INFORMATION TO USERS

This manuscript has been reproduced from the microfilm master. UMI films the text directly from the original or copy submitted. Thus, some thesis and dissertation copies are in typewriter face, while others may be from any type of computer printer.

The quality of this reproduction is dependent upon the quality of the copy submitted. Broken or indistinct print, colored or poor quality illustrations and photographs, print bleedthrough, substandard margins, and improper alignment can adversely affect reproduction.

In the unlikely event that the author did not send UMI a complete manuscript and there are missing pages, these will be noted. Also, if unauthorized copyright material had to be removed, a note will indicate the deletion.

Oversize materials (e.g., maps, drawings, charts) are reproduced by sectioning the original, beginning at the upper left-hand corner and continuing from left to right in equal sections with small overlaps. Each original is also photographed in one exposure and is included in reduced form at the back of the book.

Photographs included in the original manuscript have been reproduced xerographically in this copy. Higher quality 6" x 9" black and white photographic prints are available for any photographs or illustrations appearing in this copy for an additional charge. Contact UMI directly to order.

Mercury Absorption in Aqueous Solutions

Approved by
Dissertation Committee:

Gary Rochelle
Gary T. Rochelle, Supervisor
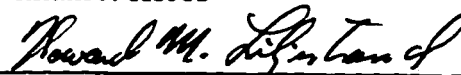
Roger T. Bonnecaze
Roger T. Bonnecaze

Matthew J. Hall
Matthew J. Hall

William J. Koros
William J. Koros

Howard M. Liljestrand
Howard M. Liljestrand

Mercury Absorption in Aqueous Solutions

by

Lingbing Zhao, B.S., M.S.

Dissertation

Presented to the Faculty of the Graduate School of

The University of Texas at Austin

in Partial Fulfillment

of the Requirements

for the Degree of

Doctor of Philosophy

The University of Texas at Austin

May, 1997

UMI Number: 9803077

UMI

300 North Zeeb Road
Ann Arbor, MI 48103

To Bin

Acknowledgments

Mercury Absorption in Aqueous Solutions

Publication No._____

Lingbing Zhao, Ph.D.

The University of Texas at Austin, 1997

Supervisor: Gary T. Rochelle

The absorption of elemental Hg vapor into various aqueous solutions was measured in a stirred cell contactor at 25°C and 55°C. The gas film mass transfer coefficient was measured using concentrated acidic permanganate solution. The liquid film mass transfer coefficient was obtained by mercury desorption from $HgCl_2$ injected into acidic stannous chloride solution.

Acidic permanganate strongly absorbs mercury with overall second order kinetics. NaOCl strongly absorbs Hg even at high pH. Low pH, high Cl^- and high temperature favor mercury absorption. Aqueous free Cl_2 was the active species that reacted with mercury. However, chlorine desorption was evident at high Cl^- and pH < 9. A fast gas phase reaction occurred between Hg° and Cl_2 at room temperature. Cl_2 concentration, moisture, and solid surface area contributed positively to mercury removal.

Aqueous solutions containing Hg(II) also absorb Hg$^\circ$. The addition of strong acids, such as HNO_3 or H_2SO_4, greatly enhanced Hg$^\circ$ absorption in Hg(II). However, HCl inhibited Hg$^\circ$ absorption in Hg(II).

Succinic acid-NaOH buffer solution greatly enhanced Hg$^\circ$ absorption in Hg(II) but $NaHCO_3$-NaOH inhibited Hg absorption. Under most conditions, oxygen in the gas phase did not have any effect on Hg$^\circ$ absorption in Hg(II). However, oxygen had a positive effect on Hg absorption in Hg(II) when HCl or $NaHCO_3$-NaOH was present in the solution.

The addition of $MnSO_4$ to Hg(II) only slightly enhanced Hg absorption while NaCl, $MgSO_4$, $FeCl_3$, $CaCl_2$ and $MgCl_2$ all inhibited Hg absorption in Hg(II).

Hg$^\circ$ absorption in Hg(II) was further enhanced by adding oxidants. The addition of H_2O_2 to HNO_3 gave the most Hg$^\circ$ removal. Both $K_2Cr_2O_7$ and $K_2Cr_2O_7$-HNO_3 enhanced Hg$^\circ$ absorption in Hg(II) and the positive effect of adding HNO_3 was more apparent than that of adding $K_2Cr_2O_7$. At 10^{-5} M Hg(II), 0.26 M H_2O_2-0.8M HNO_3 gave the most mercury removal, followed by 0.03 M $K_2Cr_2O_7$-0.8 M HNO_3, and then 0.1 or 0.8 M HNO_3, or 0.8 M H_2SO_4.

Solutions typical of limestone slurry did not remove Hg$^\circ$. Sodium sulfite and sodium thiosulfate were the main species tested in this research. Other typical limestone slurry additives, such as succinic acid, $FeSO_4$, $CaCl_2$, $MnSO_4$, $MgSO_4$, and $MgCl_2$, did not make any difference when sulfite and/or thiosulfate were present in the solution.

Aqueous sodium sulfide and aqueous polysulfide were not effective for Hg$^\circ$ absorption.

Table of Contents

xii

List of Tables

List of Figures

xvi

xvii

xviii

xix

Chapter 1 Introduction

1.1 MERCURY AND POLLUTION

Our community values the environment and clean air. Interest in controlling the emission of air toxic metals has intensified in the wake of passage of the 1990 Clean Air Act Amendments (CAAA). Among the eleven metals specified in the CAAA, mercury deserves the greatest attention both because of the emission rates and its potential hazard (Vogg et al., 1986).

Mercury is toxic to human because it acts primarily on the neurological system. Elemental mercury is actually relatively non-toxic. However, the divalent inorganic mercury compounds are considerably more toxic and organic methylmercury is more toxic yet by a factor of 10. While methylmercury is seldom present as an atmospheric emission from industrial processes, complex chemical reactions occur by which methylmercury is produced from elemental mercury or divalent mercury after they are deposited onto the soil or into lakes and streams. In lakes, methyl mercury is concentrated up the food chain so that large fish can have mercury concentrations in their flesh that is 10^6 times that in the surrounding water (Gilmour and Henry, 1991). Unacceptable levels of mercury are now even present in pristine areas of the upper Midwest and New England. Very serious problems have also been uncovered in Florida (Volland, 1991).

Mercury pollution of the environment has led to severe poisoning in several foreign countries as well as the United States (Slemr et al., 1985). To a

great extent the pollution with mercury has functioned as a trigger to the concern of the general public and of administration and industry of environmental pollution. This is particularly true for Japan, where epidemic intoxication with methyl mercury, due to contamination of sea food, occurred and caused the so called "Minamata Disease" (Takizawa, 1979). Following a severe drought that destroyed the wheat crop, Iraq imported seed grain which had been treated with a methylmercury fungicide. Many people mistakenly ate the seed which resulted in 450 deaths (Bakir et al., 1973). A Subsequent study estimated that a likely total of 5000 people died in this tragedy.

Even in other countries where no such catastrophe has occurred, mercury pollution is the issue which more than anything else has focused attention on pollution problems. The mercury problem is of general interest because it represents a pollution situation that we are likely repeatedly to encounter in the future in various parts of the world. Thus mercury pollution is of world-wide extent although the problems may not have been recognized everywhere yet (Ramel, 1973). The potential impact of fossil fuel combustion, in terms of the toxic metal emissions that can contribute to environmental pollution, is significant. At an estimated rate of coal combustion of 700×10^9 kilograms per year in utility boilers in the United States (Smith, 1980), the yield of uncontrolled fly ash emissions would be approximately 56×10^9 kilograms per year. For a trace element present in fossil fuel at a level of 1 part per million and assuming a 98 percent collection efficiency of the control device, the stack emissions would be about 1000 kilograms per year. If this element is mercury, where the collection efficiency of the control device is poor (Billing and Matson, 1972), and 98 percent

2

of the coal-bound mercury is emitted into the atmosphere, then the 1 part per million component would result in stack emissions of 55000 kilograms per year.

In January of 1990, a series of studies was completed addressing mercury contamination of lakes and streams in northern Minnesota (Swain, 1989). Researchers identified a three-fold increase in mercury deposition since the mid-1800's. Sorenson et al. (1989) concluded that airborne anthropogenic emissions are the chief cause, and most of the contamination appears to enter the lakes from wet deposition. Slemr and Langer (1992) have found that industrial pollution is causing mercury in the atmosphere to increase at a steady rate. Analyses of dated soil, peat bog and lake sediment records indicated that the total gaseous mercury has nearly doubled since the 1800's. The authors attributed more than 90 percent of the increase to human activities like coal burning, waste incineration and ore refinement. They said that although the current levels did not pose a health threat, they could become one by the mid-21st century if the increases continued at the current rate.

Mercury is generated from both natural and anthropogenic sources (Lindqvist et al., 1985). Degassing from mineral deposits, emissions from forest fires and volcanic eruptions, biological formation and photoreduction to produce elemental mercury from natural waters are examples of natural mercury sources (Hall et al., 1993). Energy production, waste incineration and smelting-refining are the major industrial processes that release mercury into the atmosphere. The total natural inputs of mercury to the atmosphere are 5.4×10^6 pounds per year while those resulting from man's activities total 7.8×10^6 pounds per year on a global scale (Nriagu et al., 1988).

3

Among man-made mercury emissions, energy production contributes 64% of the total amount and 33% is due to waste incineration (Nriagu et al., 1988). Since combustion of fossil fuels constitutes the primary means of energy production, combustion produces a significant portion of mercury emissions. Coal is one of the most commonly used fossil fuels. The concentration of mercury in coal varies from 0.01 to 8.0 ppm, depending on the type and the origin of the coal (Radian Corporation, 1989).

Since Congress approved the Clean Air Act in 1970 and Clean Air Act Amendment in 1990, over hundreds of billions of dollars have been invested in federal, state and local funds to assure a clean air and environment. Among these, public utilities alone comprised 35% of the all-industry total for air pollution control costs (Vatavuk, 1990). However, due to the limitations of current available technology, some of the air pollutants are still hard to remove from stack emissions. Mercury is among them. In fact, mercury is one of the most difficult species to remove due to its high volatility and low reactivity.

1.2   RESEARCH OBJECTIVE

The specific objectives of this work were to quantify primary phenomena and major problems that may arise in the use of limestone slurry or other reagents for mercury emissions control from coal-fired power plants. Elemental mercury and mercuric chloride vapor are the two primarily forms of mercury emissions. Due to its high water solubility and relatively low vapor pressure (1.06×10^6 gmole/l-atm at 25°C, Clever, 1985), almost all of the mercuric chloride ($HgCl_2$) is removed by conventional wet scrubber systems via physical absorption.

4

Elemental mercury, however, is unaffected in these systems because of its low solubility and high volatility (Wesnor, 1993; Noblett et al., 1993).

The most common Flue Gas Desulfurization system currently used in the industry is limestone slurry scrubbing. The major components of limestone slurry solution are sulfite and other aqueous cations and anions, such as Ca^{++}, Mg^{++}, Na^+ and Cl^-, as shown in table 1.1. Our initial research objective was to assess the effect of limestone slurry scrubbing on mercury removal.

Table 1.1   Typical limestone slurry scrubbing solution composition.

Composition	Concentration (mM)
S(IV)	10
Ca^{++}	50
Mg^{++}	50
Cl^-	100
Na^+	20
pH	5-6

The limited solubility of elemental mercury vapor in water suggests that its absorption rate should be controlled by liquid film resistance. Any reasonable rate of mercury absorption will require that it be converted to more soluble products such as Hg^{2+} by reaction in the mass transfer boundary layer. Thus an aqueous oxidant is essential to the removal of mercury. If the solution itself is an oxidant, mercury removal would be accomplished by reacting with the oxidant. In limestone slurry scrubbing, the coexistence of reducing agents ($SO_3^=$ and $S_2O_3^=$) and possible oxidizing free radicals generated by sulfite oxidation (Owens, 1984) complicate the process. Even if elemental mercury is absorbed, the generated Hg^{2+} may be reduced back to elemental mercury by sulfite or other reducing agents in the mass transfer boundary layer or bulk solution. These

5

reactions would reduce total mercury removal by desorbing the produced elemental mercury. Desorption from reactions in the bulk solution would be limited by liquid film diffusion of mercury.

Based on above discussed reasons, limestone slurry scrubbing might not be effective for mercury removal. Other approaches, such as using aqueous oxidizing solution to absorb mercury, would be another scope of our research.

Previous investigators have reported substantial mercury removal in acidic permanganate solution (Monkman et al., 1956; Hara, 1975). EPA method 29 uses two impingers in series, with hydrogen peroxide and nitric acid in the first impinger and acidic permanganate in the second impinger, to speciate between elemental mercury and mercuric chloride vapor (Environmental Protection Agency, 1992). The effects of other strong oxidants on mercury removal, such as hypochlorite and potassium persulfate, have been reported elsewhere (Nene and Rane, 1981; Metzger and Braun, 1987). Although almost all of these previous works are qualitative in nature, it sheds light on the means to remove mercury. Despite the many differences in properties and oxidation potential of different oxidants, they seem to have one thing in common. Mercury was absorbed because it was oxidized to a more soluble form, Hg^{++}. Therefore, our approach was to contact elemental mercury vapor with either aqueous or gaseous oxidants, oxidized it and scrubbed it into the solution.

In summary, the objectives of this research were:

(1) Measure and model mercury absorption into aqueous solution typical of limestone slurry scrubbing.

6

(2) Quantify the reaction kinetics and clarify the mechanisms of mercury reaction with oxidants in aqueous solutions.

Although primarily directed at developing technologies for mercury abatement from power plant emissions, this work also provides basic scientific data for the advantages of the entire chemical engineering community.

Chapter 2 Literature Review

2.1 UNDERSTANDING MERCURY

In the periodic table of the elements, mercury is categorized in the group of elements known as the transition metals. It occupies Group IIB along with the elements Zn and Cd, yet it has some rather unusual physical and chemical properties that distinguish itself from the other transition metals. For example, mercury is the only metal that is a liquid at normal room temperature. As a result, elemental mercury has a substantial vapor pressure, even at room temperature, and it is relatively easily vaporized. This is one of the reasons that mercury is found everywhere, including ambient air, work area atmospheres and natural waters.

Mercury exists in ambient air predominantly in the gaseous form as individual mercury atoms rather than in the particulate phase, as is the case for other transition metals, e.g., Cd, Zn, Cu, Ni and Pb. The relatively high first ionization potential for mercury (241 kcal/mole), even if compared with those of the noble metals Ag (175 kcal/mole), Pd (192 kcal/mole), Pt (207 kcal/mole) and Au (213 kcal/mole), places it in the same position with the inert gas Ra (248 kcal/mole). This may explain the existence of mercury in the atmosphere primarily in the reduced form (Hg°), even though the atmospheric environment is well known for its oxidizing properties, as demonstrated by the formation of acid rain and the occurrence of oxidants and photochemical smog (Schroeder et al.,

1991). The unique absorbency at 253.7 nm of elemental mercury permits the use of cold vapor atomic absorption spectroscopy for mercury analysis.

Mercury is found in nature in many forms but predominantly it is present as cinnabar, HgS. In the United States, the average mined ore contains approximately 5 pounds of mercury per ton of ore.

2.1.1 Physical-Chemical Properties

Literature review gave most of the physical-chemical properties of mercury. They are listed in table 2.1.

Table 2.1 Physical-chemical properties of elemental mercury and mercuric chloride.

Property	25°C	55°C
$D_{Hg-H_2O}{}^a$ (cm^{2}sec^{-1})	1.19×10^{-5}	2.21×10^{-5}
$D_{Hg^{++}-H_2O}{}^b$ (cm^{2}sec^{-1})	8.47×10^{-6}	1.65×10^{-5}
$H_{Hg}{}^c$ (atm M^{-1})	8.91	35.64
$D_{Hg(g)-N_2}{}^d$ (cm^{2}sec^{-1}) (1atm)	0.13	0.16
$D_{Hg(g)-Air}{}^e$ (cm^{2}sec^{-1}) (1atm)	0.15	0.18
Vapor pressure of liquid Hg^{oc} (atm)	2.70×10^{-6}	2.43×10^{-5}
Vapor pressure of solid HgCl$_2{}^c$ (atm)	2.53×10^{-7}	4.57×10^{-6}
Water solubility of liquid Hg^{oc} (M)	3.05×10^{-7}	6.82×10^{-7}
Water solubility of solid HgCl$_2{}^c$ (M)	0.269	0.575
Henry's constant of Hg^c (atm M^{-1})	8.91	35.64
Henry's constant of HgCl$_2{}^c$ (atm M^{-1})	9.41×10^{-7}	7.95×10^{-6}

[a] estimated using Sitaraman et al.'s eqn. (1963), see Appendix B for detailed calculation
[b] obtained from Lide (1994)   [c] obtained from Clever et al. (1985)
[d] obtained from Mullaly and Jacques, 1924; Spier, 1940; Nakayama, 1968
[e] obtained from Mikhailov and Kochegarova (1967)

2.1.2 Transportation and Fate of Mercury Emissions

Mercury is released into the atmosphere not only by industrial processes and other human activities, but also from many natural sources. Once discharged in the atmosphere, mercury vapor and small particulates of divalent inorganic mercury compounds can stay there for long times and travel long distances. Ultimately it is deposited on the soil or into lakes, rivers, and oceans.

Atmospheric dispersion models have been developed to predict the rate of deposition of mercury at various distance from a point source, such as a specific power plant (Vaughan et al., 1975). After deposition in lakes and streams, mercury is accumulated in the sediments where it can be converted to methylmercury by microorganisms, principally sulfate-reducing bacteria. However, the mechanism by which methylmercury becomes incorporated in the food chain in the lake is not fully understood. A model named Mercury in Temperate Lakes (MTL) is being developed by the Electric Power Research Institute (EPRI) to simulate the complex mercury interaction in lakes (Douglas, 1991). By combining atmospheric, soil and lake dispersion models, the impact of mercury emission can be estimated.

2.1.3 Characteristics of Mercury in Flue Gases

Knowledge of the vapor pressure of mercury is important in determining how much mercury is discharged to the atmosphere from various processes when the conditions are such that the vapor is in equilibrium with liquid mercury in the system. Typically, the concentration of Hg is in the range of 0.0001 to 0.0006 ppm from Coal Fired Power Plant emissions and 0.01 to 0.1 ppm from Waste

10

Incineration emissions (Hall, 1991). Since the concentration of mercury in the flue gas does not approach the equilibrium value even as it cools when passing through various gas treatment systems, homogeneous condensation of mercury vapor does not occur. However, at lower temperatures mercury vapor may be adsorbed onto fly ash particles or other surfaces.

The form of mercury in the flue gas may determine the optimum method of separation. Generally, there are three phases in coal combustion where trace elements exist in different physical forms (Gleiser, 1993). For those elements that are not volatilized or, if volatilized, condense and coalesce later, the removal mechanism usually is filtration in the dust collector which can achieve at least 90% removal. However, in comparison to these elements, a great portion of the mercury emission often exists as gas at very low concentration, namely, 0.1-0.6 ppb, which is extremely difficult to separate.

Mercury, which is mainly present in the coal as mercury sulfide, is oxidized to HgO during combustion. The oxide is converted to the elemental form which is the thermodynamically stable species at the high temperatures of the combustion zone. Most of the mercury in the coal is vaporized and, generally, about 10% is associated with the fly ash. The remaining 90% of the total mercury is in the vapor phase at the air preheater outlet (Noblett et al., 1993). Elemental mercury and a less volatile form, mercuric chloride are the two primarily forms in the vapor phase. The relatively high concentration of HCl (150 mg/m^3) in the flue gases makes the existence of $HgCl_2$ possible (Meij, 1991). This explanation was also supported by other researchers (DeVito et al, 1992; Brna, 1992; Nakazato, 1990). On the other hand, some other investigators even found low

11

coal chlorine contents could produce a significant amount of ionic mercury (Felsvang, 1993). The relative ratios of the oxidized to the elemental form of mercury have primarily been speculative to date. A recently developed mercury speciation method has been reported and the limited results indicate 50-90% of the mercury in these measurements is oxidized (Bloom, 1991). Essentially all water soluble mercuric chloride ($HgCl_2$) is removed by conventional FGD systems, while elemental mercury is unaffected (Wesnor, 1993; Noblett et al., 1993). Therefore, the overall removal efficiency of mercury will depend on the speciation of mercury inlet in the flue gas. This might also be one of the reasons that mercury removal efficiencies are widely scattered in different power plants.

2.1.4 The Question of Permanent Capture and Ultimate Disposal

Bergstrom (1986) reported that over a period of 14 days, 20-15% of the mercury in fly ash from a fabric filter evaporated at room temperature. Lindberg (1987) studied the loss of mercury vapor from solid wastes and storage ponds near chlor-alkali plants in the eastern United States. In controlled experiments he reported that the evaporation of mercury escalated dramatically as the surface temperature of the solid waste increased above 70°F. Further, at temperatures near 86°F, the measured mercury concentrations in the vicinity of a waste pond approached the EPA's 1 $\mu g/m^3$ ambient air quality standard. Similarly, a study demonstrated that evaporation of mercury from soils rich in volcanic ash was essentially parallel to the mercury vaporization function which is exponential with temperature (Siegel and Siegel, 1988). These studies suggest a substantial problem in maintaining mercury capture using a dry scrubber system. This would

be a particular concern in warm climates where dark fly ash may attain a temperature of 140°F, baking in the summer sun before being covered.

2.2 CONTROL TECHNOLOGIES

2.2.1 Control the Mercury Content of the Fuel

One of the direct approaches to reducing mercury emissions from combustion is to reduce the mercury content of the fuel. In the case of coal, switching to a coal with a lower average mercury concentration or to a cleaned coal in which a reduced mercury has been achieved through the cleaning process will result in lower emissions. The mercury content of coal varies widely. In a study of 101 coals the observed mercury concentration varied from 0.2 to 1.6 ppm. Literature values were found in the range from 0.01 to 8.0 ppm for subbituminous coal, and from < 0.01 to 3.3 ppm for bituminous coal (Radian Corporation, 1989). For a coal with a heating value of 13100 Btu/lb, the mercury emissions per 10^{12} Btu input would range from 0.7 to 620 pounds for the extreme concentrations of 0.01 and 8.0 ppm mercury, respectively. Although the freedom to switch to a coal lower in mercury content will probably be restricted by other considerations, the option of coal switching as a means of reducing mercury emissions is one to be considered.

Coal cleaning is another means of reducing the input of mercury to the combustion system. In coal cleaning, most of the trace elements are removed to the same extent as the ash. Mercury removal, however, is lower and much more variable than many of the other trace elements (DeVito et al., 1993). As in the case of switching to low mercury coal, other considerations may take precedence

13

over the use of a cleaned coal for the specific purpose of lowering mercury input, but again, it is an option that may prove useful.

2.2.2 Particulate Control Devices

Devices to control particulate emissions are now standard on coal combustion facilities. The degree to which such devices reduce mercury emissions depends on the conditions upstream of and within the device. Mercury is assumed to be entirely in the elemental vapor state when it leaves the combustion chamber. Mercury vapor will pass through the collection device unaffected because the concentration in the flue gas is far below the equilibrium value. However, if the flue gas has been sufficiently cooled, some of the mercury vapor may be sorbed onto fly ash particles or other surfaces. In this case, the electrostatic precipitator (ESP), baghouse, or other collection device would remove some or all of the particles carrying mercury.

2.2.2.1   Electrostatic Precipitator (ESP)

Radian (1989) reported that, in the literature prior to 1965, an average of 50% mercury removal was reported by the data on ESPs. However, the report pointed out that much of the data was suspect because of the failure to close mass balances due to analytical difficulties. Huang et al.. (1991) summarized mercury removal efficiencies in the literature and showed a mercury collection efficiency of 25-50% for cold and 0% for hot electrostatic precipitators. The authors also added that there were deficits in the mass balance for mercury in some of the results so that these values can only be considered tentative.

14

2.2.2.2   *Fabric Filter*

Fabric filters effectively remove particles from flue gas so that mercury removal depends on the association of mercury with particles in the same manner as that for ESP, which is discussed in section 2.2.2.1. Data for fabric filters is equally sparse and inconclusive. A range of 50-90% mercury removal was indicated in a limited numbers of fabric filter systems (Smith, 1987; Chow, 1991).

2.2.3   Wet Scrubbing

Flue Gas Desulfurization (FGD) systems, using limestone slurry scrubbing for removing sulfur dioxide, cool the flue gas and, as a result, some mercury may be adsorbed onto fly ash particles and be removed from the flue gas in the particulate collection device. Mercury removal efficiency in wet FGD process has the same wide ranges of values as seen with particulate collection devices. The literature reported 20-90% mercury removal based on very few available results (Radian Corporation, 1989; Huang et al., 1991).

Multistage condensing wet scrubbers and electrostatic precipitators followed by wet scrubbers (ESP/WS) are proven technology in Europe. Their use was originally directed to the economical removal of acid gases. However, Reimann (1986) reported 80-90% mercury removal with an ESP/WS configuration and the use of the organo-sulfur precipitant, to capture and stabilize the mercury in the scrubber blow down. More recently, greater than 90% mercury removal was reported by employing a two stage condensing wet scrubber. Since elemental mercury vapor did not completely condense at the 100-140°F operating temperatures of wet scrubber, the outlet emissions were entirely elemental

mercury. Some vendors thus believe that scrubbers work better when the dominant species is the highly soluble mercuric chloride. However, some removal of elemental mercury can be expected by the mechanism of fine particle impacting, diffusion, and possibly by dissolution in acidic zones (Volland, 1991).

Other investigators reviewed the operating conditions for mercury removal in wet flue gas desulfurization systems. Their results are listed in table 2.2.

Table 2.2   Parameters affecting removal of vapor-phase mercury in wet absorber (Noblett et al., 1993).

Parameter	Comments
L/G	Increased gas/liquid surface area increases removal.
Absorber Internals	Trays or packing can increase gas/liquid surface area and improve removal. Position of headers and nozzles can affect spray coverage and spray interaction, affecting surface area.
Tower Height	Increased tower height or tower width will increase contact time and may improve removal.
Slurry Chemistry (including pH)	If there is significant liquid-film resistance, slurry chemistry could affect the form of absorbed substance and/or solubility of compounds containing the substance.
Additives or Neutralizing Agents	If removal is influenced by liquid-film resistance, then complexing, precipitating, or increasing solubility of the absorbed substance could improve removal.
Gas Velocity	Gas velocity will affect gas/liquid contact time.
Oxidation Mode	Oxidation mode may affect form and solubility of absorbed substances, affecting removal in situations where liquid resistance is important.

Vogg et al. (1986) studied mercury removal by wet scrubbing methods in laboratory scale experiments. They showed that mercuric chloride could be conveniently and very effectively eliminated from the gas phase through condensation. They also observed the possibility of mercury loss if divalent mercury was reduced, e.g. by sulfur dioxide. They then suggested that this could be counteracted by higher chloride concentrations, by a strongly acid scrubbing

16

solution, or if possible, by lowering the temperatures or adding oxidants, such as ferric chloride.

2.2.4 Spray-Dryer Scrubbing

Spray dryer absorption is an alternative technology for desulfurization of flue gases. A wide range of 20-95% mercury removal was reported based on a few sets of data (Gleiser, 1993).

2.2.5 Modified Mercury Control Processes

The first option of modifying a FGD system is the use of carbon. Felsvang et al. conducted spray dryer absorption tests in three pilot plants used for control of mercury emissions from coal-fired power plants. By injecting activated carbon, improvements of mercury removal were achieved (Felsvang, 1993). Similar modified FGD technology increased the mercury removal efficiency to 60-90% (Gleiser, 1993; Guest, 1991). Commercial processes for injection of activated carbon in spray dryer systems for incinerators have been available (Niro, 1987), but the applicability to coal-fired power plants still is a problem.

Another option is to use additives specifically designed for mercury removal. Japanese investigators have applied a liquid chelating agent injection system and a sodium hypochlorite injection system to a limestone slurry scrubber and have achieved 90% mercury removal (Nakazato, 1990). The addition of a chlorine containing material such as sodium chloride improved overall mercury removal by changing the speciation of inlet mercury, based on testing pilot scale coal-fired power plants (Felsvang, 1993).

Other additives, such as sodium sulfide and sodium hydrosulfide for spray dryer systems and polysulfide for wet scrubbing systems have also been reported (Zohourslsen, 1991; Guest, 1991). Since the highly stable and non-volatile mercuric sulfide species is formed, this process theoretically should achieve near permanent capture of the mercury. However, the use of sodium sulfide prompts certain safety concerns with handling as well as concern for corrosion problems. Some experimental work using these additive systems on incinerator flue gas were conducted with promising results, but no work has been reported in which the systems have been applied to coal combustion flue gas.

A German company has commercialized a simplified sulfur dioxide and mercury scrubbing process called MercOx (Parkinson, 1996). In their process, a 35% aqueous solution of hydrogen peroxide is sprayed into the flue gas. Elemental mercury is oxidized by hydrogen peroxide to Hg(II) and remains in the solution. In a parallel reaction, a water spray converts SO_2 to sulfuric acid. As a result, all gaseous pollutants are converted and trapped in the solution. Dissolved mercury is removed by ion exchange and the acids are neutralized to salts and precipitated gypsum. In recent pilot test treating a 500 m^3/hr flue gas stream at a sludge incinerator, mercury concentrations were reduced from a few hundred $\mu g/m^3$ to 20 $\mu g/m^3$, well below the 50 $\mu g/m^3$ German limit. The capital cost for a 18000 m^3/hr unit is only about one quarter that of a conventional system while the operating cost is 20-25% less.

2.3 MERCURY EMISSION STANDARDS

Following the emphasis on the regulation of sulfur oxides, nitrogen oxides, and particulate matter in the 1970s and 1980s, attention broadened to include concern over air toxics in the mid 1980s and this has continued (Schroeder et al., 1987). The Clean Air Amendments (CAAA) of 1990 addressed the subject of air toxics under section 112. This section calls for the promulgation of emission standards for pollutants not previously regulated under the National Ambient Air Quality Standards. A list of 189 elements and chemicals is specified in the law as subject to control. For mercury emission, because of the wide variability of mercury levels in coal, difficulties in sampling and analysis, and variations in the way in which mercury is partitioned in the various combustors in use, the information on utility emissions was insufficient for promulgation of regulation. Thus, the law mandates three studies related to health effects, control technologies and costs of control to develop the required information.

2.3.1 Coal-Fired Power Plants

Since the CAAA prohibits EPA from setting standards on mercury emissions from utility power plants until all of the studies have been completed, it will undoubtedly take considerable time for the results of the studies to be reviewed and decisions made as to whether any standards will be set for mercury. It would seem that late 1996 or early 1997 might be the earliest that anything definite regarding new standards will be decided.

2.3.2 Municipal Waste Combustors

As a result of extensive research on mercury's impact on the ecosystem, Sweden has set a mercury emissions limit for Municipal Solid Waste incinerators equivalent to about 40 μg/dscm corrected to 7% oxygen. The Dutch limit is equivalent to about 70 μg/dscm. The new German limit for the sum of cadmium and mercury emissions is 140 μg/dscm corrected to 7% oxygen (Volland, 1991). Most recently, U. S. EPA has set the limit for large and small Municipal Waste Combustion plants to be 80 μg/dscm (35 gr/million dscf) or 85% reduction in mercury emissions (Federal Register, 1995). This mercury emission standard went into effect on June 19, 1996 for new sources and December 19, 1995 for existing sources.

2.4 THEORY OF SIMULTANEOUS MASS TRANSFER WITH CHEMICAL REACTION

2.4.1 Film Theory

Several models have been developed to describe mass transfer at a fluid phase boundary. The earliest and simplest is the film theory proposed by Whitman (1923). This model is based on the assumption that for a fluid flowing turbulently over a solid, the entire resistance to mass transfer resides in a stagnant film in the fluid next to the surface. It pictures a stagnant film of thickness at the surface of the liquid next to the gas. While the rest of the liquid is kept uniform in composition by agitation, the concentration in the film falls from $\frac{P_i}{H}$ at its surface to C^* at its inner edge, where C^* is the average concentration of dissolved gas in the bulk liquid. There is no convection in the film, and dissolved gas crosses it by

molecular diffusion alone. The mass transfer coefficient is equal to $\dfrac{D}{\delta}$, where δ is the thickness of the stagnant film.

2.4.2 Penetration Theory

Higbie (1935) suggested a penetration theory for transfer across a gas-liquid interface. This theory assumes that the liquid surface consists of small fluid elements that contact the gas phase for an average time, after which they penetrate into the bulk liquid. Each element is then replaced by another element from the bulk liquid phase. The penetration theory predicts the mass transfer coefficient to be $2\sqrt{\dfrac{D}{\pi t_s}}$, where t_s is the exposure time of the fluid element.

2.4.3 Surface Renewal Theory

On the basis of the penetration theory, Danckwerts (1970) suggested that the constant exposure time in penetration theory be replaced by an average exposure time determined from an assumed time distribution. The chance of an element being replaced on the surface was independent of the time during which it had been exposed. For this model the mass transfer coefficient is equal to $\sqrt{D\,s}$, where s is the rate of surface renewal and is equal to the reciprocal of the exposure time of the elements.

2.4.4 The Effects of Chemical Reactions

The above discussed three models may be used to predict the effect of a chemical reaction on the rate of absorption. Predictions based on the three models are closely similar, except in regard to the effect of the diffusivity of the solute gas and of dissolved reactants on the rate of absorption. For instance, the film model

21

predicts that mass transfer coefficient is proportional to diffusivity while both penetration and surface renewal theory predict that it varies as $\sqrt{D}$. It is difficult to make an accurate test of this dependence, since the diffusivities of typical solute gases do not cover a wide range and are difficult to determine accurately. For the same reasons, the dependence of mass transfer coefficient on the diffusivity is usually of relatively lesser importance. In most cases the film theory would lead to almost the same predictions as the penetration and surface renewal theory. Furthermore, the difference between predictions made on the basis of the three models discussed above will be less than the uncertainties about the values of the physical quantities used in the calculation. The three models can thus be regarded as interchangeable for many purposes, and it is then merely a question of convenience which of the three is used.

The governing equation, in the case of an irreversible first-order reaction, is given by the material balance:

$$D \frac{\partial^2 C}{\partial x^2} = \frac{\partial C}{\partial t} + k_1 C \tag{2-1}$$

with the following boundary conditions:

1. $C = 0$ at $x > 0$ and $t = 0$ (2-2)
2. $C = \frac{P_i}{H}$ at $x = 0$ and $t > 0$ (2-3)

3. $C = 0$ at $x = \infty$ and $t > 0$ (2-4)

The solution using the surface renewal model is detailed in Danckwerts (1970), where $\overline{C}$ is the average concentration over time:

$$\overline{C} = \frac{P_i}{H} \exp\left(-\frac{x\, k^\circ_1}{D} \sqrt{1 + \frac{D\, k_1}{k^\circ_1{}^2}}\right) \tag{2-5}$$

22

The average rate of absorption per unit area of gas-liquid interface, or flux, is obtained from:

$$N = - D \left(\frac{d\bar{C}}{dx}\right)_{x=0} = k^{\circ}_{l} \left(\frac{P_i}{H}\right)\sqrt{1 + \frac{D k_l}{k^{\circ}_l{}^2}} \qquad (2\text{-}6)$$

Similarly, for second-order irreversible reaction, this theory predicts the average flux to be:

$$N = k^{\circ}_{l} \left(\frac{P_i}{H}\right)\sqrt{1 + \frac{2 D k_2 P_i}{3 k^{\circ}_l{}^2}} \qquad (2\text{-}7)$$

If the reaction is fast enough (large k_1 and k_2), the simplified fluxes are:

$$N = \left(\frac{P_i}{H}\right)\sqrt{D k_l} \qquad (2\text{-}8)$$

and

$$N = \left(\frac{P_i}{H}\right)\sqrt{\frac{2 D k_2 P_i}{3}} \qquad (2\text{-}9)$$

In the above derivation, N is flux, k_1 and k_2 are first-order and second-order rate constants, D is the diffusion coefficient in liquid phase, k°_l is liquid film physical mass transfer coefficient, H is Henry's constant, P_i is interfacial partial pressure of the dissolving gas, C is the concentration of the gas in the liquid, x is the distance below the gas-liquid surface and t is time.

In the above expressions, the quantity $\sqrt{1 + \frac{D k_l}{k^{\circ}_l{}^2}}$ is known as the enhancement factor E. E is a measure of the amount of dissolved gas which reacts in the diffusion film near the surface, compared to that which reaches the bulk liquid in the unreacted state. If E is 1, it represents a physical absorption with no reaction, in which case the dissolved gas diffuses form the surface to the bulk without reaction on the way. If E » 1, the dissolved gas all reacts in the film and none diffuses in the unreacted state into the bulk of the liquid. Thus the film

23

thickness, or the value of k°_1, is irrelevant and does not appear in the expression for flux N.

2.5 AQUEOUS PHASE REACTIONS

2.5.1 Reduction of Hg^{++} by Sulfite

There are several aqueous phase reactions that involve mercury species. The most important one is reduction of Hg^{2+} by sulfite. Munthe et al. (1991) proposed that Hg^{2+} could be reduced by aqueous sulfite solutions with the formation of an unstable intermediate, $HgSO_3$, followed by decomposition to Hg^+ which in turn is rapidly reduced to Hg°. Using the empirical equation derived by Dyrssen and Wedborg (1991), they calculated that $logK_1 = 12.7$ and $logK_2 = 11.4$ where K_1 and K_2 are equilibrium constants of the following two equations, respectively:

$$Hg^{2+} + SO_3^{2-} \longleftrightarrow HgSO_3 \qquad (2\text{-}10)$$

$$HgSO_3 + SO_3^{2-} \longleftrightarrow Hg(SO_3)_2^{2-} \qquad (2\text{-}11)$$

On the other hand, the reaction:

$$HgSO_3 \longrightarrow Hg^+ + SO_3^- \qquad (2\text{-}12)$$

should be considered according to the observed dependence of apparent rate constants on the concentration of excess HSO_3^-. The Hg^+ ion formed would then be rapidly reduced to elemental Hg by the following two reactions:

$$Hg^+ + HSO_3^- \longrightarrow Hg^{\circ} + SO_3^- + H^+ \qquad (2\text{-}13)$$

$$Hg^+ + Hg^+ \longrightarrow Hg^{\circ} + Hg^{2+} \qquad (2\text{-}14)$$
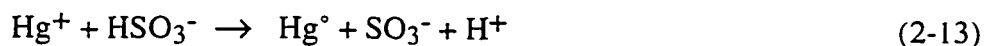
When a low concentration of $SO_2(g)$ ($5g/m^3$, $25°C$) was present, the rate of conversion of $Hg(SO_3)_2^{2-}$ to $Hg°$ was significant at $pH < 5.5$. At higher concentrations of $SO_2(g)$, significant reduction occurs at slightly lower pH.

2.5.2 Reaction between $HgCl_2$ and $S_2O_3^=$

The reaction between $HgCl_2$ and $S_2O_3^=$ is also reported in literature (Barbieri et al., 1960):

$$2SSO_3^= + 3HgCl_2 + 2H_2O \rightarrow HgCl_2 \cdot 2HgS \text{ (s)} + 2SO_4^= + 4Cl^- + 4H^+ \quad (2\text{-}15)$$

$$2S_3O_6^= + 3HgCl_2 + 4H_2O \rightarrow HgCl_2 \cdot 2HgS \text{ (s)} + 4SO_4^= + 4Cl^- + 8H^+ \quad (2\text{-}16)$$
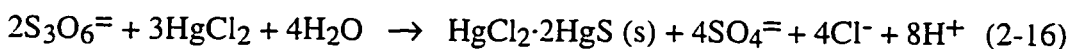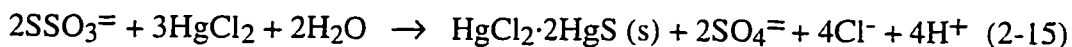
2.5.3 Oxidation of $Hg°$ and Hg^{++} by $KMnO_4$-H_2SO_4

It is well known that acidic $KMnO_4$ solution reacts with $Hg°$ (Monkman et al., 1956). Recent work performed at Radian indicates that $KMnO_4$ also reacts with Hg^{++} even though the products are not known yet (personal communication with Dr. Carl Richardson, 1994). Hara (1975) studied the reaction of $Hg°$-air with $KMnO_4$-H_2SO_4 in a impinger system. The author concluded that dissolved $KMnO_4$ changed to MnO_2, and granules of MnO_2 precipitated out gradually. The greater part of captured mercury was adsorbed on precipitated MnO_2, and the amount of mercury captured in liquid phase was very little. He further indicated that $KMnO_4$ played a great part in the capture of mercury, and H_2SO_4 was necessary for the adsorption of mercury on MnO_2.

Although $KMnO_4$-H_2SO_4 has been used in mercury analytical procedures and in mercury flue gas field sampling, no kinetic information has been reported so far. The most probable stoichiometry is shown below:

$$3Hg + 2KMnO_4 + 4H_2SO_4 \rightarrow 3HgSO_4 + K_2SO_4 + 2MnO_2(s) + 4H_2O \quad (2\text{-}17)$$

2.5.4 Oxidation of Hg° and Reduction of Hg²⁺ by H₂O₂

Aqueous H_2O_2 can either act as a source of oxidizing agent for $Hg^°$ or a reducing agent for Hg^{2+} (Brosset, 1987):

$$Hg^° + H_2O_2 + 2H^+ \rightarrow Hg^{2+} + 2H_2O \qquad (2\text{-}18)$$

$$Hg^{2+} + H_2O_2 + 2OH^- \rightarrow Hg^° + O_2 + 2H_2O \qquad (2\text{-}19)$$
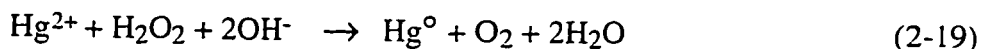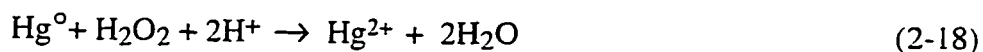
The oxidation predominates when pH is below 5.5 and the reduction predominates when pH is above 5.5.

2.5.5 Oxidation of Hg° by Chlorine, Hypochlorous Acid and Hypochlorite

Menke and Wallis (1980) studied the rate of $Hg^°$ removal by Cl_2 at different levels of relative humidity. Excess chlorine was present so the pseudo first order rate constant could be obtained. However, due to the complexity of the reaction, an upper limit of the rate constant was reported instead. The authors pointed out that their results may indicate the formation of products other than $HgCl_2$.

The kinetics of absorption of mercury in aqueous hypochlorous acid and hypochlorite were studied in a disc column at 30°C by Nene and Rane (1981). Table 2.3 gives the concentration ranges of the reactants used in their study.

Table 2.3   Concentration ranges of reactants used in Nene and Rane's study (1981).

Compound	Concentration Range (M)
HOCl	$2.6 - 9.5 \times 10^{-3}$
NaOCl	$6.7 \times 10^{-3} - 0.03$
KOCl	5.5×10^{-3}
NaCl	4.4
KCl	0.34

26

The authors found that hypochlorous acid was much more reactive than hypochlorite. In the case of hypochlorite, reactivity was further increased in the presence of sodium chloride. They also compared the reactivity of sodium and potassium hypochlorites and found the latter was more reactive with mercury. They found that the reaction between mercury and hypochlorite was first order with respect to each of them.

Kobayashi (1987) investigated the oxidation of elemental mercury by bubbling Hg° vapor into NaOCl. The concentration of dissolved mercury increased as OCl^- concentration was increased from 0.0014 to 0.014 mM. The initial rate of mercury oxidation was reported to be independent of the OCl-concentration, suggesting that the oxidation rate was not the rate-determining step under the experimental conditions. The author concluded that the reaction was zero order in OCl^-. He then proposed the following possible reactions to account for the observed 1:2 stoichiometry:

$$Hg^\circ(g) \leftrightarrow Hg^\circ(aq) \tag{2-20}$$

$$Hg^\circ(aq) + 2\,OCl^- + 4H^+ + 2e \rightarrow Hg^{2+} + 2Cl^- + 2H_2O \tag{2-21}$$

$$Hg^\circ(aq) + 2HClO + 2H^+ + 2e \rightarrow Hg^{2+} + 2Cl^- + 2H_2O \tag{2-22}$$
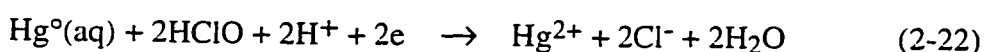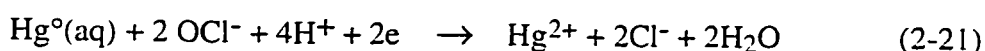
This mechanism was consistent with the observation that the concentration of dissolved mercury increased from 0.33 to 0.57 mg/l when pH was decreased from 8.1 to 1.2.

2.5.6 Oxidation of Hg° by Ozone

The oxidation of elemental mercury by aqueous ozone was studied by Iverfeldt and Lindqvist (1986) and more recently by Munthe (1992). The former

reported that the absorption of mercury in the water phase was increased by three orders of magnitude with O_3 present. The latter reported a second order rate constant of $(4.7 \pm 2.2) \times 10^7$ $M^{-1}s^{-1}$.

2.5.7   Oxidation of Hg° by Organoperoxy Compounds

Wigfield and Perkins (1985) studied the aqueous oxidation of $Hg°$ by a series of peroxy compounds including peracetic acid, m-chloroperoxybenzoic acid, ethylhydroperoxide and tert-butyl hydroperoxide. The authors found that peracetic acid and m-chloroperoxybenzoic acid oxidized $Hg°$ to Hg^+ and Hg^{++}, suggesting that the presence of a carbonyl group enhances the reactivity of peroxides. Control experiments with acetic and benzoic acid did not result in $Hg°$ oxidation.

2.6   GAS PHASE REACTIONS

The reactions of elemental mercury vapor with flue gas components were investigated by using a 17 kW propane fired flue gas generator and a continuous flow reactor (Hall et al., 1991). It was concluded that elemental mercury was readily oxidized by Cl_2 and HCl both at room and at elevated temperatures up to 900°C. Mercury also reacted with oxygen if a catalyst, such as activated carbon, was present. A slow reaction between elemental mercury and NO_2 was also observed at 340°C. On the other hand, NH_3, N_2O, SO_2 or H_2S did not react with elemental mercury under similar conditions. They proposed the following possible reactions:

$$Hg°_{(g)} + Cl_{2(g)} \rightarrow HgCl_{2(s, g)} \qquad (2\text{-}23)$$

$$2Hg°_{(g)} + Cl_{2(g)} \rightarrow Hg_2Cl_{2(s)} \qquad (2\text{-}24)$$

28

$$Hg^\circ_{(g)} + 2HCl_{(g)} \rightarrow HgCl_{2(s, g)} + H_{2(g)} \qquad (2\text{-}25)$$

$$2Hg^\circ_{(g)} + 4HCl_{(g)} + O_{2(g)} \rightarrow 2HgCl_{2(s, g)} + 2H_2O_{(g)} \qquad (2\text{-}26)$$

$$4Hg^\circ_{(g)} + 4HCl_{(g)} + O_{2(g)} \rightarrow 2Hg_2Cl_2(s) + 2H_2O_{(g)} \qquad (2\text{-}27)$$

$$Hg^\circ_{(g)} + NO_{2(g)} \rightarrow HgO_{(s, g)} + NO_{(g)} \qquad (2\text{-}28)$$

$$Hg^\circ_{(g)} + \text{activated carbon} \rightarrow Hg_{(ads.)} \qquad (2\text{-}29)$$

$$Hg_{(ads.)} + O_{2(g)} \leftrightarrow \text{products} \qquad (2\text{-}30)$$
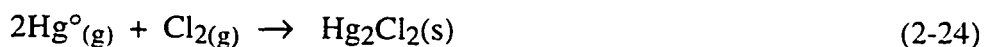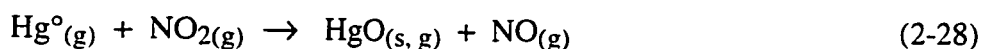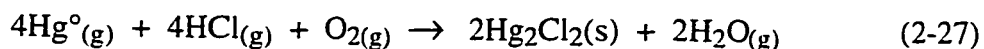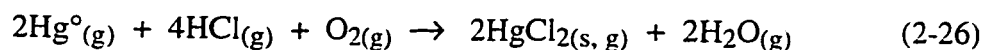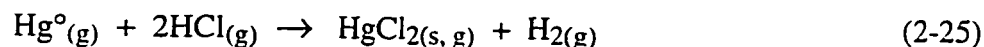
2.7 EXISTING PROBLEMS

One of the primary reasons that additional studies of mercury emissions are required is that much uncertainty exists regarding the performance of various control technologies with respect to reducing mercury emissions. There is so much scatter in the results reported that definitive performance measures cannot be established with any confidence. This variability in the data was due, in part, to the fact that the mercury concentrations encountered are extremely low so that difficulties with sampling and analysis can produce unreliable data. Another problem is that there is a lack of fundamental understanding of the mechanisms involved when mercury is removed from flue gas. It is clear that temperature is a factor because both electrostatic precipitators and wet sulfur dioxide scrubbers remove mercury more effectively at low temperature than at high temperature. This is not the result of homogeneous condensation of mercury vapor at equilibrium because the concentration of mercury in flue gas is in the mg/m^3 range, while the equilibrium concentration of mercury vapor is orders of magnitude higher. Many reports in the literature indicate that mercury retained in the system is found associated with the fly ash. Thus the nature of the fly ash

29

becomes an important factor. Variations in the fly ash between tests may play a roll in the observed different results.

Additional technologies used to modify the existing FGD systems have achieved some successes in mercury emission control (Niro, 1987), but achievable removals for these processes when applied to the more dilute mercury concentrations found in flue gases from coal-fired power plants are not yet known.

Chapter 3 Experimental Apparatus and Analytical Methods

The rate of mercury absorption was measured in the stirred cell reactor system shown in figure 3.1. Two identical reactors, one stainless steel and the other coated with Teflon, were tested for mercury absorption/desorption. As will be discussed in detail in chapter 5, results from permanganate experiments conducted in the old reactor necessitated the construction of the second Teflon coated stirred tank reactor.
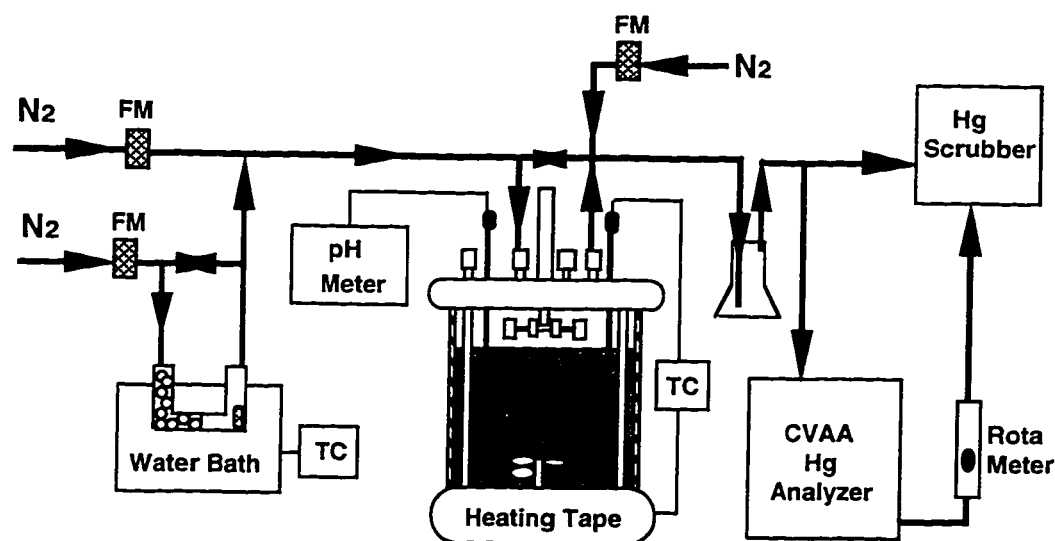
Figure 3.1 The stirred tank reactor systems for mercury absorption. Mercury permeation tube is inside the U-tube immersed in water bath. TC is temperature controller, FM is mass flow meter.

3.1 TEFLON COATED STIRRED TANK REACTOR

The purpose of the stirred tank reactor experiments was to simulate absorption of mercury across the gas-liquid interface of a droplet, a bubble or packing in a commercial absorber. The solution composition was varied in order to find the most efficient absorbent for mercury abatement under typical limestone slurry scrubbing conditions or for add-on commercial application to existing wet scrubber systems. The stirred tank reactor system was designed to provide a bulk gas phase with a known mercury concentration in contact with liquid solution. The area of gas-liquid contact at the interface is known by maintaining a flat, undisturbed surface.

Figure 3.2 gives the dimensions of the glass reactor. The cylindrical reactor had a 10 cm diameter and 16 cm height. The total volume of the reactor was 1.295 liters. The volume of solution used in each experiment was 1.06 liters. The gas-liquid contact area was 81 cm^2. The reactor vessel was a thick glass cylinder with Teflon coated 316 stainless steel plates sealed to the top and bottom by thick gasket clamps. Four $\frac{3}{8}$ inch wide, equally-spaced, Teflon-coated, 316 stainless steel baffles were welded to the bottom plate. The length of the baffles was long enough to extend to the main body of the gas phase. The bottom plate contained ports for liquid inlet and outlet. The top plate contained ports for the gas inlet and outlet, solution injection, Teflon coated thermocouple (Omega K type), Epoxy Body Gel-Filled pH probe (Accumet SN 5115079) and a glass U-tube pressure gage partially filled with water. Viton lip seals (JM Clipper Oil Seals) were used for both gas and liquid phase. The advantage of the Viton seal

was that it resisted acid or strong oxidizer corrosion. It also provided a reliable seal against leak compare to earlier spring seals. The Viton seals must be replaced regularly, depending on the frequency of the agitation and the degree of corrosion of the liquid.
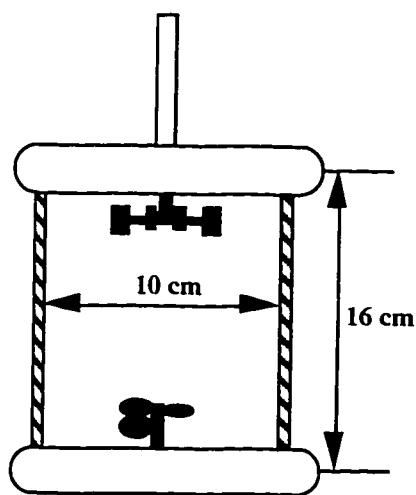
Figure 3.2   Dimensions of the gas-liquid contactor.

The gas inlet was at the near center of the top plate, directly above the gas agitator blade, to ensure that the inlet gas was properly mixed. The proper mix of gas was also ensured by four baffles extended from the liquid phase to the gas phase. The reactor was equipped with Teflon-coated gas phase and liquid phase agitators which were independently controlled. The dimensions of the agitators are given in figure 3.3. The gas agitator was a six-blade flat turbine with a diameter of 6.35 cm. The liquid phase was agitated by a three-blade marine type

agitator with a diameter of 5.08 cm. FisherBrand StedFast Stirrers (Model SL 1200) were used to drive gas and liquid phase agitators. Both agitator speeds were measured by a hand-held Ono Sokki HT-4100 digital tachometer, and for most of the experiments the agitation speed for both gas and liquid phases was between 500 and 700 rpm.

Gas Phase Agitator   **Liquid Phase Agitator**
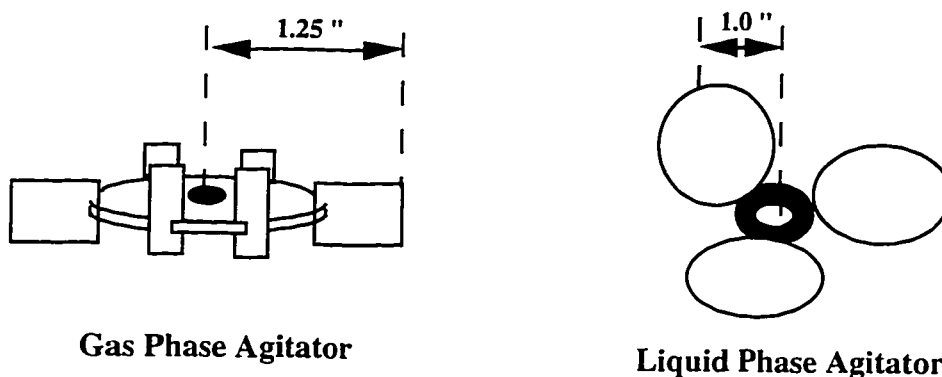
Figure 3.3   Agitator design and dimension.

Quarter inch Teflon tubing, fittings and valves were used for all connections before the mercury analyzer. Larger diameter flexible tubing, such as 1 inch Tygon tubing was used in the vent line to keep the reactor pressure low (near 1 atm). An empty 100 ml glass Erlenmeyer flask was connected after the reactor outlet and before the analyzer to capture any water vapor or liquid.

The mercury permeation tube was immersed in a water bath with temperature maintained by Lauda Immersion Circulator B. The experiments were

34

performed at both 25 and 55°C. The solution temperature was measured by an Omega K type Teflon coated thermal couple inserted into the reactor. An Omegalux FGH101-060 heating tape wrapped around the glass cylinder of the reactor was controlled by an Omega temperature controller which was connected to the thermal couple. Solution pH was continuously measured by an Accumet SN 5115079 Pencil-Thin Epoxy Body Gel-Filled pH probe inserted into the reactor and a Corning pH meter 125.

3.2   ELEMENTAL MERCURY SOURCE

Synthetic flue gas was prepared by mixing a known amount of elemental mercury vapor with nitrogen or air to produce a constant flow rate of mercury vapor to the reactor. Elemental mercury vapor was obtained from a commercially available mercury permeation tube (VICI Metronics) which emits steady trace amounts of mercury into a known dilution flow rate. By maintaining a reservoir of the liquid mercury at a constant temperature in the water bath, the mercury vapor pressure remains constant and provides the constant driving force for diffusion through the membrane wall. Actual rates of mercury diffusion can be obtained from manufacturer for a particular permeation tube. Two types of mercury permeation tubes were used in this study to provide different inlet mercury concentrations. The manufacturer calibrated permeation rate was used to determine the absolute amount of mercury in the gas stream.

The safety procedures in handling mercury can be found in appendix A. Specifications of the two mercury permeation tubes are listed in table 3.1.

Table 3.1   Specifications of the two permeation tubes used in the study.

	Tube 1	Tube 2
Type	H. E.	H. E. SR
Batch or I.D. Number	497-58697	497-65339
Tube Length (cm)	2	4
Part Number	137-030-0030-SR	137-040-0030-S56
Operating Temperature (°C)	70	90
Permeation Rate (ng/min)	167	811

The absolute mercury concentration was calculated by the following equation:

$$C = \frac{K_m P}{F} \qquad (3-1)$$

where:

C = mercury concentration (ppm by volume) (3-2)

P = permeation rate (ng/min) (3-3)

F = carrying gas flow rate (cc/min) (3-4)

K_m = 0.122, the molar constant (3-5)

The flow rate of all gas streams was maintained by Brooks mass flow controllers. The flow rate of the carrier gas (nitrogen) was kept less than 100 cc/min to ensure sufficient heat exchange between the permeation tube and water bath. The mixture of mercury and nitrogen entered the reactor through the gas inlet on the top of the plate, and mercury vapor was absorbed across an unbroken interface into a well-mixed solution. Nitrogen was added to dilute the gas before and after the reactor by a factor of ten, respectively. Nitrogen dilution into the reactor brought the total gas flow rate to 1 liter per minute. This ensures a fast absorption/desorption and adsorption/desorption equilibrium, which gave good, reproducible results. As will be discussed in more detail in chapter 8, lower gas

flow rate (200 cc/min) resulted in non-reproducible results. Nitrogen dilution after the reactor minimized the effect of water vapor on Hg analysis by cold vapor atomic absorption spectrophotometer.

3.3   GAS PHASE MERCURY ANALYSIS

Typically, the concentration of mercury is in the range of 0.0001 to 0.0006 ppm from Coal Fired Power Plant emissions and 0.01 to 0.1 ppm from Waste Incineration emissions (Hall, 1991). Since our mercury analyzer can only measure total elemental mercury concentration at the lowest level of 0.001 ppm, 0.01 to 0.1 ppm mercury was used in the gas inlet.

A Cold Vapor Atomic Absorption Spectrophotometer (LDC Analytical, model 3200) was used for gas phase elemental mercury analysis. At the unique absorbency at 253.7 nm of elemental mercury, this method can measure mercury concentration at a level as low as 0.001 ppm. However, due to the limitations of the voltage readout device, the lowest detectable concentration was 0.005 ppm in our analyzer. Gas after the reactor was continuously analyzed for mercury and recorded by the strip chart recorder (Soltec Model 1242). Based on experimental results discussed in chapter 4, the analyzer configuration and gas phase mercury analysis techniques used were as follows:

(1)   10 mV full scale output port

(2)   10 to 15 times nitrogen dilution of the reactor outlet gas

(3)   constant 150-200 cc/min flow into analyzer and monitored by rotameter after the analyzer

(4)   125 ml glass flask before the analyzer to catch condensed water

(5)   calibration conducted both before and after the experiment. The

calibration equation based on the above two calibrations assuming

linear analyzer drifting was used

3.4   LIQUID PHASE MERCURY ANALYSIS

It is desirable to know the concentration of mercury in all chemical forms

in the liquid phase, which also provides a mean for examining the accuracy of the

gas phase material balance. Whenever feasible, liquid samples were withdrawn

from the reactor at different stages of the absorption. Those samples are dumped

into impingers, reduced by $SnCl_2$-H_2SO_4 or $NaBH_4$ solution, collected on the

gold column and flushed out to elemental mercury analyzer (Hatch et al., 1968).

All liquid mercury analyses were conducted at Radian International, LLC in

Austin, TX.

3.5   TYPICAL GAS FLOW PATH AND EXPERIMENTAL OPERATION

In a typical experiment, the mercury analyzer was turned on at least two

hours before the experiment. Carrier gas nitrogen was passed through the

mercury permeation tube. The permeation tube was inside a glass U-tube and the

U-tube was immersed in a water bath. An inverted 2000 ml volumetric flask was

filled with distilled water to automatically replenish any evaporated water from

the constant temperature bath. This ensured a constant water bath depth and thus

constant heating area for the U-tube. Experiments with lower water bath depth

tended to give lower mercury concentration. When the water in the constant

temperature bath was refilled to the top, an increased mercury concentration was

38

recorded. Distilled water was used in the constant temperature bath to protect and extend the life of the instrument.

The gas with elemental mercury vapor was mixed downstream with pure nitrogen to bring total flow rate to 1 l/min. This gas stream was then fed into the reactor over the solution. The reactor outlet gas was diluted ten to fifteen times with nitrogen. The permanganate scrubbing solution was prepared from equal volume of 0.1 M potassium permanganate and 10 % sulfuric acid. The majority of the gas went through the permanganate scrubber before being vented to the hood. Only a small portion (150-200 cc/min) of the gas was passed through the mercury analyzer. The gas flow rate through the analyzer was continuously monitored by a rotameter after the analyzer to ensure a constant flow rate through the analyzer in the same experiment. Rotameter off-gas was passed through the permanganate scrubber before being vented to the hood.

3.6 MINOR DIFFERENCES IN EXPERIMENTAL CONDITIONS AND OPERATIONS

The experimental conditions described in section 3.5 were the optimized conditions derived from numerous try-and-error attempts. In the early stage of this research, slightly different experimental conditions were used. The total gas flow rate into the reactor was in the range of 100 to 200 cc/min. The flow rate of the diluting nitrogen was 1 to 2 l/min, significantly lower than that used later. A glass coil condenser immersed in ice bath was once used after the reactor to collect water. Experiments showed that the condensed water was actually trapped inside the condenser and was very difficult to get it out. As a result, reactor outlet mercury was still in contact with water inside the condenser. Finally, a 125 ml

39

glass Erlenmeyer flask was used to trap any condensed water. It was first used immersed in ice bath. Later the ice bath was eliminated. When running experiments at 25°C, there was no visible water collected in the trap. However, the water trap flask was an essential device when conducting experiments at 55°C. Visible water drops were collected in the flask. Without the water knock-out flask, those water drops would very likely plug the small tubes inside the mercury analyzer and stop the flow into the analyzer completely.

3.7   LIST OF INSTRUMENTS USED IN THE RESEARCH

Table 3.2 gives the instruments and their model or specifications used in this research.

Table 3.2   List of instruments used in the research.

Instrument	Model
Brooks Mass Flow Meter	9203HCO 37102, 9203HCO 37104 9205HCO 37101, 9310HCO 38404/2 9310HCO 38406/2, 8707HCO 33415
Brooks Mass Flow Controller	5878
Soltec Strip Chart Recorder	1242
Corning pH Meter	125
Lauda Constant Temperature Bath	Immersion Circulator B
Omegalux Heating Tape	FGH 101-060
Pencil-Thin Epoxy Body Gel-Filled pH probe	Accumet SN 5115079
JM Clipper Oil Seals (Viton lip seals)	0037-06362
FisherBrand StedFast Stirrers	SL 1200
Omega Temperature Controller	Rebuilt for K type Thermocouple
Soar Digital Multimeter	5030
Proportional Electric Temperature Controller	Versa-Therm 2156-4
Corning Hot Plate Stirrer	PC-351
Elemental Mercury Detector	mercuryMonitor™ 3200

Chapter 4 Calibration of the Apparatus

4.1   MERCURY ANALYZER CALIBRATION

A MercuryMonitor™ 3200 Elemental Mercury Detector from LDC Analytical was used for all gas phase mercury analysis. This analyzer is specially designed for application requiring the measurement of 253.7 nm ultraviolet light. The method used to determine the amount and/or concentration of elemental mercury present uses a photometric detector which measures the luminous intensity of monochromatic light that has passed through the sample and compares it with the luminous intensity of an equal light beam of fixed value such as a reference beam. Through the electronics of the instrument the result of the measurement is displayed as absorbance units.

4.1.1   Analyzer Output Choice

There are two different voltage outputs in the mercury analyzer, one is 1 volt per absorbance unit output and the other 10 mV full scale output. Both output ranges were tested for mercury detection sensitivity. Figures 4.1 and 4.2 give the results with an external digital voltmeter (Soar Model 5030). For approximately the same mercury concentration, using the 10 mV full scale output port gave a much bigger voltage response than that of 1 V per absorbance unit output port. This indicates that 10 mV full scale output port is more sensitive and flexible when large mercury concentration change occurs in one experiment when continuous mercury monitoring is necessary. We only used the 10 mV full scale output port for all our subsequent experiments.

41
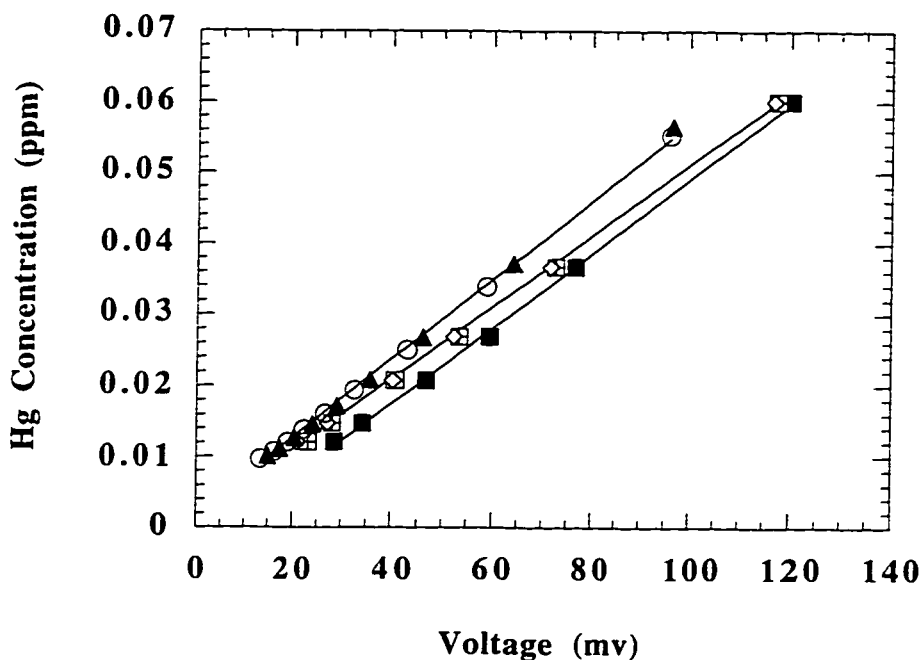
Figure 4.1   Calibration of mercury analyzer using 1 volt per absorbance unit output port. Analyzer absorbance units sensitivity was set at R. The gas flow rate was 200 cc/min.

4.1.2   Analyzer Drift and Linearity

The calibrated mercury concentration ranged from 0.005 ppm to 0.1 ppm. These calibration experiments were performed on different days with different combinations of gas synthesis systems. Not all the data points fell on the same line exactly, even when all other conditions were kept the same. This is probably due to the analyzer drift. Analyzer drift was further confirmed by calibrations conducted before and after the experiments when different readings were obtained

42

in later runs. From figures 4.1 and 4.2, it is obvious that linearity has been achieved over the possible range of the available permeation tubes. A minimum concentration of 0.005 ppm mercury was achieved. Lower mercury concentration could be measured as long as sufficient time was allowed for steady state to be reached and mercury loss (such as adsorption on tube wall) to be eliminated.
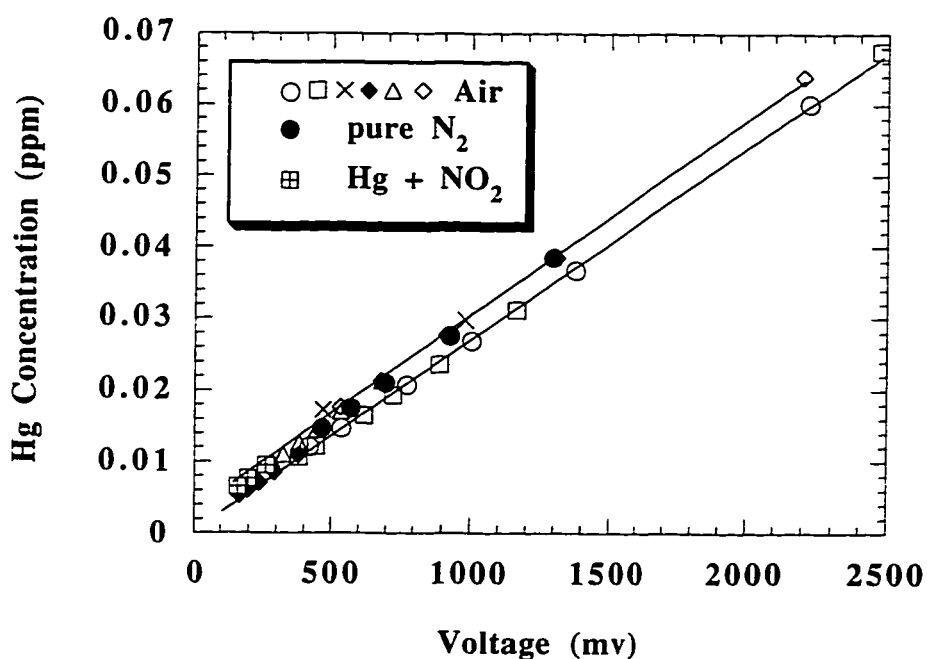
Figure 4.2   Calibration of mercury analyzer using 10 mV full scale output port. Analyzer absorbance units sensitivity was set at R. The gas flow rate was 200 cc/min. No drying tube was used when NO_2 was added to the gas phase.

4.1.3 Interferences for Mercury Analysis

Possible interferences for mercury detection were investigated. Since water vapor could easily condense inside the system tubes or on the cell wall inside the analyzer, a 125 ml water knock out flask was installed before the analyzer. This flask is especially needed when running experiments at 55°C. In the mean time, heavy diluting nitrogen (10 times of the reactor outlet gas at 25°C and 15 times at 55°C) was used to decrease the possible interferences of water vapor.

Instead of using nitrogen as carrier gas and air as diluting gas, only pure nitrogen was used. As shown in figure 4.2, results with nitrogen alone give an almost identical calibration line as that of those with air present. Therefore, air does not interfere with mercury detection.

Additional experiments with NO_2 and SO_2 mixed with mercury were conducted as well. Mercury concentration decreased steadily when the drying tube (contained $Mg(ClO_4)_2$) was used before the analyzer. When the drying tube was eliminated from the system, the calibration lines were the same as those of mercury with air or nitrogen. We concluded that NO_2 and SO_2 did not interfere with mercury analysis when the drying tube was eliminated. For consistency, the drying tube was not included in the apparatus for all subsequent experiments.

Later in February 1996, an experiment was designed to test the effect of SO_2 once again. The test was conducted under conditions similar to actual experiments (approximately the same relative humidity of the reactor outlet gas, heavy N_2 dilution after reactor outlet and water knock out flask). 97 ppb Hg in

N_2 bypassed the reactor first and a stable reading was obtained. While the gas stream still bypassed the reactor, 47 ppm SO_2 was added to the Hg-N_2 stream and the Hg-N_2 flow rate was adjusted to keep 97 ppb Hg in the mixture. The same steady state analyzer reading was obtained. After this, the SO_2 was shut off and the original Hg-N_2 stream was shifted to pass over distilled water inside the reactor. The same analyzer reading was obtained. Then 47 ppm SO_2 was added to the Hg-N_2 stream again and passed over distilled water. The same analyzer reading was obtained. After this, the same Hg-SO_2-N_2 stream was shifted to bypass the reactor. The same analyzer reading was obtained. Then the same Hg-SO_2-N_2 stream was shifted to pass over water again. The same analyzer reading was obtained. After this, SO_2 concentration was decreased to 23 ppm but Hg concentration was kept constant and the gas stream was passed over water, the same analyzer reading was obtained. The gas stream was bypassed again with and without SO_2. The same analyzer reading was obtained in both cases. When "same analyzer reading was obtained", it means that the reading was within less than 4% error.

The effect of gas flow rate into the analyzer was also investigated. A fixed concentration of mercury vapor was fed into the analyzer and the steady state absorbance units and voltage were recorded. The flow rate of the mercury vapor was changed and different steady state absorbance units and voltage were recorded. The results are shown in figure 4.3. The mercury analyzer reading was proportional to the flow rate of the mercury vapor being fed through the analyzer. When flow rate was increased by a factor of 4.2, both the absorbance units and the voltage response increased by a factor of 1.1. In order to monitor the flow rate

and to keep a constant flow rate into the analyzer in the same experiment, a rotameter was connected to the outlet of the analyzer. The flow rate into the mercury analyzer was usually kept at 150-200 cc/min.
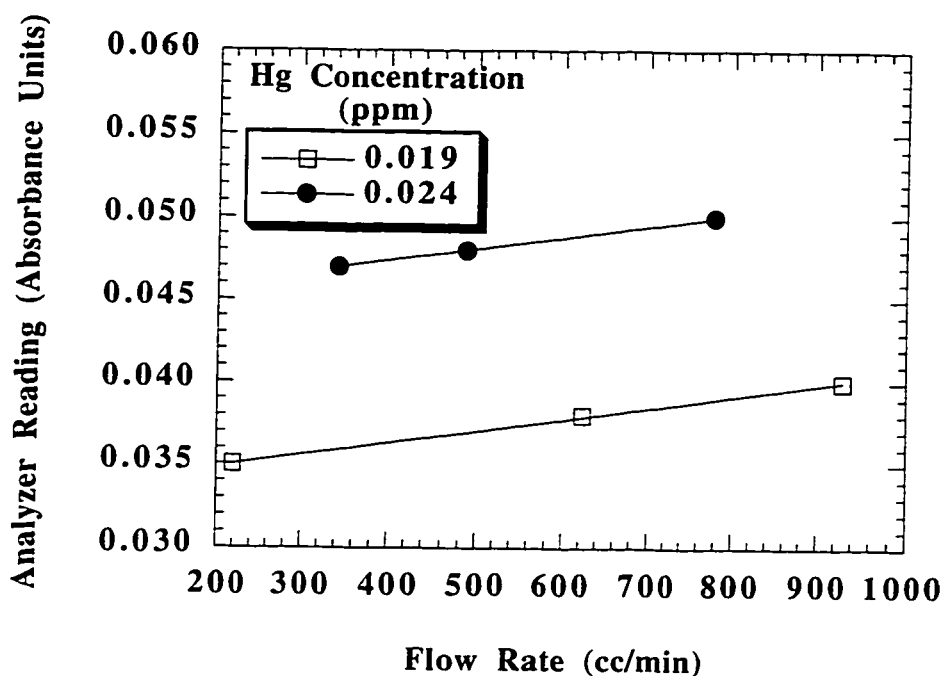
Figure 4.3   The dependence of mercury analyzer reading on gas flow rate passed through the analyzer.

4.1.4   Summary

On the basis of above experimental results, the 10 mV full scale output port was chosen to be the analyzer output. To account for the effect of analyzer drifting, calibration was conducted both before and after the experiments. The calibration equation obtained from the above two calibration results assuming a

46

linear analyzer drift was used in data analyses. To minimize the interferences of water vapor, large nitrogen dilution (10 to 15 times of the reactor outlet gas flow rate) and a water knock out flask were necessary to ensure reliable results.

4.2 LIQUID FILM MASS TRANSFER COEFFICIENT

Mass transfer coefficients were measured in the stainless steel stirred tank reactor by McGuire (1990) using sulfur dioxide. Due to the unique characteristics of mercury, it was necessary to recalibrate the same reactor with mercury. The following calibration was conducted in the stainless steel reactor, not the new Teflon coated reactor. However, the same correlation was used for experiments conducted in the Teflon coated reactor later.

4.2.1 Mercury Desorption from Water without Reducing Agent at 25°C

The objective of this experiment was to measure the liquid film mass transfer coefficient, $k^{\circ}_{l, Hg}$, by desorbing elemental mercury from water. Liquid mercury was put into a beaker with distilled water, stirred for 48 hours while being exposed to the ambient air. The clear mercury solution was then decanted into the stirred tank reactor. Nitrogen or air was flowed above this solution to desorb dissolved elemental mercury. If all the dissolved mercury was in the elemental form and the partial pressure of the desorbed mercury, $P_{Hg, out}$, was small so that it could be neglected, the slope of $\ln(C_{Hg}/C_{Hg, initial})$ versus time should give the liquid film mass transfer coefficient, $k^{\circ}_{l, Hg}$. Here C_{Hg} is the concentration of mercury in liquid phase at time t and $C_{Hg, initial}$ is the initial liquid phase mercury concentration.

Figure 4.4 gives the results of two mercury desorption experiments. 1.1 l/min air was used in one experiment while 0.2 l/min nitrogen was used in the other. The gas and liquid agitation speeds were approximately the same in these two experiments. The initial mercury concentration in the liquid phase $C_{Hg, initial}$ was 1×10^{-4} M by flame atomic absorption spectrophotometer analysis. Since the solubility of liquid mercury in water is only 3.05×10^{-7} M without oxygen, there must be some oxidized forms of mercury present in the liquid phase. This was consistent with the fact that mercury solution was prepared in the presence of air. The measured initial mercury concentration $C_{Hg, initial}$ was also close to the reported liquid mercury solubility data with the presence of oxygen.

Using the modified k°_l value from SO_2 data, the range of mercury flux, liquid phase driving force and total mercury in liquid phase can be obtained. The results are listed in table 4.1. The high end of the liquid phase driving force in one of the experiments (0.9 µM) was two times larger than the solubility limit of liquid mercury at 25°C (0.3 µM). This raised the possibility that dissolved oxidized mercury species were reduced to elemental mercury in the mass transfer boundary layer.

Table 4.1   Mercury desorption from distilled water without the presence of reducing agent at 25°C.

gas flow rate $(\frac{l}{min})$	n_g (rpm)	n_l (rpm)	N_{Hg} $(\frac{mole}{s\text{-}m^2}) \times 10^9$	liquid phase driving force (M) $\times 10^7$	total Hg in liquid phase (M) $\times 10^4$
air 1.1	155	284	high 12.1 low 6.2	high 8.9 low 4.6	1.0 1.0
N_2 0.2	117	250	high 3.6 low 2.9	high 2.9 low 2.3	- -

* The solubility of liquid mercury at 25°C in water without oxygen is 3.05×10^{-7} M

48
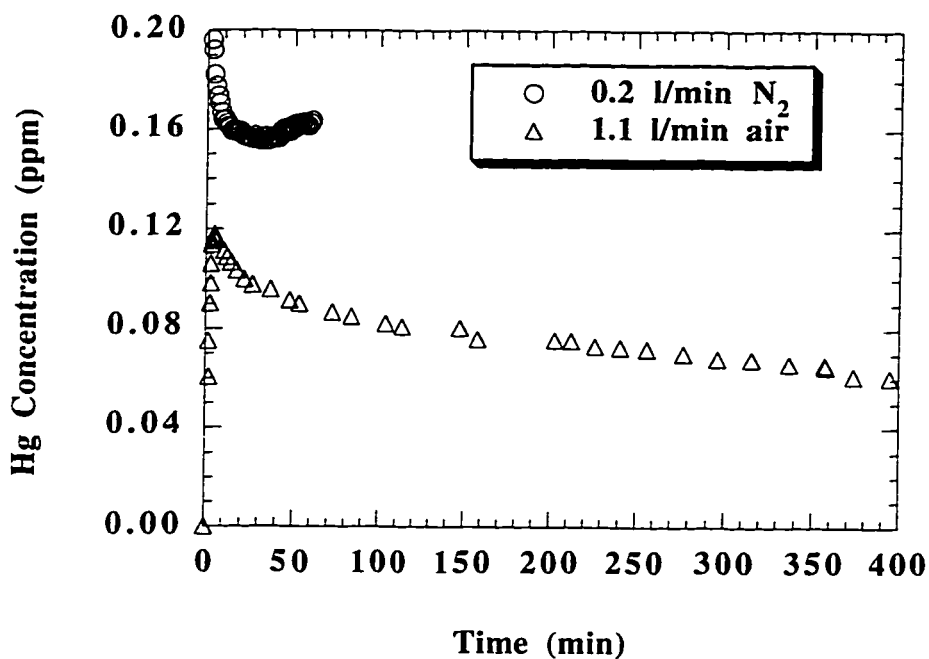
Figure 4.4   Mercury desorption from distilled water at 25°C   Either nitrogen or air was used as stripping gas. Gas and liquid phase agitation speeds were 136 and 267 rpm, respectively.

In order to ensure that only elemental mercury is present in the solution, mercury desorption from a reducing environment is necessary. In addition, pure nitrogen should be used as the stripping gas rather than air to further reduce the possibility of oxidation. A large stripping gas flow rate, such as 1 l/min, should be used to obtain a large liquid phase driving force and a large mercury flux.

49

4.2.2 Mercury Desorption from Water in the Presence of Reducing Agent at 25°C

4.2.2.1   Theoretical Basis

The mercury desorption method was improved by adding a small amount of $HgCl_2$ to a $SnCl_2$-H_2SO_4 reducing solution. The produced elemental mercury did not exceed its solubility limit. This ensures that all the mercury in the liquid phase exists in its elemental form. The liquid phase mass balance gives:

$$\frac{V \, dC_{Hg}}{dt} = -k^{\circ}{}_{l, \, Hg} \, A \, (C_{Hg} - \frac{P_{Hg,out}}{H_{Hg}}) \qquad (4\text{-}1)$$

Assuming $P_{Hg, \, out}$ is negligible compare to C_{Hg}, this leads to:

$$\frac{dC_{Hg}}{C_{Hg}} = -\frac{k^{\circ}{}_{l, \, Hg} \, A}{V} \, dt \qquad (4\text{-}2)$$

Integration of the above differential equation results in:

$$C_{Hg} = C_{Hg, \, initial} \, \exp(-\frac{k^{\circ}{}_{l, \, Hg} \, A}{V} \, t) \qquad (4\text{-}3)$$

From the gas phase mass balance:

$$G \, (P_{Hg, \, out} - P_{Hg, \, in}) = RT \, k^{\circ}{}_{l, \, Hg} \, A \, (C_{Hg} - \frac{P_{Hg, \, out}}{H_{Hg}}) \qquad (4\text{-}4)$$

Assume $C_{Hg} \gg \frac{P_{Hg, \, out}}{H_{Hg}}$ and the stripping nitrogen has no mercury in it so that $P_{Hg, \, in} = 0$. The Combination of liquid and gas phase mass balance gives:

$$\ln P_{Hg, \, out} = \ln(\frac{RT \, C_{initial} \, k^{\circ}{}_{l, \, Hg} \, A}{G}) - \frac{k^{\circ}{}_{l, \, Hg} \, A}{V} \, t \qquad (4\text{-}5)$$

From the plot of $\ln P_{Hg, \, out}$ versus time, the liquid film mass transfer coefficient $k^{\circ}{}_{l, \, Hg}$ can be obtained either from the slope or the intercept.

4.2.2.2   Experimental Procedure

Elemental mercury was produced by injecting a low concentration of $HgCl_2$ into a strong reducing solution. The recommended reducing solution was 1% $SnCl_2$, 10% H_2SO_4 and 1% NaCl. The resulted reducing solution is a turbid,

skim milk like mixture. Initial runs with this turbid solution did not give good results and k°_l values obtained from these experiments were lower than those from clear solution experiments. This is not surprising since mercury might adsorb on the surface of suspended solids in the solution and the adsorption/desorption complicated the process. Clear reducing solution was obtained by filtering the solution using cellulose acetate membrane filter (0.2 μm pore size, Micro Filtration Systems).

In a typical experiment, 10^{-7} M mercuric chloride was injected into fresh prepared reducing solution using a septum and a long needle well below the surface of the solution inside the reactor. The purpose of this procedure was to keep an undisturbed process during injection and prevent mercury loss at the time of $HgCl_2$ injection. Before and during the addition of $HgCl_2$, pure nitrogen was continuously passed over the liquid phase and the liquid phase agitator was set at a very low speed. This should minimize the accumulation of reduced elemental mercury in the gas-liquid interface. After $HgCl_2$ injection, the gas and liquid phase agitation speed were immediately adjusted to desired values. This moment was time zero. The gas phase outlet mercury concentration was then recorded continuously as the experiment proceeded.

4.2.2.3 Results and Discussion

Figure 4.5 gives the results of the mercury desorption experiments. The slope of each experiment was obtained from the linear part of the data, usually those after the initial mercury accumulation periods. The resulting k°_l values from the slope and the material balance are given in table 4.2. The total amount

51

of Hg desorbed was estimated by integrating the gas outlet concentration over time. As shown in table 4.2, the recovery of Hg was always less than 100% and varied from 7 to 80%.
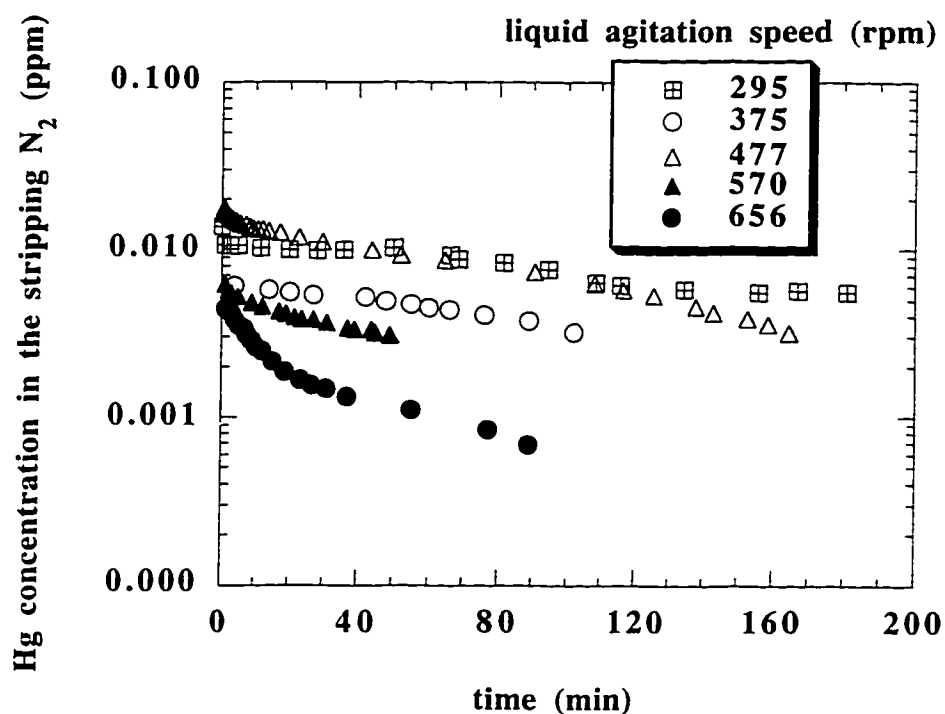
Figure 4.5   Hg desorption from water when 10^{-7} M $HgCl_2$ was injected into clear 0.05 M $SnCl_2$-1 M H_2SO_4-0.2 M NaCl at 25°C. Stripping N_2 flow rate was 1 l/min.

Mercury desorption gave the following $k^o_{l, Hg}$ - n_l correlation:

$$k^o_{l, Hg} = 2.42 \times 10^{-7} \, (\, n_l \,)^{0.73} \text{ m/sec} \qquad (4\text{-}6)$$

Table 4.2   Hg desorption from water at 25°C when 10^{-7} M $HgCl_2$ was injected into filtered 1% $SnCl_2$-10% H_2SO_4-1% NaCl solution. Stripping N_2 flow rate was 1 l/min.

T (°C)	n_l (rpm)	length of experiment (min)	$k°_{l, Hg}$ from slope $(\frac{m}{s})$ x 10^5	Hg desorbed* (%)
24	295	181	1.64	80
26	375	102	1.74	37
28	477	165	1.96	66
26	570	49	2.51	18
26	656	89	2.90	7

* Integration only accounted for the length of the experiments.

4.2.3 CO_2 Desorption from Water at 25°C

The CO_2 desorption method was developed to check the reliability of the previously described mercury desorption results. The advantage of using CO_2 is that it is unlikely to adsorb on the solid metal surfaces, thus eliminating interferences that might be significant in mercury desorption measurements.

The theoretical basis is essentially the same as that for mercury desorption. The $k°_l$ values were obtained from the plot of $lnP_{CO_2, out}$ versus time, where the following equation applies:

$$lnP_{CO_2, out} = ln \left(\frac{RT \, C_{initial} \, k°_l \, A}{G}\right) - \frac{k°_l A}{V} t \qquad (4-7)$$

Aqueous CO_2 was produced by injecting sodium carbonate solution into 10% sulfuric acid. A septum and a long needle well below the liquid surface were used to inject sodium carbonate. The initial injected 0.03 mM Na_2CO_3 was too small to cause significant CO_2 production. The highest CO_2 concentration produced was around 20 ppm, which was in the noise range of the CO_2 analyzer. The initial added Na_2CO_3 was then increased to 6.5 mM. This concentration was below the solubility limit of CO_2 at 1 atm.

53

By examining the raw data of two experiments with 6.5 mM Na_2CO_3 injection, we found that the calibration of the CO_2 analyzer was not accurate due to the interference of water vapor. A wet calibration method was used instead. This was accomplished by feeding CO_2 into the reactor filled with 10% sulfuric acid to ensure the same amount of moisture contained in the outlet mercury as that of the actual desorption experiment. During the wet CO_2 analyzer calibration, the reactor outlet CO_2 concentration dropped immediately but increased gradually until a stable reading. This was expected since CO_2 dissolved in water initially and gradually saturated the water. A steady state analyzer reading was obtained when CO_2 absorption and desorption reached equilibrium.

A typical experiment started with the wet CO_2 analyzer calibration. Then 6.5 mM Na_2CO_3 was injected in 10% sulfuric acid and the outlet CO_2 concentration was recorded continuously. Figure 4.6 gives the results of these experiments. A straight line can be easily identified in each plot. The k°_l values obtained from the slope and the material balance are tabulated in table 4.3. Nearly 100% recovery of CO_2 was obtained. This contrasts with only 7 to 80% recovery in mercury desorption. The k°_l values obtained from CO_2 desorption were converted to k°_l of mercury by using

$$k^\circ_{l, Hg} = k^\circ_{l, CO2} \sqrt{\frac{D_{Hg.H2O}}{D_{CO2.H2O}}} \qquad (4\text{-}8)$$

and the result is:

$$k^\circ_{l, Hg} = 1.93 \times 10^{-7} \, (n_l)^{0.72} \qquad (4\text{-}9)$$

54

CO$_2$ concentration in stripping N$_2$ (ppm)

10^4

liquid agitation speed (rpm)

■	291
⊞	429
●	506
○	641
△	698

10^3

10^2

0   50   100   150   200   250

time (min)
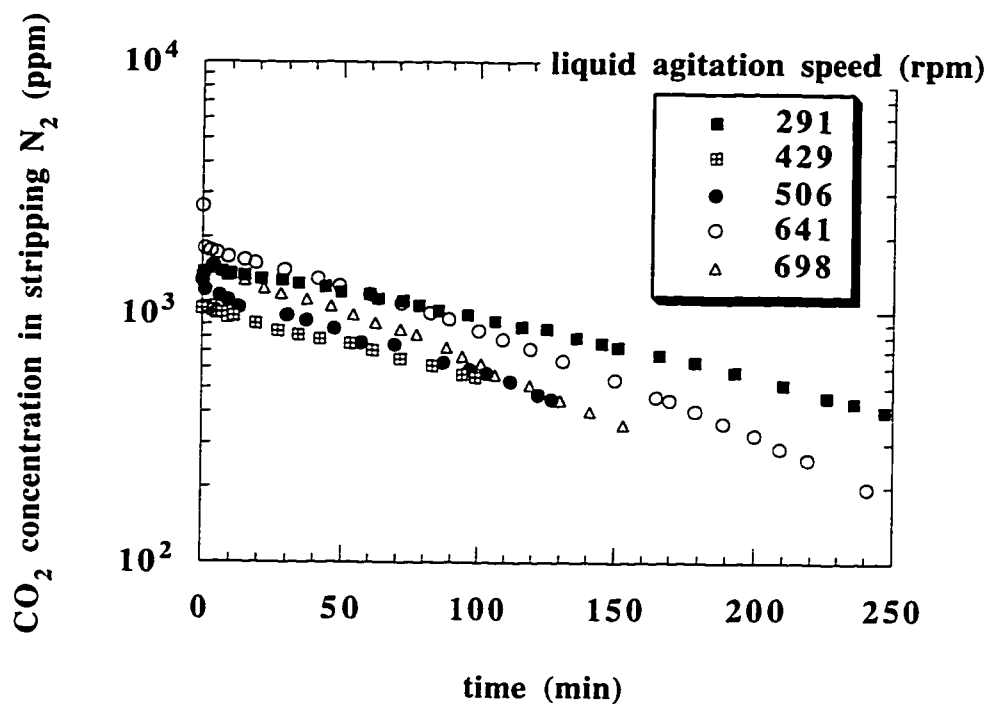
Figure 4.6 CO$_2$ desorption from water at 22-24°C when 6.5 mM Na$_2$CO$_3$ was injected into 10% sulfuric acid. Stripping N$_2$ flow rate was 1 l/min.

Table 4.3 Calibration of the liquid film mass transfer coefficient by CO$_2$ desorption from water when initially injecting 6.5 mM Na$_2$CO$_3$ into 10% sulfuric acid.

T (°C)	slope	nl (rpm)	$k^°_l$ from slope $(\frac{m}{s}) \times 10^5$	desorbed (%)
23	0.00529	291	1.198	121[*]
24	0.00655	429	1.483	101
22	0.00745	506	1.685	101
23	0.00912	641	2.065	117[*]
24	0.00949	698	2.147	100

[*] Raw data based on dry bypass analyzer calibration were adjusted by the factor obtained from later wet analyzer calibration. This might also explain greater than 100% recovery.

55

4.2.4 Comparison of $k^{\circ}_{l, Hg}$ Obtained from Different Methods

The k°_{l} values obtained from SO_2 absorption (McGuire, 1990) were converted to k°_{l} of mercury by using

$$k^{\circ}_{l, Hg} = k^{\circ}_{l, SO2} \sqrt{\frac{D_{Hg.H2O}}{D_{SO2.H2O}}} \qquad (4\text{-}10)$$

The correlations of the liquid phase mass transfer coefficient of mercury, $k^{\circ}_{l, Hg}$ with liquid phase agitation speed, n_l are listed below:

$$k^{\circ}_{l, Hg} = 1.93 \times 10^{-7} \, (\, n_l \,)^{0.72} \text{ m/sec} \quad \text{(from modified } CO_2 \text{ desorption)} \quad (4\text{-}11)$$

$$k^{\circ}_{l, Hg} = 2.42 \times 10^{-7} \, (\, n_l \,)^{0.73} \text{ m/sec} \quad \text{(from the slope of Hg desorption)} \quad (4\text{-}12)$$

$$k^{\circ}_{l, Hg} = 2.67 \times 10^{-7} \, (\, n_l \,)^{0.74} \text{ m/sec} \quad \text{(from modified } SO_2 \text{ absorption)} \quad (4\text{-}13)$$

Figure 4.7 gives the correlation of $k^{\circ}_{l, Hg}$ with n_l from these three different methods. The slopes of these three lines are approximately the same. However, mercury desorption gave k°_{l} values about 10% lower than those predicted from SO_2 data and 20 % higher than those from CO_2 desorption. From later permanganate results shown in chapter 5, it was clear that the stainless steel reactor was not appropriate for mercury experiments. The discrepancies might have been caused by the low reliability of the stainless steel reactor. Other possible explanations might include the errors associated with the estimated mercury diffusion coefficient in water, or the reactor characteristics might have been changed since those SO_2 measurements were made.

In all following chapters, we used k°_{l} values from mercury desorption, that is:

$$k^{\circ}_{l, Hg} = 2.42 \times 10^{-7} \, (\, n_l \,)^{0.73} \text{ m/sec} \qquad (4\text{-}14)$$

4.2.5 Liquid Film Mass Transfer Coefficient of mercury, $k^\circ_{l, Hg}$ at 55°C

The same factor was used as that measured by McGuire to modify $k^\circ_{l, Hg}$ at 25°C to obtain $k^\circ_{l, Hg}$ at 55°C. The correlation is:

$$k^\circ_{l, Hg} = 7.64 \times 10^{-7} \, (n_l)^{0.64} \text{ m/sec} \quad (55°C) \tag{4-15}$$
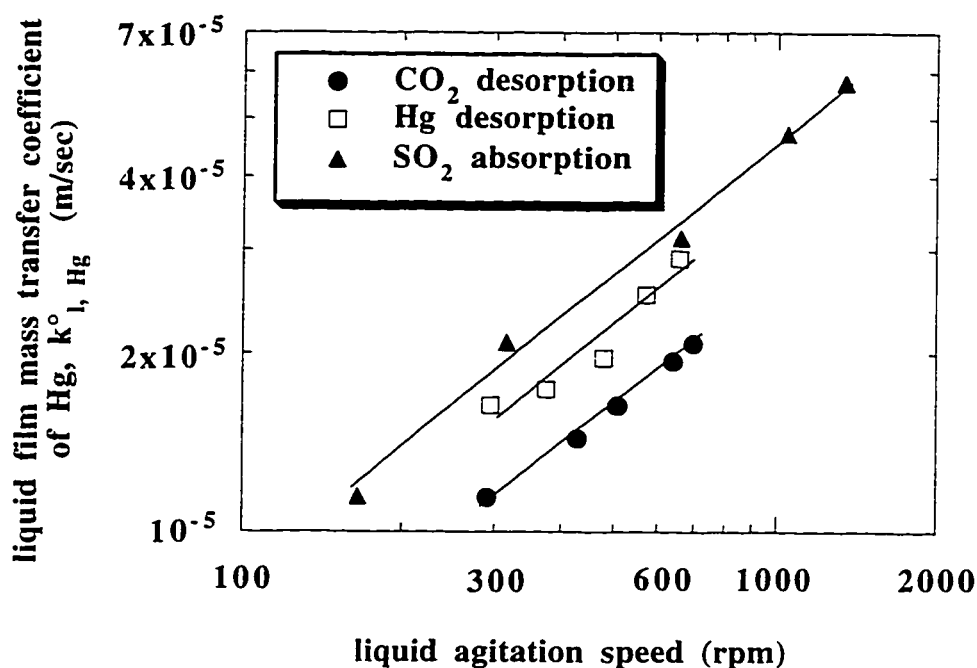
Figure 4.7 Comparison of liquid film mass transfer coefficient of mercury obtained from different methods at 25°C.

4.3 GAS FILM MASS TRANSFER COEFFICIENT CALIBRATION

Mercury absorption into concentrated permanganate was used to calibrate the gas film mass transfer coefficient of mercury, $k_{g, Hg}$. Detailed description can be found in chapter 5.

Chapter 5 Mercury Absorption in Aqueous Permanganate

Aqueous acidic permanganate is known to be an effective solvent for elemental Hg vapor (Monkman et al., 1956; Hara, 1975). EPA method 29 specifies permanganate as the scrubbing solution for determination of elemental mercury in gas streams (Environmental Protection Agency, 1992). Permanganate has been used to collect mercury in flue gas field sampling procedures (Shendrikar et al., 1984). Even though permanganate is an expensive reagent, it is effective at low concentration for mercury removal, so it may be commercially useful for air pollution control or removal of mercury from other gases. No previous work was found giving the rate of reaction of permanganate with mercury. Therefore, the objective of this study was to quantify the kinetics in a well-characterized gas liquid contactor.

5.1   EXPERIMENTAL METHOD

All experiments were performed in the well-characterized stirred cell reactor described in Chapter 3. The stainless steel reactor was used initially. Figure 5.1 gives the results of mercury absorption in $KMnO_4$ in the stainless steel reactor. Most of the permanganate decomposed within three hours when initial injected permanganate did not exceed 3 mM. Bubbles were observed rising from the surface of the stainless steel baffles inside the reactor. It was later speculated that permanganate oxidized some of the iron in the reactor parts. The produced Mn^{2+} expedited permanganate decomposition. Data analysis of the figure 5.1 results gave a complicated second order dependence on mercury with scattered

data. It was under these circumstances that we decided to build a new Teflon coated reactor. With the new Teflon coated reactor, permanganate did not degrade under the same conditions as those of the old reactor. Data analysis gave reproducible, reasonable kinetics, as will be shown in detail later in this chapter.
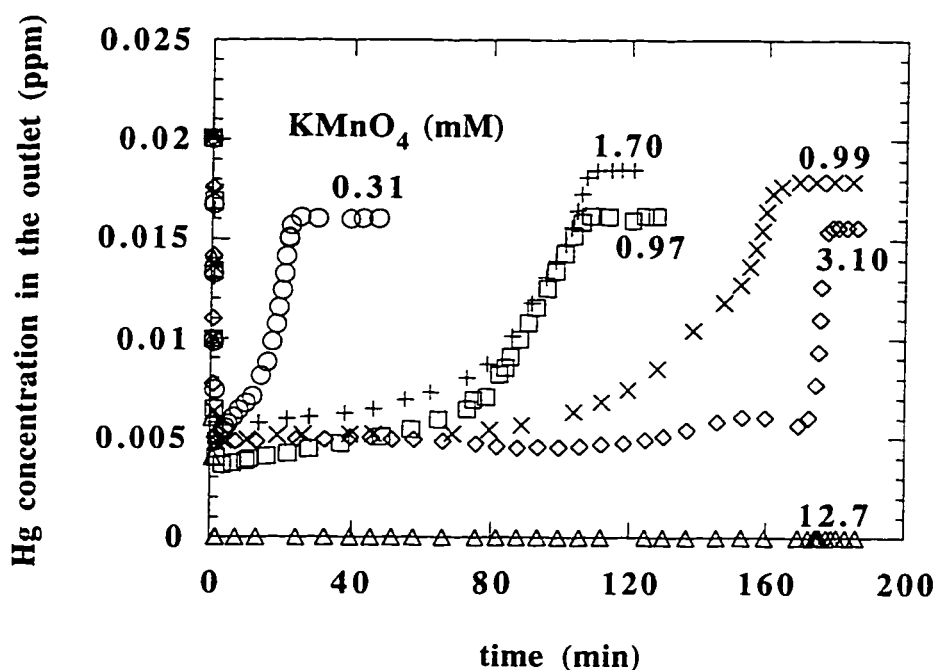
Figure 5.1   Hg absorption in $KMnO_4$-1.8M H_2SO_4 at 25°C in the old stainless steel reactor. The inlet mercury was 0.02 ppm. Total Hg-N_2 flow rate was 1 l/min.

The liquid film mass transfer coefficient, $k°_{l, Hg}$, was determined by mercury and CO_2 desorption, as described in detail in chapter 4. The gas film mass transfer coefficient, $k_{g, Hg}$ was determined by mercury absorption into concentrated permanganate solution.

59

A stock solution of 0.1 M potassium permanganate was prepared from $KMnO_4$ solid (EM Science), standardized by $Na_2C_2O_4$ (Baker Analyzed Reagent) titration and stored in a brown bottle. Before titration, several drops of concentrated sulfuric acid was added to the permanganate sample to bring the solution acidity to 0.5-1 M and the solution was heated to 75-85°C. The sample was immediately titrated with 0.6-40 mM sodium oxalate depending on the initial concentration of $KMnO_4$. Usually $KMnO_4$ served as a self indicator. If the sample solution was too dilute, several drops of 0.5 mM ferroin (indicator) were added to the solution. At the endpoint the solution color turned from pale blue to red (Harris, 1987).

1.8 M sulfuric acid solution was prepared by weighing a certain amount of concentrated sulfuric acid (EM Science) and diluted with distilled water to a desired volume.

In a typical experiment, 1.06 liters of 1.8 M sulfuric acid was put into the reactor while elemental mercury in nitrogen was bypassed the reactor. After the mercury analyzer gave a stable reading, the mercury stream was passed over 1.8 M sulfuric acid inside the reactor. This was the wet analyzer calibration. Again after the analyzer gave a stable reading, known amounts of the above permanganate solution or freshly prepared diluted permanganate solutions were sequentially injected into 1.8 M sulfuric acid using a syringe with a long needle. The outlet elemental mercury concentration was analyzed continuously and recorded by the strip chart recorder (Soltec Model 1242).

The rate of mercury absorption was calculated from the gas phase material balance. A four-point calibration was performed before and after each run to

account for the effect of base line drifting of the mercury analyzer. MnO_4^- addition to the liquid phase was determined by weighing the syringe before and after the injection.

5.2 MASS TRANSFER WITH SIMULTANEOUS CHEMICAL REACTION

The rate of reaction between elemental mercury vapor and $KMnO_4$ is given by the mechanism:

$$Hg + MnO_4^- \rightarrow \text{Products} \tag{5-1}$$

$$\text{reaction rate} = k_2 \, [Hg] \, [MnO_4^-] \tag{5-2}$$

Using surface renewal theory (Danckwerts, 1970), the flux of mercury, N_{Hg}, should be given by:

$$N_{Hg} = \frac{P_{Hgi}}{H_{Hg}} \sqrt{k_2 \, [MnO_4^-]_i \, D_{Hg\text{-}H2O}} \tag{5-3}$$

where:

$$P_{Hgi} = P_{Hgb} - \frac{N_{Hg}}{k_g} \quad \text{(significant)} \tag{5-4}$$

$$[MnO_4^-]_i = [MnO_4^-]_b - \frac{N_{Hg}}{k^o_{l.MnO4^-}} \quad \text{(negligible)} \tag{5-5}$$

The value of $k^o_{l, Hg}$ obtained from mercury desorption experiments in an identical reactor (old stainless steel reactor) was modified to give $k^o_{l, MnO4^-}$:

$$k^o_{l, MnO4^-} = k^o_{l, Hg} \sqrt{\frac{D_{MnO4^-\text{-}H2O}}{D_{Hg\text{-}H2O}}} \tag{5-6}$$

The value of $k_{g, Hg}$ is provided in detail in the next section. All physical constants used in the calculation are tabulated in table 5.1.

Table 5.1   Physical properties of Hg and MnO_4^-.

	25°C	55°C
$D_{Hg-H_2O}{}^a$ (cm^{2}sec^{-1})	1.19×10^{-5}	2.21×10^{-5}
$D_{MnO_4^- - H_2O}{}^b$ (cm^{2}sec^{-1})	1.63×10^{-5}	3.18×10^{-5}
$H_{Hg}{}^c$ (atm M^{-1})	8.91	35.64
$k_{g.Hg}$ (mole sec^{-1} atm^{-1} m^{-2})	$0.0344\ (n_g)^{0.38}$	$0.0344\ (n_g)^{0.38}$
$k^\circ_{l,\ Hg}$ (m sec^{-1})	$2.42 \times 10^{-7}\ (n_l)^{0.73}$	$7.64 \times 10^{-7}\ (n_l)^{0.64}$
$k^\circ_{l,\ MnO_4^-}$ (m sec^{-1})	$2.83 \times 10^{-7}\ (n_l)^{0.73}$	$9.15 \times 10^{-7}\ (n_l)^{0.64}$

[a] estimated using Sitaraman et al.'s eqn. (Sitaraman et al., 1963) (refer to appendix B)
[b] obtained from Lide, (1994   [c] obtained from Clever et al. (1985)

5.3   RESULTS AND DISCUSSION

Figure 5.2 gives the experimental results for mercury absorption in permanganate. At 2.3 mM $KMnO_4$, the mercury removal is practically the same as with 0.6 mM $KMnO_4$. This indicates that the absorption of mercury into 2.3 mM $KMnO_4$ is gas phase controlled. This leads to the measurement of the gas film mass transfer coefficient. 3 mM $KMnO_4$ was injected into 1.8 M sulfuric acid with a fixed gas and liquid phase agitation speed. Mercury absorption was observed immediately. After steady state absorption was achieved, the gas agitation speed was increased and a different mercury absorption rate was observed. This process was repeated several times. k_g can be calculated from:

$$k_g = \frac{N_{Hg}}{P_{Hg.\ out}} \qquad (5\text{-}7)$$

The results are given in table 5.2 and figure 5.3. The obtained gas phase mass transfer coefficient of mercury in this reactor (Teflon coated) is:

$$k_{g.\ Hg}\ A = 2.784 \times 10^{-4}\ (n_g)^{0.38} \qquad (5\text{-}8)$$

These $k_{g, Hg}$ A values are smaller than those measured by McGuire with SO_2 absorption into NaOH solution in an identical reactor (old stainless steel reactor) (McGuire, 1990), as shown in table 5.2 and figure 5.3. One explanation could be unknown differences between the current Teflon-coated reactor and the earlier stainless steel reactor. McGuire showed that k_gA is independent of temperature from 25 to 55°C. We used the same $k_{g, Hg}$ A correlation for both 25 and 55°C.
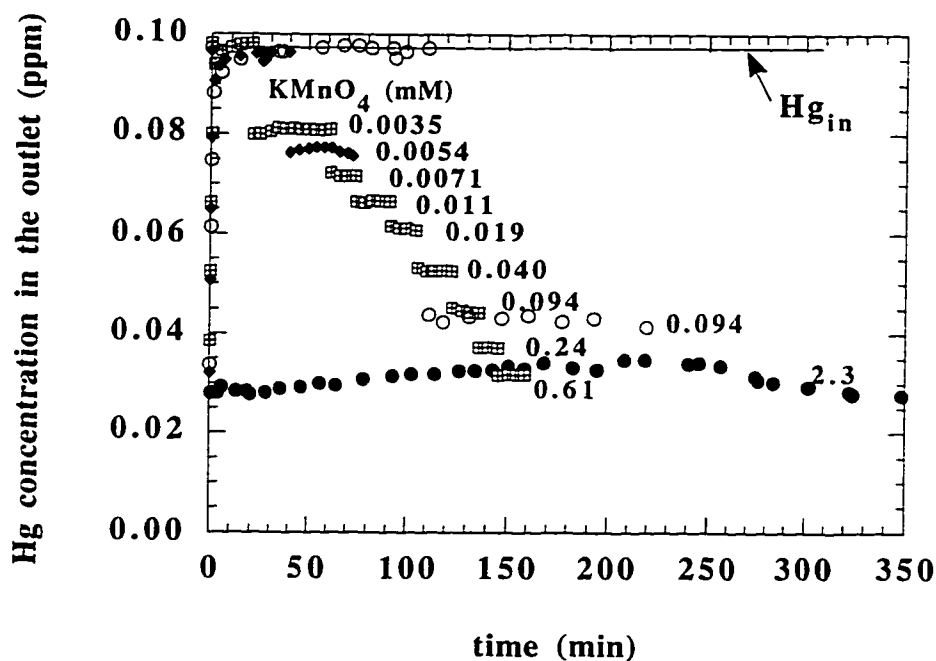
Figure 5.2   Effect of $KMnO_4$ on mercury removal during mercury absorption in $KMnO_4$-1.8M H_2SO_4 solution at 25°C. The inlet mercury was 0.097 ppm, total $Hg-N_2$ flow rate was 1 l/min.

63

Table 5.2 Calibration of gas film mass transfer coefficient by mercury absorption in 3 mM $KMnO_4$-1.8 M H_2SO_4 solution at 25°C. Hg_{in} was 9.9×10^{-8} atm and total Hg-N_2 flow rate was 1 l/min.

$P_{Hgb} \times 10^8$ (atm)	n_g (rpm)	$k_g A \times 10^3$ (mole sec^{-1} atm^{-1})	
		this work	McGuire*
2.63	164.5	1.91	2.39
2.43	208.5	2.13	2.87
2.26	286.5	2.37	3.65
2.10	344	2.58	4.19
1.98	415	2.76	4.83
1.82	540	3.07	5.91
1.68	708	3.39	7.25
1.64	776	3.50	7.78
1.57	925	3.68	8.89

* The values of $k_g A_{.Hg}$ were obtained from the values of $k_g A_{.SO2}$ measured by McGuire (1990), corrected using $k_g A_{.Hg} = k_g A_{.SO2} \sqrt{\dfrac{D_{Hg\text{-}N2}}{D_{SO2\text{-}N2}}}$, where $D_{Hg\text{-}N2} = 0.126$ cm^{2}sec^{-1} (Nakayama, 1968) and $D_{SO2\text{-}N2} = 0.130$ cm^{2}sec^{-1} (Marrero and Mason, 1972) at 25°C.

Gas phase control can be further illustrated in figure 5.4. With 3.7 mM $KMnO_4$, which was considered gas phase controlled, changes in gas agitation speed resulted in dramatic changes in mercury absorption rate. On the other hand, with 0.035 mM $KMnO_4$, variation of the gas or liquid agitation speed did not cause a significant change in absorption rate. At 0.035 mM $KMnO_4$, absorption was controlled by fast reaction near the gas-liquid interface and not by gas film diffusion.

Table 5.3 gives the results of mercury absorption into different concentrations of $KMnO_4$. The detailed results can be found in appendix C. It is obvious that mercury removal is responsive to the amount of MnO_4^- present in the solution. Figure 5.5 gives the dependence of normalized flux, $\dfrac{N_{Hg}}{P_{Hgi}}$, on the interfacial permanganate concentration $[MnO_4^-]_i$. These results are consistent with a reaction between Hg and MnO_4^- that is first order in MnO_4^-. For both 0.02

and 0.1 ppm inlet mercury, all data were fit with one line, as shown in figure 5.5. This indicates that the reaction is first order in Hg. The average value of the second order rate constant, k_2, is $(1.6 \pm 0.2) \times 10^7$ $M^{-1}s^{-1}$ at 25°C and (12.6 ± 5.3) $\times 10^7$ $M^{-1}s^{-1}$ at 55°C at a 95% confidence level. Figure 5.6 gives the k_2 values at 25 and 55°C. The experimental data for k_2 were correlated with the following expression:

$$k_2 = 1.018 \times 10^{17} \exp\left(\frac{-6730}{T}\right) \qquad (5\text{-}9)$$

The activation energy was calculated to be 56.0 kJ/mole (13.4 kcal/mole).
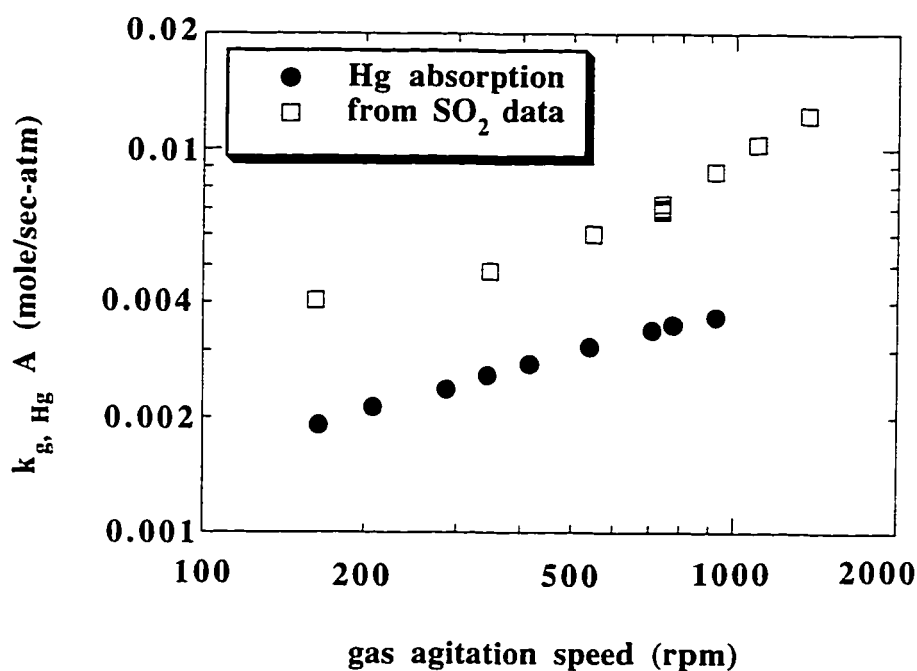
Figure 5.3 Comparison of gas film mass transfer coefficient of mercury obtained in two reactors using different methods. $kgA_{,SO2}$ from McGuire, 1990 was corrected by $kgA_{, Hg} = kgA_{,SO2}\sqrt{\dfrac{D_{Hg\text{-}N2}}{D_{SO2\text{-}N2}}}$.
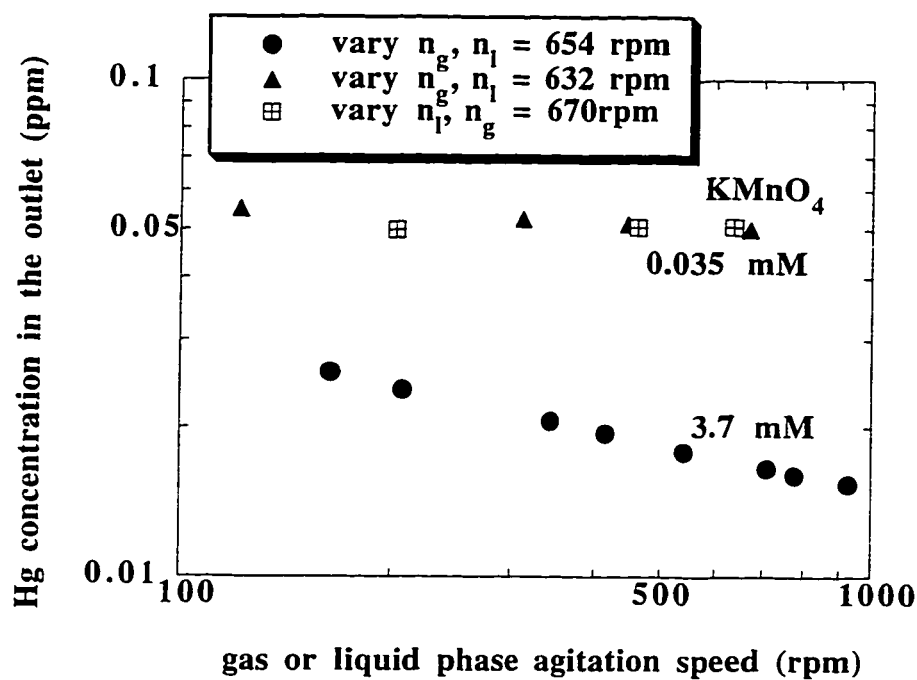
Figure 5.4   Effect of agitation speed on mercury removal during Hg absorption in KMnO$_4$/1.8M H$_2$SO$_4$ solution at 25°C. The inlet mercury was 0.097 ppm, total Hg/N$_2$ flow rate was 1 l/min. n_g was gas phase agitation speed and n_l was liquid phase agitation speed.

66

Table 5.3   The effect of $KMnO_4$ during mercury absorption in $KMnO_4$ and 1.8 M H_2SO_4 solution. Total Hg-N_2 flow rate was 1 l/min.

T (°C)	P_{Hgin} x10^8 (atm)	P_{Hgb} x10^8 (atm)	N_{Hg} x10^9 ($\frac{gmol}{s\text{-}m^2}$)	$[MnO_4^-]_b$ (mM)	$k_{g,Hg}$ ($\frac{gmol}{s\text{-}atm\text{-}m^2}$)	$k_1°, MnO4^-$ x10^5 ($\frac{m}{s}$)	k_2 x10^{-7} ($\frac{1}{M\text{-}s}$)
25	2.0	1.5	0.4	0.003	0.4	3.2	1.4
25	2.0	1.4	0.5	0.008	0.4	3.2	1.5
25	2.0	1.3	0.6	0.014	0.4	3.3	1.5
25	2.0	1.1	0.8	0.034	0.4	3.3	1.5
25	2.0	1.0	0.9	0.061	0.4	3.3	1.5
25	2.0	0.8	1.0	0.168	0.4	3.3	1.5
25	9.9	8.0	1.6	0.002	0.4	3.2	1.4
25	9.9	4.4	4.7	0.093	0.4	3.2	1.5
25	10.0	7.3	2.5	0.007	0.4	3.2	1.3
25	10.0	6.8	3.0	0.011	0.4	3.2	1.5
25	10.0	6.2	3.5	0.019	0.4	3.2	1.5
25	10.0	5.4	4.2	0.040	0.4	3.2	1.5
25	10.0	4.6	4.9	0.094	0.4	3.2	1.5
25	10.0	3.8	5.7	0.242	0.4	3.2	1.5
25	10.0	3.2	6.2	0.612	0.4	3.2	1.4
25	9.9	5.4	3.9	0.033	0.4	3.3	1.6
25	9.9	5.4	3.9	0.035	0.4	3.3	1.5
55	10.0	6.4	2.8	0.012	0.4	5.5	11.8
55	10.0	6.0	3.1	0.017	0.4	5.5	12.6
55	10.0	5.4	3.6	0.029	0.4	5.5	12.6
55	10.0	4.9	4.0	0.049	0.4	5.5	12.6
55	10.0	4.2	4.5	0.102	0.4	5.5	12.6
55	10.0	3.5	5.1	0.247	0.4	5.5	12.9
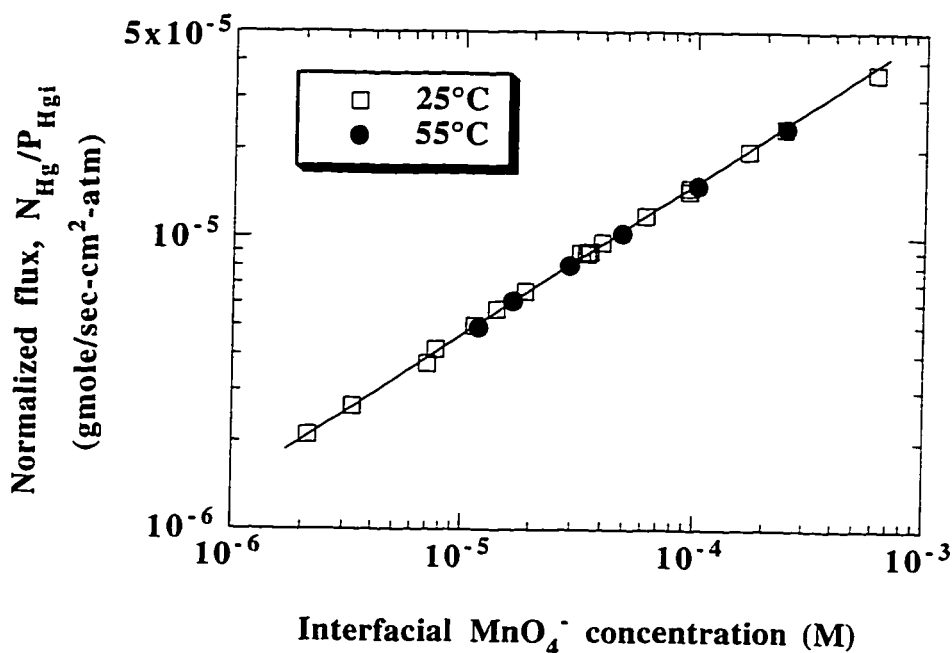
Figure 5.5 The dependence of normalized flux on $[MnO_4^-]_i$ during mercury absorption in $KMnO_4$-1.8 M H_2SO_4. Total Hg/N_2 flow rate was 1 l/min.

Other investigators studied the kinetics of MnO_4^- reaction with other reagents. Table 5.4 shows that the rate of permanganate reaction with mercury is faster than most reagents, but slower than reaction with hydrated electrons. The second order reaction of elemental mercury and ozone was also reported with a rate constant of 4.7×10^7 $M^{-1}s^{-1}$ (Munthe, 1992), which was in the same order of magnitude but faster than mercury reaction with permanganate.
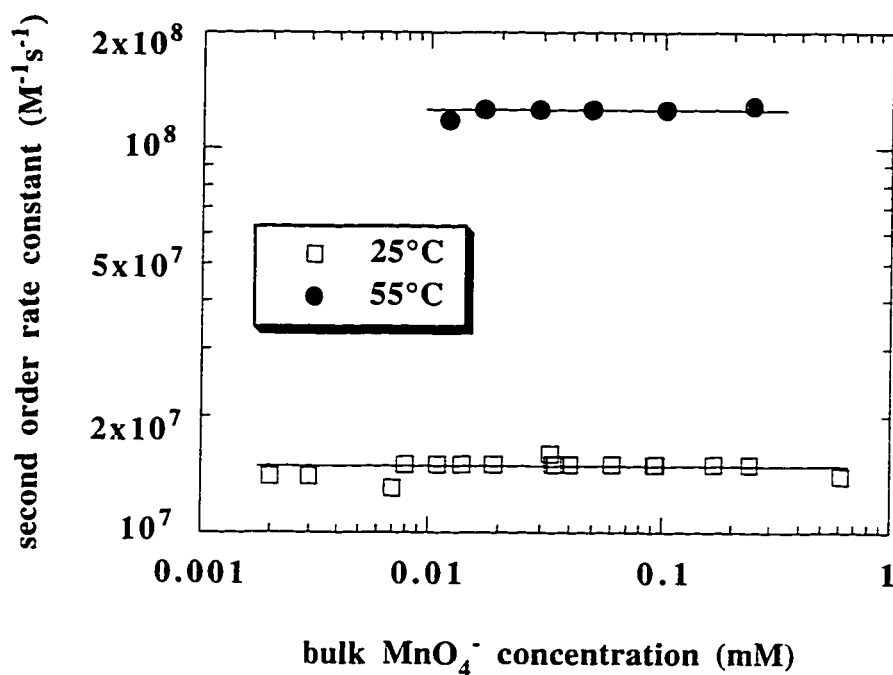
Figure 5.6   Reaction kinetics of mercury absorption in $KMnO_4/1.8$ M H_2SO_4 at 25 and 55°C. Total Hg-N_2 flow rate was 1 l/min.

Table 5.4   Second order reaction rate constants of MnO_4^- with different reactants.

Reactant	Medium	T (°C)	pH	k_2 ($M^{-1}s^{-1}$)	References
$[H_2Fe(CN)_6]^{2-}$	Na_3PO_3	15	2	5.2×10^5	Rawoof and Sutter, 1967
MnO_2-Mn (adsorbed)	-	25	8	1.4×10^6	Benschoten and Lin, 1992
NO vapor	NaOH	25	-	4.4×10^6	Uchida et al., 1983
H_2O radical	-	23	3	7.9×10^6	Baxendale et al., 1965
Hg vapor	$1.8M$ H_2SO_4	25	0	1.6×10^7	this work
Hg vapor	$1.8M$ H_2SO_4	55	0	12.6×10^7	this work
hydrated electron	MeOH	25	7	2.2×10^{10}	Thomas et al., 1964
hydrated electron	MeOH	25	13	3.7×10^{10}	Thomas et al., 1964
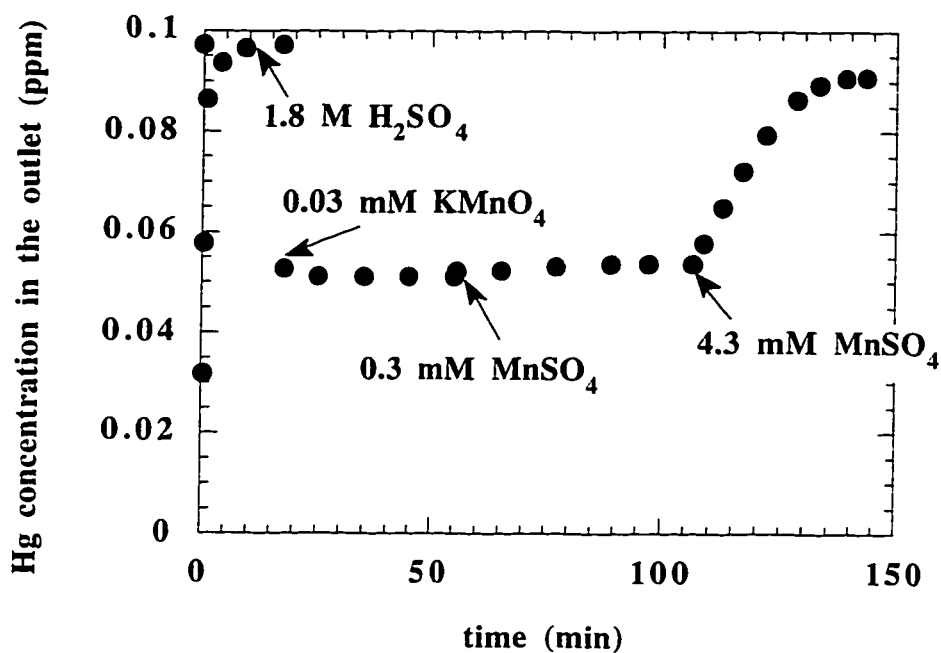
Figure 5.7   The effect of Mn^{2+} on permanganate decomposition during mercury absorption in 3.3×10^{-5} M $KMnO_4/1.8$ M H_2SO_4 at 25°C. The inlet mercury was 0.097 ppm, total Hg/N_2 flow rate was 1 l/min.

The effect of $MnSO_4$ was investigated as well. Figure 5.7 indicates that 4.3 mM $MnSO_4$ was adequate to seriously weaken mercury absorption in 0.03 mM $KMnO_4$. In the case of figure 5.7, the addition of 4.3 mM $MnSO_4$ decreased mercury removal from 95% to 10%.

70

Chapter 6 Mercury Absorption in Aqueous Oxidants Catalyzed by Mercury(II)

Elemental mercury was absorbed in $HgCl_2$ based aqueous solutions with $HgCl_2$-water as a base case for comparison purposes. The effects of strong acid, oxidants, salts, buffer solution and some combinations of them were investigated. The presence of HNO_3 or H_2SO_4 greatly enhanced mercury absorption. However, HCl inhibited mercury absorption. The addition of 0.1 M H_2O_2 to 0.8 M HNO_3 absorbed much more mercury than that of only with 0.8 M HNO_3. Both $K_2Cr_2O_7$ and $K_2Cr_2O_7$-HNO_3 enhanced mercury absorption and the positive effect of adding HNO_3 was more apparent than that of adding $K_2Cr_2O_7$. $MnSO_4$ only mildly enhanced mercury absorption. Other salts, such as $FeCl_3$, $CaCl_2$, $MgCl_2$, $MgSO_4$ and NaCl, inhibited mercury absorption in $HgCl_2$. NaOH-succinic acid buffer solution greatly enhanced while $NaHCO_3$/NaOH inhibited mercury absorption in $HgCl_2$.

6.1 PREVIOUS WORK

EPA method 29 for field sampling of mercury specifies the use of hydrogen peroxide and nitric acid in the first impinger and permanganate and sulfuric acid in the following impinger (Environmental Protection Agency, 1992). This method assumes that hydrogen peroxide and nitric acid absorb divalent mercury but not elemental mercury vapor. However, results obtained at the High Sulfur Test Center indicate that the EPA mercury speciation method may not be reliable (Peterson et al., 1995). Several other researchers have indicated that the oxidation of elemental mercury by hydrogen peroxide may be important in the

71

atmospheric environment (Lindqvist et al., 1984; Brosset, 1987; Kobayashi, 1987).

More recently, a German company has commercialized a sulfur dioxide and mercury scrubbing process called MercOx (Parkinson, 1996). In their process, a 35% aqueous solution of hydrogen peroxide is sprayed into the flue gas. Elemental mercury is oxidized by hydrogen peroxide to Hg(II) and remains in the solution. In a parallel reaction, the water spray converts SO_2 to sulfuric acid. As a result, all gaseous pollutants are converted and trapped in the solution. Dissolved mercury is removed by ion exchange and the acids are neutralized to salts and precipitated gypsum. In recent pilot test treating 500 m^3/hr of flue gas stream at a sludge incinerator, mercury concentrations were reduced from a few hundred $\mu g/m^3$ to 20 $\mu g/m^3$, well below the 50 $\mu g/m^3$ German limit.

The combination of hydrogen peroxide and a polyvalent metal ion has also been suggested as a potential oxidizer for elemental mercury. Kobayashi (1987) studied the mixtures of hydrogen peroxide with thirteen metal ions (Fe^{3+}, Mn^{2+}, Zn^{2+}, Pb^{2+}, Cu^{2+}, Co^{2+}, Ni^{2+}, Cd^{2+}, Sb^{3+}, Bi^{3+}, VO_3^-, Ca^{2+} and Al^{3+}). Among these, only Fe^{3+} enhanced mercury absorption and the reaction was first order in hydrogen peroxide and Fe^{3+}, respectively. Munthe and McElroy (1992), however, concluded that the reactions between aqueous elemental mercury and hydrogen peroxide, or Fe^{3+}, or a mixture of the two, were not significant.

Other researchers have studied the effect of Hg^{++} on elemental mercury removal. Qualitative results obtained by Morita et al. (1983) reported that the rate of mercury absorption increased with increasing Hg^{++} concentration and with increasing oxidation potential of dichromate solutions in sulfuric acid. The

combination of Hg^{++} and dichromate absorbed mercury more efficiently than either component alone. Strong mercury absorption in $HgCl_2/H_2SO_4$ was also observed (Morita et al., 1983). Allgulin (1974) found that solution containing mercury(II) ions ranging from 0.02 g/l to saturation and at least one anion selected from the group Cl^-, Br^-, I^- and SO_4^{2-} was effective for removing Hg°.

The objective of this study was to investigate the role of Hg(II) and other oxidants on elemental mercury absorption in a variety of aqueous solutions.

6.2 EXPERIMENTAL METHODS

All experiments were performed in the well-characterized stirred cell reactor described in Chapter 3. In a typical experiment, mercury diluted with nitrogen (1 l/min) bypassed the reactor. After the mercury analyzer gave a stable reading, the $Hg-N_2$ stream was shifted to flow above 0.8 M nitric acid or other background solution, such as other acid, buffer solution or water. Again after the analyzer reached a stable reading, a known amount of 30 wt% hydrogen peroxide solution or mercuric chloride solution prepared from solid was injected using a syringe with a long needle into the reactor and the outlet mercury concentration was recorded continuously by a strip chart recorder (Soltec Model 1242). Each active liquid phase ingredient was injected sequentially rather than mixed outside the reactor. Prior to each injection, the same amount of solution was extracted from the reactor to keep the final liquid volume constant during mercury absorption.

The reactor outlet gas was immediately diluted with nitrogen by a factor of 10 at 25°C and 15 at 55°C to minimize water vapor interference on mercury

73

analysis. A three-point calibration of the analyzer (cold vapor atomic absorption) was conducted both before and after the experiment. The mercury concentration obtained when the Hg-N_2 was passed over the background solution of the actual experiment was used as the inlet mercury concentration (wet calibration). The rate of mercury absorption was calculated from the gas phase material balance. The bulk hydrogen peroxide concentration was determined by titration with potassium iodide and certified 1 N sodium thiosulfate solution (Appendix D). $HgCl_2$ or other reagent additions to the liquid phase were determined by weighing the syringe before and after the injection. The specifications of the reagents used are listed in table 6.1.

Table 6.1   Specifications of the chemicals used in the experiments.

Chemical Name	Specification	Manufacturer
Nitric Acid	70 wt%, GR	EM Science
Sulfuric Acid	95-98 wt%, GR	EM Science
Hydrochloric Acid	36.5-38 wt%, GR	EM Science
Succinic Anhydride	Practical	Matheson Coleman & Bell Manufacturing Chemists
Hydrogen Peroxide	30 wt%, Reagent	EM Science
Mercuric Chloride	Analytical Reagent	Mallinckrodt Chemical, Inc.
Potassium Iodide	GR	EM Science
Sodium Thiosulfate	Certified 1 N Solution	Fisher Scientific
Potassium Dichromate	Crystal, A.C.S. Reagent	MCB Manufacturing Chemists
Manganese Sulfate Monohydrate	GR	EM Science
Magnesium Chloride Hexahydrate	Crystal, GR	EM Science
Ferric Chloride	Lumps, AR	Mallinckrodt Chemical, Inc.
Ferrous Sulfate	Crystal, A.C.S. Reagent	Spectrum Chemical Mfg. Corp.
Calcium Chloride Anhydrous	4 Mesh/Desiccant	Spectrum Chemical Mfg. Corp.
Sodium Bicarbonate	Powder A.C.S. Reagent	Matheson Coleman & Bell Manufacturing Chemists
Sodium Hydroxide	Pellets	Spectrum Chemical Mfg. Corp.

6.3 DETERMINATION OF MASS TRANSFER CHARACTERISTICS AND PHYSICAL PROPERTIES OF MERCURY

The determination of the gas phase mass transfer coefficient, $k_{g, Hg}$, was discussed in chapter 4 and its value is listed in table 6.2. The value of the liquid phase mass transfer coefficient of Hg, $k^{o}_{l, Hg}$, obtained from mercury desorption experiments in an identical reactor, was modified to give $k^{o}_{l, Hg^{++}}$:

$$k^{o}_{l, Hg^{++}} = k^{o}_{l, Hg} \sqrt{\frac{D_{Hg^{++}-H2O}}{D_{Hg-H2O}}}$$

(6-1)

The portion of $[Hg(II)]_b$ resulting from mercury absorption was obtained by integration of the gas phase material balance. The nominal concentration of injected mercuric chloride was used for the portion of $[Hg(II)]_b$ resulting from mercuric chloride injections. All other physical constants used in the calculation are tabulated in table 6.2.

Table 6.2   Physical properties of Hg and Hg^{++}.

	25°C	55°C
$D_{Hg-H2O}{}^a$ $(cm^2 s^{-1})$	1.19×10^{-5}	2.21×10^{-5}
$D_{Hg^{++}-H2O}{}^b$ $(cm^2 s^{-1})$	8.47×10^{-6}	1.65×10^{-5}
$H_{Hg}{}^c$ $(atm M^{-1})$	8.91	35.64
$k_{g,Hg}$ $(mol \ s^{-1} \ atm^{-1} \ m^{-2})$ Typical Value	$0.0344 \ (n_g)^{0.38}$ 0.4	$0.0344 \ (n_g)^{0.38}$ 0.4
$k^{o}_{l, Hg}$ $(m \ s^{-1})$ Typical Value	$2.42 \times 10^{-7} \ (n_l)^{0.73}$ 2.6×10^{-5}	$7.64 \times 10^{-7} \ (n_l)^{0.64}$ 4.7×10^{-5}
$k^{o}_{l, Hg^{++}}$ $(m \ s^{-1})$ Typical Value	$2.04 \times 10^{-7} \ (n_l)^{0.73}$ 2.2×10^{-5}	$6.59 \times 10^{-7} \ (n_l)^{0.64}$ 4.0×10^{-5}

[a] estimated by method of Sitaraman et al. (1963) (see appendix B)
[b] obtained from Lide (1994)   [c] obtained from Clever et al. (1985)

6.4 RESULTS AND DISCUSSION

6.4.1 Absorption in Mercury(II)

For most experiments the results are reported as normalized flux, K_g', analogous to the overall gas phase mass transfer coefficient:

$$K_g' = \frac{N_{Hg}}{P_{Hgi}} \qquad (6\text{-}2)$$

Figure 6.1 gives the results of two independent tests. With only distilled water in the liquid phase, injections of $HgCl_2$ resulted in step decreases of the outlet mercury concentration.
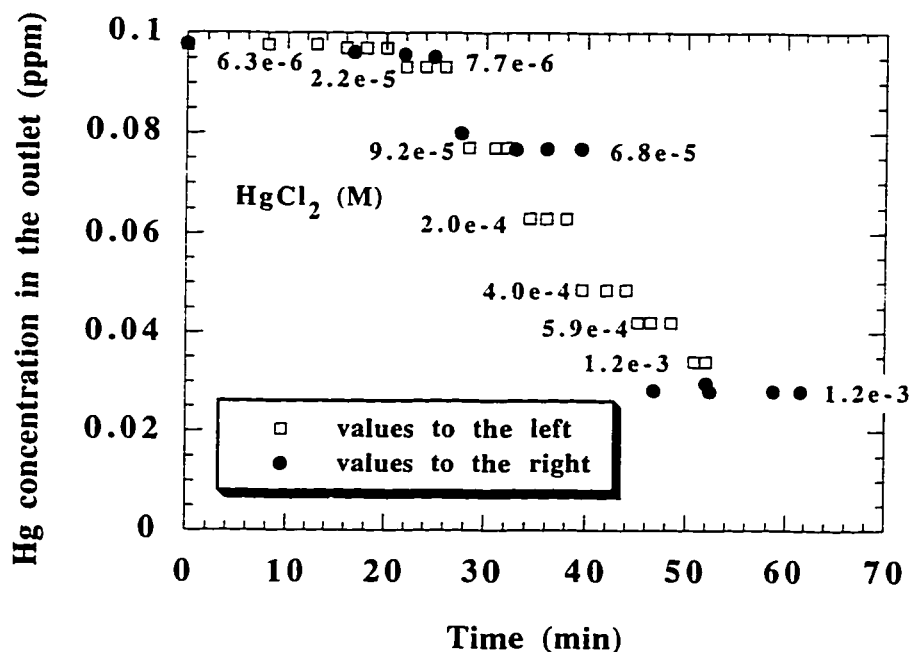
Figure 6.1 Hg absorption in distilled water with sequential $HgCl_2$ injections at 25°C. Hg-N_2 flow rate was 1 l/min. Solution pH was 4.82-4.14. Two different legends represent two independent runs under the same conditions.

The normalized flux, K_g', increases with $HgCl_2$ (figure 6.2). The log-log slope is greater than 0.5, indicating that without strict pH control, the apparent reaction between elemental mercury and mercuric chloride is not a simple second order reaction . Experimental results in table 6.3 indicate that the injection of more $HgCl_2$ resulted in lower solution pH, as pH was reduced from 4.82 with 0.008 mM $HgCl_2$ to 4.14 with 1 mM $HgCl_2$. Lower pH enhanced mercury removal by mercury(II), as shown in later sections.
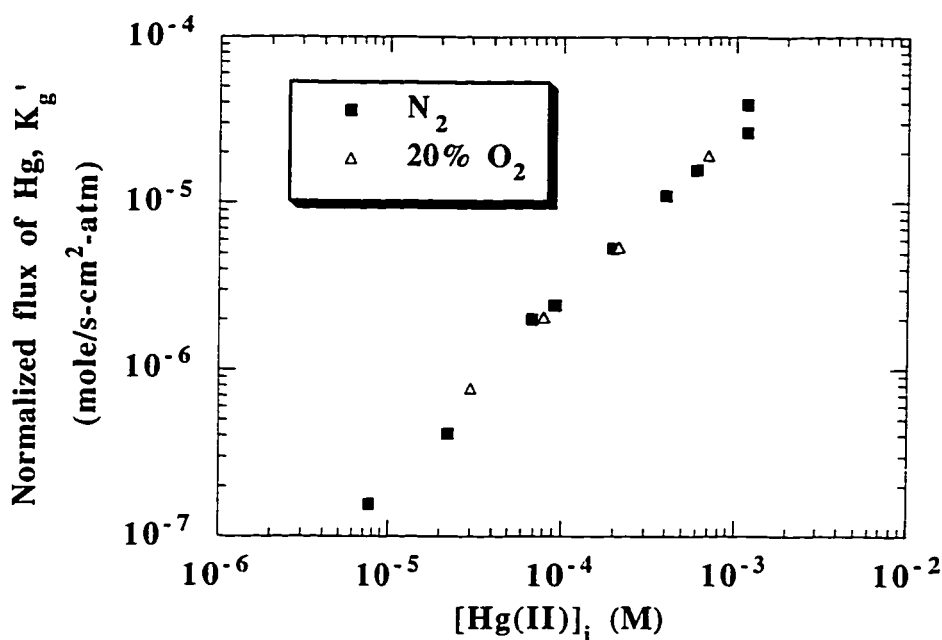
Figure 6.2   Hg absorption in distilled water with sequential $HgCl_2$ injections at 25°C. Hg-N_2 or Hg-air flow rate was 1 l/min. Solution pH was 4.82-4.14.

The effect of oxygen was investigated by mixing air with elemental mercury vapor instead of pure nitrogen. This resulted in 20% oxygen (by volume) in the gas phase. Known amounts of $HgCl_2$ were injected into distilled water or other reagents and the results are given in figure 6.2. The presence of O_2 in the gas phase makes no difference in Hg absorption in Hg(II) at 25°C.

Table 6.3 Mercury absorption in distilled water with sequential $HgCl_2$ injections at 25°C. Total $Hg-N_2$ or Hg-air flow rate was 1 l/min. $P_{Hg,in}$ was 1.02×10^{-7} atm. $k_{g,Hg}$ was 0.39 gmol/s-atm-m^2. $k_l^\circ._{Hg^{++}}$ was 2.2×10^{-5} m/s at 25°C.

O_2 (%)	Time (min)	P_{Hgb} $\times 10^8$ (atm)	P_{Hgi} $\times 10^8$ (atm)	$N_{Hg} \times 10^9$ ($\frac{mole}{s-m^2}$)	Hg^{++} injected (mM)	pH
0	16.0	10.2	10.1	0.06	0.006	-
0	22.0	9.8	9.7	0.40	0.022	-
0	28.4	8.1	7.6	1.84	0.091	-
0	34.4	6.6	5.8	3.10	0.195	-
0	39.6	5.1	4.0	4.39	0.395	-
0	45.2	4.4	3.1	4.97	0.593	-
0	50.8	3.6	2.1	5.67	1.164	-
0	16.8	10.1	10.0	0.16	0.008	4.82
0	27.6	8.4	8.0	1.59	0.068	4.45
0	52.0	3.1	1.6	6.08	1.157	4.14
20	36.0	9.4	9.2	0.71	0.030	5.10
20	48.0	8.3	7.9	1.63	0.080	4.90
20	60.8	6.6	5.8	3.13	0.212	4.74
20	66.0	4.1	2.7	5.26	0.694	4.51

6.4.2 Absorption by Mercury (II) with the Addition of a Strong Acid or Buffer Solution

With a solution of a strong acid, we have found that the rate of reaction between elemental mercury vapor and mercuric chloride is given by the mechanism:

$$Hg + Hg(II) \xrightarrow{H^+} Products \tag{6-3}$$

At constant pH the reaction rate is given with the second order rate constant, k_2:

$$\text{reaction rate} = k_2 \, [\text{Hg}] \, [\text{Hg(II)}] \tag{6-4}$$

Using approximate surface renewal theory (Danckwerts, 1970), the flux of elemental mercury, N_{Hg}, should be given by:

$$N_{Hg} = \frac{P_{Hgi}}{H_{Hg}} \sqrt{k_2 \, D_{Hg\text{-}H2O} \, [\text{Hg(II)}]_i} \tag{6-5}$$

where:

$$P_{Hgi} = P_{Hgb} - \frac{N_{Hg}}{k_{g.Hg}} \tag{6-6}$$

$$[\text{Hg(II)}]_i = \frac{N_{Hg}}{k^\circ_{l.Hg^{++}}} + [\text{Hg(II)}]_b \tag{6-7}$$

6.4.2.1 Mercury Absorption in 0.8 M Nitric Acid

Elemental mercury vapor was absorbed into 0.8 M nitric acid with sequential injection of mercuric chloride. Without any other oxidants, injection of mercuric chloride into 0.8 M nitric acid resulted in a step decrease in outlet mercury concentration. All of the experimental data are tabulated in table 6.4. Detailed results can be found in appendix E.

Figure 6.3 plots normalized flux, N_{Hg}/P_{Hgi} versus $[\text{Hg(II)}]_i$. The reaction is first order in Hg and Hg(II), respectively. The kinetic data at 55°C was difficult to obtain and unstable compared to that at 25°C. This was probably due to the difficulties encountered in cleaning the reactor from residual $HgCl_2$ using the reducing agent $NaBH_4$. Sometimes, the reactor had to be first soaked in $NaBH_4$ to get rid of the residual $HgCl_2$ and then soaked in H_2O_2 to neutralize the effect of $NaBH_4$. In contrast, soaking the reactor in $NaBH_4$ before each experiment when conducting experiments at 25°C did not cause any difficulties and abnormal

results. As shown in figure 6.3, when the injected $HgCl_2$ exceeded 3×10^{-5} M at 55°C, K_g' tended to flatten out. With $HgCl_2$ less than 3×10^{-5} M, the overall second order rate constant k_2 is $(7.8 \pm 2.1) \times 10^6$ $M^{-1}s^{-1}$ at 25°C and $(13.4 \pm 8.0) \times 10^6$ $M^{-1}s^{-1}$ at 55°C. The experimental data for k_2 were correlated with the following expression:

$$k_2 = 2.90 \times 10^9 \exp\left(\frac{-1765}{T}\right) \tag{6-8}$$

Table 6.4   Effect of Hg(II) on mercury absorption in 0.8 M HNO_3. $P_{Hg,in}$ was 1.0×10^{-7} atm. $k_{g,Hg}$ was 0.4 gmol/s-atm-m^2. $k_l°_{,Hg^{++}}$ was 2.2×10^{-5} m/s at 25°C and 4.0×10^{-5} m/s at 55°C.

T (°C)	$P_{Hg,b}$ $\times 10^8$ (atm)	$P_{Hg,i}$ $\times 10^8$ (atm)	N_{Hg} $\times 10^9$ ($\frac{mole}{s \cdot m^2}$)	Hg^{++} injected (µM)	$[Hg(II)]_i$ (µM)	k_2 $\times 10^{-6}$ ($\frac{1}{M \cdot s}$)
25	9.5	9.3	0.6	0.68	0.65	4.6*
	8.6	8.2	1.4	2.84	2.77	7.3
	7.8	7.3	2.0	6.74	6.64	7.7
	8.4	8.0	1.6	3.82	3.75	7.2
	7.0	6.3	2.8	17.20	17.07	7.8
	6.0	5.0	3.7	41.24	41.08	8.6
	5.3	4.2	4.2	89.96	89.77	7.6
	8.3	7.9	1.7	4.17	4.09	7.3
	6.9	6.1	2.9	17.54	17.41	8.5
	5.8	4.9	3.7	46.85	46.68	8.3
	5.0	3.9	4.4	110.96	110.76	7.9
55	9.5	9.4	0.5	1.49	1.48	13.1
	8.9	8.7	1.0	5.67	5.64	13.5
	7.9	7.4	1.8	29.98	29.93	11.4
	7.3	6.7	2.3	83.59	83.53	7.7*
	7.3	6.7	2.3	161.55	161.50	4.0*
	8.4	8.0	1.4	10.06	10.02	18.6
	7.9	7.5	1.8	24.06	24.01	13.8
	8.8	8.6	1.1	7.12	7.10	12.6
	8.1	7.7	1.6	22.63	22.59	11.6
	7.8	7.3	1.9	49.56	49.52	7.5*
	7.2	6.5	2.4	127.12	127.06	6.0*

*represents data excluded from rate constant regression

At 10^{-5} M Hg(II), K_g' was 3.5×10^{-6} with 0.8 M HNO_3 and 1.6×10^{-7} $\frac{\text{mole}}{\text{s-cm}^2\text{-atm}}$ without acid at 25°C, as shown in figures 6.2 and 6.3. This indicates that the presence of HNO_3 greatly enhanced Hg absorption by mercury(II).
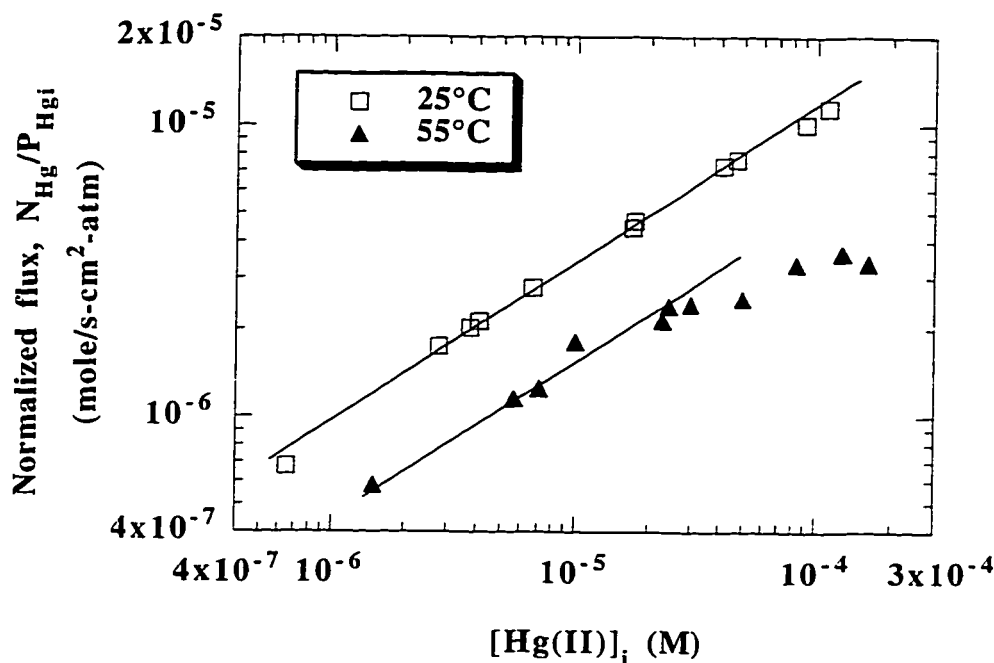
Figure 6.3   Hg absorption in 0.8 M HNO_3 with sequential $HgCl_2$ injection at 25 and 55°C. Total $Hg-N_2$ flow rate was 1 l/min.

6.4.2.2   Effects of HNO_3, H_2SO_4 and HCl

Figure 6.4 gives the results at 25°C when nitric acid, sulfuric acid or buffer solution was present in the solution. The base line is absorption in water without acid addition. Hg flux was significantly lower with 0.01 M HNO_3 and no acid than with 0.8 M HNO_3. The difference was most significant at low Hg(II) and

81

diminished at higher Hg(II). For example, at 10^{-5} M Hg(II), the normalized flux of mercury increased a factor of 32 with 0.8 M HNO₃ compared to that with HgCl₂ alone. While at 10^{-3} M Hg(II), the normalized flux of mercury only increased a factor of 1.5.
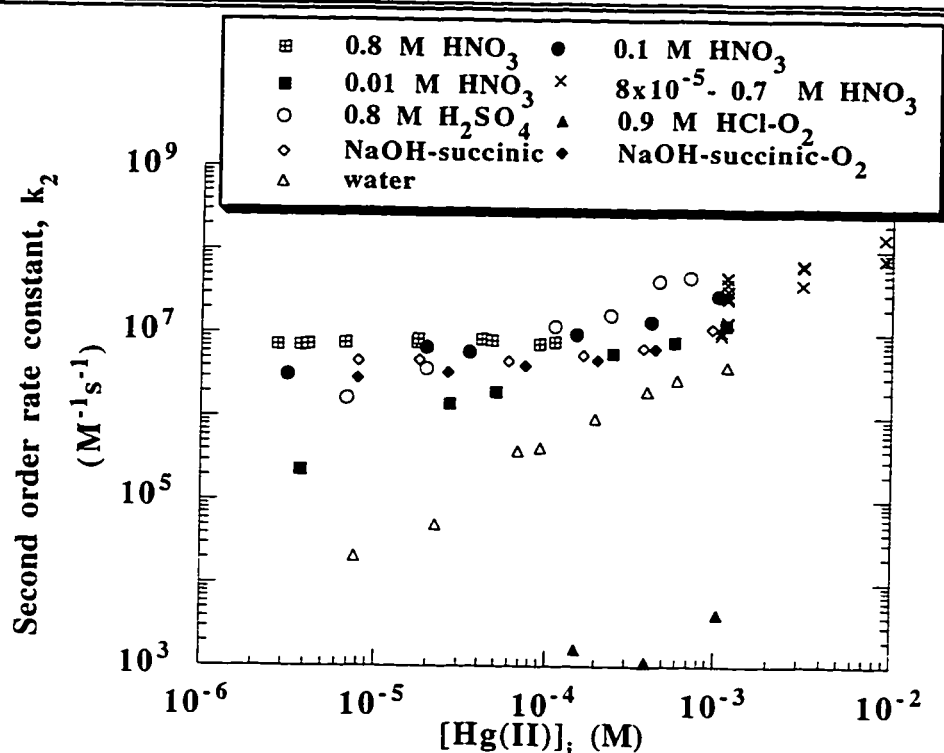
Figure 6.4   The dependence of second order rate constant k_2 on [Hg(II)]$_i$ with various acids and buffers in the solution at 25°C. k_2 was obtained from eqn (6-5). N_2 was in the gas phase unless otherwise indicated in the legends. Experiments with O_2 were with 20% (by volume) O_2. Total Hg-N_2 or Hg-air flow rate was 1 l/min.

The effect of HNO₃ is apparent in comparison of mercury absorption in 0.01, 0.1 and 0.8 M HNO₃ with sequential HgCl₂ injection. k_2 was lower in

82

0.01M HNO_3 than in 0.1 M HNO_3 at the same Hg(II) level. Figure 6.4 also shows that k_2 in 0.01 M HNO_3 was greater than with no HNO_3 at the same level of Hg(II). However, there was very little increase in k_2 when HNO_3 was increased from 0.1 M to 0.8 M. At high Hg(II), concentration differences in HNO_3 did not make much difference in k_2. The results of HNO_3 injections from 8×10^{-6} to 0.7 M indicate that at Hg(II) greater than 1 mM, increased Hg(II) was the primary reason of high mercury absorption compared to the increased HNO_3 acidity.

For the other acid systems studied, keeping a high and constant level of H^+ was essential to obtain an overall second order reaction between elemental mercury and Hg(II). When a high level of HNO_3 existed, injections of $HgCl_2$ did not change the solution pH significantly. However, when a small amount of HNO_3 was present, injections of $HgCl_2$ decreased the solution pH significantly. k_2 increased as the injected amount of Hg(II) was increased. This was the effect of both increased Hg(II) and lower pH associated with increased $HgCl_2$. This is the primary reason that k_2 depend on Hg(II).

The effect of 0.8 M H_2SO_4 on Hg absorption at 25°C is comparable to that of 0.8 M HNO_3.

The effect of HCl was studied in a similar manner with only elemental mercury vapor and nitrogen in the gas. $HgCl_2$ was sequentially injected into 0.8 M HCl at 25°C to give 10^{-6} to 10^{-3} M $HgCl_2$. The outlet Hg concentration exceeded the inlet Hg concentration and increased as the concentration of injected $HgCl_2$ increased. The same phenomenon was observed when 0.9 M HCl was used in another effort. This indicates that the presence of HCl in $HgCl_2$ not only

did not remove mercury but reduced some of the injected $HgCl_2$ to elemental form.

$HgCl_2$ was sequentially injected into 0.9 M HCl with 20% oxygen in the gas phase. Although a finite amount of mercury removal was detected, the presence of HCl inhibited Hg absorption in Hg(II), as shown in figure 6.4. However, in the absence of oxygen, the outlet Hg concentration exceeded the inlet Hg concentration and increased as the amount of injected $HgCl_2$ increased.

6.4.2.3   Effect of NaOH-succinic acid buffer

From the results with various degrees of HNO_3 and $HgCl_2$ in the solution, it seems that pH plays an important role. Thus a 0.01 M NaOH-0.01 M succinic acid buffer solution was used to keep a reasonably constant pH at 5.6 while subsequently injecting $HgCl_2$. The results are shown in figure 6.4. k_2 was comparable to that with 0.8 M HNO_3, even though the buffer solution pH was much higher. This indicates that 0.01 M NaOH-0.01 M succinic acid buffer greatly enhances Hg absorption in Hg(II). With 20% oxygen in the gas phase, k_2 did not change significantly. This indicates that oxygen has negligible effect on Hg absorption in 0.01 M NaOH-0.01 M succinic acid buffer with sequential $HgCl_2$ injection.

6.4.2.4   Effect of NaHCO₃-NaOH buffer

With only nitrogen and Hg in the gas phase, $NaHCO_3$-NaOH buffer was used to maintain the solution pH at 9.49-9.56. $HgCl_2$ injections into $NaHCO_3$-NaOH buffer gave 10^{-6} to 10^{-3} M Hg(II). The outlet Hg concentration increased as the amount of $HgCl_2$ injected increased, as shown in table 6.5. For all the

84

HgCl$_2$ injections performed, the outlet Hg concentration exceeded the inlet Hg concentration. This indicates that the injected HgCl$_2$ was somehow reduced to elemental mercury and got stripped out of the solution.

The presence of 20% O$_2$ contributed to inhibiting the reduction of injected HgCl$_2$, but not enough to cause Hg absorption. When the injected HgCl$_2$ was increased to a certain high value, such as 5.26×10^{-4} M, 20% O$_2$ was no longer enough to prevent HgCl$_2$ from being reduced.

Table 6.5   The effect of oxygen on Hg absorption in NaHCO$_3$-NaOH buffer solution at 25°C.

O$_2$	HgCl$_2$ (M)	pH	Results
0	10^{-6}	9.56	Hg$_{out}$ > Hg$_{in}$
0	10^{-4}	↓	Hg$_{out}$ > Hg$_{in}$
0	10^{-3}	9.49	Hg$_{out}$ > Hg$_{in}$
20	2.17×10^{-5}	9.63	Hg$_{out}$ = Hg$_{in}$
20	1.47×10^{-4}	9.61	Hg$_{out}$ = Hg$_{in}$
20	5.26×10^{-4}	9.55	Hg$_{out}$ > Hg$_{in}$

6.4.3   Mercury Absorption in Hydrogen Peroxide and Nitric Acid

The rate of reaction between elemental mercury vapor and hydrogen peroxide is given by the mechanism:

$$\text{Hg} + \text{H}_2\text{O}_2 \xrightarrow{\text{H}^+} \text{Hg(II)} + \text{Other Products} \qquad (6\text{-}9)$$
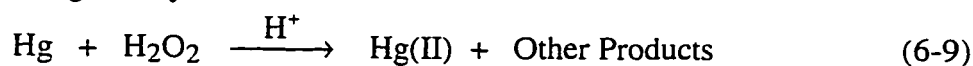
Since the reaction product Hg(II) catalyses Hg absorption, the rate of reaction at constant pH with the third order rate constant, k_3, is given by:

$$\text{reaction rate} = k_3 \, [\text{Hg}] \, [\text{Hg(II)}] \, [\text{H}_2\text{O}_2] \qquad (6\text{-}10)$$

Using surface renewal theory, the flux of elemental mercury, N_{Hg}, should be given by:

$$N_{Hg} = \frac{P_{Hgi}}{H_{Hg}} \sqrt{k_3 \, D_{Hg\text{-}H2O} \, [\text{Hg(II)}]_i \, [\text{H}_2\text{O}_2]_i} \qquad (6\text{-}11)$$

where:

$$P_{Hgi} = P_{Hgb} - \frac{N_{Hg}}{k_{g.Hg}} \qquad (6\text{-}12)$$

$$[H_2O_2]_i \approx [H_2O_2]_b \qquad (6\text{-}13)$$

$$[Hg(II)]_i = \frac{N_{Hg}}{k^o{}_{l.Hg^{++}}} + [Hg(II)]_{b,\ initial\ injected} + [Hg(II)]_{absorbed} \qquad (6\text{-}14)$$

6.4.3.1 Hydrogen Peroxide and 0.8 M Nitric Acid

Figure 6.5 gives typical responses when H_2O_2 was injected into 0.8 M HNO_3. Hg outlet concentration dropped when additional H_2O_2 was injected. It kept decreasing as absorption proceeded. This phenomenon can be explained by the accumulation of absorbed mercury species (mainly Hg(II)). This assumption was verified by the results with $HgCl_2$ injection shown in figure 6.6. Hg outlet concentration dropped dramatically when $HgCl_2$ was injected. This indicates that Hg(II) catalyzes Hg absorption in H_2O_2-HNO_3. The experimental data are tabulated in table 6.6.

Table 6.6 Hg^o absorption in H_2O_2-Hg(II) with 0.8M HNO_3. Total Hg-N_2 flow rate was 1 l/min. $[H_2O_2]_b$ was determined by titration.

Temp. & $P_{Hg, in}$	$P_{Hg, b}$ ppb	$[H_2O_2]_b$ M	$[Hg(II)]_i$ x 10^7 M	N_{Hg} x 10^{10} $\frac{mole}{s\text{-}m^2}$	$k_{g.Hg}$ $\frac{mole}{s\text{-}atm\text{-}m^2}$	$k_l{}^{o,Hg^{++}}$ x 10^5 $\frac{m}{s}$	k_3 x 10^{-8} $\frac{l}{M^2\text{-}s}$
25 °C	19.9	0.1	0.01	0.1	0.4	2.2	3.9
20.1 ppb	19.9	0.1	0.01	0.2	0.4	2.2	4.1
	19.8	0.1	0.02	0.2	0.4	2.2	3.8
	19.8	0.1	0.02	0.2	0.4	2.2	4.1
	19.8	0.1	0.02	0.3	0.4	2.2	4.4
	19.4	0.4	0.04	0.6	0.4	2.2	4.0
	19.3	0.4	0.1	0.7	0.4	2.2	3.9
	19.2	0.4	0.1	0.8	0.4	2.2	4.8

Table 6.6 (continue)

25 °C	78.5	1.0	1.1	17.0	0.4	2.2	3.2
97.5 ppb	78.2	1.0	1.1	17.3	0.4	2.2	3.1
	74.2	1.0	1.5	20.8	0.4	2.2	3.8
	69.7	1.0	1.9	24.8	0.4	2.2	4.7
	69.2	1.0	2.0	25.3	0.4	2.2	4.8
	93.4	0.2	0.2	3.7	0.4	2.2	3.2
	83.1	0.6	0.7	12.9	0.4	2.2	3.9
	81.8	0.6	0.9	14.1	0.4	2.2	3.7
	80.2	0.6	1.1	15.5	0.4	2.2	4.0
	74.5	0.9	1.6	20.5	0.4	2.2	3.9
	72.1	0.9	1.9	22.8	0.4	2.2	4.0
	70.8	0.9	2.1	23.9	0.4	2.2	4.1
	95.3	0.1	0.1	2.0	0.4	2.2	3.1
	94.9	0.1	0.1	2.3	0.4	2.2	3.5
	88.5	0.3	0.5	8.1	0.4	2.2	3.7
	86.6	0.3	0.6	9.8	0.4	2.2	4.3
	82.3	0.6	0.8	13.6	0.4	2.2	3.9
	79.6	0.6	1.0	16.0	0.4	2.2	4.7
	61.7	0.3	24.6	32.0	0.4	2.2	3.4
	43.2	0.3	183.0	48.6	0.4	2.2	3.1
	42.9	0.3	183.0	48.9	0.4	2.2	3.2
	28.7	0.3	1090.0	61.5	0.4	2.2	4.0
55 °C	95.1	0.1	0.1	2.0	0.4	4.1	90.6
97.5 ppb	94.4	0.1	0.1	2.5	0.4	4.1	90.4
	87.2	0.2	0.3	8.4	0.4	4.1	86.6
	86.1	0.2	0.4	9.3	0.4	4.1	97.3
	90.0	0.2	0.2	6.1	0.4	4.0	86.0
	87.0	0.2	0.4	8.6	0.4	4.0	82.3
	78.8	0.4	0.7	15.2	0.4	4.0	84.4
	78.2	0.4	0.7	15.7	0.4	4.0	81.8
	77.1	0.4	0.8	16.6	0.4	4.0	89.5
	69.3	0.7	1.1	22.9	0.4	4.0	92.6
	91.3	0.1	0.1	5.1	0.4	4.0	86.2
	91.3	0.1	0.2	5.1	0.4	4.0	86.2
	91.3	0.1	0.2	5.1	0.4	4.0	86.7
55 °C	93.5	0.1	0.1	3.3	0.4	4.0	82.4
97.6 ppb	92.4	0.1	0.1	4.2	0.4	4.0	86.7
	91.8	0.1	0.2	4.7	0.4	4.0	85.2
	84.8	0.3	0.4	10.4	0.4	4.0	81.4
	81.9	0.3	0.6	12.8	0.4	4.0	88.8
	79.6	0.3	0.8	14.6	0.4	4.0	91.1
	76.1	0.4	0.9	17.5	0.4	4.0	85.9
	74.9	0.4	1.0	18.4	0.4	4.0	87.1
	70.2	0.6	1.3	22.3	0.4	4.0	86.8
	66.9	0.6	1.5	24.9	0.4	4.0	91.2
	61.5	0.8	2.2	29.3	0.4	4.0	87.6
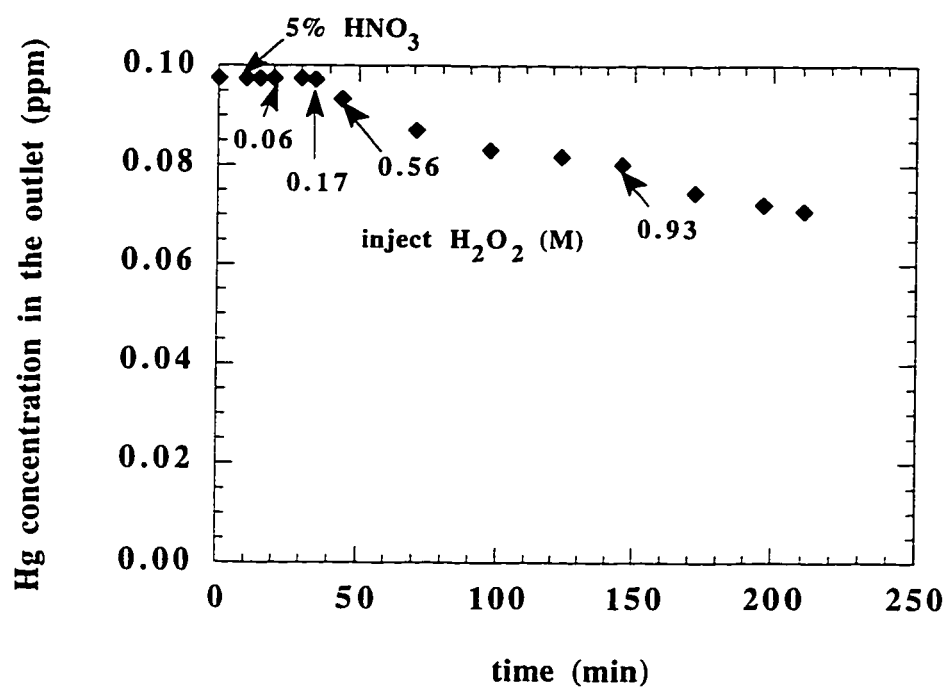
Figure 6.5   Hg absorption in $H_2O_2/0.8$ M HNO_3 at 25°C. Total Hg-N_2 flow rate was 1 l/min.
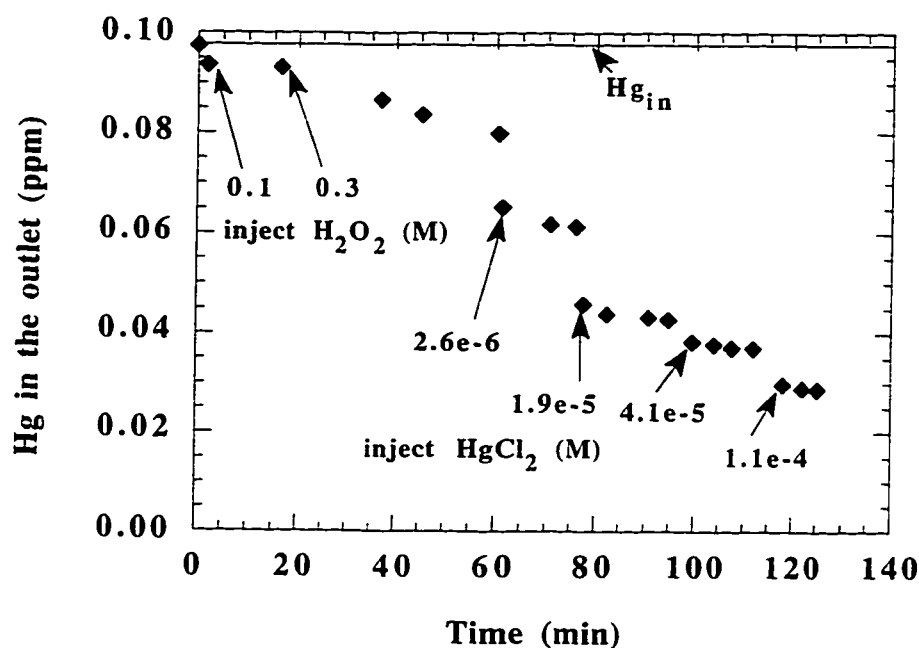
Figure 6.6 Effect of H_2O_2 and Hg(II) on Hg absorption in H_2O_2-0.8 M HNO_3 at 25°C. Total $Hg-N_2$ flow rate was 1 l/min.

Figure 6.7 plots normalized flux, N_{Hg}/P_{Hgi} versus the product of $[H_2O_2]_i$ and $[Hg(II)]_i$. The third order rate constant is $(4.0 \pm 1.1) \times 10^8$ $M^{-2}s^{-1}$ at 25°C and $(88.8 \pm 9.9) \times 10^8$ $M^{-2}s^{-1}$ at 55°C. The experimental data for k_3 were correlated with the following expression:

$$k_3 = 2.13 \times 10^{23} \exp\left(\frac{-10110}{T}\right) \tag{6-15}$$

At our conditions 0.1 mM Hg(II) was sufficient to get 50% gas film resistance. Therefore, there may be specific conditions where elemental Hg will be absorbed by the first impinger in EPA method 29. As a result mercury

89

speciation by sequential absorption in peroxide and permanganate impingers may not give accurate or even reproducible results. In particular, the anomalous results on Hg injection at Shawnee (Peterson et al., 1995) may be explained as absorption of elemental mercury in the first H_2O_2-HNO_3 impinger.
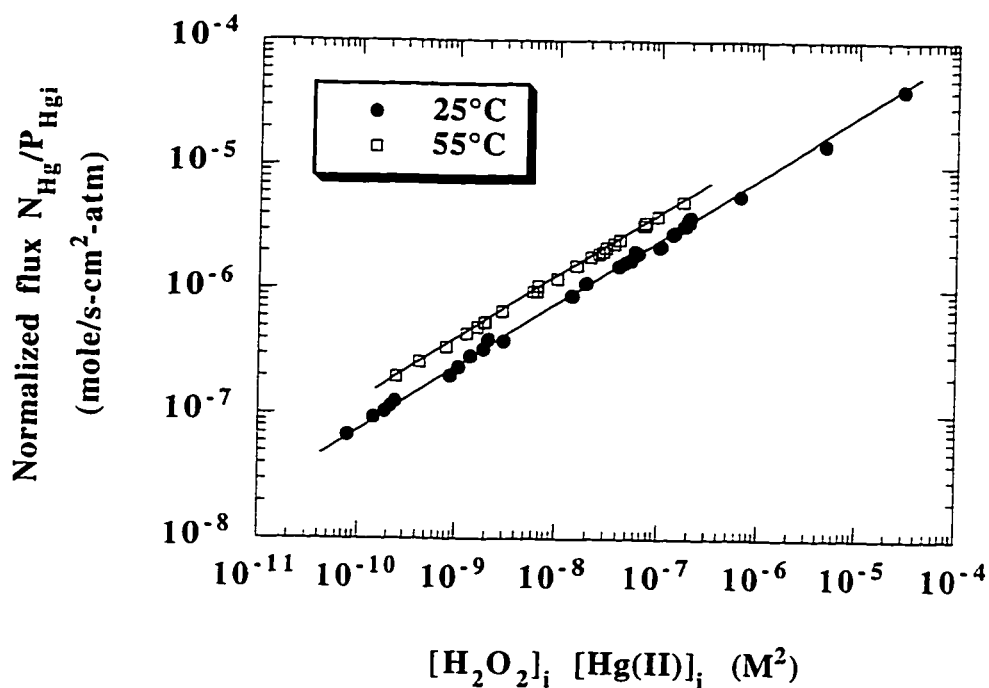
Figure 6.7 The dependence of normalized mercury flux on the product of $[H_2O_2]_i$ and $[Hg(II)]_i$ during mercury absorption in $H_2O_2/0.8$ M HNO_3. Total Hg/N_2 flow rate was 1 l/min. The inlet Hg was tested at 20 and 98 ppb. The injected H_2O_2 was varied between 0.1 and 1.0 M while Hg^{++} was varied between 0 and 1.1×10^{-4} M.

6.4.3.2   *Effect of FeCl₃ in H₂O₂ and HNO₃*

The effect of Fe^{3+} was investigated by adding $FeCl_3$ to H_2O_2-0.8 M HNO_3 with and without external $HgCl_2$ injection. The results are given in figures 6.8 and 6.9.
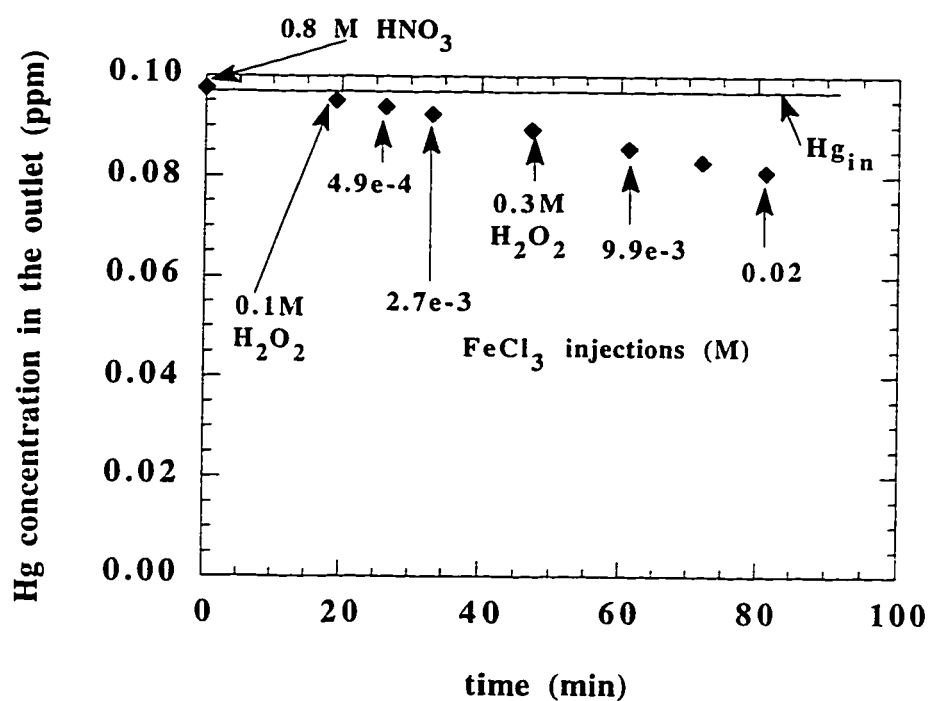
Figure 6.8   The effect of $FeCl_3$ on Hg absorption in H_2O_2-0.8 M HNO_3 at 25°C. Total Hg-N_2 flow rate was 1 l/min.

Two injections of 0.1 and 0.25 M H_2O_2 into 0.8 M HNO_3 gave normal responses. However, four $FeCl_3$ additions ranged from 4.9×10^{-4} to 0.02 M injected between and after the two H_2O_2 injections gave no indication of additional mercury absorption. When 0.4 M H_2O_2, 0.1 mM $HgCl_2$ and 0.8 M

HNO$_3$ were present in the solution, the injection of 0.2 M FeCl$_3$ resulted in noticeable additional mercury removal. However, more FeCl$_3$ injection of 0.4 M gave no additional mercury removal. In figure 6.9, the abnormal high mercury removal obtained from 0.8 M HNO$_3$ might have just been the effects of residual HgCl$_2$ from the last experiment. Nevertheless, it is still effective to see the net effect of individually injected reagent on Hg removal.
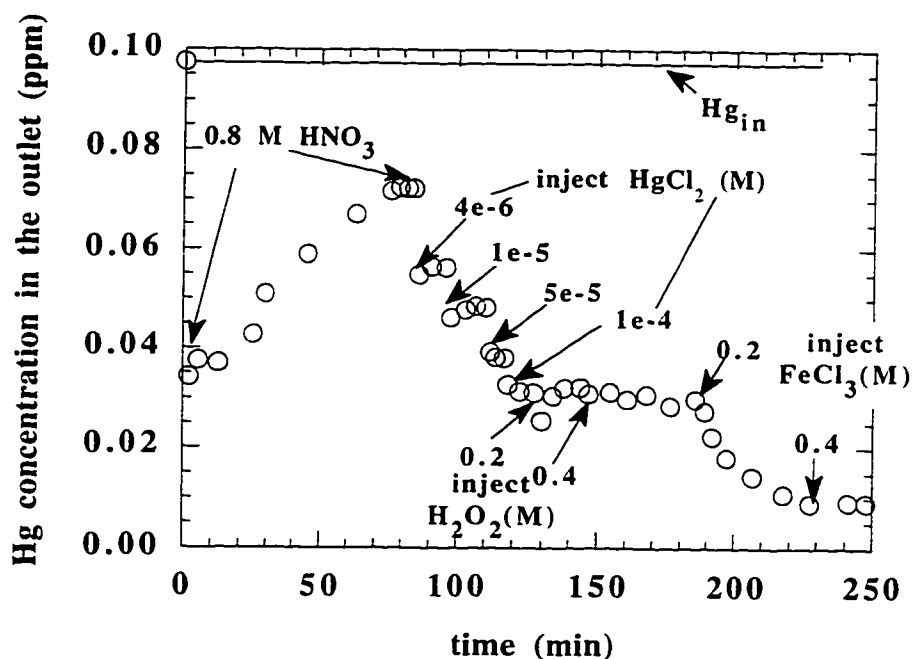
Figure 6.9   The effect of FeCl$_3$ on Hg absorption in H$_2$O$_2$-0.8 M HNO$_3$ with external HgCl$_2$ injections at 25°C. Total Hg-N$_2$ flow rate was 1 l/min.

6.4.3.3   Effect of FeSO₄ in the presence of H₂O₂ and HNO₃

The effect of Fe^{2+} was investigated with 0.3 M H₂O₂-0.8 M HNO₃ in the solution. As shown in figures 6.10 and 6.11, the injection of 0.004 to 0.2 M FeSO₄ gave very little, if any, additional mercury removal.
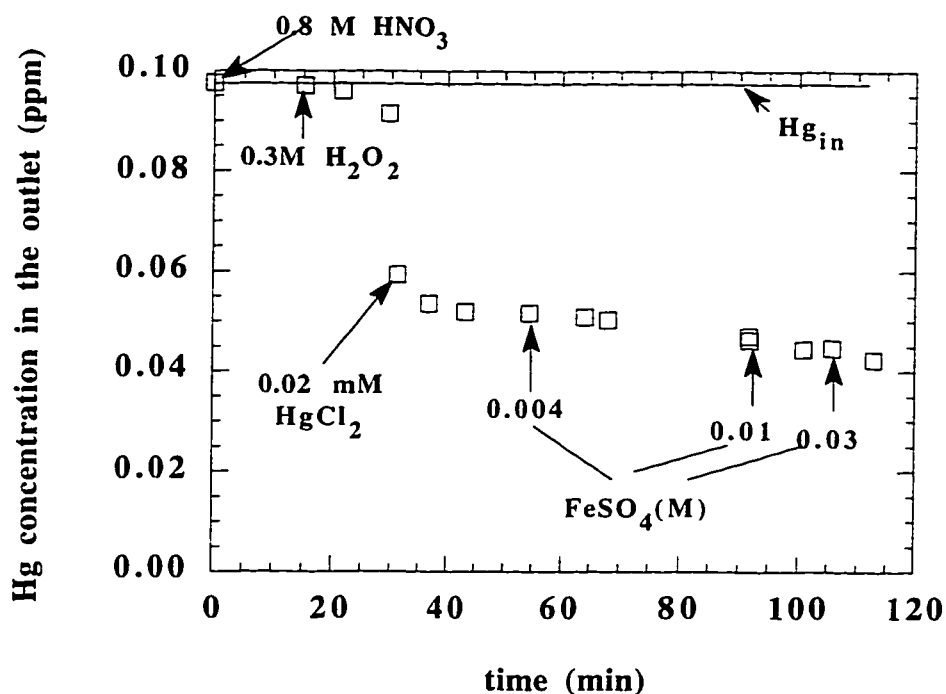
Figure 6.10 The effect of FeSO₄ on Hg absorption in H₂O₂-0.8 M HNO₃ with external HgCl₂ injection at 25°C. Total Hg-N₂ flow rate was 1 l/min.
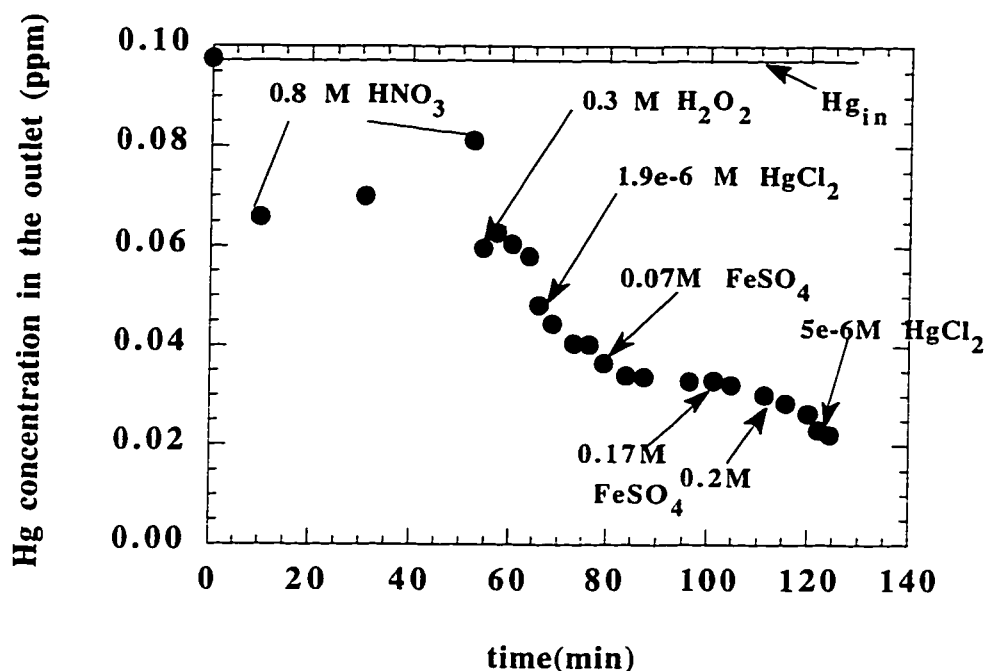
Figure 6.11 The effect of FeSO₄ on Hg absorption in H₂O₂-0.8 M HNO₃ with external HgCl₂ injections at 25°C. Total Hg-N₂ flow rate was 1 l/min.

6.4.3.4 Effect of FeCl₃ or FeSO₄ with only H₂O₂ present (no HNO₃)

Pure water was put into the reactor and was heated and maintained at 55°C. After the bypassed Hg-N₂ reached steady state, a known amount of FeCl₃ solution was injected into the reactor. After reaching steady state, another known amount of FeCl₃ or H₂O₂ was injected. Table 6.7 gives the results of this experiment. A phenomenon was observed for all of the last four H₂O₂ injections that once H₂O₂ was injected into the reactor, the outlet Hg concentration dropped

94

immediately and stabilized for a while, then it increased back to the inlet Hg concentration. One explanation could be that H_2O_2 decomposed. Hg removal was evident only after H_2O_2 and Fe^{3+} concentrations exceeded certain limits.

Table 6.7   Hg absorption in H_2O_2-$FeCl_3$ at 55°C. The Hg-N_2 flow rate was 1 l/min and the inlet Hg was 97.5 ppb.

P_{Hgb} ppb	$\dfrac{N_{Hg}}{P_{Hgi}} \times 10^7$ $\dfrac{mole}{sec\text{-}cm^2\text{-}atm}$	Reagent Injected	Concentration of Injected Reagent mM	Solution pH	k_1 $\dfrac{1}{sec}$
94.8	2.3	H_2O	0.0	7.20	2
94.6	2.4	Fe^{3+}	0.2	2.62	2
94.3	2.7	H_2O_2	0.4	2.70	3
92.9	3.9	Fe^{3+}	1.9	1.56	8
92.8	4.0	Fe^{3+}	8.8	0.92	8
77.2	21.5	H_2O_2	3.8	0.82	265
76.3	22.8	H_2O_2	4.2	0.74	298
70.6	31.9	H_2O_2	9.6	0.77	582
65.5	42.0	H_2O_2	45.9	0.75	1009

In another case, as shown in figure 6.12, the injection of 2 mM $FeSO_4$ to 0.1 M H_2O_2 (no HNO_3) resulted in very little additional Hg removal. External injections of $HgCl_2$ after this resulted in the usual step decrease of the outlet mercury.

95
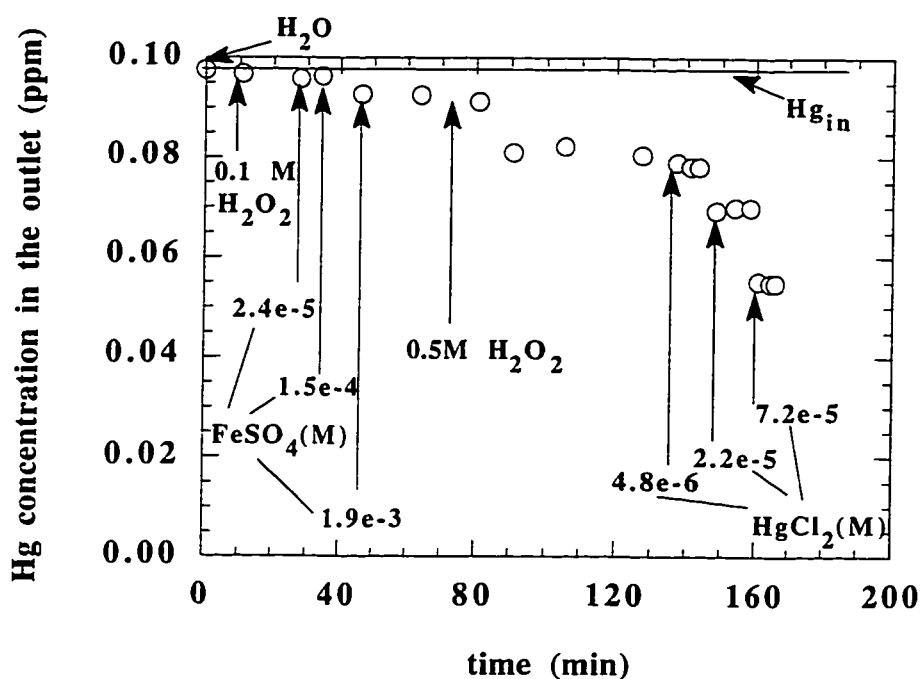
Figure 6.12 The effects of $FeSO_4$ and $HgCl_2$ on Hg absorption in H_2O_2 at 25°C. Total Hg/N_2 flow rate was 1 l/min.

The above results indicate that the presence of Fe^{3+} or Fe^{2+} had no immediate effect on elemental mercury removal. In contrast, as little as 10^{-6} M $HgCl_2$ resulted in dramatic elemental mercury absorption.

In some of the experiments discussed before, HNO_3 seemed to have Hg removal capability, although we speculated that those were not the effect of HNO_3 but rather of residual $HgCl_2$. In order to test this hypothesis, an experiment was designed to test the effect of HNO_3. The results are given in figure 6.13. Three nitric acid injections of 0.1, 0.5 and 0.8 M did not change

outlet mercury concentration. After 0.012 mM $HgCl_2$ was injected into the solution, subsequent 1.5 and 2.9 M HNO_3 injections did not decrease the outlet Hg concentration further. Rather, the 2.9 M HNO_3 injection increased the outlet Hg concentration. This was due to the decrease in $HgCl_2$ concentration when HNO_3 was injected into the solution. The above results prove that HNO_3 alone has no effect on Hg removal. Thus the earlier results suggesting effects of HNO_3 on Hg removal were merely the effects of residual $HgCl_2$. The residual $HgCl_2$ effect was also evident in figure 6.9 with only water present.
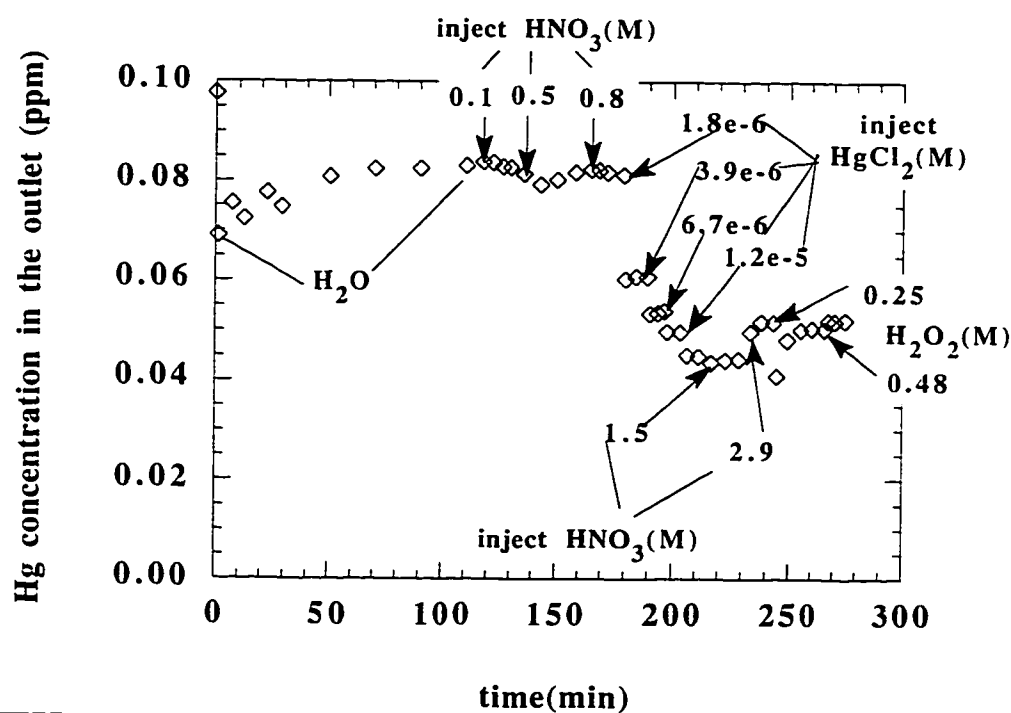
Figure 6.13   The effect of HNO_3 on Hg absorption in H_2O_2-Hg(II) at 25°C. Total Hg-N_2 flow rate was 1 l/min.

6.4.4 Absorption in Mercury(II) and Potassium Dichromate

The rate of reaction between elemental mercury vapor, Hg(II) and potassium dichromate in 0.8 M nitric acid is given by the mechanism:

$$Hg + Hg(II) + Cr_2O_7^= \xrightarrow{\quad H^+ \quad} \text{Products} \tag{6-16}$$
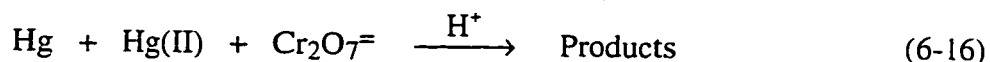
When a fixed amount of HNO_3 and $Cr_2O_7^=$ are present in the solution, the reaction rate can be written as:

$$\text{reaction rate} = k_2 \, [Hg] \, [Hg(II)] \tag{6-17}$$

where k_2 is the pseudo-second-order rate constant.

Using surface renewal theory (Danckwerts, 1970), the flux of elemental mercury, N_{Hg}, should be given by:

$$N_{Hg} = \frac{P_{Hgi}}{H_{Hg}} \sqrt{k_2 \, D_{Hg\text{-}H2O} \, [Hg(II)]_i} \tag{6-18}$$

in the case of constant $Cr_2O_7^=$ concentration.

In the above equations,

$$P_{Hgi} = P_{Hgb} - \frac{N_{Hg}}{k_{g.Hg}} \tag{6-19}$$

$$[Cr_2O_7^=]_i \approx [Cr_2O_7^=]_b \tag{6-20}$$

$$[Hg(II)]_i = [Hg(II)]_{b,\text{ initial injected}} + [Hg(II)]_{absorbed} - \frac{N_{Hg}}{k^o l.Hg^{++}} \tag{6-21}$$

Figure 6.14 gives typical results when $K_2Cr_2O_7$ was used to absorb elemental mercury. The results show that $K_2Cr_2O_7$ alone (without Hg(II) or HNO_3) removes little (if any) Hg, even with $K_2Cr_2O_7$ as high as 39 mM (not shown in figure 6.14 for this particular concentration). However, the combination of $K_2Cr_2O_7$ and $HgCl_2$ absorbs Hg more efficiently than either component alone, as shown in figures 6.15 and 6.16. The presence of HNO_3 further enhanced Hg absorption. In addition, 0.8 M HNO_3 has more positive effects on Hg removal

than increasing $K_2Cr_2O_7$ alone. Solutions with all three components - Hg(II), HNO_3 and $K_2Cr_2O_7$ were the most efficient for mercury absorption compared to those with only one or two components.
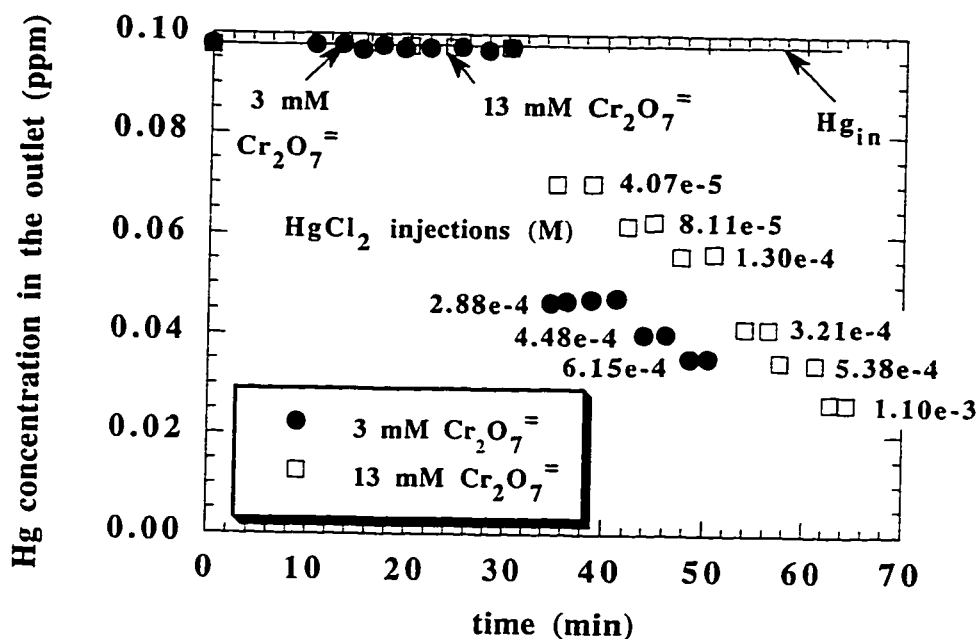
Figure 6.14 Hg absorption in $K_2Cr_2O_7$ and Hg(II) at 25°C. Total Hg-N_2 flow rate was 1 l/min.

Of different combinations of Hg(II), $K_2Cr_2O_7$ and HNO_3 tested, only $K_2Cr_2O_7$-0.8 M HNO_3 with sequential $HgCl_2$ injections exhibited a simple pseudo-second order reaction behavior. The data are tabulated in table 6.8. The pseudo-second order rate constant was 1.4×10^7 $M^{-1}s^{-1}$ at 25°C.

99
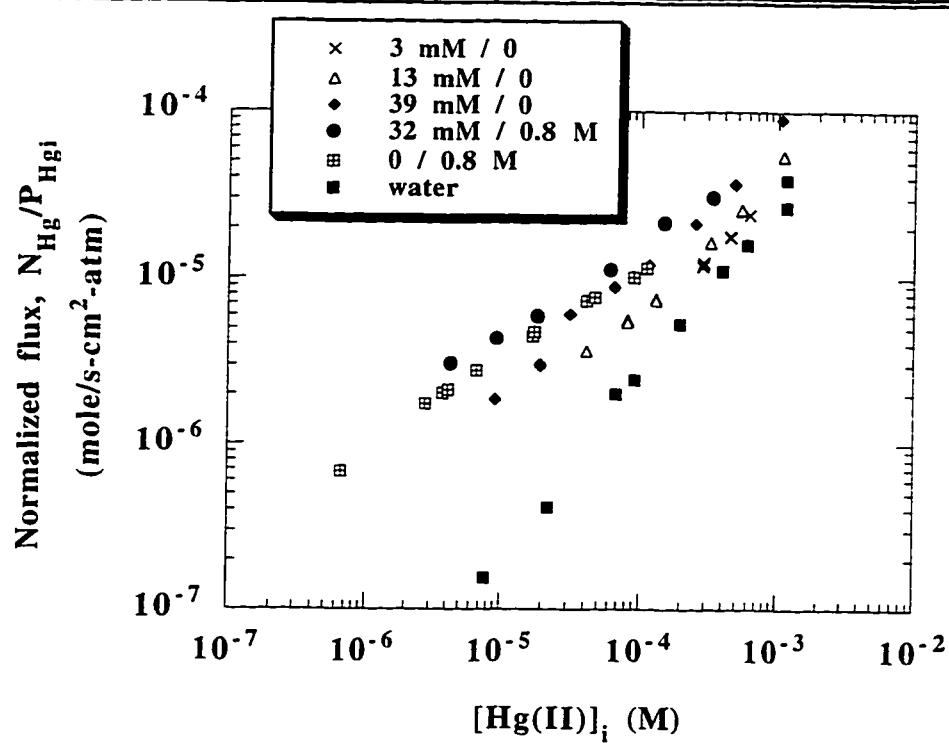
Figure 6.15 The effect of $K_2Cr_2O_7$ and HNO_3 on Hg absorption in Hg(II) at 25°C. Total Hg-N_2 flow rate was 1 l/min. Legends indicate the initial concentrations of $K_2Cr_2O_7$ and HNO_3, respectively.

Table 6.8   Mercury absorption in $K_2Cr_2O_7$-0.8 M HNO_3 with sequential $HgCl_2$ injections at 25°C. Total Hg-N_2 flow rate was 1 l/min. The inlet mercury was 97.6 ppb. Solution pH ranged from 0.37 to 0.47. $k_{g,Hg}$ was 0.4 gmol/s-atm-m^2. $k_1°_{,Hg^{++}}$ was 2.2×10^{-5} m/s. k_2 is the pseudo-second order rate constant with a constant $K_2Cr_2O_7$ concentration of 32.3 mM.

$P_{Hg, b}$ (ppb)	$[Hg(II)]_i$ $\times 10^5$ (M)	N_{Hg} $\times 10^9$ $(\frac{mole}{s\text{-}m^2})$	k_2 $\times 10^{-7}$ $(\frac{1}{M\text{-}s})$
73.3	0.4	2.2	1.5
66.9	0.9	2.7	1.4
60.8	1.8	3.3	1.3
48.1	6.1	4.4	1.4
37.2	14.7	5.4	2.1
32.4	33.0	5.8	1.9
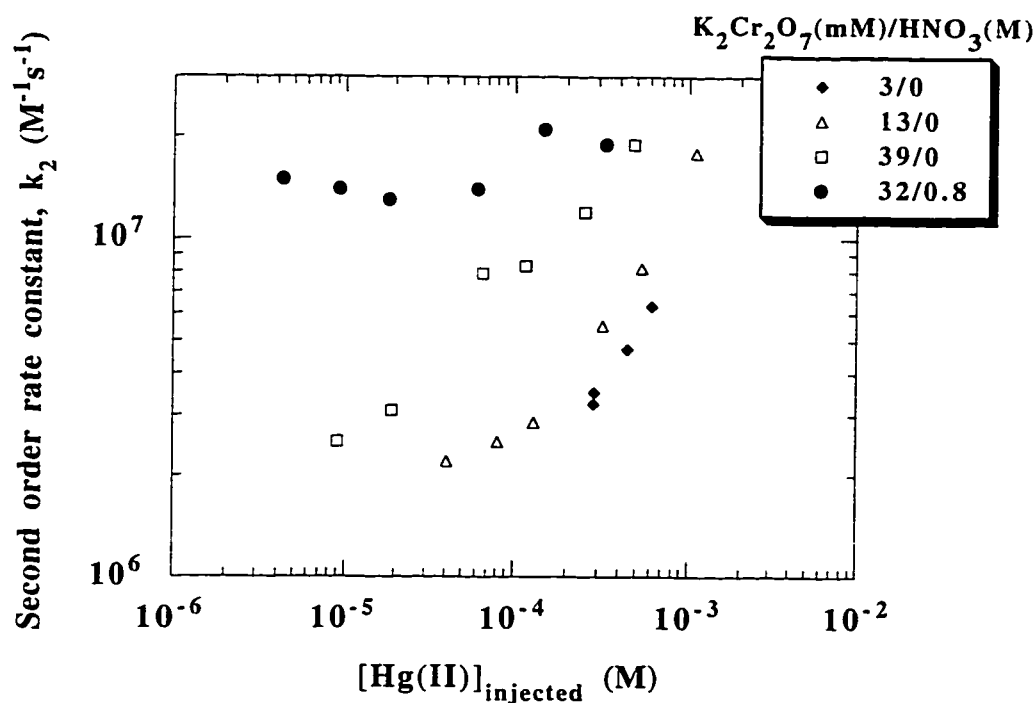
Figure 6.16   The effect of $K_2Cr_2O_7$ and HNO_3 on Hg absorption at 25°C. k_2 was obtained from equation (6-18). Legends indicate the initial concentrations of $K_2Cr_2O_7$ and HNO_3, respectively.

6.4.5 Mercury Absorption in Mercury(II) and Manganese(II) Sulfate

The rate of reaction between elemental mercury vapor, Hg(II) and manganese(II) sulfate is given by the mechanism:

$$Hg \ + \ Hg(II) \ + \ Mn(II) \ \rightarrow \quad Products \tag{6-22}$$
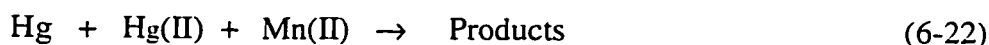
The rate of reaction is:

$$reaction \ rate = k_3 \ [Hg] \ [Hg(II)] \ [Mn(II)] \tag{6-23}$$

Using surface renewal theory (Danckwerts, 1970), the flux of elemental mercury, N_{Hg}, should be given by:

$$N_{Hg} = \frac{P_{Hgi}}{H_{Hg}} \ \sqrt{k_3 \ D_{Hg-H2O} \ [Hg(II)]_i \ [Mn(II)]_i} \tag{6-24}$$

where:

$$P_{Hgi} = P_{Hgb} - \frac{N_{Hg}}{k_{g.Hg}} \tag{6-25}$$

$$[Mn(II)]_i \cong [Mn(II)]_b \tag{6-26}$$

$$[Hg(II)]_i \ = [Hg(II)]_b - \frac{N_{Hg}}{k°_{l.Hg^{++}}} + [Hg(II)]_{absorbed} \tag{6-27}$$

If $[Hg(II)]_b \gg [Hg(II)]_{absorbed}$, then:

$$[Hg(II)]_i \ = [Hg(II)]_b - \frac{N_{Hg}}{k°_{l.Hg^{++}}} \tag{6-28}$$

Figure 6.17 gives the results of mercury absorption in distilled water with sequential $HgCl_2$ and $MnSO_4$ injections at 25°C. No nitric acid or other reagent was present in the solution. The additions of $MnSO_4$ enhanced mercury absorption in Hg(II). However, the enhancement was not significant since substantial amounts of $MnSO_4$ were needed.

Quantitative results are listed in table 6.9. At $MnSO_4$ less than 0.22 M, a third order rate constant of 4.4×10^7 $M^{-2}s^{-1}$ was obtained. A rate constant of 3.3-3.9 $\times 10^7$ $M^{-2}s^{-1}$ was obtained for $MnSO_4$ greater than 0.23 M.

Table 6.9   Effect of Hg(II) and Mn(II) on mercury absorption in $HgCl_2$-$MnSO_4$ at 25°C. Total Hg-N_2 flow rate was 1 l/min. The inlet Hg was 97.7 ppb. $k_{g,Hg}$ was 0.4 gmol/s-atm-m². $k_l°, Hg^{++}$ was 2.2×10^{-5} m/s.

$P_{Hg,b}$ (ppb)	N_{Hg} $\times 10^9$ $(\frac{mole}{s\text{-}m^2})$	$[Hg(II)]_b$ $\times 10^5$ (M)	$[Mn(II)]_b$ (M)	pH	k_3 $\times 10^{-7}$ $(\frac{1}{M^2\text{-}s})$
79.2	1.7	1.8	0.04	-	4.4
76.4	1.9	1.8	0.06	-	4.2
73.4	2.2	1.7	0.08	-	4.1
66.9	2.7	3.5	0.08	-	4.3
58.3	3.5	3.9	0.17	3.89	4.7
56.5	3.7	3.8	0.22	3.81	4.4
55.3	3.8	3.7	0.28	3.72	3.9*
54.4	3.9	3.6	0.38	3.61	3.3*
66.9	2.7	2.9	0.10	4.04	4.3
64.5	3.0	3.0	0.13	3.96	4.3
62.4	3.1	3.0	0.15	3.90	4.4
60.7	3.3	2.9	0.19	3.84	4.4
56.1	3.7	4.2	0.23	3.76	3.9*
55.4	3.8	4.2	0.26	3.72	3.8*
54.3	3.9	4.1	0.31	3.66	3.6*
53.8	3.9	4.0	0.35	3.61	3.4*

*represents data excluded from rate constant regression

6.4.6   Effects of Negative Salts

The effects of five different salts on mercury absorption in Hg(II) was investigated by sequentially injecting $HgCl_2$ and salts.
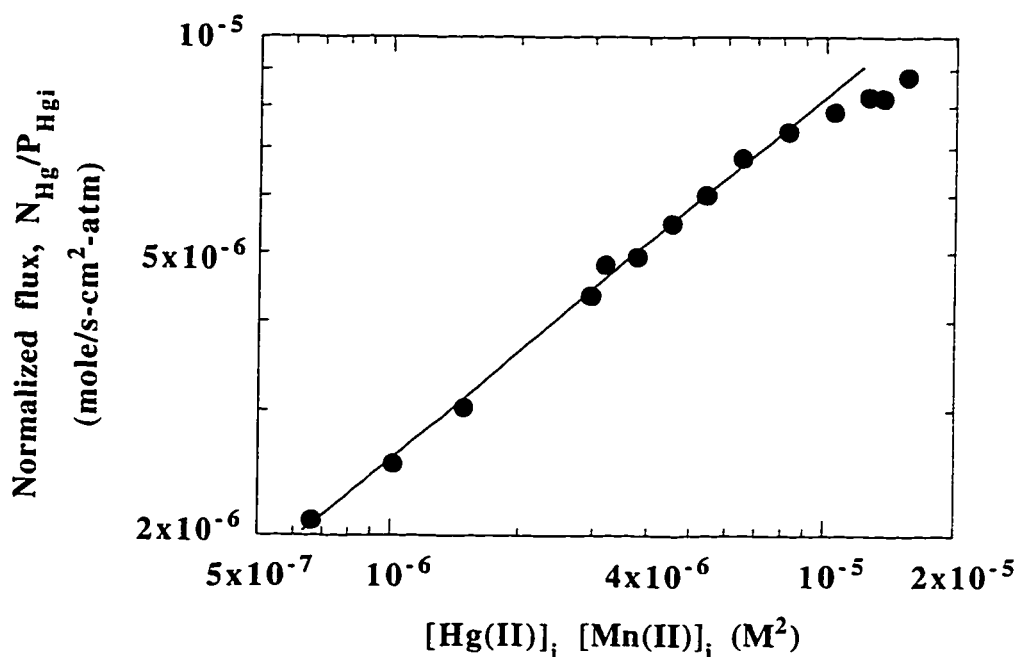
Figure 6.17   Hg absorption in water with sequential $HgCl_2$ and $MnSO_4$ injections at 25°C. The injected Hg(II) ranged from 17 to 42 µM while Mn(II) ranged from 40 to 380 mM.

6.4.6.1   The Effect of NaCl

The K_g' of mercury was smaller than that of $HgCl_2$ alone when 0.1 M NaCl was present in the solution. This indicates that the addition of NaCl inhibited mercury absorption in Hg(II). The comparison is illustrated in figure 6.22.

Table 6.10 summarizes the results of Hg absorption in Hg(II)-NaCl at 25°C with and without oxygen. In the experiment with 20% oxygen mixed with

elemental mercury vapor, 8.8×10^{-6} and 5.5×10^{-5} M $HgCl_2$ were injected into 1 M NaCl solution in which pH was maintained at 6.77-6.78. No mercury removal was observed. Another 3.54×10^{-4} M $HgCl_2$ injection caused the outlet Hg concentration to decrease immediately but gradually increase to near the inlet Hg concentration. pH ranged from 6.72 to 6.73 at this last injection. In an earlier experiment, no O_2 was present in the gas phase and the NaCl concentration was 10 times lower (0.1 M NaCl). Measurable Hg removal was observed when $HgCl_2$ was injected and the normalized Hg flux was lower than with pure water by two orders of magnitude (refer to figure 6.18). This indicates that NaCl inhibits Hg absorption in Hg(II) and the magnitude of the negative effect on Hg removal is proportional to the concentration of NaCl. NaCl inhibits Hg absorption in Hg(II) and the magnitude of the negative effect on Hg removal is proportional to the concentration of NaCl.

Table 6.10   The effect of oxygen and NaCl on Hg absorption in NaCl at 25°C.

NaCl (M)	O_2 (%)	$HgCl_2$ injected (M)	pH	Results or K_g' ($\frac{mole}{s \cdot m^2 \cdot atm}$)
1	20	8.8×10^{-6}	6.78	0
1	20	5.5×10^{-5}	6.77	0
1	20	3.5×10^{-4}	6.72	$Hg_{out} < Hg_{in}$*
0.1	0	5.2×10^{-6}	-	5.8×10^{-4}
0.1	0	1.3×10^{-4}	-	1.9×10^{-2}
0.1	0	3.5×10^{-4}	-	4.6×10^{-2}

* The $HgCl_2$ injection caused the outlet Hg concentration to decrease immediately but gradually increased to near the inlet Hg concentration. So the K_g' value was very small in this case.

6.4.6.2   The Effect of MgSO₄

The presence of $MgSO_4$ inhibited the Hg removal ability of Hg(II). The addition of 9.8×10^{-5} M $HgCl_2$ to 0.02 M $MgSO_4$ gave less Hg removal than 6.8×10^{-5} M $HgCl_2$ alone without $MgSO_4$. The results are given in figure 6.18.
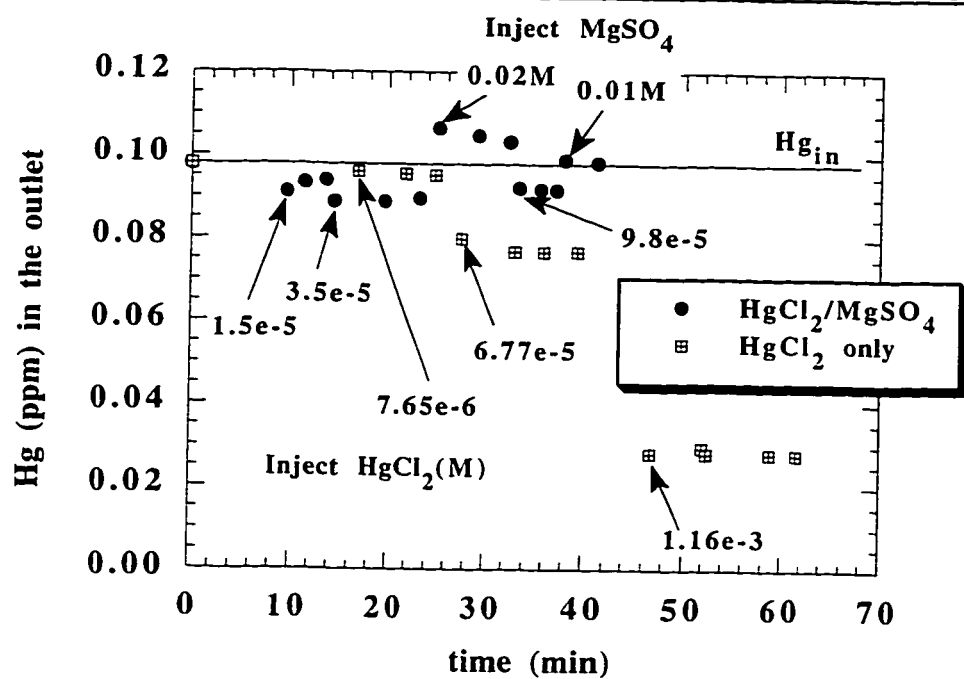
Figure 6.18   The effect of $MgSO_4$ on Hg absorption in Hg(II) at 25°C. Total Hg-N_2 flow rate was 1 l/min.

6.4.6.3   The Effect of FeCl₃

$FeCl_3$ alone did not remove Hg. The presence of $FeCl_3$ inhibited the Hg removal ability of Hg(II). The addition of 1.6×10^{-5} M $HgCl_2$ to 0.01 M $FeCl_3$ had

106

the same Hg removal as 7.7×10^{-6} M $HgCl_2$ alone without $FeCl_3$. The results are given in figure 6.19.
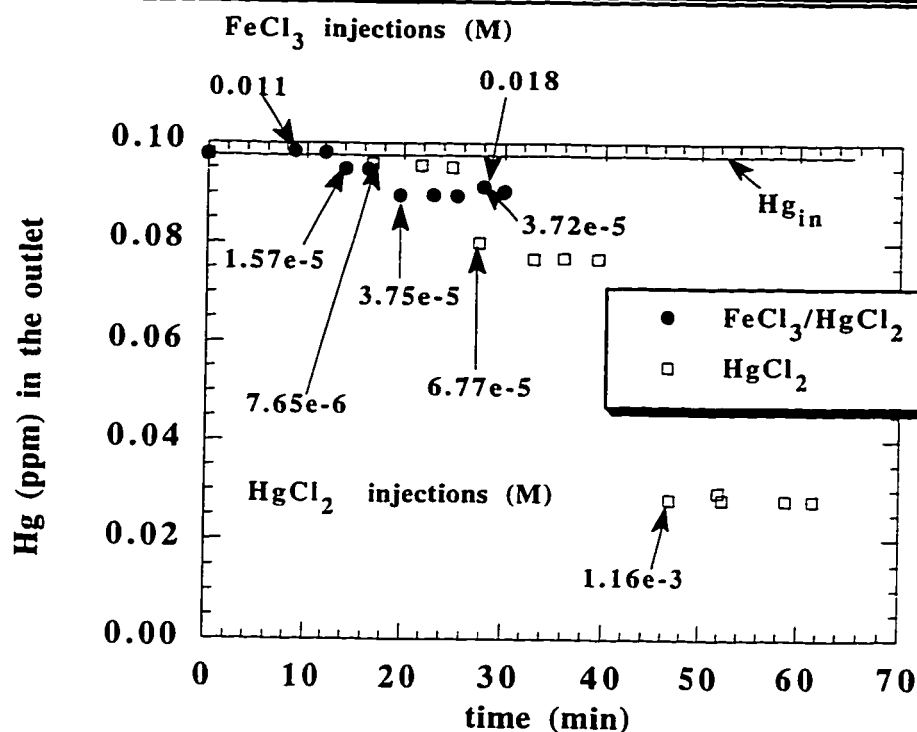
Figure 6.19 The effect of $FeCl_3$ on Hg absorption in Hg(II) at 25°C. Total Hg-N_2 flow rate was 1 l/min.

6.4.6.4   The Effect of $CaCl_2$

$CaCl_2$ alone did not remove Hg. The presence of $CaCl_2$ inhibited the Hg removal ability of Hg(II). The addition of 2.3×10^{-4} M $HgCl_2$ to 0.09 M $CaCl_2$ had less Hg removal than 6.8×10^{-5} M $HgCl_2$ without $CaCl_2$. The results are given in figure 6.20.

107
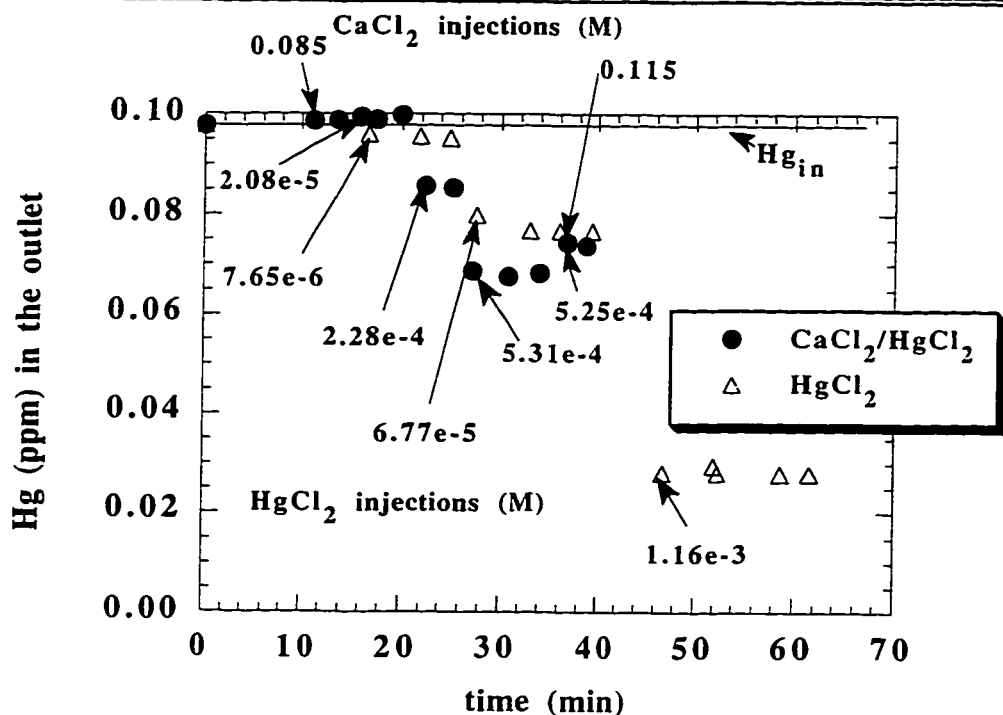
Figure 6.20 The effect of CaCl$_2$ on Hg absorption in Hg(II) at 25°C. Total Hg/N$_2$ flow rate was 1 l/min.

6.4.6.5 The Effect of MgCl$_2$

MgCl$_2$ alone did not remove Hg. The presence of MgCl$_2$ inhibited the Hg removal ability of Hg(II). This was concluded from the fact that 2.1×10^{-5} M HgCl$_2$ in 0.04 M MgCl$_2$ had almost the same Hg removal capability as that of 7.7×10^{-6} M HgCl$_2$ without MgCl$_2$. The results are given in figure 6.21.

108
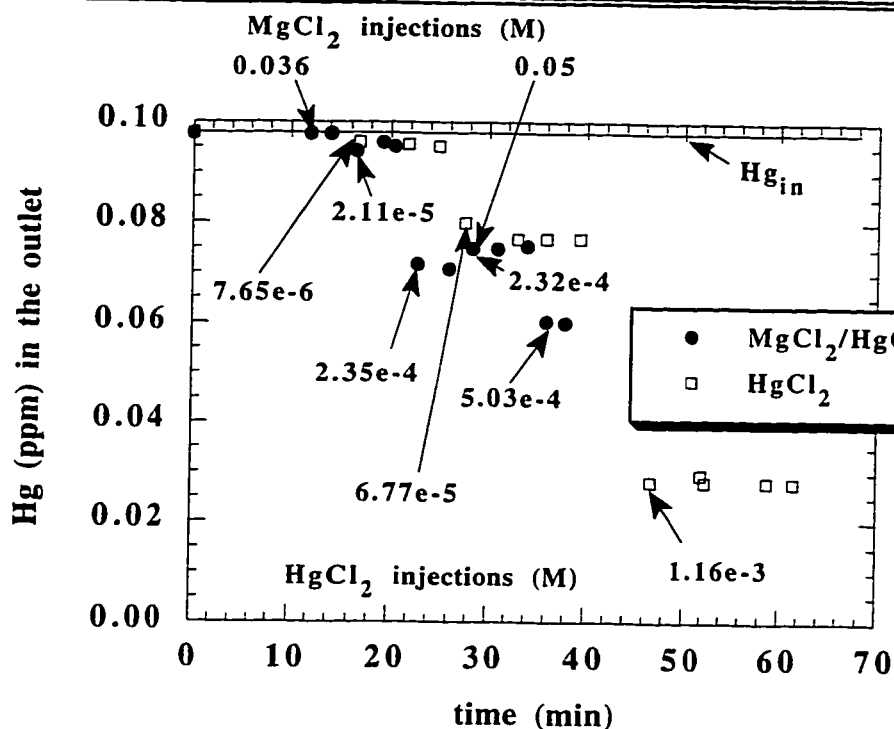
Figure 6.21 The effect of $MgCl_2$ on Hg absorption in Hg(II) at 25°C. Total Hg/N_2 flow rate was 1 l/min.

Figure 6.22 summarizes the effects of the above discussed five different salts. The overall third-order rate constant, k_3', assuming a second-order dependence on Hg(II), was obtained from:

$$N_{Hg} = \frac{P_{Hgi}}{H_{Hg}} \sqrt{k_3' \, D_{Hg\text{-}H2O} \, [Hg(II)]_i^2}$$

(6-29)

All of the above salts inhibited the Hg removal ability of Hg(II).

109
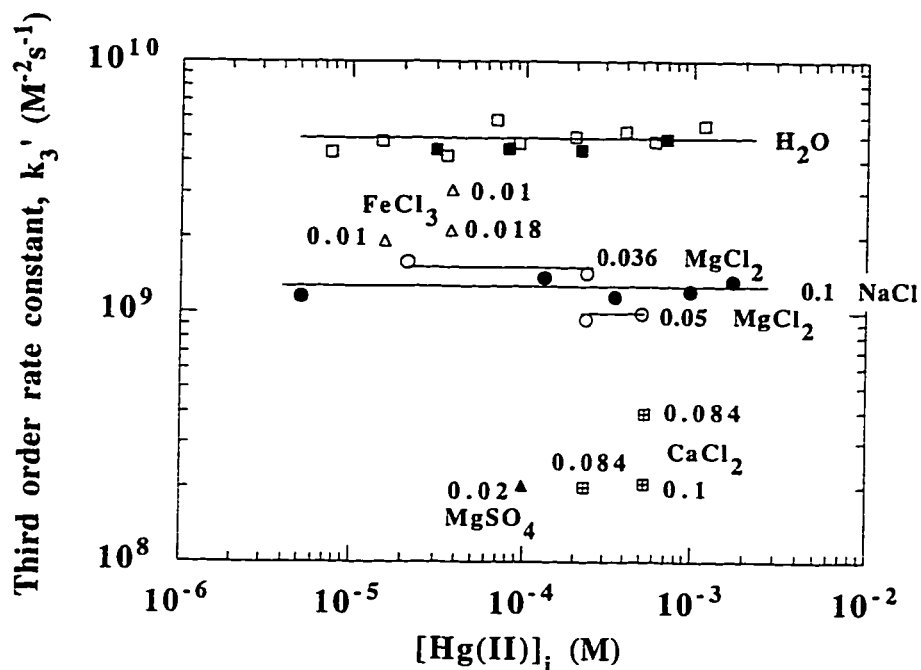
Figure 6.22 The effect of salts (concentrations in M) on Hg absorption at 25°C. k_3' was obtained from equation (6-29). Filled squares represent data with 20% O_2 while empty squares with N_2 only. All other legends represent data with N_2.

6.4.7 SUMMARY OF RESULTS

Table 6.11 gives the summary of rate constants obtained for different aqueous systems. The second and third order rate constants, k_2 and k_3, are calculated from $N_{Hg} = \frac{P_{Hgi}}{H_{Hg}} \sqrt{k_2 \, D_{Hg-H2O} \, [Hg(II)]_i}$ (6-30)

or:

$$N_{Hg} = \frac{P_{Hgi}}{H_{Hg}} \sqrt{k_3 \, D_{Hg-H2O} \, [Hg(II)]_i \, [\text{other active reagent}]_i} \qquad (6-31)$$

respectively.

110

Table 6.11 Summary of the second and third order rate constants, k_2 and k_3, for mercury absorption in different aqueous systems.

Aqueous Solution	T °C	$k_2 \times 10^{-6}$ $\dfrac{1}{M\text{-}s}$	$k_3 \times 10^{-8}$ $\dfrac{1}{M^2\text{-}s}$
$HgCl_2$-0.8 M HNO_3	25 55	7.8 ± 2.1 13.4 ± 8.0	-
$HgCl_2$-H_2O_2-0.8 M HNO_3	25 55	-	4.0 ± 1.1 88.8 ± 9.9
$HgCl_2$-$K_2Cr_2O_7$-0.8 M HNO_3	25	14	4.3^{*}
$HgCl_2$-$MnSO_4$	25	-	0.44

* was measured at 32 mM $K_2Cr_2O_7$ and various $HgCl_2$ in 0.8 M HNO_3

Although the aqueous systems studied were diversified, they all exhibited first order dependence on Hg(II). To compare different systems, the Hg(II) concentration must be specified along with other active liquid or gas components. The effectiveness of the system for Hg removal is expressed as normalized flux, K_g'. The results are listed in table 6.12. At 10^{-5} M Hg(II), 0.26 M H_2O_2-0.8M HNO_3 gives the best mercury removal, followed by 0.03 M $K_2Cr_2O_7$-0.8 M HNO_3, and then 0.1 or 0.8 M HNO_3, or 0.8 M H_2SO_4.

111

Table 6.12 Comparison of K_g' and k_2 at three Hg(II) levels among different systems at 25°C. Data inside parentheses are extrapolated values rather than experimental data. "-" indicates that either no experimental data available or extrapolation was not possible.

Liquid & Gas Composition	Hg(II) M	K_g' x 10^6 $\dfrac{\text{mole}}{\text{s-atm-cm}^2}$	k_2 x 10^{-6} * $\dfrac{1}{\text{M-s}}$	Solution pH
water N$_2$ or 20 % O$_2$	10^{-5} 10^{-4} 10^{-3}	0.16 2.9 29	0.02 0.6 5.6	4.82 ↓ 4.14
0.01 M HNO$_3$ N$_2$	10^{-5} 10^{-4} 10^{-3}	1.3 7.0 41	1.1 3.3 11.0	~ 2
0.1 M HNO$_3$ N$_2$	10^{-5} 10^{-4} 10^{-3}	2.78 13 60	5.2 11.0 24.0	~ 1
0.8 M HNO$_3$ N$_2$	10^{-5} 10^{-4} 10^{-3}	3.5 13 (40)	7.8 7.8 (7.8)	~ 0
0.8 M H$_2$SO$_4$ N$_2$	10^{-5} 10^{-4} 10^{-3}	1.8 13 (100)	2.2 11.0 (67.0)	~ 0
0.8 or 0.9 M HCl N$_2$	10^{-5} 10^{-4} 10^{-3}	Hg$_{out}$ > Hg$_{in}$ and Hg$_{out}$ » Hg$_{in}$ as HgCl$_2$ was increased	-	~ 0.07
0.9 M HCl 20 % O$_2$	10^{-5} 10^{-4} 10^{-3}	(0.021) 0.125 0.75	0.00029 0.001 0.0038	~ 0
0.26 M H$_2$O$_2$ 0.8 M HNO$_3$ N$_2$	10^{-5} 10^{-4} 10^{-3}	11.5 39 (141)	88.2 101.0 (133.0)	~ 0
3 mM K$_2$Cr$_2$O$_7$ N$_2$	10^{-5} 10^{-4} 10^{-3}	0.42 4.0 (37.5)	0.12 1.1 (9.4)	-
13 mM K$_2$Cr$_2$O$_7$ N$_2$	10^{-5} 10^{-4} 10^{-3}	(1.1) 6.8 46	(0.81) 3.1 14.0	4.37 ↓ 4.15
39 mM K$_2$Cr$_2$O$_7$ N$_2$	10^{-5} 10^{-4} 10^{-3}	2.0 12.5 82	2.7 10.0 45.0	4.80 ↓ 4.02
32 mM K$_2$Cr$_2$O$_7$ 0.8 M HNO$_3$ N$_2$	10^{-5} 10^{-4} 10^{-3}	4.5 15 (48)	14.0 14.0 14.0	0.47 ↓ 0.37

112

0.1 M MnSO$_4$ N$_2$	10^{-5} 10^{-4} 10^{-3}	2.3 (8.0) (50)	3.5 (4.3) (16.7)	~ 4.0
0.011 M FeCl$_3$ N$_2$	10^{-5} 10^{-4} 10^{-3}	0.14 (2.3) (36)	0.017 (0.353) (8.65)	2.38 ↓ 2.41
0.084 M CaCl$_2$ N$_2$	10^{-5} 10^{-4} 10^{-3}	0.02 0.4 9.1	0.000267 0.0107 0.552	9.42 ↓ 9.09
0.036 M MgCl$_2$ N$_2$	10^{-5} 10^{-4} 10^{-3}	0.16 1.6 16	0.017 0.17 1.71	5.57 ↓ 5.39
0.02 M MgSO$_4$ N$_2$	10^{-5} 10^{-4} 10^{-3}	- 0.5 -	- 0.0167 -	-
0.1 M NaCl N$_2$	10^{-5} 10^{-4} 10^{-3}	0.125 1.38 12.5	0.01 0.13 1.0	-
0.01 M NaOH 0.01 M succinic acid N$_2$ or 20 % O$_2$	10^{-5} 10^{-4} 10^{-3}	2.6 9.0 41	4.5 5.4 11.0	5.61 ↓ 5.56
NaHCO$_3$ / NaOH buffer N$_2$ or 20% O$_2$**	10^{-5} 10^{-4} 10^{-3}	Hg$_{out}$ > Hg$_{in}$ and Hg$_{out}$ » Hg$_{in}$ as HgCl$_2$ was increased	-	9.56 ↓ 9.49

* The second order rate constant k_2 was calculated from $N_{Hg} = \dfrac{P_{Hgi}}{H_{Hg}} \sqrt{k_2\ D_{Hg-H2O}\ [Hg(II)]_i}$

** O$_2$ contributed positively to Hg absorption. Refer to section 6.4.2.4 for more information

113

Chapter 7 Mercury Absorption in Aqueous Hypochlorite and Chlorine

Elemental mercury absorption in sodium hypochlorite was investigated over a wide range of hypochlorite concentration and solution pH. Aqueous free chlorine was the active species that oxidized Hg°. An apparent overall second order reaction was observed between Hg° and aqueous free chlorine with $k_2 = 1.7$ x 10^{15} $M^{-1}s^{-1}$ at 25°C and 1.4 x 10^{17} $M^{-1}s^{-1}$ at 55°C. Chlorine desorption was evident at high Cl^- when pH was less than 9. Because of Cl_2 desorption at low to intermediate pH with high Cl^-, kinetic information was difficult to obtain in that region. However, data gathered at low to intermediate pH with low Cl^- agreed well with results of high pH with high Cl^-, when concentration was corrected for the effect of ionic strength.

Because of chlorine desorption at low to intermediate pH with high Cl^-, the reaction between gaseous chlorine and Hg° vapor was further investigated. A fast reaction occurred between Hg° and chlorine at room temperature on apparatus surfaces. Chlorine concentration, moisture, and solid surface area contributed positively to mercury removal.

7.1 PREVIOUS WORK

7.1.1 Mercury Oxidation by Hypochlorite

The capability of hypochlorite to dissolve mercury has long been recognized. Parks and Baker (1969) described the recovery of mercury by contacting mercury containing material with a hypochlorite solution maintained at

pH of 4.5 to 9.5 to dissolve mercury in the hypochlorite solution. Nguyen (1979) demonstrated the use of hypochlorite to treat mercury-containing waste water from chlor-alkali plants. Nene and Rane (1981) reported quantitative results on mercury absorption in 5.8-27 mM sodium hypochlorite and 2.6-9.5 mM hypochlorous acid. They concluded that hypochlorous acid was much more reactive than hypochlorite. With hypochlorite, reactivity further increased in the presence of sodium or potassium chloride. Potassium hypochlorite was more reactive than sodium hypochlorite.

7.1.2 Gas Phase Reaction of Mercury and Chlorine

Medhekar et al. (1979) reported surface reaction of mercury with chlorine at 250°C to form a compound with a stoichiometric formula of $(HgCl_2)_n$. Cylindrical test cells made from four different materials were tested. Their initial observations rated the reactivity in the sequence: Teflon-coated stainless steel > stainless steel > quartz > Inconel. However, it was also observed that after several runs the reaction rate became faster until it eventually became independent of the surface material. They concluded that it was likely that the reaction products formed on the surface $(HgCl_2)$ coated the surfaces and thus made all surfaces essentially the same.

Other investigators observed reaction between mercury and chlorine as well. McCannon and Woodfin (1977) reported that a reduced amount of mercury vapor was detected by atomic absorption if the gas mixture contained more than a few ppm chlorine. The reduction in mercury vapor concentration was attributed to the formation of reaction products between mercury and chlorine. Menke and

Wallis (1980) studied the gas phase reaction of mercury with chlorine in a cylindrical quartz tube with four levels of Cl_2 concentration (0, 0.5, 1.5 and 3.8 ppm) and two levels of relative humidity (13% and 80%). They concluded that at constant mercury concentration, the rate of the formation of $Hg-Cl_2$ reaction product (possibly $HgCl_2$) increased with chlorine concentration and relative humidity. They also observed adsorption of $Hg-Cl_2$ reaction product on the quartz walls.

7.2   EXPERIMENTAL METHOD

All experiments were performed in the well-characterized stirred cell reactor with Teflon surfaces described in chapter 3.

In a typical experiment, 1.06 liters of distilled water was put into the reactor while $Hg°$ in nitrogen bypassed the reactor. After the mercury analyzer gave a stable reading, the mercury stream was passed over the distilled water inside the reactor. This condition was used to calibrate the analyzer. After the analyzer gave a stable reading, known amounts of sodium hypochlorite solution (Fisher Scientific, Purified Grade, 4-6 wt%) were sequentially injected into the water using a syringe with a long needle. In some experiments, a small amount ($\leq$ 1 ml) of 0.01 or 0.1 M HCl (EM Science, 36.5-38 wt%, GR) or NaOH (Spectrum Chemical, pellets) solution was injected to modify pH while $Hg-N_2$ was passed over the solution. The outlet concentration of $Hg°$ was analyzed continuously and recorded by the strip chart recorder (Soltec Model 1242).

The rate of mercury absorption was calculated from the gas phase material balance. A three-point calibration was performed before and after each run to

account for the effect of base line drifting of the mercury analyzer. Hypochlorite addition to the liquid phase was determined by titration (Appendix F). When hypochlorite was too dilute to be titrated, the syringe was weighed before and after the injection to obtain the amount of hypochlorite injected.

During the studies of gas phase reaction of mercury and chlorine (Matheson Gas Products, 972 ppm Cl_2 with N_2 balance), a variety of apparatus configurations were used. The largest Teflon surface area was exposed with all of the tubing and the reactor in the gas flow path. When the gas stream bypassed the reactor, the surface area of the reactor was excluded. When the gas stream bypassed the reactor and all of the tubing before the analyzer, the least amount of surface area was exposed to the Hg-Cl_2 stream.

7.3 MASS TRANSFER WITH SIMULTANEOUS CHEMICAL REACTION

In aqueous hypochlorite solution, the distribution of OCl^-, $HOCl$ and Cl_2 depends on solution pH and $[Cl^-]$. Since lower pH gives higher Hg removal, it is possible that free Cl_2 is the active species that reacts with Hg. Due to the wide concentration ranges of NaCl and NaOCl in the solution, the ionic strength has a significant impact on the interpretation of experimental results. The activities of the aqueous species were used instead of concentrations. The activity of free Cl_2 can be obtained from the two equilibria:

$$HOCl \xleftrightarrow{K_1} H^+ + OCl^- \tag{7-1}$$

$$Cl_2 + H_2O \xleftrightarrow{K_2} HOCl + Cl^- + H^+ \tag{7-2}$$
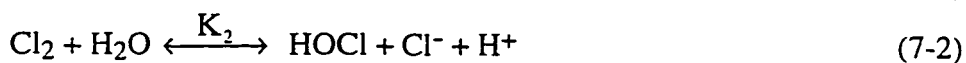
where:

$$K_1 = \frac{a_{H^+}\, a_{OCl^-}}{a_{HOCl}} \tag{7-3}$$

117

$$K_2 = \frac{a_{HOCl}\, a_{Cl^-}\, a_{H^+}}{a_{Cl_2}}$$ (7-4)

and:

[Total NaOCl] = [Cl$_2$] + [OCl$^-$] + [HOCl] (7-5)

$a_{H^+} = 10^{(\text{-measured pH})}$ (7-6)

$a_{HOCl} = \gamma_{HOCl}$ [HOCl] (7-7)

$a_{OCl^-} = \gamma_{OCl^-}$ [OCl$^-$] (7-8)

$a_{Cl_2} = \gamma_{Cl_2}$ [Cl$_2$] (7-9)

$a_{Cl^-} = \gamma_{Cl^-}$ [Cl$^-$] (7-10)

$a_{NaCl} = \gamma_{NaCl}$ [NaCl] (7-11)

Thus:

$$a_{Cl_2} = \frac{[\text{Total NaOCl}]}{\dfrac{1}{\gamma_{Cl_2}} + \dfrac{K_2}{\gamma_{HOCl}\, a_{Cl^-}\, a_{H^+}} + \dfrac{K_1\, K_2}{\gamma_{OCl^-}\, a_{Cl^-}\, a_{H^+}^2}}$$ (7-12)

By using the following assumptions,

$\gamma_{Cl_2} = \gamma_{HOCl} = 1$ (γ of molecule is near 1) (7-13)

$\gamma_{Cl^-} = \gamma_{OCl^-} = \gamma_{NaCl}$ (7-14)

equation (7-12) can be simplified to:

$$a_{Cl_2} = \frac{[\text{Total NaOCl}]}{1 + \dfrac{K_2}{\gamma_{NaCl}\, [\text{Cl}^-]\, a_{H^+}} + \dfrac{K_1\, K_2}{\gamma_{NaCl}^2\, [\text{Cl}^-]\, a_{H^+}^2}}$$ (7-15)

γ_{NaCl} is the mean activity coefficient of aqueous NaCl solution ($\gamma_{NaCl} = \sqrt{\gamma_{Cl^-}\, \gamma_{Na^+}}$) and its value is determined using the effective NaCl concentration:

[NaCl]$_{\text{effective}}$ = [NaCl] + [NaOCl] (7-16)

γ_{NaCl} is 0.996, 0.903, 0.779 and 0.657 for 0.001, 0.01, 0.1 and 1 M NaCl at 25°C, respectively. γ_{NaCl} is 0.768 for 0.1 M NaCl and 0.655 for 1 M NaCl at

118

55°C (Robinson and Harned, 1941; Lobo and Quaresma, 1989). The temperature dependence of equilibrium constants is given in table 7.1.

Table 7.1   Equilibrium constants at two different temperatures.

Equilibrium Constant	25°C	55°C
K_1 (M)*	3.00×10^{-8}	4.46×10^{-8}
K_2 (M^2)‡	3.94×10^{-4}	7.10×10^{-4}

*obtained from Atkins (1990)   ‡Obtained from Connick and Chia (1959)

We have found that the rate of reaction between elemental mercury vapor and hypochlorite is given by the mechanism:

$$Hg \ + \ Cl_{2(aq)} \ \xrightarrow{\ H^+ \ or \ OH^- \ } \ Products \qquad (7\text{-}17)$$

At constant pH the reaction rate is given with the second order rate constant, k_2:

$$reaction \ rate = k_2 \ [Hg] \ [Cl_2] \qquad (7\text{-}18)$$

Using surface renewal theory with fast reaction near the gas-liquid interface, the flux of elemental mercury, N_{Hg}, should be given by:

$$N_{Hg} = \frac{P_{Hgi}}{H_{Hg}} \ \sqrt{k_2 \ D_{Hg\text{-}H2O} \ [Cl_2]_i} \qquad (7\text{-}19)$$

where:

$$P_{Hgi} = P_{Hgb} - \frac{N_{Hg}}{k_{g.Hg}} \qquad (7\text{-}20)$$

$$[Cl_2]_i \ \approx \ [Cl_2]_b \qquad (7\text{-}21)$$

7.4   MERCURY ABSORPTION IN SODIUM HYPOCHLORITE

Figure 7.1 gives the results of Hg° absorption in aqueous sodium hypochlorite. Although there is no indication of the presence of NaCl in NaOCl by the manufacturer, it is reasonable to assume that for every mole of NaOCl,

there is one mole of NaCl in NaOCl solution. This assumption is based on the

fact that NaOCl was manufactured by bubbling chlorine through NaOH:

$$Cl_2 + 2NaOH \leftrightarrow NaOCl + NaCl + H_2O \qquad (7\text{-}22)$$

Injections of NaOCl resulted in step decreases in the outlet Hg°

concentration. This indicates that NaOCl (with NaCl) absorbs mercury readily

even at high pH. All the systems that we have studied previously absorb Hg well

only at low pH with the presence of strong acid and oxidizer. Hypochlorite is the

only oxidizer we have tested that substantially removes mercury at high pH.
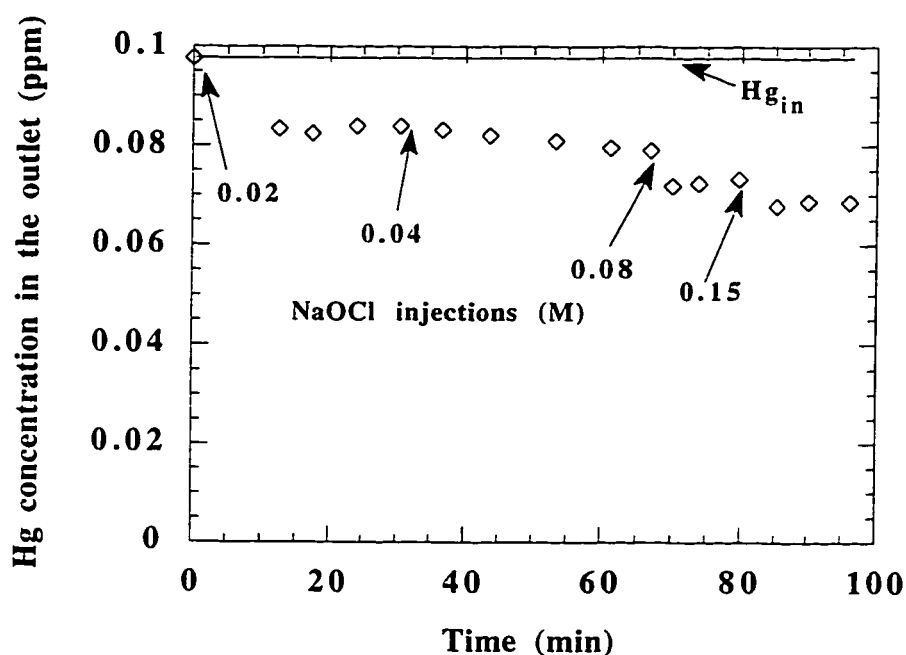
Figure 7.1 Hg absorption in NaOCl at 25°C. NaOCl concentration is obtained from the cumulative amount injected. pH ranged from 10.7 to 11.2. NaCl concentration is assumed to be the same as that of the cumulative amount of NaOCl. Total Hg-N_2 flow rate was 1 l/min.

120
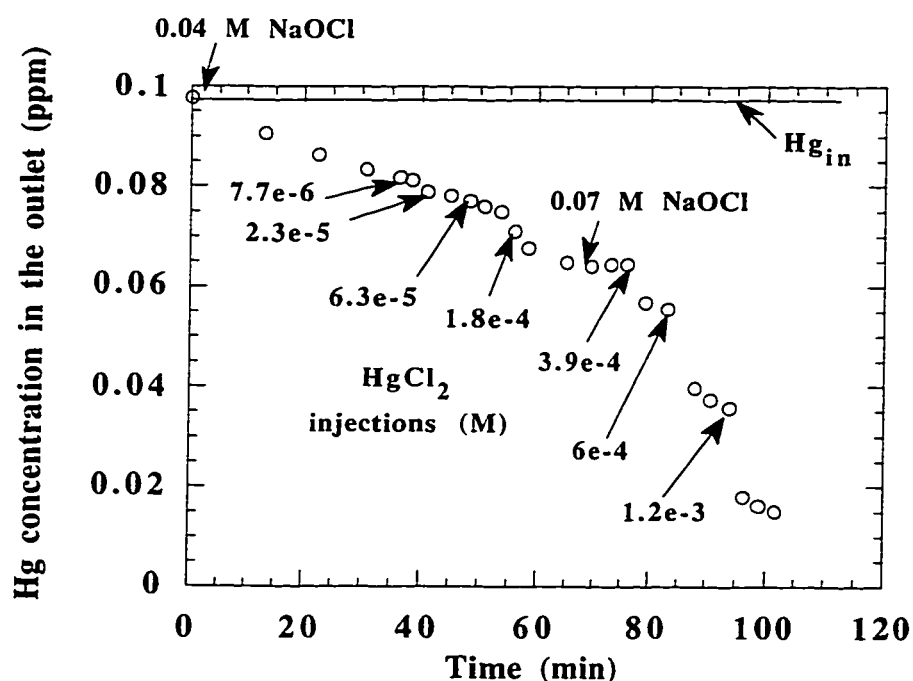
Figure 7.2 Hg absorption in NaOCl and HgCl₂ at 25°C. The concentrations of NaOCl and HgCl₂ are cumulative amounts from injection quantities. pH ranged from 10.2 to 11.1. NaCl concentration is assumed to be the same as that of cumulative amount of injected NaOCl. Total Hg-N₂ flow rate was 1 l/min.

When a small concentration of $HgCl_2$ was injected into relatively large amount of NaOCl, the net effect of $HgCl_2$ was not apparent. However, when relatively large changes in $HgCl_2$, such as 10^{-4} M, were made in 0.1 M NaOCl, the net effect of $HgCl_2$ was significant, as shown in the step decreases in the outlet Hg concentration in figure 7.2. $HgCl_2$ itself did not help to absorb more Hg (refer to section 7.4.4), but rather it reduced the solution pH. Lower pH favors Hg absorption in NaOCl, as shown in section 7.4.2. Small $HgCl_2$ addition to large

121

amount of NaOCl did not lower solution pH significantly. On the contrary, large addition of $HgCl_2$ to relatively dilute NaOCl lowers solution pH significantly and thus absorbs Hg more readily.

7.4.1 Effect of NaCl

The effect of NaCl was investigated by injecting NaOCl into 0.1 and 1 M NaCl solution. The results are given in figure 7.3.
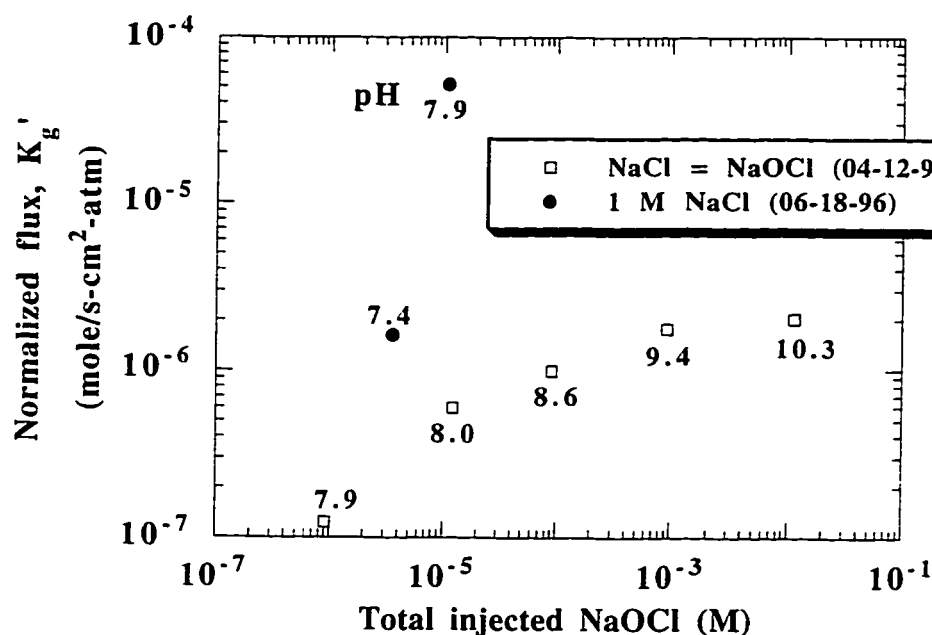

Figure 7.3   The effect of NaCl on Hg absorption in NaOCl at 25°C. Total Hg-N_2 flow rate was 1 l/min.

With a trace amount of NaOCl, the existence of 1 M NaCl greatly enhanced mercury absorption. At 10^{-5} M NaOCl, the normalized flux was

increased by a factor of 70. Controlled pH experiments described later in this chapter indicate that lower pH favors mercury absorption. From the chlorine hydrolysis reaction:

$$Cl_2 + H_2O \leftrightarrow HOCl + H^+ + Cl^- \tag{7-23}$$
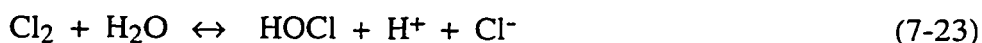
It is obvious that lower pH and higher Cl^- produce more free Cl_2 in the solution. Therefore it is probable that free chlorine is the active species reacting with mercury.

Because of the positive effect of NaCl on mercury absorption in NaOCl, two levels of high NaCl were tested. Figure 7.4 gives the results with 0.1 and 1 M NaCl at controlled pH. The low pH was obtained by adding HCl. At 0.1 M NaCl, injections of both 9.2×10^{-7} and 2.9×10^{-6} M NaOCl caused the outlet Hg to decrease immediately. However, the outlet Hg increased shortly after NaOCl was injected. The outlet mercury concentration continuously increased until it approached the inlet mercury concentration. With 1 M NaCl, injections of NaOCl in the same range caused the outlet mercury concentration to decrease and stabilize at the reduced value. The results indicate that the presence of NaCl either helped absorbed mercury stay in the solution, or it produced enough free chlorine to continuously absorb mercury, or the produced free chlorine desorbed and reacted with Hg on apparatus surfaces.
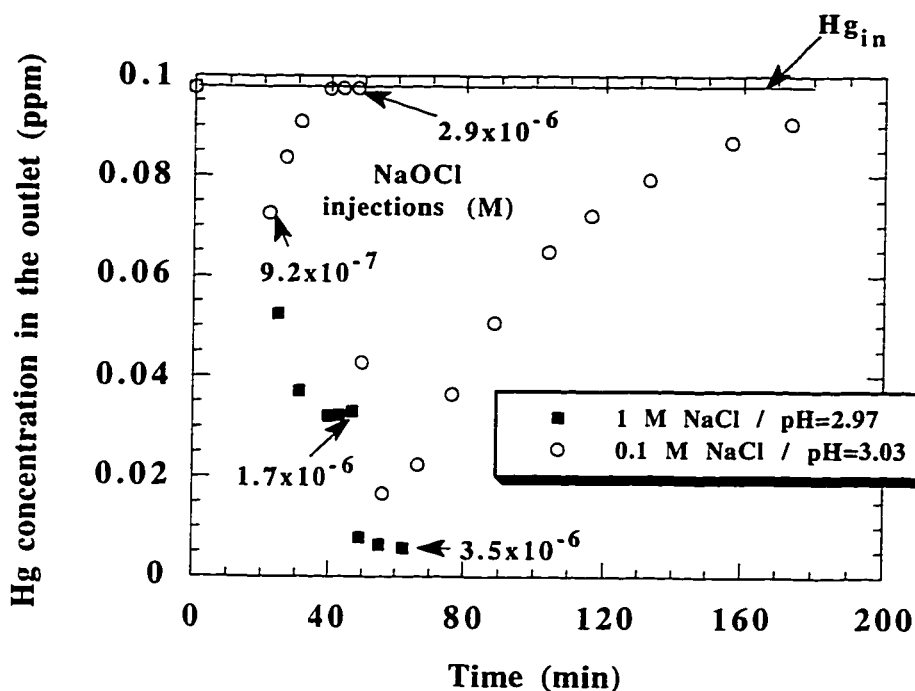
Figure 7.4   The effect of NaCl on Hg absorption in NaOCl at 25°C and pH 3. Total Hg-N_2 flow rate was 1 l/min.

7.4.2   Effect of pH

Figure 7.5 gives the effect of pH on mercury absorption in NaOCl with 1 M NaCl. Lower pH favors mercury absorption. This further indicates that aqueous free chlorine is the active ingredient reacting with Hg. At very high pH, such as pH 11, large amount of NaOCl needs to be injected to reach or near gas phase control. However, at pH 10 or lower, gas phase control was fairly easy to achieve. At intermediate pH, there were some K_g' that exceeded k_g. This extra

amount of Hg removal might have been caused by surface reaction of Hg with desorbed chlorine, which will be discussed in section 7.5.
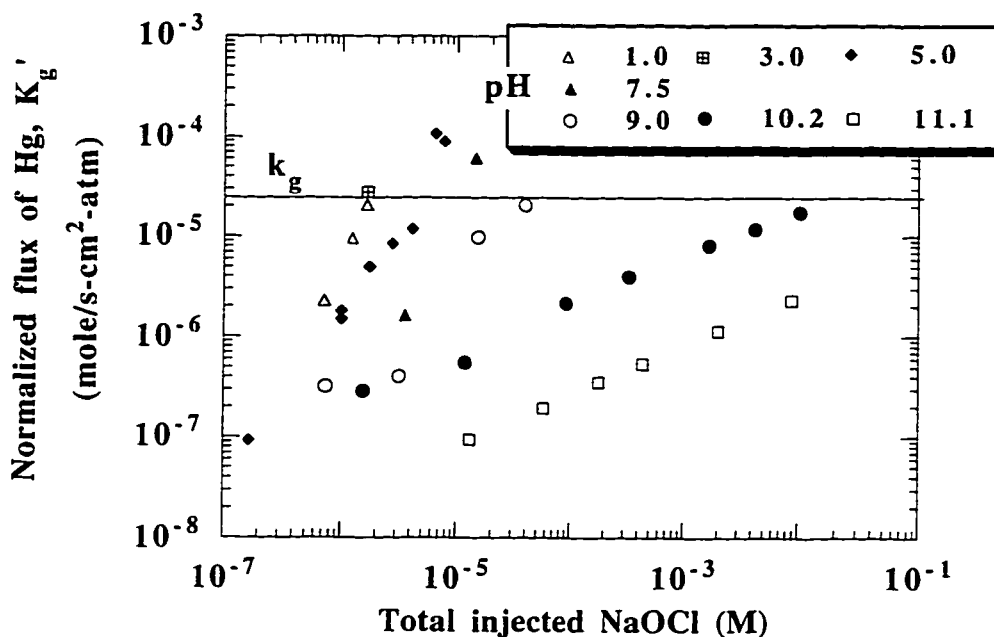

Figure 7.5   The effect of pH during Hg absorption in 1 M NaCl with sequential injections of NaOCl at 25°C. No external $HgCl_2$ injections were made. Total Hg-N_2 flow rate was 1 l/min. Data points for pH < 9 represent the maximum fluxes associated with each injection of NaOCl.

Figure 7.6 gives the activity coefficient of NaCl for concentrations upto 1 M at 25°C. γ_{NaCl} is 0.768 for 0.1 M NaCl and 0.655 for 1 M NaCl at 55°C (Robinson and Harned, 1941).

125
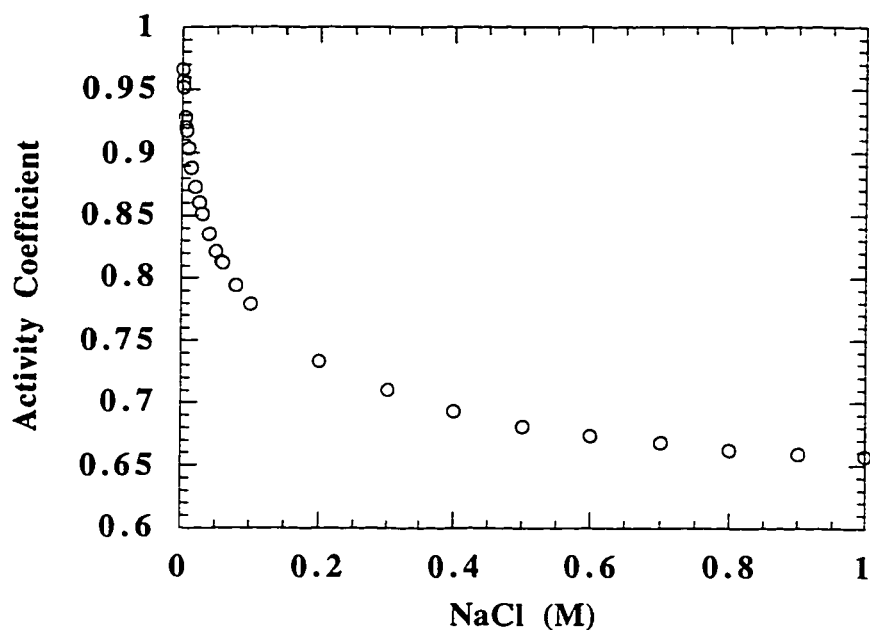
Figure 7.6   The dependence of activity coefficient of NaCl on its concentration
at 25°C (Lobo and Quaresma, 1989).

Figure 7.7 gives the dependence of normalized flux, K_g', on the estimated

activity of free aqueous Cl_2 using equation (7-15). 9×10^{-7} to 1 M NaCl and a pH

range of 4.9 to 11.1 were used in these experiments. By assuming a 1:1 ratio of

NaOCl to NaCl, results without externally adding NaCl to NaOCl were fitted

successfully with controlled NaCl-controlled pH results. The data are tabulated in

tables 7.2a, 7.2b and 7.2c.

○ 9×10^{-7}-0.15 M NaOCl=NaCl, pH=4.9-11.1, 0-0.6 mM $HgCl_2$
♦   1 M NaCl, pH = 9.0-11.1, no $HgCl_2$
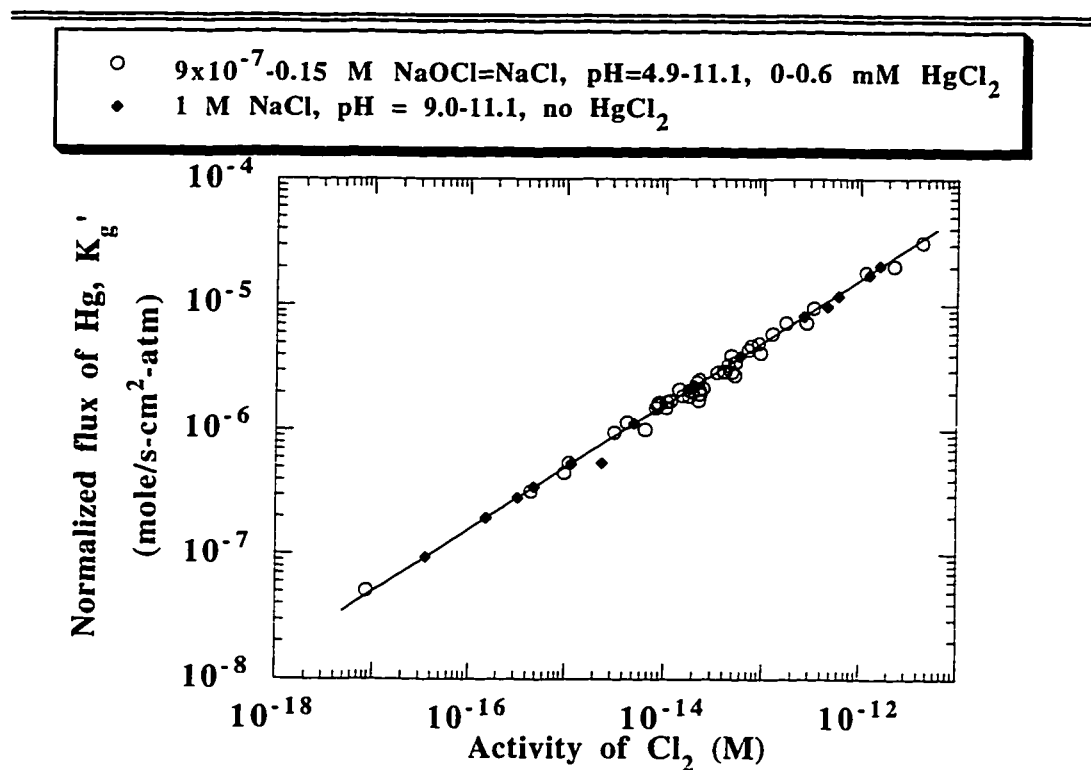
Figure 7.7   Hg absorption in NaOCl-NaCl at 25°C. The wide pH range was obtained by adding NaOCl, $HgCl_2$ or NaOH. Total Hg-N_2 flow rate was 1 l/min.

Table 7.2a   Mercury absorption in NaOCl with or without $HgCl_2$ injection at 25°C. The inlet Hg was 97.7 ppb. $k_{g, Hg}$ = 0.39 mole/s-atm-m^2 and $k°_{l, Hg^{++}}$ = 2.2×10^{-5} m/s. NaCl concentration was assumed to be the same as that of the cumulative amount of NaOCl. Total Hg-N_2 flow rate was 1 l/min.

Run ID	Time	P_{Hgb} $\times 10^8$	P_{Hgi} $\times 10^8$	N_{Hg} $\times 10^{10}$	Injected [Hg^{++}]	[Hg^{++}]$_i$	Injected [NaOCl]	γ_{NaCl}	a_{Cl_2}	pH	k_2 $\times 10^{-15}$
	min	atm	atm	$\frac{mole}{s-m^2}$	M	M	M		M		$\frac{1}{M-s}$
03-06-96	22.4	9.0	8.8	10.2	0	5.2E-08	3.71E-02	0.80	4.3E-15	11.12	2.1
	36.4	8.6	8.2	14.2	7.7E-06	7.7E-06	3.71E-02	0.80	1.2E-14	10.90	1.7
	41.0	8.3	7.8	16.7	2.3E-05	2.3E-05	3.70E-02	0.80	1.4E-14	10.86	2.2

127

Date										
	48.4	8.1	7.6	18.4	6.3E-05	6.3E-05	3.70E-02	0.80	2.1E-14	10.77	1.8
	56.0	7.4	6.8	23.9	1.8E-04	1.8E-04	3.69E-02	0.80	5.3E-14	10.57	1.5
	76.0	6.7	6.0	29.7	1.7E-04	1.7E-04	7.00E-02	0.76	9.1E-14	10.71	1.8
	79.2	6.0	5.0	36.4	3.9E-04	3.9E-04	6.99E-02	0.76	1.7E-13	10.57	2.0
	88.0	4.1	2.8	51.8	6.0E-04	6.0E-04	6.98E-02	0.76	1.1E-12	10.16	2.0
03-07-96	12.4	8.7	8.4	12.8	0	6.2E-08	2.02E-02	0.84	8.3E-15	10.73	1.8
	66.8	8.3	7.9	16.7	0	1.1E-07	4.13E-02	0.79	2.3E-14	10.80	1.3
	70.0	7.5	6.9	23.0	0	1.4E-07	7.83E-02	0.75	4.4E-14	10.91	1.6
	90.0	7.2	6.5	25.8	0	1.8E-07	1.50E-01	0.72	4.8E-14	11.16	2.2
03-27-96	68.0	8.4	8.0	15.7	0	8.4E-08	3.78E-02	0.80	2.3E-14	10.76	1.1
	69.6	8.2	7.8	17.0	0	9.1E-08	3.90E-02	0.80	2.5E-14	10.76	1.3
03-28-96	133.2	6.9	6.1	28.9	2.9E-05	3.0E-05	9.04E-02	0.74	7.6E-14	10.85	2.0
	138.0	6.4	5.5	32.9	1.6E-04	1.6E-04	9.04E-02	0.74	1.3E-13	10.74	1.9
	151.0	5.4	4.4	41.2	3.9E-04	4.0E-04	8.98E-02	0.74	3.3E-13	10.53	1.8
04-01-96	38.8	8.6	8.3	14.0	0	7.7E-08	3.90E-03	0.92	1.1E-14	10.00	1.8
	42.0	8.6	8.2	14.3	0	8.1E-08	3.90E-03	0.92	2.2E-14	9.84	0.9
	52.4	8.5	8.1	15.1	0	9.2E-08	3.63E-03	0.92	1.8E-14	9.86	1.3
04-02-96	28.4	8.6	8.3	13.8	0	7.1E-08	2.58E-03	0.93	8.8E-15	9.87	2.1
	42.8	8.4	8.1	15.2	4.8E-06	4.9E-06	2.58E-03	0.93	1.5E-14	9.75	1.6
	47.2	8.4	8.0	15.5	4.8E-06	4.9E-06	2.58E-03	0.93	2.3E-14	9.66	1.1
	60.0	7.7	7.2	21.3	1.3E-05	1.3E-05	2.58E-03	0.93	4.8E-14	9.50	1.2
	74.4	3.4	1.9	58.5	1.3E-04	1.3E-04	2.35E-03	0.93	4.4E-12	8.46	1.5
04-03-96	37.2	8.8	8.4	12.7	0	6.8E-08	1.17E-03	0.95	1.0E-14	9.50	1.5
	52.4	8.3	7.9	16.5	0	9.6E-08	1.17E-03	0.95	1.8E-14	9.38	1.6
	64.8	8.0	7.5	19.1	0	1.2E-07	1.17E-03	0.95	2.2E-14	9.33	1.9
	76.0	7.8	7.2	21.0	0	1.4E-07	7.22E-03	0.89	3.5E-14	10.00	1.6
	79.2	7.8	7.2	21.2	0	1.4E-07	7.22E-03	0.89	4.0E-14	9.97	1.4
	84.8	7.7	7.2	21.3	0	1.5E-07	7.22E-03	0.89	4.2E-14	9.96	1.4
	95.6	7.1	6.4	26.7	0	1.8E-07	2.72E-02	0.82	9.5E-14	10.32	1.2
	113.2	7.0	6.3	27.7	0	2.1E-07	6.63E-02	0.76	7.2E-14	10.74	1.8
04-12-96	25.6	10.2	10.2	0.5	0	2.7E-09	9.04E-07	0.97	8.6E-18	7.86	2.0
	56.4	9.6	9.5	5.2	0	2.6E-08	1.23E-05	0.97	1.1E-15	7.95	1.8
	94.0	9.2	9.0	8.6	0	5.4E-08	9.08E-05	0.97	3.2E-15	8.64	1.9
	111.2	8.7	8.3	13.3	0	8.6E-08	9.34E-04	0.95	8.8E-15	9.44	1.9
	115.2	8.3	7.9	16.1	0	1.0E-07	1.13E-02	0.87	1.9E-14	10.31	1.4
04-26-96	30.4	9.9	9.8	3.1	0	1.6E-08	8.60E-06	0.97	4.4E-16	8.00	1.5
	50.0	9.7	9.6	4.3	9.3E-06	9.4E-06	8.59E-06	0.97	9.7E-16	7.80	1.4
	60.0	9.2	8.9	9.0	3.0E-05	3.0E-05	8.56E-06	0.97	6.5E-15	7.25	1.0
	66.8	7.8	7.3	20.4	7.7E-05	7.7E-05	8.56E-06	0.97	5.2E-14	6.50	1.0
	73.2	6.0	5.0	36.4	2.0E-04	2.0E-04	8.53E-06	0.97	2.8E-13	5.80	1.3
	78.0	4.0	2.6	53.2	4.4E-04	4.4E-04	8.52E-06	0.97	2.3E-12	4.89	1.2

Table 7.2b Hg absorption in NaOCl with 1 M NaCl at 25°C with pH varied from 9.0 to 11.1 (obtained by adding NaOH). γ_{NaCl} is 0.657. $k_{g, Hg}$ was 0.39 mole/s-atm-m^2 and $k^{\circ}_{l, Hg++}$ was 2.2×10^{-5} m/s. No external HgCl$_2$ injection was made. Hg-N$_2$ flow rate was 1 l/min.

Run ID	Time min	$P_{Hg,b}$ $\times 10^8$ atm	$P_{Hg,i}$ $\times 10^8$ atm	$N_{Hg} \times 10^{10}$ $\dfrac{mole}{sec\ m^2}$	Injected [NaOCl] M	a_{Cl_2} M	pH	$k_2 \times 10^{-15}$ $\dfrac{1}{M\text{-}s}$
05-20-96	45.2	5.3	4.3	41.6	1.5E-05	4.5E-13	9.04	1.4
	71.0	4.0	2.6	53.3	3.9E-05	1.6E-12	8.97	1.7
05-31-96	16.8	9.9	9.8	2.8	1.6E-06	3.3E-16	10.12	1.7
	26.0	9.6	9.5	5.2	1.2E-05	2.4E-15	10.13	0.8*
	43.6	8.3	7.8	16.8	9.1E-05	1.8E-14	10.13	1.7
	100.0	7.2	6.6	25.7	3.3E-04	5.8E-14	10.16	1.8
	120.0	5.7	4.7	38.6	1.7E-03	2.7E-13	10.18	1.7
	127.2	5.0	3.8	44.8	4.3E-03	5.9E-13	10.21	1.5
	138.0	4.2	2.9	51.2	1.0E-02	1.2E-12	10.24	1.6
05-21-96	27.2	10.1	10.1	1.0	1.3E-05	3.5E-17	11.07	1.7
	33.6	10.0	10.0	1.9	5.8E-05	1.5E-16	11.07	1.7
	44.4	9.8	9.8	3.4	1.8E-04	4.8E-16	11.07	1.7
	48.8	9.6	9.5	5.1	4.4E-04	1.2E-15	11.07	1.7
	59.2	9.1	8.8	10.0	2.0E-03	5.0E-15	11.08	1.7
	98.0	8.2	7.7	17.6	8.8E-03	2.0E-14	11.10	1.7

* represents data not included in rate constant regression

Table 7.2c Hg absorption in NaOCl with 0.1 or 1 M NaCl at 55°C with pH varied from 9.3 to 10.1 (obtained by adding NaOH). γ_{NaCl} is 0.655 (1M NaCl) or 0.768 (0.1 M NaCl). $k_{g, Hg}$ was 0.39 mole/s-atm-m^2 and $k^{\circ}_{l, Hg++}$ was $3.9\text{-}4.0 \times 10^{-5}$. Total NaOCl represents cumulatively injected concentration. No external HgCl$_2$ injection was made.

Run ID	Time min	$P_{Hg,b}$ $\times 10^8$ atm	$P_{Hg,i}$ $\times 10^8$ atm	$N_{Hg} \times 10^{10}$ $\dfrac{mole}{sec\ m^2}$	Injected [NaOCl] M	[NaCl] M	a_{Cl_2} M	pH	$k_2 \times 10^{-17}$ $\dfrac{1}{M\text{-}s}$
07-17-96	14.0	9.7	9.6	4.2	9.1E-07	1	9.4E-17	10.06	1.2
	20.0	9.3	9.1	7.1	3.0E-06	1	3.0E-16	10.07	1.2
	29.2	8.5	8.2	13.3	1.1E-05	1	1.2E-15	10.03	1.2
	41.2	6.3	5.5	30.7	3.3E-05	1	5.1E-15	9.97	3.6*
	79.2	4.5	3.4	44.2	8.9E-05	1	1.6E-14	9.94	6.1*
07-23-96	34.4	7.1	6.4	24.6	1.2E-05	0.1	5.2E-15	9.31	1.6
	60.4	5.3	4.4	37.9	3.1E-05	0.1	9.5E-15	9.39	4.6*

* represents data not included in rate constant regression

129

7.4.3   Effect of Temperature

Figure 7.8 gives the results of experiments conducted at 25 and 55°C.

For controlled pH and NaCl experiments with pH $\geq$ 9 and Cl$^-$ $\geq$ 0.1 M, an overall second order reaction between Hg and Cl$_2$ was observed. The combination of high pH and low Cl$^-$ also gave good results. In addition, the same second order behavior was obtained with low Cl$^-$ and low pH, such as with pH = 4.9 and Cl$^-$ = 8.5x10^{-6} M.
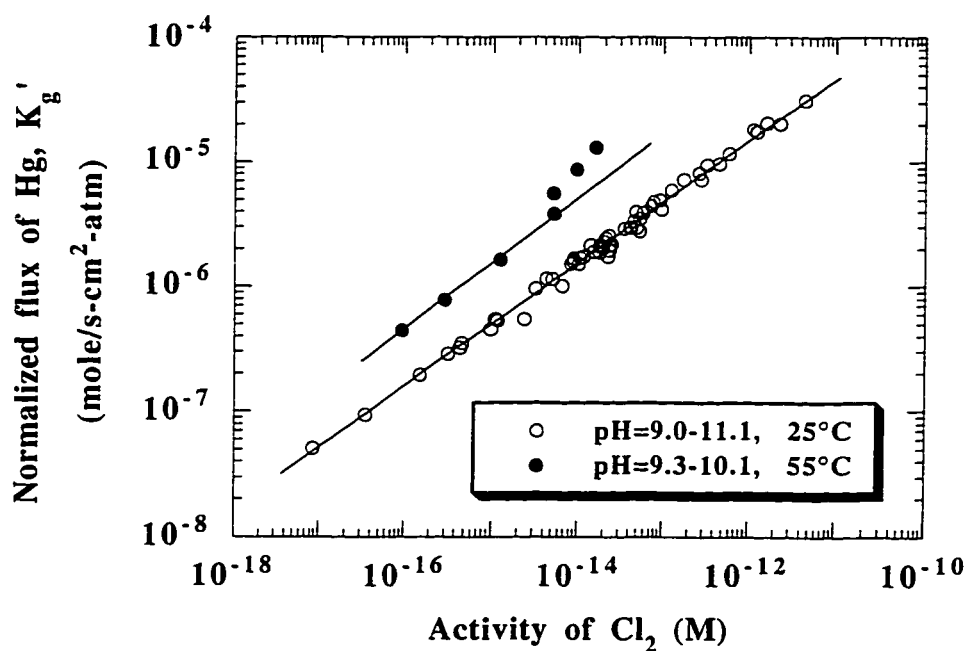
Figure 7.8   Hg absorption in NaOCl-NaCl at 25 and 55°C.   Data at 25°C included some low to intermediate pH results with low Cl$^-$.   No HgCl$_2$ injection was made. Total Hg-N$_2$ flow rate was 1 l/min.

High temperature favors mercury absorption. At 25°C, all data points gave reasonably good fit to second order kinetics. However, high chlorine points at 55°C tended to give higher mercury flux, as shown in figure 7.8. The data of high pH at 55°C are given in table 7.2c. The free chlorine concentration was again calculated from equation (7-15).

The second order rate constant appears to be 1.7×10^{15} $M^{-1}s^{-1}$ at 25°C and 1.4×10^{17} $M^{-1}s^{-1}$ at 55°C.

7.4.4 Effect of HgCl₂

The effect of $HgCl_2$ can be determined from table 7.2a. Since results obtained with external $HgCl_2$ injections (ranged from 4.8×10^{-6} to 1.0×10^{-3} M) gave the same second order rate constant as those without external $HgCl_2$ injection, it was concluded that the addition of $HgCl_2$ did not affect Hg absorption in NaOCl-NaCl solution. The same conclusion can be reached from the results of low to intermediate pH with $Cl^- \geq 0.1$ M (refer to figure 7.11). However, solution pH was lowered by the injection of $HgCl_2$. Lower pH resulted in more free aqueous chlorine and thus absorbed more Hg. It is only in this sense that $HgCl_2$ helped to absorb more Hg.

7.4.5 Results with pH < 9 and Cl⁻ ≥ 0.1 M

At pH > 9, no Cl_2 desorption was apparent. Results with pH as low as 4.9 and low Cl^- (8.5 µM) also agreed well with those of pH > 9 (no Cl_2 desorption was experienced at low pH with low Cl^-. This is expected since such a low amount of Cl^- (8.5 µM) did not result in significant amount of Cl_2). However, at pH < 9 and $Cl^- \geq 0.1$ M, K_g' was lower than expected, as shown in figure 7.9.

131

During these experiments at low pH, the outlet mercury decreased immediately after NaOCl was injected and increased shortly after. Therefore, it is probable that severe chlorine stripping was occurring.
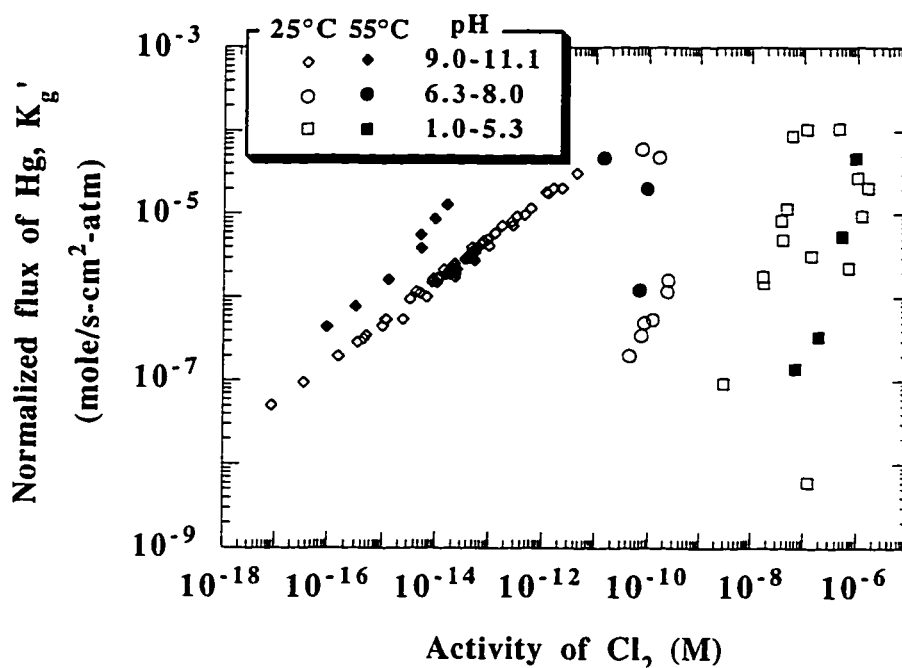
Figure 7.9 Hg absorption in NaOCl-NaCl at 25 and 55°C. Low and intermediate pH results are all with Cl⁻ ≥ 0.1 M. High pH data at 25°C included some low to intermediate pH results with low Cl⁻. All data were those of without external $HgCl_2$ injection except some low to intermediate pH results with low Cl⁻. Data points for low and intermediate pH represent the maximum fluxes associated with each injection of NaOCl. Total Hg-N_2 flow rate was 1 l/min.

At intermediate pH, Cl_2 desorption was experienced only at low NaOCl injections, such as 2.6×10^{-6} M total NaOCl. After each injection of NaOCl, the

132

outlet Hg concentration decreased then increased to a steady-state value which was less than the inlet Hg concentration. With high NaOCl injection, solution pH was always higher than intermediate pH. So this was the same situation as that of pH > 9 and no chlorine desorption was experienced. Due to the complicated chlorine desorption process, it is possible that the activity of free chlorine estimated by equation (7-15) did not represent actual free chlorine activity in the solution.
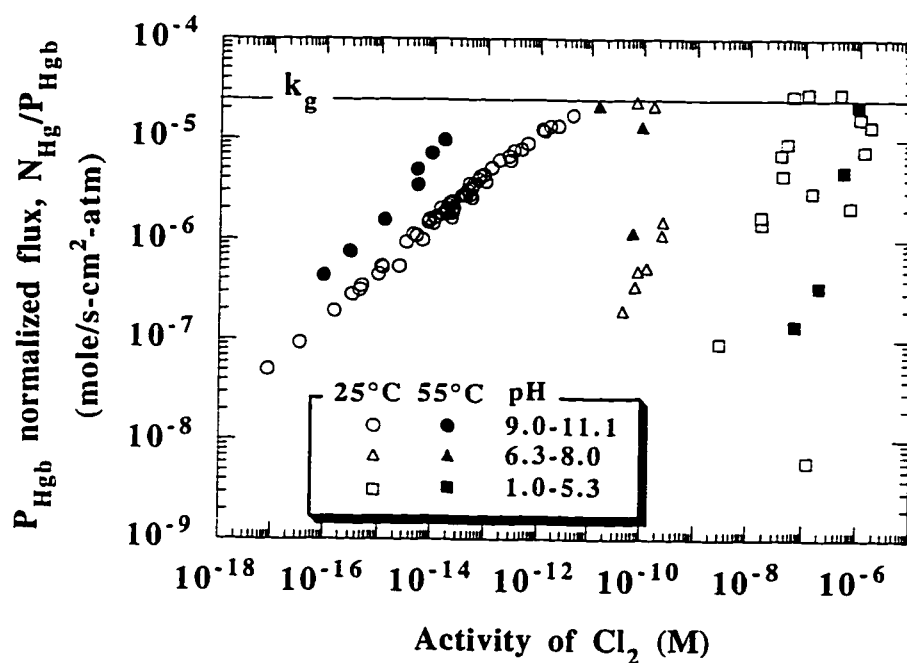
Figure 7.10 The effect of gas phase control on Hg absorption in NaOCl-NaCl at 25 and 55°C. Data points for low and intermediate pH represent the maximum fluxes associated with each injection of NaOCl. Total Hg-N_2 flow rate was 1 l/min.

At low and intermediate pH, NaOCl injection resulted in Cl_2 desorption, with lower than expected Hg flux. High NaOCl injection gave results near or at gas phase control, as shown in figure 7.10. There are even several points that exceeded the gas phase control line. This may have been caused by additional reaction of mercury with chlorine in the gas phase catalyzed by the Teflon surface. Because of Cl_2 desorption, the pH effects, and the high reactivity of Cl_2 with Hg, both in the aqueous solution and gas phase, the kinetics was complicated at low to intermediate pH.
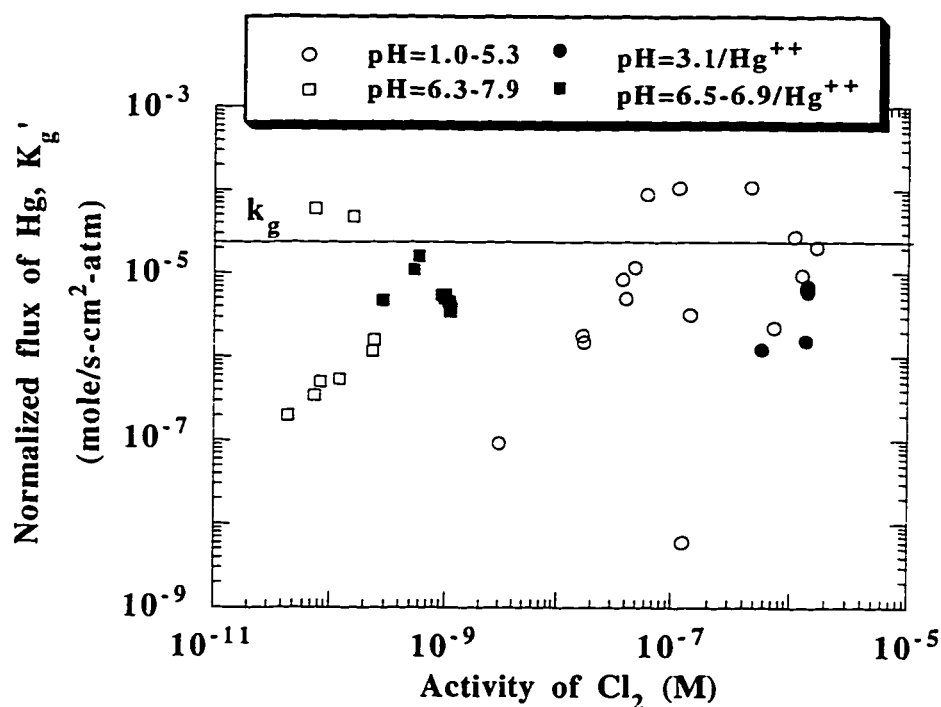
Figure 7.11 Effect of $HgCl_2$ on Hg absorption in NaOCl-NaCl at 25°C. The low pH was obtained by adding HCl. 0.1 or 1 M NaCl was present. No external $HgCl_2$ was injected except indicated in the legends otherwise. Data points represent the maximum fluxes associated with each injection of NaOCl. Total $Hg-N_2$ flow rate was 1 l/min.

134

External $HgCl_2$ injections were made in low and intermediate pH experiments with $Cl^- \geq 0.1$ M. The results are given in figure 7.11. It indicates one more time that $HgCl_2$ did not affect Hg absorption in NaOCl-NaCl.

Results of the experiments at low and intermediate pH with high Cl^- are given in tables 7.3a, 7.3b, and 7.3c. Detailed results are listed in appendix G.

Table 7.3a   Hg absorption in NaOCl-NaCl at low to intermediate pH at 25°C. Data represent the maximun flux in any single reagent addition. The inlet Hg was 97.7 ppb. $k_{g, Hg} = 0.39$ mole/s-atm-m^2 and $k^{\circ}_{l, Hg^{++}} = 2.2 \times 10^{-5}$ m/s. No external $HgCl_2$ injection was made in all of the experiments. $[Hg^{++}]_i = [Hg^{++}]_{absorbed} + \dfrac{N_{Hg}}{k^{\circ}_{l.\,Hg^{++}}}$.   *with 1 M NaCl.

Run ID	time	P_{Hgb} $\times 10^8$	P_{Hgi} $\times 10^8$	N_{Hg}	$[Hg^{++}]_i$ $\times 10^8$	injected NaOCl $\times 10^6$	pH	a_{Cl_2}	k_2
				$\dfrac{mole}{s\text{-}m^2}$					$\dfrac{1}{M\text{-}s}$
	min	atm	atm		M	M		M	
05-10-96	21.6	7.6	7.0	2.2E-09	11.3	0.9	3.04	1.4E-07	4.8E+08
0.1 M NaCl	66.4	2.3	0.6	6.7E-09	37.7	2.9	3.03	4.6E-07	1.7E+11
05-16-96*	24.4	3.5	2.1	5.7E-09	28.1	1.7	2.98	1.1E-06	4.7E+09
05-17-96	18.0	10.2	10.2	6.2E-12	0.0	0.1	0.96	1.2E-07	2.0E+03
1 M NaCl	22.0	8.2	7.8	1.7E-09	8.0	0.7	0.96	7.2E-07	4.7E+07
	80.8	4.0	2.6	5.3E-09	28.5	1.7	0.93	1.6E-06	1.7E+09
05-23-96	20.8	10.1	10.1	9.4E-11	0.5	0.2	4.96	3.0E-09	1.9E+07
1 M NaCl	29.2	8.5	8.2	1.5E-09	6.8	1.0	4.99	1.7E-08	1.3E+09
	38.8	5.6	4.6	3.9E-09	18.5	2.7	5.08	3.7E-08	1.3E+10
	90.0	5.0	3.8	4.5E-09	26.4	4.1	5.15	4.8E-08	2.0E+10
	97.2	2.4	0.8	6.6E-09	37.5	7.7	5.32	6.0E-08	8.6E+11
05-28-96*	28.4	5.4	4.3	4.1E-09	21.4	1.2	1.04	1.2E-06	4.9E+08
05-29-96	13.0	6.8	6.0	3.0E-09	14.3	1.7	4.85	4.0E-08	4.0E+09
1 M NaCl	63.7	2.3	0.6	6.7E-09	36.5	6.4	4.97	1.1E-07	6.7E+11
05-07-96	11.2	9.7	9.6	4.7E-10	2.3	0.9	6.31	8.2E-11	2.0E+10
0.1 M NaCl	18.4	9.0	8.8	1.0E-09	4.9	3.4	6.42	2.3E-10	3.9E+10
05-08-96	21.2	10.0	10.0	2.0E-10	1.0	0.9	6.55	4.5E-11	5.9E+09
0.1 M NaCl	31.8	9.8	9.7	3.4E-10	1.7	2.1	6.67	7.4E-11	1.1E+10
	39.8	9.6	9.5	5.1E-10	2.6	4.1	6.74	1.2E-10	1.6E+10
	70.0	2.9	1.3	6.3E-09	32.2	12.6	7.05	1.6E-10	9.6E+13
06-18-96	6.8	8.7	8.3	1.3E-09	6.3	3.6	7.17	2.4E-10	7.1E+10
1 M NaCl	16.8	2.7	1.1	6.4E-09	30.4	14.4	7.87	7.4E-11	3.2E+14

135

Table 7.3b   Hg absorption in NaOCl-NaCl at low and intermediate pH at 55°C. Data represent the maximun flux in any single reagent addition. Total Hg-N_2 flow rate was 1 l/min. The inlet Hg was 97.7 ppb. $k_{g, Hg}$ = 0.39 mole/s-atm-m^2 and $k°_{l, Hg^{++}}$ = 4.0x10^{-5} m/s. No external $HgCl_2$ injection was made in all of the experiments. $[Hg^{++}]_i$ = $[Hg^{++}]_{absorbed}$ + $\dfrac{N_{Hg}}{k°_{l. Hg^{++}}}$.

Run ID	time	P_{Hgb} x10^8	P_{Hgi} x10^8	N_{Hg} x10^9	absorb $[Hg^{++}]$ x10^8	$[Hg^{++}]_i$ x10^8	injected [NaOCl] x10^6	pH	a_{Cl2}	k_2
	min	atm	atm	$\dfrac{mole}{s\text{-}m^2}$	M	M	M		M	$\dfrac{1}{M\text{-}s}$
07-18-96	32.0	10.1	10.0	0.1	0.1	0.5	0.1	2.88	7.0E-08	1.6E+07
1M NaCl	46.8	9.8	9.7	0.3	0.3	1.1	0.4	2.91	1.9E-07	3.5E+07
55°C	74.0	6.3	5.6	3.0	2.6	10.1	1.0	2.95	5.3E-07	3.2E+09
	96.0	2.7	1.2	5.8	7.5	22.0	1.9	2.94	9.6E-07	1.3E+11
07-24-96	10.8	8.9	8.6	1.1	0.3	2.9	2.6	7.23	6.6E-11	1.3E+12
1M NaCl	28.8	3.8	2.5	5.0	3.0	15.6	8.6	7.46	9.3E-11	2.5E+14
55°C	42.0	2.7	1.2	5.8	6.6	21.2	13.7	8.03	1.4E-11	8.9E+15

Table 7.3c   Hg absorption in NaOCl-NaCl at low and intermediate pH with external $HgCl_2$ injections at 25°C. Data represent the maximun flux in any single reagent addition. The inlet Hg was 97.7 ppb. $k_{g, Hg}$ = 0.39 mole/s-atm-m^2 and $k°_{l, Hg^{++}}$ = 2.2x10^{-5} m/s. Injected NaOCl was the cumulative amount. Total Hg-N_2 flow rate was 1 l/min.

Run ID& [NaCl]$_{initial}$	time	P_{Hgb} x10^8	P_{Hgi} x10^8	N_{Hg} x10^9	$[Hg^{++}]_b$	$[Hg^{++}]_i$	injected [NaOCl]	pH	a_{Cl2}	k_2
	min	atm	atm	$\dfrac{mole}{s\text{-}m^2}$	M	M	M		M	$\dfrac{1}{M\text{-}s}$
05-06-96	20.0	6.8	6.1	2.9	0	1.5E-07	1.1E-05	6.78	2.9E-10	5.2E+11
0.1 M	60.8	5.1	4.0	4.4	7.4E-06	7.7E-06	1.1E-05	6.55	5.2E-10	1.5E+12
	76.0	4.4	3.1	5.0	2.9E-05	3.0E-05	1.1E-05	6.51	5.8E-10	2.9E+12
06-19-96	22.8	6.6	5.8	3.1	0	1.6E-07	5.6E-06	6.87	9.3E-10	2.1E+11
1 M	33.6	7.0	6.4	2.7	2.2E-06	2.4E-06	5.4E-06	6.81	1.1E-09	1.1E+11
	38.0	7.2	6.6	2.5	7.6E-06	7.8E-06	5.4E-06	6.80	1.1E-09	9.0E+10
	42.8	7.4	6.8	2.4	2.6E-05	2.6E-05	5.3E-06	6.80	1.1E-09	7.4E+10
06-20-96	14.0	9.0	8.7	1.1	0	5.1E-08	9.6E-07	3.06	5.7E-07	1.7E+07
1 M	24.4	6.0	5.1	3.6	0	1.7E-07	2.4E-06	3.07	1.4E-06	2.4E+08
	27.2	6.2	5.3	3.5	2.8E-06	3.0E-06	2.3E-06	3.07	1.4E-06	2.1E+08
	32.8	6.4	5.5	3.3	4.1E-05	4.1E-05	2.3E-06	3.07	1.4E-06	1.8E+08
	44.0	6.2	5.4	3.4	2.7E-04	2.7E-04	2.3E-06	3.08	1.4E-06	2.0E+08
	61.6	8.7	8.4	1.3	1.0E-03	1.0E-03	2.3E-06	3.08	1.4E-06	1.2E+07

Appendix H gives the results when interfacial chlorine activity is used instead of bulk chlorine activity. Although this approach somewhat improves the results at low pH with high Cl^-, the K_g' is still lower compared to those of high pH results.

7.5 GAS PHASE REACTION OF ELEMENTAL MERCURY AND CHLORINE

Due to chlorine desorption at $Cl^- \geq 0.1$ M and pH < 9, kinetic information was difficult to obtain under these conditions. In order to understand this phenomenon, various amounts of chlorine were added to elemental Hg in the gas phase. It was estimated from previous experiments that the desorbed Cl_2 during Hg absorption in NaOCl would not exceed 1 ppm. Thus it was assumed that adding a fixed amount of Cl_2 greater than 1 ppm to the gas phase would minimize the effect of chlorine desorption.

Hg-Cl_2 was bypassed the reactor, absorbed into pure water and 1 M NaCl at different pH values. With the coexistence of chlorine and elemental mercury in the gas phase, less elemental mercury was detected at the outlet. Furthermore, higher chlorine concentration gave lower outlet elemental mercury concentration. This was experienced in every experiment. Thus it was concluded that more chlorine resulted in more reaction between elemental mercury and Cl_2.

At the same inlet Cl_2 concentration, the degree of surface contact of the Hg-Cl_2 gas mixture affects results. It was shown that more solid surface area gave less elemental mercury in the outlet. When Hg-Cl_2 bypassed the reactor and Teflon tubes upstream of the analyzer and flowed directly to the mercury analyzer, the Hg-Cl_2 was only exposed to the surface of the gas blending tube and

of the analyzer. This is the first mode of operation in table 7.4. It gave the least amount of surface area exposure. Comparison of this mode to the second mode of normal bypassing shows that solid surface area, even with Teflon coated reactor surface and Teflon tubes, contributes to more reaction between elemental mercury and chlorine.

Table 7.4   Summarized results of chlorine reaction with elemental mercury at 25°C. The inlet Hg concentration was 97 ppb.

Mode	Mode Description	Estimated Teflon Surface Area (m^2)	Inlet Cl_2 (ppm)	Outlet Hg (ppb)
1	Hg & Cl_2 bypassed the reactor and connected directly to Hg analyzer	0.0025	0 5 11 38	97 97 89 17
2	Hg & Cl_2 bypassed the reactor	0.019	0 5 30	97 14 1 - 5
3	only Hg absorbed in H_2O Cl_2 added after the reactor	0.034	0 1.5 10	86 85 81
4	Hg & Cl_2 absorbed in H_2O	0.034	0 1 10	87 71 9 - 14

The third mode in table 7.4 indicates that only Hg absorbed into water. Chlorine was added to the gas stream after the reactor. Under this mode of operation, chlorine was not exposed to a lot of moisture. Less Hg removal was expected.

The fourth mode in table 7.4 is Hg and chlorine absorbed in water. In this mode of operation, Hg was blended with chlorine before the reactor and absorbed into water with all the normal tubing system. In this mode, more mercury loss was observed. This indicates that moisture contributes positively to Hg reaction

138

with Cl_2. It is also expected that chlorine react with Hg quite readily at the water surface.

The history of the experiments also seems to influence the results. Table 7.5 gives the comprehensive experimental results. Each block in the table represents one experiment while each line inside the block represents one mode of operation. If a very high level of chlorine was introduced at the beginning of the experiment, it tended to give more reaction between mercury and chlorine even if a very small amount of chlorine was present later. This indicates that once the reactor or surface was coated with high levels of the reaction product of chlorine and mercury, more reaction could be expected.

Table 7.5   Summary of Hg removal when Cl_2 was added to the gas phase. The experiments were conducted at 25°C with 15 l/min N_2 dilution before the Hg analyzer. Hg-Cl_2-N_2 or Hg-N_2 flow rate was 1 l/min and the inlet Hg was 97 ppb.

Apparatus Configuration	Mode of Operation	Cl_2 ppm	Outlet Hg Concentration ppb
normal tubing system	bypass(dry)	10	97
with Ö*	water	10	38-14
	bypass	10	40-34
	bypass	0	97
	bypass	10	29
normal tubing system	bypass(dry)	0	97
no Ö	bypass(dry)	10	93
§ on Teflon tube‡	water	10	9 (started to decrease after 14 min)
	bypass	10	30-3
	bypass	0	90
	bypass	10	0
	bypass	0	69 (stopped run at this reading)
only Hg absorbed into	bypass(dry)	0	97
water, Cl_2 was added	bypass(dry)	10	94
after the reactor	water	0	86
no Ö	water	10	81
§ on Teflon tube	bypass	10	89

only Hg was absorbed	bypass(dry)	0	97
into water, Cl₂ was added	bypass(dry)	1.5	95
after the reactor	water	0	85
no Ò	water	1.5	84.5
§ on Teflon tube	bypass	1.5	95
Hg/Cl₂ was absorbed into	bypass(dry)	0	97
water	bypass(dry)	1.4	94
no Ò	water	0	87
§ on Teflon tube	water	1.4	71 after 128 min., kept at 87 in the first 39 min.
	bypass	1.4	82
	bypass	0	87
Hg/Cl₂ was absorbed into	bypass(dry)	3	97 (not tested for dry bypass without Cl₂)
1M NaCl, pH = 2.96	1 M NaCl	3	81
no Ò, § on Teflon tube	bypass	3	88
Hg/Cl₂ was absorbed into	bypass(dry)	3	97 (not tested for dry bypass without Cl₂)
1M NaCl, pH=6.64-7.27	1 M NaCl	0	93
no Ò	1 M NaCl	3	88
§ on Teflon tube	bypass	3	91
normal tubing system	bypass	0	97
no Ò	bypass	30	5
no §	bypass	0	83
	bypass	30	3
	bypass	0	stopped run at 79
normal tubing system	bypass	0	97
no Ò	bypass	30	0.7
no §	bypass	0	80
	bypass	6	3
	bypass	0	76
	bypass	14	1
	bypass	0	74
	bypass	6	1.3
	bypass	0	81
	bypass	6	1.3
	bypass	0	stopped run at 75
normal tubing system	bypass	0	97
no Ò	bypass	4.6	14 (stayed at 97 for 10 min.)
no §	bypass	0	81
	bypass	4.6	6
	bypass	0	78
the gas mixture was	bypass	0	97
connected directly to the	bypass	4.6	97
analyzer inlet with	bypass	38.5	22-57
normal 15 l/min N₂	bypass	0	97
dilution	bypass	10.6	89
no Ò	bypass	28.5	92
no §	bypass	38	17
	bypass	0	96

* Ò denotes water knock-out flask   ‡ § denotes heating tape

140

Chapter 8 Mercury Absorption in Simulated Limestone Slurry, Sulfide, and Polysulfide Solutions

Many coal-fired power plants and municipal solid waste incinerators have been equipped with various flue gas desulfurization systems, mainly for the control of sulfur dioxide emissions. Mercury is removed in those systems. Field data showed a mercury collection efficiency of 25-50% for cold and 0% for hot electrostatic precipitators (Huang et al., 1991). A range of 50 to 90% mercury removal was indicated in a limited number of fabric filter systems (Smith, 1987; Chow, 1991). The most common system, limestone slurry scrubbing, appears to remove total mercury with an efficiency of 20-90% based on very few available results (Radian Corporation, 1989; Huang et al., 1991).

Vogg et al. (1986) studied mercury removal by wet scrubbing methods in laboratory scale experiments. They showed that mercuric chloride could be conveniently and very effectively eliminated from the gas phase through condensation. They also observed the possibility of mercury loss if divalent mercury was reduced, e.g. by sulfur dioxide. They then suggested that this could be counteracted by higher chloride concentrations, by a strongly acid scrubbing solution, or if possible, by lowering the temperatures or adding oxidants, such as ferric chloride.

The objective of this study was to test the effectiveness of limestone slurry scrubbing on mercury removal. Experimental results indicate that solutions with sulfite or thiosulfate did not absorb elemental mercury vapor, even with the presence of oxygen in the gas phase. Additives, such as ferrous sulfate and

141

succinic acid used in limestone slurry scrubbing, usually for sulfur dioxide removal, did not contribute to mercury removal either. Thus it is concluded that solutions typical of limestone slurry scrubbing did not remove elemental mercury under our experimental conditions.

Aqueous sodium sulfide and polysulfide were tested for mercury absorption as well. Neither of the above reagents remove gaseous elemental mercury effectively under our experimental conditions.

8.1 EXPERIMENTAL METHOD

All experiments were performed in the well-characterized stirred cell reactor described in Chapter 3. Two modes of experimental operation were developed over the course of the research. The initial mode of operation is called Batch-with-Low-Gas-Flow-Rate. Batch means that all the liquid components were put into the reactor prior to mercury absorption. In this mode of operation, the initial unsteady-state stage was recorded along with the rest of the experiment, usually at steady-state. Because of the initial uncontrollable behavior with this batch mode of operation, it is difficult to interpret experimental data. Low-Gas-Flow-Rate means that the Hg/N_2 or Hg/air flow rate into the reactor was either 100 cc/min or 200 cc/min.

An improved experimental method was introduced later. It is named Injection-with-High-Gas-Flow-Rate. Injection means that with only background solution, such as water or nitric acid in the reactor, the active reagents were sequentially injected. This method is superior because of its reliability and reproducibility. In every experiment, a base line was recorded with Hg/N_2 or

Hg/air absorbed into the background solution where no mercury absorption was expected. All other data were then compared to the base line to determine the effects of injected reagents. High-Gas-Flow-Rate means that the Hg/N_2 or Hg/air flow rate into the reactor was 1000 cc/min. The High-Gas-Flow-Rate method gave reproducible and reasonable results for Hg absorption into distilled water. Because of the very limited solubility of elemental mercury in water, it is generally believed that water does not absorb elemental mercury. However, with low gas flow rate, there was always a certain amount of mercury loss in the reactor. This was probably due to the fact that mercury adsorbed on solid walls of the reactor system. With 1 l/min of gas flow rate, no visible mercury loss was observed when Hg was absorbed from Hg/N_2 into distilled water.

The following described in detail the procedures with the Injection-with-High-Gas-Flow-Rate method. In a typical experiment, 1.06 liters of distilled water or other background solution was put into the reactor while elemental mercury in nitrogen or air was bypassed the reactor. After the mercury analyzer gave a stable reading, the mercury stream was passed over the solution inside the reactor. This was the wet analyzer calibration. Again after the analyzer gave a stable reading, known amounts of the proposed reagent solution were sequentially injected into the reactor using a syringe with a long needle below the liquid surface. The outlet elemental mercury concentration was analyzed continuously and recorded by the strip chart recorder (Soltec Model 1242).

The rate of mercury absorption was calculated from the gas phase material balance. A four-point calibration was performed before and after each run to account for the effect of base line drifting of the mercury analyzer. Reagent

143

addition to the liquid phase was determined by weighing the syringe before and after the injection. The specifications of the reagents used are listed in table 8.1.

Table 8.1   Specifications of the chemicals used in the experiments.

Chemical Name	Specification	Manufacturer
Sodium Sulfite	powder, A.C.S. Reagent	Spectrum Chemical Mfg. Corp.
Sodium Thiosulfate	Crystal, A.C.S. Reagent	Spectrum Chemical Mfg. Corp.
Sublimed Sulfur	Powder, Baker Analyzed	J. T. Baker Inc.
Succinic Anhydride	Practical	Matheson Coleman & Bell Manufacturing Chemists
Ferrous Sulfate	Crystal, A.C.S. Reagent	Spectrum Chemical Mfg. Corp.
Mercuric Chloride	Analytical Reagent	Mallinckrodt Chemical, Inc.
Sodium Hydroxide	Pellets, U.S.P./N.F.	Spectrum Chemical Mfg. Corp.
Sulfuric Acid	95-98 wt%, GR	EM Science
Manganese Sulfate Monohydrate	GR	EM Science
Magnesium Sulfate Anhydrous	-	Fisher Scientific
Magnesium Chloride Hexahydrate	Crystal, GR	EM Science
Sodium Sulfide Nonahydrate	Crystal, A.C.S. Reagent	Spectrum Chemical Mfg. Corp.

8.2   SIMULATED LIMESTONE SLURRY SCRUBBING

Sulfite is the major component in limestone slurry. Solutions typical of limestone slurry scrubbing were tested for mercury removal. Although earlier results using Batch-with-Low-Gas-Flow-Rate indicated that elemental mercury was substantially absorbed in sulfite and/or thiosulfate solutions, later results using Injection-with-High-Gas-Flow-Rate indicated no significant mercury absorption. Because the reactor system is more likely to be a mercury sink at low gas flow rate than at high gas flow rate, and because of the difficulties and uncertainties in data interpretation associated with the batch mode of operation, we believe the results obtained using Injection-with-High-Gas-Flow-Rate. In addition, Injection-with-High-Gas-Flow-Rate was tested and confirmed in the permanganate system prior to the application of the method to limestone slurry scrubbing system. This further increased its credibility and reliability.

144

8.2.1 Sulfite and / or Thiosulfate

8.2.1.1 Results with Injection-with-High-Gas-Flow-Rate Method

The application of Injection-with-High-Gas-Flow-Rate provides an opportunity to examine the net effect of each of the solution components on mercury removal. A higher gas flow rate of 1 l/min was an integral part of the method. Figure 8.1 gives the results of two independent measurements with this method. With 19.7% O_2 in the gas phase, neither S(IV) injection into $S_2O_3^=$/succinic acid/Fe^{2+} solution nor $S_2O_3^=$ injection into succinic acid/Fe^{2+} solution made a positive contribution to Hg removal. This suggests that neither sulfite nor thiosulfate are effective mercury removal reagents, even with oxygen. Although high mercury removal was achieved in both runs, it was probably the effects of the initial solution rather than S(IV) or $S_2O_3^=$. Reactor system contamination could be the possible cause for this high mercury removal.

Table 8.2 gives the results using Injection-with-High-Gas-Flow-Rate. Elemental mercury was mixed with nitrogen. Some experiments also included oxygen or NO_2 in the gas phase. Each block in the table represents one independent experiment. Each line represents one reagent injection, as described by the column of Reagents Injected. Each injected reagent concentration is the cumulative concentration, resulting from multiple injections of the same reagent. In the column of Hg Removal, each line represents the differential effect of each reagent injection. Little mercury removal was achieved for most of the experiments. There are three experiments with 40 to 75% mercury removal that might have been caused by reactor or flow path contamination.

145
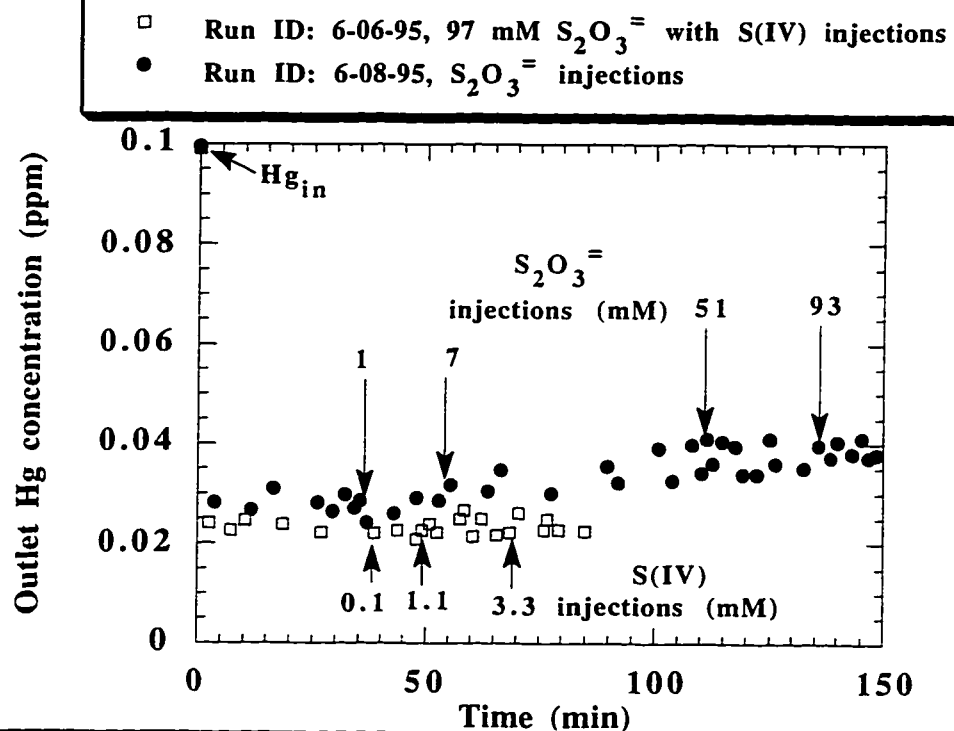
Figure 8.1 Effects of S(IV) and $S_2O_3^=$ injections on Hg absorption in 0.02M succinic acid and 0.02 mM Fe^{2+} with 19.7 % O_2 in the gas phase at 55°C. Total gas flow was 1 l/min and the initial solution pH was 5.

In experiment 01-02-96 (table 8.2), 97 ppb Hg, 100 ppm NO_2, 15% O_2, and N_2 were in the gas phase. 50 mM $Na_2S_2O_3$, 20 mM succinic acid and 0.02 mM $FeSO_4$ were individually injected into the reactor. None of the injections caused visible mercury absorption. After that, 1.76×10^{-5} M $HgCl_2$ was injected and a small amount of Hg removal was observed. Another 2.90×10^{-4} M $HgCl_2$ injection resulted in more Hg removal. The final solution turned light grayish with very little, almost undetectable precipitant. The results are given in figure

146

8.2. Compared to the results with only $HgCl_2$ injection and no other reagents, the presence of $Na_2S_2O_3$-succinic acid-$FeSO_4$ in the solution and NO_2-O_2 in the gas phase decreased the effect of $HgCl_2$ on mercury absorption.
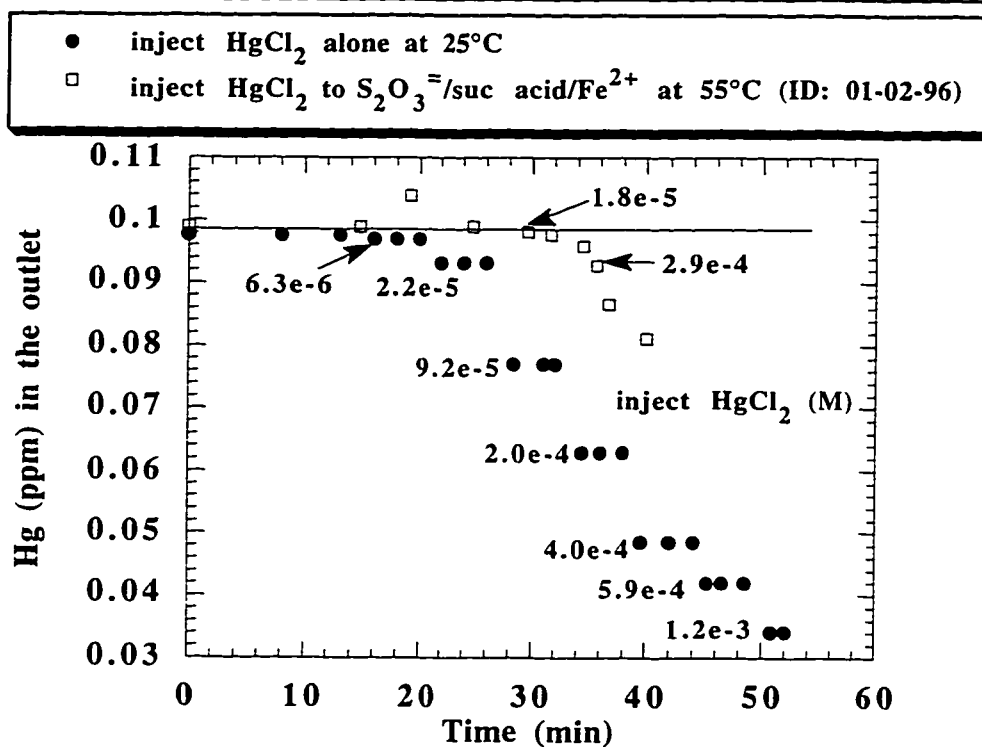
Figure 8.2   Comparison of $HgCl_2$ effect on Hg removal in water at 25°C with N_2 in the gas phase and in 50 mM $Na_2S_2O_3$-20 mM succinic acid-0.02 mM $FeSO_4$ at 55°C with 100 ppm NO_2-15% O_2 in the gas phase.

Table 8.2   Hg absorption in simulated limestone slurry solution using Injection-with-High-Gas-Flow-Rate method. The inlet elemental Hg concentration was 97 ppb, total gas flow rate was 1 l/min.

Run ID	T °C	O_2 %	Reagents Injected	Injected Concentration mM	pH	Hg Removal
12-20-95*	25	0	S(IV)	≥ 218	9.7-9.8	none
12-26-95*	25	15	S(IV) $S_2O_3^=$	≥ 180 47	9.9-10	none none
01-03-96	25	0	$S_2O_3^=$ $HgCl_2$	52 0.026-0.30	7.1-7.7	none none
01-02-96*	55	15	$S_2O_3^=$ succinic $FeSO_4$ $HgCl_2$	50 20 0.02 0.018-0.29	7.4 3.1	none none none some
01-05-96	25	19	$S_2O_3^=$ $HgCl_2$	52 0.024-0.32	6.8-7.0	none none
01-18-96	25	0	succinic $S_2O_3^=$	20 21 (turbid)	3.2-3.5	10% none
01-26-96	55	20	$FeSO_4$ succinic $S_2O_3^=$	0.03 21.3 86.3 (turbid)	-	none negligible small
01-29-96	55	20	$FeSO_4$ $FeSO_4$ $FeSO_4$ succinic succinic NaOH $S_2O_3^=$ $S_2O_3^=$	0.02 0.1 0.3 9.9 26.0 adjust pH to 5.1 21.6 63.6	2.5-5.1	negligible small small none none small none none
02-01-96	55	20	$FeSO_4$ succinic succinic NaOH $S_2O_3^=$ $S_2O_3^=$ $S_2O_3^=$	0.02 9.7 19.8 adjust pH to 5.1 35.1 68.3 107.6	3.1-5.2	small none none none none none none
02-05-96	55	20	$FeSO_4$ succinic NaOH $S_2O_3^=$ S(IV) H_2SO_4	0.02 20.6 adjust pH to 5.06 57.0 11.3 adjust pH to 5.0	- 2.6 5.1 5.3 6.5 5.0	negligible negligible none small small none
01-19-96	25	0	succinic succinic	23 45	2.8-3.1	none none

148

06-13-95	55	20	FeSO$_4$ succinic S$_2$O$_3$$^=$ S$_2$O$_3$$^=$	0.02 20 1.4 67	-	none 40% 7% 5%
06-08-95	55	20	succinic+FeSO$_4$ S$_2$O$_3$$^=$ S$_2$O$_3$$^=$ S$_2$O$_3$$^=$ S$_2$O$_3$$^=$	20+0.2 (not injected) 1.1 6.6 50.5 93	5.0	65% none none none none
06-06-95	55	20	S$_2$O$_3$$^=$+succinic+FeSO$_4$ S(IV) S(IV) S(IV)	97+20+0.2 (not injected) 0.1 1.1 3.3	5.0	75% none none none

* with 100 ppm NO$_2$ in the gas phase

8.2.1.2   Results using Batch-with-Low-Gas-Flow-Rate

Prior to using Injection-with-High-Gas-Flow-Rate, earlier experiments were conducted with low gas flow rate (100 or 200 cc/min) and no reagent injection. Experiments using this method tended to give more mercury removal. The results are given in table 8.3 and figure 8.3.

Table 8.3   Hg absorption in simulated limestone slurry solution using Batch-with-Low-Gas-Flow-Rate.

Condition		Gas Phase			Liquid Phase					Results
Run ID	T	Flow Rate	Hg$_{in}$	O$_2$	S(IV)	S$_2$O$_3$$^=$	Succinic Acid	FeSO$_4$	pH	Hg removal
	°C	l/min	ppb	%	mM	mM	mM	mM		%
05-02-95	25	0.2	100	0	10	0	20	0.02	5.0	12
05-24-95	25	0.1	100	15	0	0	0	0	-	12
05-05-95	25	0.2	100	15	10	0	20	0.02	5.0	22*
05-04-95	25	0.2	100	15	10	0	20	0.02	5.0	22
05-16-95	55	0.1	200	15	7	0	20	0.02	5.1	20
05-17-95	55	0.1	200	15	397	0	20	0.02	7.5	16
05-23-95	55	0.1	210	15	0	0	20	0.02	-	16
05-25-95	55	0.1	210	15	6	0	20	0.02	2.0	5**
06-05-95	55	0.1	210	15	6.7	99.5	20	0.02	5.1	93
04-23-95	25	0.2	100	0	0	10	0	0	-	12
04-25-95	25	0.2	100	0	0	20	20	0	5.0	80
04-26-95	25	0.2	100	15	0	20	20	0	5.0	30

* 100 ppm NO$_2$ was present in the gas phase   ** 0.2 M CaCl$_2$ was present in the solution

149
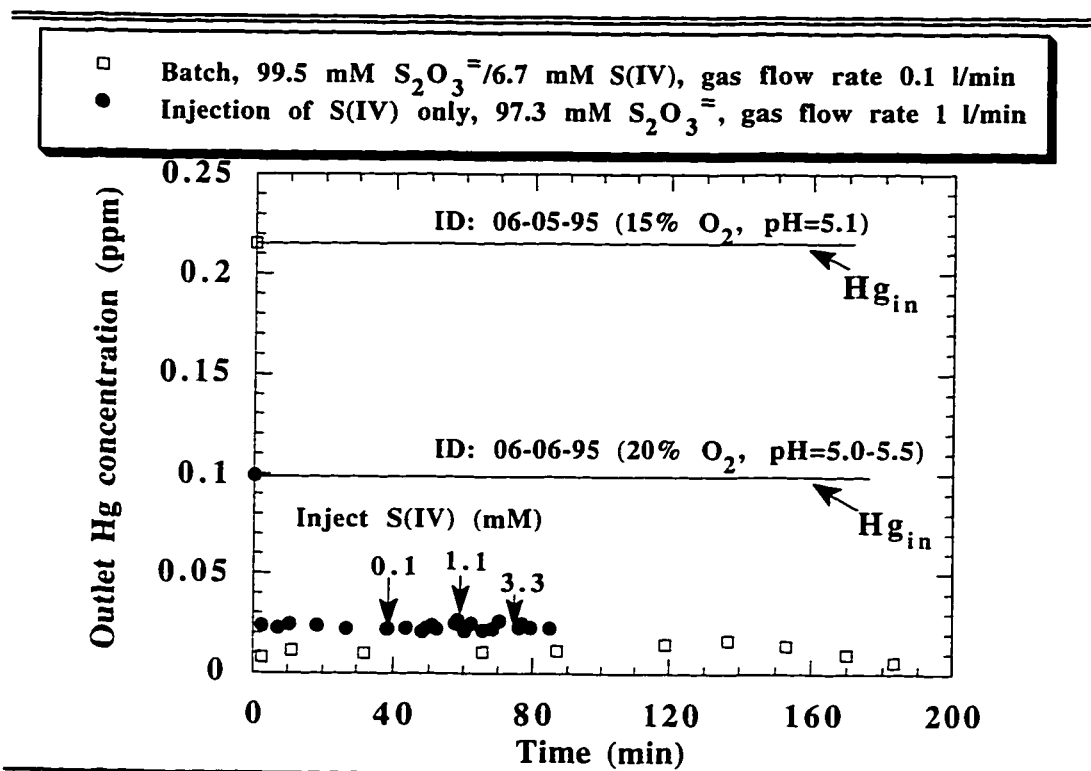
Figure 8.3 Comparison of Hg absorption using two methods at 55°C. Both of the initial solutions contained 20 mM succinic acid and 0.02 mM Fe^{2+}.

Although some experimental results in table 8.3 gave as much as 93% mercury removal, others using Batch-with-Low-Gas-Flow-Rate gave very little mercury removal, as shown in figures 8.4 and 8.5. In these runs, although 15 to 25% mercury removal was observed, the actual mercury flux was small due to the low gas flow rate. These results show that without S(IV) in solution or O_2 in the gas phase, Hg absorption is very limited and the calculated pseudo first order rate

150

constant k_1, where $k_1 = \dfrac{(\frac{N_{Hg}\, H_{Hg}}{P_{Hgi}})^2}{D_{Hg\text{-}H_2O}}$, is close to zero. When both S(IV) and O_2

were present, Hg removal was enhanced and k_1 increased to 1.0 sec^{-1}, although it

was still negligible. The results also show that 100 ppm NO_2 in the gas phase has

no apparent effect on Hg removal.
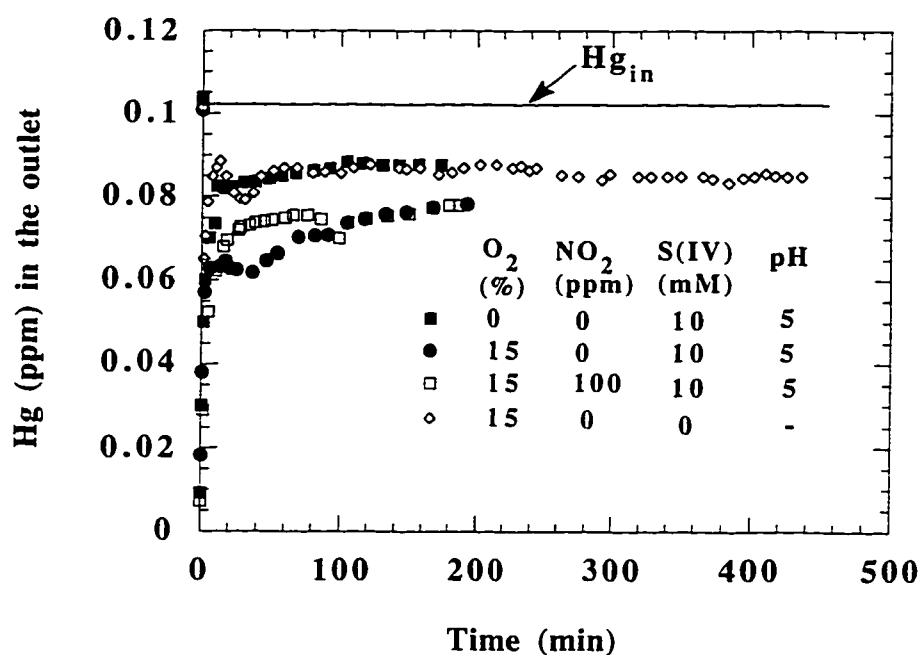
Figure 8.4   Mercury absorption in S(IV) or water at 25°C using Batch-with-Low-Gas-Flow-Rate. All S(IV) solution contained 20 mM succinic acid and 0.02 mM $FeSO_4$. Total Hg-N_2, Hg-air or Hg-air-NO_2 flow rate was 200 cc/min.

The results at typical limestone slurry scrubber temperature, 55°C, are given in figure 8.5. When 15% O_2 was present in the gas phase, water alone and solution containing S(IV) gave the same amount of Hg removal and the removal was independent of S(IV) concentration. When 200 mM $CaCl_2$ was added to the solution at pH 2, Hg removal was inhibited and the calculated k_1 was practically zero. With no $CaCl_2$, k_1 was approximately 1.0 sec^{-1} and was negligible.
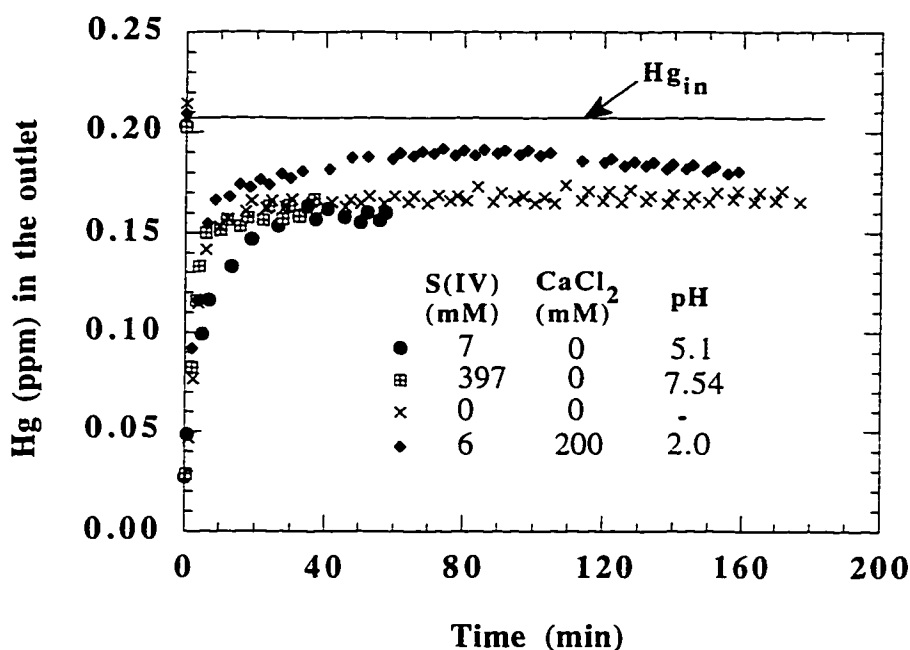
Figure 8.5   Effect of S(IV) on Hg removal in the presence of 15% O_2 at 55°C using Batch-with-Low-Gas-Flow-Rate. All S(IV) solution contained 0.02 M succinic acid and 0.02 mM $FeSO_4$. Total Hg-air flow rate was 100 cc/min.

152

Figure 8.6 gives the results of Hg absorption in a variety of other solutions using the Batch-with-Low-Gas-Flow-Rate. Polysulfide solution was prepared by reacting sublimed sulfur with NaOH at 80°C. 40% mercury removal was achieved when total flow into the reactor was 200 cc/min. 0.01 M $Na_2S_2O_3$ and 0.2 M NaOH alone gave only 10% and 5% Hg removal, respectively. At low gas flow rate, 5 to 10% removal is practically no removal. When 0.02 M succinic acid was added to 0.02 M $Na_2S_2O_3$ at pH 5, it gave 85% Hg removal without O_2 and 30% Hg removal when 15% O_2 was added to the gas mixture.
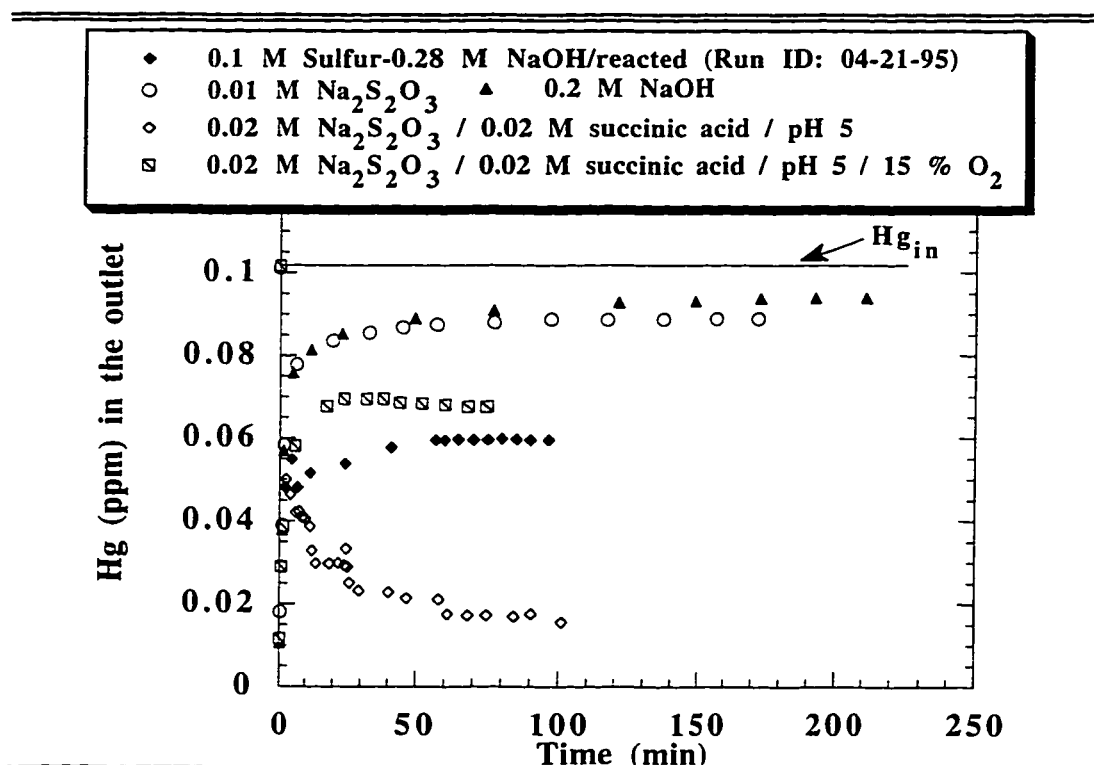
Figure 8.6   Results with Batch-with-Low-Gas-Flow-Rate method at 25°C. Gas flow rate was 200 cc/min.

8.2.2   Effects of Additives

Typical additives in limestone slurry scrubbing were tested for mercury removal. The addition of $MnSO_4$, $MgSO_4$ or $MgCl_2$ to sulfite or thiosulfate using Injection-with-High-Gas-Flow-Rate did not remove elemental mercury. Earlier results indicated that the addition of $CaCl_2$ to sulfite (using Batch-with-low-Gas-Flow-Rate) inhibited mercury absorption.

8.2.2.1   *Results using the Injection-with-High-Gas-Flow-Rate*

Table 8.4 gives the results of the addition of $MnSO_4$, $MgSO_4$ or $MgCl_2$ to sulfite or thiosulfate. Each block in the table represents one independent experiment. Each line represents one reagent injection, as indicated by the column called Reagents Injected. Each line in the column of Injected Concentration represents cumulative concentration, if it was resulted from multiple injections of the same reagent. In the column of Hg Removal, each line represents the differential effect of the reagent injection defined on the same line. For example, in the experiment with run ID of 02-22-96, 60 mM $MnSO_4$ was injected followed by 18 mM Na_2SO_3 injection. Then an additional $MnSO_4$ injection of 40 mM was conducted. This gives a cumulative $MnSO_4$ concentration of 100 mM. Another $MnSO_4$ injection of 100 mM resulted in a cumulative $MnSO_4$ concentration of 200 mM. All these injections gave no mercury removal.

In summary, results show that no mercury removal was detected with $MgSO_4$ or $MnSO_4$ injected into sulfite.

154

Experiments with $MgCl_2$ injection are also tabulated in table 8.3. Two representative runs, 02-12-96 and 02-06-96, gave no mercury removal. The experiment on 02-12-96 was repeated the next day. Similar results were obtained.

Table 8.4   Effects of additives on Hg absorption in sulfite and thiosulfate at 25°C using Injection-with-High-Gas-Flow-Rate. Total $Hg-N_2$ flow rate was 1 l/min, Hg_{in} was 97 ppb.

Run ID	Reagents Injected	Injected Concentration mM	pH	Hg Removal
02-22-96	$MnSO_4$	60		none
	S(IV)	18		none
	$MnSO_4$	100	-	none
	$MnSO_4$	200		none
02-23-96	$MgSO_4$	20		none
	S(IV)	19	-	none
	$MgSO_4$	50		none
02-07-96	$MgCl_2$	<130	-	none
	$MgCl_2$	<270	-	none
	S(IV)	18	8.71	none
	50% H_2SO_4	-	3.51	large
	50% H_2SO_4	-	1.60	none[#]
	$NaOH^Y$	-	5.97	large
	50% H_2SO_4	-	5.15	some
	50% H_2SO_4	-	2.86	none[#]
	$NaOH^Y$	-	3.89	some
02-12-96*	$MgCl_2$	<150	-	none
	S(IV)	36	9.28	negligible
	50% H_2SO_4	-	2.63	none[#]
	$NaOH^Y$	-	5.86	some^
	several 50% H_2SO_4 or $NaOH^Y$	-	-	negligible
02-06-96*	Succinic	21	-	none
	add NaOH to adjust pH to 5.09	-	5.09	none
	$S_2O_3^=$	70	4.94	none
	$MgCl_2$	<250	4.86	none
	add NaOH to adjust pH to 5.23	-	5.23	none

* with 20% O_2 in the gas phase
Y white flaky precipitant formed immediately after NaOH was injected, but disappeared quickly
the net effect of the individual injection actually increased the outlet Hg concentration
^ this injection just brought the outlet Hg concentration back down to the same as the inlet, so overall there was no Hg removal up to this injection

155

On 02-07-96, adding sulfuric acid or sodium hydroxide to adjust the pH of $MgCl_2$ - S(IV) solution resulted in dramatic Hg removal. In order to reproduce these results, another independent but similar experiment was conducted. Two $MgCl_2$ injections followed by one sulfite injection were performed. Then either sulfuric acid or NaOH was injected. No dramatic Hg removal like that of 02-07-96 was observed. Although the concentrations of $MgCl_2$ and sulfite injected in this experiment were different from those of 02-07-96, and pH values were not exactly the same in these two runs, the basic constituents and principles are the same. The lack of reproducibility suggestes that the results of 02-07-96 is unreliable.

One explanation of the dramatic mercury removal observed on 02-07-96 could be that the injections of NaOH formed flaky precipitants. Mercury may have adsorbed on the surface of the precipitants.

8.2.2.2   *Results using Batch-with-Low-Gas-Flow-Rate*

An earlier run using Batch-with-Low-Gas-Flow-Rate tested the effect of 0.2 M $CaCl_2$ and the results are shown in table 8.2. Mercury removal was inhibited and the calculated pseudo first order rate constant k_1, was practically zero. With no $CaCl_2$, k_1 was approximately 1.0 sec^{-1}.

8.2.3   Succinic Acid or Succinic Acid/Sodium Hydroxide Mixture

Figure 8.7 gives the results of a screening experiment which was designed to test the net effect of succinic acid on mercury removal. With 19.7% oxygen and a total gas flow rate of 1 l/min, 13% Hg removal was obtained when there was only water in the reactor. This amount of mercury removal might have been

the result of reactor contamination, as was mentioned earlier. 0.02 mM $FeSO_4$ was injected into the reactor and no additional Hg removal was observed. After this, the addition of 20 mM succinic acid resulted in dramatic mercury removal. Subsequent 1.4 mM $S_2O_3^=$ and 67 mM $S_2O_3^=$ made no big difference and the solution turned turbid due to the mixing of succinic acid and NaS_2O_3 at low pH.
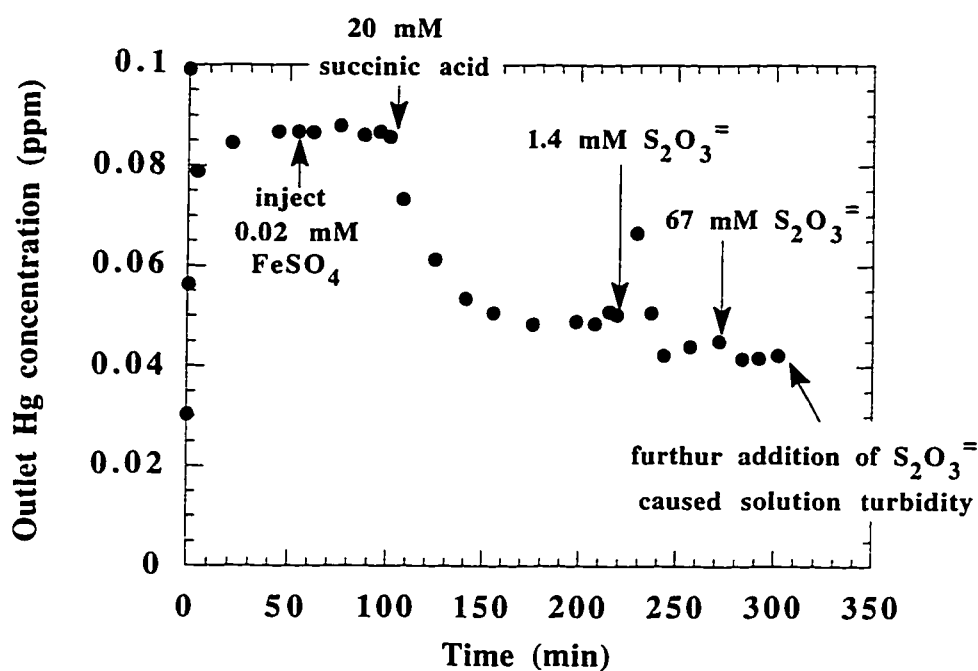
Figure 8.7   Effects of Fe^{2+}, succinic acid and $S_2O_3^=$ injections on Hg absorption in H_2O with 19.7 % O_2 in the gas phase at 55°C. Total Hg/air flow rate was 1 l/min. Solution pH was not adjusted (natural pH).

At this point, it seemed that succinic acid played an important role in Hg removal. Additional experiments were performed by injecting succinic acid alone

157

Table 8.5   Hg absorption in succinic acid-NaOH at 55°C using Injection-with-
High-Gas-Flow-Rate method. The inlet Hg was 99 ppb, total flow
rate was 1 l/min, 19.7% O_2 was present in the gas phase.

Run ID	Reagent Injection	P_{Hgb} x 10^8 (atm)	P_{Hgi} x 10^8 (atm)	Succinic acid (mM)	pH	$\dfrac{F}{P_{Hgi}}$ $(\dfrac{mole}{sec\text{-}m^2\text{-}atm})$	k_l $(\dfrac{1}{sec})$
06-20-95	suc acid alone	9.0	8.8	0.00	6.73	1.19E-02	35
		9.1	8.9	0.03	6.58	1.06E-02	28
		8.4	8.1	0.23	3.38	1.83E-02	84
		4.1	2.9	1.87	2.53	1.64E-01	6732
		3.7	2.4	5.07	2.21	2.14E-01	11390
07-03-95	1M suc acid 0.25M NaOH	9.3	9.1	0.00	6.38	8.89E-03	19
		7.3	6.8	0.29	3.64	3.44E-02	295
		7.0	6.3	1.19	3.52	4.09E-02	416
		6.9	6.2	2.67	3.38	4.25E-02	449
		6.4	5.6	8.61	3.22	5.35E-02	712
		5.8	4.9	18.30	3.16	7.05E-02	1236
06-27-95	1M suc acid 1M NaOH	9.5	9.3	0.00	5.7	7.43E-03	14
		8.4	8.0	0.33	4.05	1.90E-02	89
		7.8	7.3	1.22	4.05	2.75E-02	188
		7.7	7.2	2.58	3.97	2.81E-02	196
		7.8	7.3	8.20	4.09	2.68E-02	179
		7.9	7.4	29.10	4.22	2.58E-02	166
07-13-95	0.1M suc acid 1M NaOH	10.0	9.9	0.00	6.55	3.05E-03	2
		10.0	9.9	0.04	10.13	3.05E-03	2
		10.0	9.9	0.20	11.07	3.05E-03	2
07-13-95	1M suc acid 0.5M NaOH	10.0	9.9	1.91	5.91	3.05E-03	2
		10.0	9.9	4.79	4.59	3.05E-03	2
		10.0	9.9	17.00	3.96	3.05E-03	2
		10.0	9.9	61.70	3.73	3.05E-03	2
07-14-95	0.5M suc acid 0.5M NaOH	10.0	9.9	0.00	6.22	3.37E-03	3
		10.0	9.9	0.20	4.85	3.37E-03	3
		10.0	9.9	1.01	4.69	3.37E-03	3
		10.0	9.9	12.60	4.56	3.37E-03	3
		10.0	9.9	47.10	4.47	3.37E-03	3

and mixtures of succinic acid and NaOH. These combinations give different

solutions with pH from 2 to 12. They were tested for mercury absorption at 55°C

with 19.7% oxygen in the gas phase. The results are given in table 8.5. Each

block in the table represents one independent run with subsequent succinic acid or

succinic acid/NaOH injections. The initial three experiments seemed to remove

mercury and gave a pseudo first order rate constant of 28 to 11390. However, three subsequent experiments with similar solution conditions did not removal mercury. The discrepancies might have been caused by reactor contamination which removed Hg in the initial three experiments. We tend to believe that succinic acid alone or the mixture of succinic acid and sodium hydroxide does not absorb mercury.

8.3 SODIUM SULFIDE AND POLYSULFIDE

Although earlier results using Batch-with-Low-Gas-Flow-Rate indicated a substantial amount of mercury absorption in sulfide or polysulfide, more reliable results obtained using Injection-with-High-Gas-Flow-Rate gave no mercury removal. Thus it was concluded that sodium sulfide or polysulfide did not remove elemental mercury under our experimental conditions.

8.3.1 Results using Injection-with-High-Gas-Flow-Rate

The results of mercury absorption in sodium sulfide or polysulfide using Injection-with-High-Gas-Flow-Rate are given in table 8.6. Each block in the table represents one experiment while each line inside the block represents one injection of reagent. Most of the results gave no mercury removal when Hg was absorbed in sodium sulfide solution with or without oxygen in the gas phase. However, when the full scale of the strip chart recorder was reduced from 1 V or 500 mV to 200 mV, a small amount of mercury removal was observed, as indicated by the run with an asterisk in table 8.6. The second order rate constant k_2 ranged from 66 to 306 $M^{-1}s^{-1}$, where k_2 was calculated from:

$$N_{Hg} = \frac{P_{Hgi}}{H_{Hg}} \sqrt{k_2 \, [Na_2S]_b \, D_{Hg\text{-}H_2O}} \qquad (8\text{-}1)$$

159

The value of k_2 is much smaller than that of Hg absorption in $HgCl_2$ or $KMnO_4$. The oscillation of k_2 resulted from the fluctuation in the outlet Hg concentration. The small amount of mercury removal observed might have been the effect of the improved sensitivity of the strip chart recorder.

Table 8.6   Hg absorption in sodium sulfide and polysulfide using Injection-with-High-Gas-Flow-Rate. Total Hg-air or $Hg-N_2$ flow rate was 1 l/min, Hg_{in} was 97 ppb.

Run ID	Temp. (C°)	Gas Phase O_2 Concentration (%)	Reagent Injected	Injected Reagent Concentration (mM)	Hg Removal
01-11-96	25	0	Na_2S Na_2S Na_2S	2.6 8.3 52	none none none
01-20-96	25	0	Na_2S Na_2S Na_2S	25 71 111	<3%
01-12-96	25	20	Na_2S	23.6	none
01-12-96	55	20	Na_2S Na_2S	59.4 112	none none
01-25-96*	55	20	Na_2S Na_2S Na_2S	26 63 115	k_2 varied from 66 to 306 $M^{-1}s^{-1}$
01-22-96	25	0	polysulfide $HgCl_2$	55.6g/40 ml 0.21	none none

Polysulfide solution was obtained by heating the mixture of sublimed sulfur solid and NaOH solution around 70-80°C. As shown in table 8.5, polysulfide did not remove mercury, even with the presence of mercuric chloride.

8.3.2   Results using Batch-with-Low-Gas-Flow-Rate

As discussed earlier, experiments conducted with low gas flow rate (100 and 200 cc/min) and no reagent injection gave orders of magnitude more mercury removal than those with the new injection method and high gas flow rate. This

was experienced again when Hg was absorbed in sodium sulfide and polysulfide. In figure 8.8, 93% Hg removal was achieved when total gas flow rate was 100 cc/min and sodium sulfide was put into the reactor before Hg was fed into the reactor.
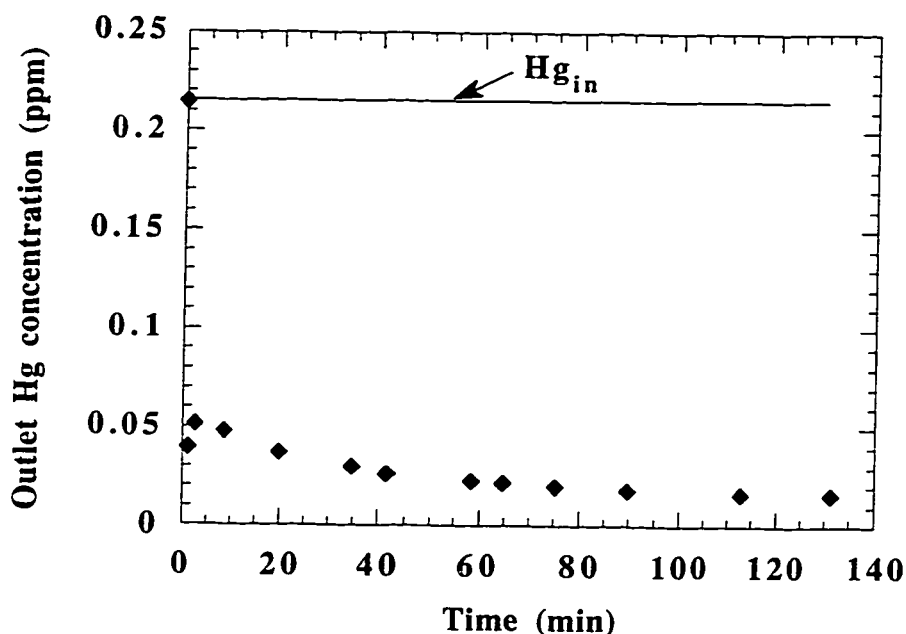
Figure 8.8   Hg absorption in 100 mM Na₂S at 55°C using Batch-with-Low-Gas-Flow-Rate. 15% O_2 was present in the gas phase. Total Hg-air flow rate was 100 cc/min. Initial solution pH was 12.86, run ID: 06-02-95.

Using Batch-with-Low-Gas-Flow-Rate, 40% mercury was absorbed by polysulfide solution. The results are summarized in table 8.7.

Table 8.7   Hg absorption in sodium sulfide and polysulfide using Batch-with-Low-Gas-Flow-Rate method.

Run ID	T ($C°$)	Gas Flow Rate (cc/min)	O_2 (%)	Hg_{in} (ppm)	Reagent in the Batch	Reagent Conc. (mM)	pH	Hg Removal (%)
06-02-95	55	100	15	0.2	Na_2S	100	12.86	93
04-21-95	25	200	0	0.1	polysulfide	‡	-	40

‡ The batch of polysulfide was obtained by mixing 0.1 M sublimed sulfur and 0.3 M NaOH at 80°C

162

Chapter 9 Conclusions and Recommendations

9.1 CONCLUSIONS

9.1.1 Strong Oxidants

Aqueous solutions with oxidation capability were effective for Hg absorption. It oxidized the sparingly soluble Hg° to a more soluble form, Hg(II), and stabilized it in the solution. Permanganate with sulfuric acid absorbed Hg° effectively even at concentration as low as 10^{-6} M.

NaOCl strongly absorbs Hg even at high pH. Low pH, high Cl^- and high temperature favor mercury absorption. Aqueous free Cl_2 was the active species that reacted with mercury. However, chlorine desorption was evident at high Cl^- and pH < 9.

Gas phase reaction was observed between Hg and Cl_2 on apparatus surfaces at room temperature. Strong mercury absorption in water was also detected with Cl_2 gas present. Chlorine concentration, moisture and surface area contribute positively to mercury removal.

9.1.2 Hg(II) without Oxidants

Hg(II) catalyzed Hg° absorption in aqueous solutions. Hg(II) alone removes Hg° effectively. The addition of a strong acid to Hg(II), such as HNO_3 or H_2SO_4, greatly enhanced Hg° absorption. However, the addition of HCl inhibited Hg° absorption in Hg(II).

Succinic acid-NaOH buffer solution greatly enhanced Hg° absorption in Hg(II) but $NaHCO_3$-NaOH inhibited Hg absorption. Under most conditions,

oxygen in the gas phase did not have any effect on Hg° absorption in Hg(II). However, oxygen had a positive effect on Hg absorption in Hg(II) when HCl or $NaHCO_3$-NaOH was present in the solution.

The addition of $MnSO_4$ to Hg(II) only slightly enhanced Hg absorption. On the other hand, NaCl, $MgSO_4$, $FeCl_3$, $CaCl_2$ and $MgCl_2$ all inhibited Hg absorption in Hg(II).

9.1.3 Hg(II) with Oxidants

When an oxidant was added to Hg(II), Hg° absorption was further enhanced. The addition of H_2O_2 to HNO_3 gave the most Hg° removal. The addition of Fe^{2+} or Fe^{3+} to Hg(II)-H_2O_2-HNO_3 has no immediate effect.

Both $K_2Cr_2O_7$ and $K_2Cr_2O_7$-HNO_3 enhanced Hg° absorption in Hg(II) and the positive effect of adding HNO_3 was more apparent than that of adding $K_2Cr_2O_7$.

At 10^{-5} M Hg(II), 0.26 M H_2O_2-0.8M HNO_3 gave the most mercury removal, followed by 0.03 M $K_2Cr_2O_7$-0.8 M HNO_3, and then 0.1 or 0.8 M HNO_3, or 0.8 M H_2SO_4.

9.1.4 Limestone Slurry Scrubbing, Na_2S and Polysulfide Solutions

Solutions typical of limestone slurry did not remove Hg° under our experimental conditions. Sodium sulfite and sodium thiosulfate were the main species tested in this research. Other typical limestone slurry additives, such as succinic acid, $FeSO_4$, $CaCl_2$, $MnSO_4$, $MgSO_4$, and $MgCl_2$, did not make any difference when sulfite and/or thiosulfate were present in the solution.

164

Aqueous sodium sulfide and aqueous polysulfide were not effective for Hg° absorption under our experimental conditions.

The Teflon-coated stirred tank reactor was appropriate and reliable for Hg° absorption. Earlier runs using the stainless steel reactor gave results that were difficult to interpret because of the interactions between mercury and stainless steel.

9.2 RECOMMENDATIONS FOR FURTHER WORK

1. Further study mercury absorption in hypochlorite over a wide range of pH by varying the inlet Hg° concentration and liquid phase agitation speed. Varying inlet Hg° will determine the order of reaction on Hg°. If the limiting step is reaction rather that diffusion, vary the liquid phase agitation would not make any difference. However, liquid phase agitation would definitely have significant impact if the limiting step is diffusion rather than reaction.

2. Explore the possible Hg° removal capabilities of other chlorine related strong oxidizers, such as $NaClO_3$, $NaClO_4$, $HClO_3$, $HClO_4$, etc.

3. Investigate surface catalyzed mercury reaction with chlorine. Teflon, glass and stainless steel are some of the surface materials that can be used. Identify the reaction product and study the effect of solid mercuric chloride. If the surface is coated with $HgCl_2$, it might give different results compare to the situation when the surface is clean.

4. Investigate possible solid adsorbents for Hg and $HgCl_2$. Na_2S impregnated activated carbon, polysulfide, calcium based adsorbents and fly ash are some of the adsorbents that might be effective.

165

5. Add mercuric chloride to elemental mercury vapor stream. Study the simultaneous absorption of mercury and mercuric chloride. It has been shown that aqueous $HgCl_2$ removes Hg° vapor. It is possible that gaseous $HgCl_2$ reacts with Hg°. Furthermore, $HgCl_2$ absorbs fairly easily in water and stays mainly in its molecular form as $HgCl_2$ in the solution. This solution removes Hg°.

6. Study the effect of sulfur dioxide and/or NOx on mercuric chloride absorption, or simultaneous mercury and mercuric chloride absorption. Since SO_2 is a reducing agent, it might reduce the absorbed $Hg(II)$ back to Hg° and desorb from the solution. On the other hand, SO_2 absorbs in the solution itself and might form complexes with $Hg(II)$, which could render a completely different picture.

Appendix A Safety Procedures in Handling Mercury

Due to the well-known health effects of mercury and its acute toxicity, special precautions must be followed when handling mercury. The American Conference of Governmental Industrial Hygienists has adopted the threshold limit value (TLV) of 0.1 mg/m^3 (0.01 ppm) for mercury vapor and inorganic compounds of mercury for an eight hour work day. Since mercury can either be absorbed through the skin or inhaled, special protection procedures must be adopted.

A.1 FIRST AID

Eye Contact: Flush with running water for 15 min., including under the eyelids.

Skin Contact: Remove contaminated clothing. Wash affected area with soap and water.

Inhalation: Remove to fresh air. Restore and/or support breathing as needed. Administer O_2 for chemical pneumonitis.

Ingestion: Gastric lavage with 5% solution of sodium formaldehyde sulfoxylate, followed by 2% $NaHCO_3$, and finally leave 250 cc of the sodium formaldehyde sulfoxylate in the stomach.

A.2 PERSONAL PROTECTION

Provide adequate exhaust ventilation to meet TLV requirements in the workplace. This was done by placing all mercury containing components of the apparatus inside the ventilation hood. When it was not being used, the mercury

source was sealed inside the U-tube without contacting the ambient air. According to the mercury Material Safety Data Sheets (MSDS), self-contained breathing apparatus can be used up to 5 mg/m^3 (0.5 ppm) with a full facepiece above 1 mg/m^3 (0.1 ppm). Since the highest inlet mercury concentration used in all experiments was 0.1 ppm, we used a half-face respirator (Cole-Parmer Instrument Company) whenever experimental personnel were near or partially inside the hood. Chemical safety glasses, rubber gloves and protective clothing appropriate for the work situation should be used to avoid body contact with mercury. Provide replacement and periodic medical exams for those regularly exposed to mercury, such as testing the blood sample for mercury concentration in a clinic. No eating or smoking in work areas.

A.3 SPILL, LEAK AND DISPOSAL PROCEDURES

Notify safety personnel of leaks or spills. Provide adequate ventilation. Clean-up spills promptly. A suction bottle with a capillary tube for small amounts can be used. Vacuum cleaners may be used provided they have special mercury absorbent exhaust filters. Calcium polysulfide with excess sulfur can be sprinkled into cracks or other inaccessible places to convert mercury globules into the sulfide. Collect picked-up or scrapped mercury in tightly sealed containers for reclaim or for disposal. Do not discharge mercury down the drain. As for disposal procedure, mercury should be salvaged for purification or sold to a salvage company when large amounts are involved.

Appendix B D_{Hg-H2O} Estimation

The diffusion coefficient of elemental mercury in water, D_{Hg-H2O}, was estimated by the equation of Sitaraman et al. (1963):

$$D_{Hg-H2O} = 16.79 \times 10^{-14} \left(\frac{M_{H2O}^{0.5} \Delta H_{H2O}^{1/3} T}{\mu_{10\% \, H2SO4} V_{Hg}^{0.5} \Delta H_{Hg}^{0.3}} \right)^{0.93} \qquad (B-1)$$

where ΔH_{Hg} and ΔH_{H2O} are the latent heats of vaporization of the solute and solvent at their normal boiling points:

$$\Delta H_{Hg} = 2.94776 \times 10^5 \text{ J/kg} \qquad (B-2)$$

$$\Delta H_{H2O} = 2.257 \times 10^6 \text{ J/kg} \qquad (B-3)$$

and $\mu_{10\%, \, H2SO4}$ is the viscosity of the reducing solvent in centipoise:

$$\mu_{10\%, \, H2SO4} = 1.256 \text{ cp } (25°C) \qquad (B-4)$$

V_{Hg} is the molar volume of solute at the normal boiling point:

$$V_{Hg} = 19 \times 10^{-3} \text{ m}^3/\text{kgatom} \qquad (B-5)$$

and M_{H2O} is the molecular weight of solvent in kg/kgmol.

The predicted D_{Hg-H2O} value is 1.19×10^{-5} cm^2/sec at 25°C and 2.21×10^{-5} cm^2/sec at 55°C.

Appendix C Results of Hg Absorption in $KMnO_4$ -1.8 M H_2SO_4

Table C-1 Detailed results of Hg absorption in $KMnO_4$-1.8 M H_2SO_4 at 25°C. Total Hg-N_2 flow rate was 1 l/min. $k_{g, Hg} = 0.4 \dfrac{mole}{s\text{-}atm\text{-}m^2}$.

Run ID	Hg_{in} ppb	Hg_b• mV	Hg_b ppb	P_{Hgb} $\times10^8$ atm	P_{Hgi} $\times10^8$ atm	N_{Hg} $\times10^{11}$ $\frac{mole}{s}$	$k°_{l,MnO_4^-}$ $\times10^5$ $\frac{m}{s}$	$[MnO_4^-]_b$ M	$[MnO_4^-]_i$ M	k_2 $\times10^{-7}$ $\frac{1}{M\text{-}s}$
02-16-95	97	543	79	8.0	7.6	1.3	3.2	2.18E-06	2.12E-06	1.4
02-19-95	97	368	43	4.4	3.3	3.8	3.2	9.35E-05	9.33E-05	1.5
02-24-95	97	639	69	7.3	6.7	2.0	3.2	7.10E-06	7.02E-06	1.3
02-24-95	97	597	63	6.8	6.0	2.4	3.2	1.14E-05	1.13E-05	1.5
02-24-95	97	557	58	6.2	5.4	2.8	3.2	1.89E-05	1.88E-05	1.5
02-24-95	97	499	56	5.4	4.4	3.4	3.2	3.99E-05	3.97E-05	1.5
02-24-95	97	439	48	4.6	3.4	4.0	3.2	9.40E-05	9.38E-05	1.5
02-24-95	97	381	40	3.8	2.4	4.6	3.2	2.42E-04	2.42E-04	1.5
02-24-95	97	339	32	3.2	1.7	5.0	3.2	6.12E-04	6.11E-04	1.4
03-03-95	97	465	53	5.4	4.4	3.2	3.3	3.26E-05	3.25E-05	1.6
03-03-95	97	483	53	5.4	4.4	3.2	3.3	3.52E-05	3.51E-05	1.5
04-19-95	19	134	15	1.5	1.4	0.3	3.3	3.30E-06	3.29E-06	1.4
04-19-95	19	122	14	1.4	1.2	0.4	3.2	7.68E-06	7.66E-06	1.5
04-19-95	19	113	12	1.3	1.1	0.5	3.3	1.41E-05	1.41E-05	1.5
04-19-95	19	100	11	1.1	0.9	0.6	3.3	3.43E-05	3.42E-05	1.5
04-19-95	19	91	9	1.0	0.7	0.7	3.3	6.10E-05	6.10E-05	1.5
04-19-95	19	78	8	0.8	0.5	0.8	3.3	1.68E-04	1.68E-04	1.5

Table C-2 Detailed results of Hg absorption in $KMnO_4$-1.8 M H_2SO_4 at 55°C. Total Hg-N_2 flow rate was 1 l/min. $k_{g, Hg} = 0.4 \dfrac{mole}{s\text{-}atm\text{-}m^2}$.

Run ID	Hg_{in} ppb	Hg_b mV	Hg_b ppb	P_{Hgb} $\times10^8$ atm	P_{Hgi} $\times10^8$ atm	N_{Hg} $\times10^{11}$ $\frac{mole}{s}$	$k°_{l,MnO_4^-}$ $\times10^5$ $\frac{m}{s}$	$[MnO_4^-]_b$ M	$[MnO_4^-]_i$ M	k_2 $\times10^{-8}$ $\frac{1}{M\text{-}s}$
07-18-95	98	245	62	6.4	5.7	2.3	5.5	1.19E-05	1.18E-05	1.2
07-18-95	98	239	58	6.0	5.2	2.5	5.5	1.68E-05	1.67E-05	1.3
07-18-95	98	231	52	5.4	4.5	2.9	5.5	2.91E-05	2.90E-05	1.3
07-18-95	98	223	47	4.9	3.9	3.2	5.5	4.85E-05	4.85E-05	1.3
07-18-95	98	213	41	4.2	3.0	3.7	5.5	1.02E-04	1.02E-04	1.3
07-18-95	98	203	34	3.5	2.2	4.1	5.5	2.47E-04	2.46E-04	1.3

Appendix D Determination of H$_2$O$_2$ by Iodometric Titration

Aqueous hydrogen peroxide concentration was determined by iodometric titration. An excess amount of potassium iodide was oxidized by hydrogen peroxide. The produced iodine was then back-titrated with thiosulfate to determine the amount of iodine produced. From the reaction stoichometry, the hydrogen peroxide concentration can be determined.

The chemistry involved can be described as follows:

$$H_2O_2 + 2\ I^- + 2\ H^+ \rightarrow I_2 + 2\ H_2O \tag{D-1}$$

$$I_2 + 2\ S_2O_3^= \rightarrow S_4O_6^= + 2I^- \tag{D-2}$$
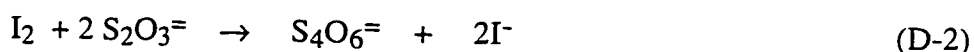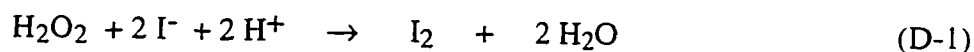
The procedures are described below:

1. Put 10 ml 0.3 M KI in 50 ml Erlenmeyer flask.

2. Add 2 ml of 1:1(by volume) H$_2$SO$_4$ to the flask

3. Add 3 drops of 1 N ammonium molybdate (reaction catalyst)

4. Extract 1 ml H$_2$O$_2$ sample from the reactor and add the sample to the flask while constantly shaking the flask

5. Let solution stand for 5-10 min.

6. Titrate liberated I$_2$ with certified 1 N thiosulfate. Add thiosulfate untill the solution turns from dark orange to pale yellow while shaking the solution. Slow down the addition of thiosulfate by adding the solution drop by drop until the solution is clear.

171

Appendix E Results of Hg Absorption in Hg(II)-H$_2$O$_2$-0.8 M HNO$_3$

Table E-1   Detailed results of Hg absorption in Hg(II)-H$_2$O$_2$-0.8 M HNO$_3$ at 25°C. Total Hg-N$_2$ flow rate was 1 l/min. $k_{g,\,Hg} = 0.4 \dfrac{\text{mole}}{\text{s-atm-m}^2}$.

Time	P_{Hgin}	P_{Hgb} x10^8	P_{Hgi} x10^{10}	N_{Hg} x10^{10}	$k^\circ_{I,Hg}$ x10^5	$k^\circ_{I,Hg^{++}}$ x10^5	$\dfrac{N_{Hg}}{k^\circ_{II,Hg^{++}}}$ x10^8	Hg^{++}* x10^8	Hg^{++} injected	Hg^{++}_i x10^7	H_2O_2‡	k_3 x10^{-8}
min	ppb	atm	atm	$\dfrac{\text{mole}}{\text{s-m}^2}$	$\dfrac{m}{s}$	$\dfrac{m}{s}$	M	M	mM	M	M	$\dfrac{1}{M^2\text{-s}}$
24.8	20.1	2.1	2.1	0.1	2.6	2.2	0.06	0.01	0	0.01	0.1	3.9
67.2	20.1	2.1	2.1	0.2	2.6	2.2	0.09	0.04	0	0.01	0.1	4.1
91.2	20.1	2.1	2.1	0.2	2.6	2.2	0.10	0.06	0	0.02	0.1	3.8
104.8	20.1	2.1	2.1	0.2	2.6	2.2	0.11	0.08	0	0.02	0.1	4.1
115.2	20.1	2.1	2.1	0.3	2.6	2.2	0.12	0.09	0	0.02	0.1	4.4
127.6	20.1	2.0	2.0	0.6	2.6	2.2	0.26	0.11	0	0.04	0.4	4.0
159.2	20.1	2.0	2.0	0.7	2.6	2.2	0.30	0.20	0	0.05	0.4	3.9
164.0	20.1	2.0	2.0	0.8	2.6	2.2	0.35	0.22	0	0.06	0.4	4.8
61.6	97.5	8.2	7.8	17.0	2.6	2.2	7.74	2.95	0	1.1	0.9	3.2
66.0	97.5	8.2	7.8	17.3	2.6	2.2	7.85	3.29	0	1.1	0.9	3.1
94.4	97.5	7.8	7.3	20.8	2.6	2.2	9.47	5.77	0	1.5	0.9	3.8
116.4	97.5	7.3	6.7	24.8	2.6	2.2	11.36	8.08	0	1.9	1.0	4.7
120.8	97.5	7.2	6.6	25.3	2.6	2.2	11.54	8.58	0	2.0	1.0	4.8
9.2	97.5	9.8	9.7	3.7	2.6	2.2	1.70	0.03	0	0.2	0.2	3.2
62.0	97.5	8.7	8.4	12.9	2.6	2.2	5.94	1.27	0	0.7	0.6	3.9
88.4	97.5	8.6	8.2	14.1	2.6	2.2	6.49	2.59	0	0.9	0.6	3.7
110.6	97.5	8.4	8.0	15.5	2.6	2.2	7.16	4.06	0	1.1	0.6	4.0
137.0	97.5	7.8	7.3	20.5	2.6	2.2	9.46	6.25	0	1.6	0.9	3.9
161.8	97.5	7.6	7.0	22.8	2.6	2.2	10.49	8.74	0	1.9	0.9	4.0
175.4	97.5	7.4	6.8	23.9	2.6	2.2	11.02	10.29	0	2.1	0.9	4.1
5.2	97.5	10.0	9.9	2.0	2.7	2.2	0.89	0.02	0	0.1	0.1	3.1
8.4	97.5	9.9	9.9	2.3	2.7	2.2	1.05	0.06	0	0.1	0.1	3.5
58.2	97.5	9.3	9.1	8.1	2.6	2.2	3.61	1.18	0	0.5	0.3	3.7
74.2	97.5	9.1	8.8	9.8	2.6	2.2	4.39	1.83	0	0.6	0.3	4.3
82.8	97.5	8.6	8.3	13.6	2.7	2.2	6.09	2.30	0	0.8	0.6	3.9
90.4	97.5	8.3	7.9	16.0	2.7	2.2	7.17	2.81	0	1.0	0.6	4.7
68.0	97.5	6.5	5.7	32.0	2.6	2.2	14.34	3.40	2.3E-06	24.6	0.3	3.4
82.4	97.5	4.5	3.3	48.6	2.7	2.2	21.74	6.00	1.8E-05	183.0	0.3	3.1
94.4	97.5	4.5	3.3	48.9	2.7	2.2	21.85	8.63	1.8E-05	183.0	0.3	3.2

| 125.2 | 97.5 | 3.0 | 1.5 | 61.5 | 2.7 | 2.2 | 27.51 | 16.34 | 1.1E-04 | 1090.0 | 0.3 | 4.0 |

* Amount of gas phase Hg absorbed in the solution obtained by integration.

‡ Cumulative injected concentration of H_2O_2.

Table E-2   Detailed results of Hg absorption in Hg(II)-H_2O_2-0.8 M HNO_3 at 55°C. Total Hg-N_2 flow rate was 1 l/min. $k_{g, Hg}$ = 0.4 mole/s-atm-m^2.

Time	P_{Hgin}	P_{Hgb} $\times 10^8$	P_{Hgi} $\times 10^{10}$	N_{Hg} $\times 10^5$	$k°_{l.Hg}$ $\times 10^5$	$k°_{l.Hg^{++}}$ $\times 10^5$	$\frac{N_{Hg}}{k°_{II.Hg^{++}}}$ $\times 10^8$	Hg^{++} * $\times 10^8$	Hg^{++} injected	$Hg^{++}{}_i$ $\times 10^8$	H_2O_2 ‡	k_3 $\times 10^{-8}$
min	ppb	atm	atm	$\frac{mole}{s\text{-}m^2}$	$\frac{m}{s}$	$\frac{m}{s}$	M	M	mM	M	M	$\frac{1}{M^2\text{-}s}$
16.4	97.5	10.0	9.9	2.0	4.8	4.1	0.48	0.07	0	0.6	0.0	90.6
35.2	97.5	9.9	9.8	2.5	4.8	4.1	0.62	0.27	0	0.9	0.0	90.4
75.2	97.5	9.1	8.9	8.4	4.8	4.1	2.04	1.27	0	3.3	0.2	86.6
78.8	97.5	9.0	8.8	9.3	4.8	4.1	2.26	1.42	0	3.7	0.2	97.3
9.6	97.5	9.4	9.3	6.1	4.7	4.0	1.52	0.13	0	1.7	0.2	86.0
52.2	97.5	9.1	8.9	8.5	4.7	4.0	2.12	1.56	0	3.7	0.2	82.3
80.8	97.5	8.3	7.9	15.2	4.7	4.0	3.78	3.12	0	6.9	0.4	84.4
84.4	97.5	8.2	7.8	15.7	4.7	4.0	3.90	3.38	0	7.3	0.4	81.8
87.2	97.5	8.1	7.7	16.6	4.7	4.0	4.11	3.59	0	7.7	0.4	89.5
101.6	97.5	7.3	6.7	22.9	4.7	4.0	5.69	4.91	0	10.6	0.7	92.6
9.6	97.5	9.6	9.4	5.1	4.7	4.0	1.26	0.11	0	1.4	0.1	86.2
19.6	97.5	9.6	9.4	5.1	4.7	4.0	1.26	0.34	0	1.6	0.1	86.2
29.6	97.5	9.6	9.4	5.1	4.7	4.0	1.27	0.58	0	1.8	0.1	86.7
3.4	97.6	9.8	9.7	3.3	4.7	4.0	0.82	0.03	0	0.8	0.1	82.4
22.0	97.6	9.7	9.6	4.2	4.7	4.0	1.04	0.34	0	1.4	0.1	86.7
38.8	97.6	9.6	9.5	4.7	4.7	4.0	1.16	0.69	0	1.8	0.1	85.2
58.8	97.6	8.9	8.6	10.4	4.7	4.0	2.59	1.38	0	4.0	0.3	81.4
80.0	97.6	8.6	8.3	12.8	4.7	4.0	3.17	2.51	0	5.7	0.3	88.8
103.0	97.6	8.3	8.0	14.6	4.7	4.0	3.62	3.95	0	7.6	0.3	91.1
109.6	97.6	8.0	7.5	17.5	4.7	4.0	4.34	4.43	0	8.8	0.4	85.9
115.6	97.6	7.8	7.4	18.4	4.7	4.0	4.58	4.93	0	9.5	0.4	87.1
141.6	97.6	7.3	6.8	22.3	4.7	4.0	5.52	7.38	0	12.9	0.6	86.8
154.8	97.6	7.0	6.4	24.9	4.7	4.0	6.19	8.80	0	15.0	0.6	91.2
204.4	97.6	6.4	5.7	29.3	4.7	4.0	7.26	15.07	0	22.3	0.8	87.6

* Amount of gas phase Hg absorbed in the solution obtained by integration.

‡ Cumulative injected concentration of H_2O_2.

Appendix F Determination of NaOCl by Iodometric Titration
(Lagowski, 1995)

An oxidation-reduction (redox) titration was used to analyze the concentration of hypochlorite ion when high concentration of NaOCl was used. The iodide ion from the KI added to the solution is oxidized to iodine by the hypochlorite ion.

$$OCl^- + 2I^- + H_2O \rightarrow I_2 + Cl^- + 2OH^- \qquad (F-1)$$
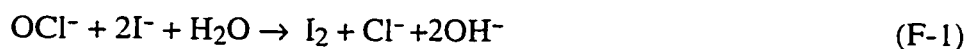
In the presence of free I^-, any I_2 produced will combine with I- to form I_3^-:

$$I^- + I_2 \rightarrow I_3^- \qquad (F-2)$$

I_3^- is called the triiodide ion. Stoichiometrically, I_3^- will react in the same ratio as the I_2 molecule. Therefore, to simplify discussion, I_2 molecule is used in all subsequent discussions even though I_3^- ion may actually be present in the solution.

The iodine produced in reaction (F-1) is titrated with standardized sodium thiosulfate. 0.5 M H_2SO_4 is added at this point to provide an acidic reaction solution.

$$2S_2O_3^= + I_2 \rightarrow 2I^- + S_4O_6^= \qquad (F-3)$$

The thiosulfate titration is continued slowly until the yellow color disappears.

$$I_2 \text{ (yellow)} + 2S_2O_3^= \rightarrow 2I^- + S_4O_6^= \text{ (colorless)} \qquad (F-4)$$
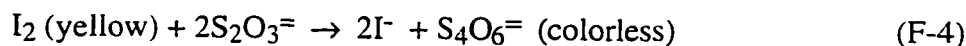
Procedure:

1. Add 1g of solid KI and 5 ml o f 0.5 M H_2SO_4 to 100 ml Erlenmeyer flask

174

2. Weigh the above solution and the Erlenmeyer flask

3. Add several drops of NaOCl from the original NaOCl bottle to the weighed Erlenmeyer flask, the solution turned to yellow instantaneously

4. Weigh the solution and the Erlenmeyer flask again

5. Immediately titrate the above solution with the standard sodium thiosulfate solution. Record the volume of titrant used.

6. Repeat the whole process several times.

Note: The density of the NaOCl solution needs to be determined before the titration. Deliver a known volume of NaOCl into the preweighed volumetric flask or beaker and then weighing the volumetric flask (or beaker)+ sample.

Data Analysis:

NaOCl concentration (M) is obtained from the following equation:

$$\frac{\text{volume of } Na_2S_2O_3 \text{ (ml)} \times 0.001 \left(\frac{1}{ml}\right) \times Na_2S_2O_3 \text{ concentration (M)}}{2 \times \dfrac{\text{weight of NaOCl sample(g)}}{\text{density of NaOCl sample} \left(\frac{g}{ml}\right)} \times 0.001 \left(\frac{1}{ml}\right)} \qquad \text{(G-5)}$$

Appendix G Results of Mercury Absorption in NaOCl-NaCl at Low and Intermediate pH

Total Hg-N$_2$ flow rate was 1 l/min. The inlet Hg was 97.7 ppb. $k_{g, Hg}$ = 0.39 mole/s-atm-m^2, $k^\circ_{l, Hg^{++} (25^\circ C)}$ = 2.2x10^{-5} m/s, $k^\circ_{l, Hg^{++} (55^\circ C)}$ =4.0x10^{-5} m/s.

Table G-1   Detailed results of Hg$^\circ$ absorption in NaOCl-NaCl at low pH at 25°C, no external HgCl$_2$ injection, [Hg^{++}]$_i$ = [Hg^{++}]$_{absorbed}$ + $\dfrac{N_{Hg}}{k^\circ_{l, Hg^{++}}}$.

Run ID	Hg ppb	time min	P$_{Hgb}$ x10^8 atm	P$_{Hgi}$ x10^8 atm	N$_{Hg}$ mole s-m^2	absorb [Hg^{++}] M	[Hg^{++}]$_i$ x10^8 M	injected [NaOCl] x10^7 M	pH	a$_{Cl2}$ x10^7 M	k$_2$ l M-s
05-10-96	72.6	21.6	7.6	7.0	2.2E-09	1.1	11.3	9.2	3.04	1.4	4.8E+08
0.1 M NaCl	83.8	26.4	8.8	8.5	1.2E-09	1.5	7.2	9.2	3.04	1.4	1.0E+08
25°C	90.8	30.8	9.5	9.4	6.1E-10	1.7	4.5	9.2	3.04	1.4	2.1E+07
	97.4	39.6	10.2	10.2	2.7E-11	1.8	1.9	9.2	3.04	1.4	3.3E+04
	97.5	43.6	10.2	10.2	1.8E-11	1.8	1.9	9.2	3.04	1.4	1.5E+04
	97.5	48.0	10.2	10.2	1.5E-11	1.8	1.9	9.2	3.04	1.4	1.0E+04
	42.8	49.6	4.5	3.2	4.9E-09	2.0	24.3	29.4	3.04	4.5	3.4E+09
	22.4	66.4	2.3	0.6	6.7E-09	7.1	37.7	29.4	3.03	4.6	1.7E+11
	36.5	76.4	3.8	2.4	5.5E-09	9.9	34.7	29.4	3.03	4.6	7.4E+09
	50.6	88.4	5.3	4.2	4.2E-09	12.6	31.7	29.4	3.03	4.6	1.4E+09
	64.8	104.0	6.8	6.0	2.9E-09	15.1	28.4	29.4	3.03	4.6	3.4E+08
	72.0	116.0	7.5	7.0	2.3E-09	16.5	26.9	29.4	3.03	4.6	1.6E+08
	79.4	132.8	8.3	7.9	1.6E-09	18.1	25.5	29.4	3.03	4.6	6.2E+07
	86.9	156.8	9.1	8.9	9.6E-10	19.5	23.9	29.4	3.03	4.6	1.7E+07
	90.6	173.6	9.5	9.3	6.3E-10	20.1	23.0	29.4	3.03	4.6	6.7E+06
05-16-96*	33.7	24.4	3.5	2.1	5.7E-09	2.3	28.1	16.7	2.98	10.6	4.7E+09
05-17-96	97.6	18.0	10.2	10.2	6.2E-12	0.003	0.03	1.2	0.96	1.2	2.0E+03
1 M NaCl	78.2	22.0	8.2	7.8	1.7E-09	0.2	8.0	7.2	0.96	7.2	4.7E+07
25°C	80.4	28.0	8.4	8.0	1.5E-09	0.6	7.5	7.2	0.96	7.2	3.4E+07
	86.2	38.0	9.0	8.8	1.0E-09	1.2	5.8	7.2	0.96	7.2	1.3E+07
	90.4	44.8	9.5	9.3	6.5E-10	1.5	4.4	7.2	0.95	7.2	4.5E+06
	96.1	54.0	10.1	10.0	1.4E-10	1.6	2.3	7.2	0.95	7.2	1.8E+05
	97.4	56.8	10.2	10.2	2.2E-11	1.6	1.7	7.2	0.95	7.2	4.4E+03
	97.1	61.6	10.2	10.2	5.6E-11	1.6	1.9	7.2	0.95	7.2	2.8E+04
	97.1	67.6	10.2	10.2	5.0E-11	1.7	1.9	7.2	0.94	7.2	2.3E+04
	48.1	69.6	5.0	3.9	4.4E-09	1.9	21.8	16.6	0.93	16.5	5.1E+08
	42.9	73.2	4.5	3.3	4.9E-09	2.6	24.6	16.6	0.93	16.5	9.2E+08

176

	39.0	77.6	4.1	2.8	5.2E-09	3.7	27.2	16.6	0.93	16.5	1.5E+09
	37.7	80.8	4.0	2.6	5.3E-09	4.4	28.5	16.6	0.93	16.5	1.7E+09
	38.7	85.2	4.1	2.7	5.3E-09	5.5	29.2	16.6	0.92	16.5	1.5E+09
	42.1	89.6	4.4	3.2	5.0E-09	6.5	28.9	16.6	0.92	16.5	1.0E+09
	49.0	94.8	5.1	4.0	4.3E-09	7.6	27.2	16.6	0.92	16.5	4.7E+08
	53.8	97.6	5.6	4.6	3.9E-09	8.2	25.8	16.6	0.91	16.5	2.9E+08
	57.2	99.4	6.0	5.1	3.6E-09	8.5	24.7	16.6	0.91	16.5	2.0E+08
05-23-96	96.7	16.0	10.1	10.1	8.9E-11	0.03	0.4	1.7	4.95	0.0	1.7E+07
1 M NaCl	96.6	20.8	10.1	10.1	9.4E-11	0.1	0.5	1.7	4.96	0.0	1.9E+07
25°C	97.0	24.8	10.2	10.1	6.3E-11	0.1	0.4	1.7	4.97	0.0	8.9E+06
	83.5	27.2	8.8	8.4	1.3E-09	0.1	5.8	9.9	4.98	0.2	8.8E+08
	81.4	29.2	8.5	8.2	1.5E-09	0.3	6.8	9.9	4.99	0.2	1.3E+09
	84.0	32.0	8.8	8.5	1.2E-09	0.4	5.9	9.9	5.00	0.2	8.5E+08
	86.9	34.8	9.1	8.9	9.6E-10	0.6	4.9	9.9	5.01	0.2	5.0E+08
	88.5	37.2	9.3	9.1	8.2E-10	0.7	4.4	9.9	5.01	0.2	3.4E+08
	53.8	38.8	5.6	4.6	3.9E-09	0.8	18.5	27.3	5.08	0.4	1.3E+10
	54.7	42.4	5.7	4.8	3.8E-09	1.5	18.7	27.3	5.08	0.4	1.2E+10
	64.0	51.2	6.7	5.9	3.0E-09	2.9	16.4	27.3	5.07	0.4	4.5E+09
	71.2	59.2	7.5	6.9	2.4E-09	3.9	14.5	27.3	5.06	0.4	2.0E+09
	78.5	70.8	8.2	7.8	1.7E-09	4.9	12.6	27.3	5.07	0.4	8.4E+08
	83.0	82.0	8.7	8.4	1.3E-09	5.7	11.6	27.3	5.08	0.4	4.4E+08
	86.0	88.8	9.0	8.8	1.0E-09	6.1	10.7	27.3	5.09	0.4	2.6E+08
	47.3	90.0	5.0	3.8	4.5E-09	6.2	26.4	41.0	5.15	0.5	2.0E+10
	50.9	93.2	5.3	4.3	4.2E-09	6.9	25.6	41.0	5.15	0.5	1.3E+10
	53.7	96.0	5.6	4.6	3.9E-09	7.4	25.0	41.0	5.15	0.5	1.0E+10
	23.3	97.2	2.4	0.8	6.6E-09	7.7	37.5	76.7	5.32	0.6	8.6E+11
	23.9	100.4	2.5	0.8	6.6E-09	8.6	38.2	76.7	5.31	0.6	6.7E+11
	24.1	104.8	2.5	0.9	6.6E-09	10.0	39.5	76.7	5.30	0.6	6.2E+11
05-28-96	51.5	28.4	5.4	4.3	4.1E-09	2.7	21.4	12.5	1.04	12.4	4.9E+08
1 M NaCl	52.2	32.2	5.5	4.4	4.1E-09	3.4	21.8	12.5	1.03	12.4	4.5E+08
25°C	53.4	34.0	5.6	4.6	4.0E-09	3.7	21.6	12.5	1.03	12.4	4.0E+08
05-29-96	64.6	13.0	6.8	6.0	3.0E-09	0.9	14.3	17.5	4.85	0.4	4.0E+09
1 M NaCl	76.2	26.4	8.0	7.5	1.9E-09	2.4	11.1	17.5	4.85	0.4	1.1E+09
25°C	83.5	38.8	8.8	8.4	1.3E-09	3.3	9.0	17.5	4.86	0.4	3.8E+08
	88.2	52.8	9.2	9.0	8.5E-10	4.0	7.8	17.5	4.87	0.4	1.5E+08
	23.7	62.0	2.5	0.8	6.6E-09	5.5	35.5	64.2	5.01	1.0	4.4E+11
	22.4	63.7	2.3	0.6	6.7E-09	6.0	36.5	64.2	4.97	1.1	6.7E+11
	23.0	65.6	2.4	0.7	6.7E-09	6.6	36.9	64.2	4.96	1.1	5.1E+11

* with 1 M NaCl and 25°C

Table G-2 Detailed results of Hg° absorption in NaOCl-NaCl at intermediate pH at 25°C, no external $HgCl_2$ injection, $[Hg^{++}]_i = [Hg^{++}]_{absorbed} + \dfrac{N_{Hg}}{k°l.\,Hg^{++}}$

Run ID	Hg	time	P_{Hgb} x10^8	P_{Hgi} x10^8	N_{Hg} x10^{10}	absorb [Hg^{++}]	[Hg^{++}]$_i$ x10^8	injected [NaOCl] x10^6	pH	a_{Cl2} x10^{10}	k_2
	ppb	min	atm	atm	mole s-m^2	M	M	M		M	$\dfrac{1}{M\text{-}s}$
05-07-96	92.4	11.2	9.7	9.6	4.7	1.2E-09	2.3	0.9	6.31	0.8	2.0E+10
0.1 M NaCl	95.0	12.8	10.0	9.9	2.4	1.5E-09	1.2	0.9	6.33	0.8	5.0E+09
25°C	94.8	14.8	9.9	9.9	2.5	1.7E-09	1.3	0.9	6.34	0.8	5.7E+09
	95.5	16.0	10.0	10.0	1.9	1.8E-09	1.1	0.9	6.35	0.7	3.3E+09
	86.2	18.4	9.0	8.8	10.2	2.5E-09	4.9	3.4	6.42	2.3	3.9E+10
	90.1	20.0	9.4	9.3	6.7	3.1E-09	3.4	3.4	6.43	2.3	1.5E+10
	90.9	21.6	9.5	9.4	6.0	3.6E-09	3.1	3.4	6.45	2.2	1.3E+10
	91.5	24.4	9.6	9.5	5.5	4.3E-09	2.9	3.4	6.46	2.1	1.1E+10
	91.6	28.0	9.6	9.5	5.5	5.2E-09	3.0	3.4	6.47	2.1	1.1E+10
	67.4	29.6	7.1	6.4	27.1	6.4E-09	12.9	13.0	6.95	2.1	5.6E+11
	53.9	32.0	5.6	4.7	39.1	1.0E-08	18.6	13.0	6.96	2.1	2.3E+12
	40.4	35.2	4.2	2.9	51.1	1.7E-08	24.7	13.0	6.97	2.0	1.0E+13
	26.9	38.0	2.8	1.2	63.1	2.4E-08	30.9	13.0	6.90	2.5	7.2E+13
	20.2	42.4	2.1	0.4	69.1	3.7E-08	35.0	13.0	6.79	3.4	7.1E+14
	18.9	48.0	2.0	0.2	70.3	5.5E-08	37.3	13.0	6.66	4.8	1.8E+15
	18.8	52.0	2.0	0.2	70.4	6.8E-08	38.6	13.0	6.60	5.6	1.7E+15
	18.9	57.2	2.0	0.2	70.3	8.5E-08	40.2	13.0	6.57	6.1	1.3E+15
05-08-96	95.5	21.2	10.0	10.0	2.0	9.6E-10	1.0	0.9	6.55	0.4	5.9E+09
0.1 M NaCl	93.9	31.8	9.8	9.7	3.4	1.7E-09	1.7	2.1	6.67	0.7	1.1E+10
25°C	96.7	34.4	10.1	10.1	0.9	1.9E-09	0.6	2.1	6.68	0.7	7.0E+08
	96.8	36.4	10.1	10.1	0.8	2.0E-09	0.5	2.1	6.69	0.7	5.4E+08
	91.9	39.8	9.6	9.5	5.1	2.3E-09	2.6	4.1	6.74	1.2	1.6E+10
	95.6	43.6	10.0	10.0	1.8	2.9E-09	1.1	4.1	6.75	1.2	1.9E+09
	95.7	45.6	10.0	10.0	1.8	3.1E-09	1.1	4.1	6.75	1.2	1.8E+09
	95.7	48.0	10.0	10.0	1.8	3.3E-09	1.1	4.1	6.86	0.9	2.4E+09
	95.8	52.8	10.0	10.0	1.7	3.7E-09	1.1	4.1	6.87	0.9	2.3E+09
	70.0	54.8	7.3	6.7	24.7	4.9E-09	11.7	12.6	7.41	0.5	1.9E+12
	56.4	58.0	5.9	5.0	36.8	9.4E-09	17.6	12.6	7.40	0.5	7.2E+12
	42.9	60.8	4.5	3.3	48.9	1.5E-08	23.7	12.6	7.40	0.5	3.0E+13
	29.4	66.0	3.1	1.5	61.0	2.8E-08	30.4	12.6	7.05	1.5	6.8E+13
	27.7	70.0	2.9	1.3	62.5	3.9E-08	32.2	12.6	7.05	1.6	9.6E+13
	29.8	79.7	3.1	1.6	60.6	6.7E-08	34.1	12.6	7.04	1.6	6.1E+13
	32.8	88.0	3.4	2.0	57.9	8.9E-08	35.2	12.6	6.89	2.5	2.3E+13
	35.7	94.6	3.7	2.3	55.3	1.1E-07	35.7	12.6	6.89	2.5	1.5E+13

38.7	102.0	4.1	2.7	52.6	1.2E-07	36.3	12.6	6.88	2.5	9.9E+12
41.6	108.8	4.4	3.1	50.0	1.4E-07	36.7	12.6	6.86	2.7	6.5E+12

Run ID										
06-18-96	82.7	6.8	8.7	8.3	13.3	2.1E-09	6.3	3.6	7.17	2.4	7.1E+10
1 M NaCl	88.5	8.0	9.3	9.1	8.2	2.7E-09	4.0	3.6	7.27	1.7	3.2E+10
25°C	91.5	10.0	9.6	9.4	5.5	3.3E-09	2.8	3.6	7.35	1.3	1.7E+10
	92.2	11.6	9.7	9.5	4.9	3.7E-09	2.6	3.6	7.39	1.1	1.5E+10
	25.8	16.8	2.7	1.1	64.1	1.2E-08	30.4	14.4	7.87	0.7	3.2E+14
	26.6	18.8	2.8	1.2	63.5	1.8E-08	30.7	14.4	7.80	1.0	2.0E+14
	26.8	20.4	2.8	1.2	63.2	2.2E-08	31.0	14.4	7.74	1.2	1.5E+14

Table G-3 Detailed results of $Hg°$ absorption in NaOCl-NaCl at low to intermediate pH at 25°C with external $HgCl_2$ injection. $[Hg^{++}]_i =$ $[Hg^{++}]_{injected} + [Hg^{++}]_{absorbed} + \dfrac{N_{Hg}}{k°_{l.\ Hg^{++}}}$

Run ID & initial [NaCl]	Hg ppb	time min	P_{Hgb} x10^8 atm	P_{Hgi} x10^8 atm	N_{Hg} x10^9 mole s-m²	absorb [Hg++] x10^8 M	injected [Hg++] M	[Hg++]i M	injected [NaOCl] x10^6 M	pH	a_{Cl2} M	k_2 1/M-s
05-06-96	65.4	20.0	6.8	6.1	2.9	1.3	0	1.5E-07	11.0	6.78	2.9E-10	5.2E+11
25°C	66.7	21.6	7.0	6.3	2.8	1.5	0	1.4E-07	11.0	6.78	2.9E-10	4.5E+11
0.1 M	68.3	23.6	7.2	6.5	2.6	1.8	0	1.4E-07	11.0	6.77	2.9E-10	3.7E+11
	68.3	25.4	7.2	6.5	2.6	2.0	0	1.4E-07	11.0	6.75	3.1E-10	3.5E+11
	63.7	33.4	6.7	5.9	3.0	3.0	7.4E-06	7.6E-06	11.0	6.73	3.3E-10	5.4E+11
	59.2	41.2	6.2	5.3	3.4	4.2	7.4E-06	7.6E-06	11.0	6.70	3.5E-10	7.9E+11
	56.1	45.6	5.9	4.9	3.7	4.9	7.4E-06	7.7E-06	11.0	6.62	4.4E-10	8.6E+11
	51.6	53.6	5.4	4.4	4.1	6.3	7.4E-06	7.7E-06	11.0	6.60	4.6E-10	1.3E+12
	48.5	60.8	5.1	4.0	4.4	7.7	7.4E-06	7.7E-06	11.0	6.55	5.2E-10	1.5E+12
	43.5	66.8	4.6	3.3	4.8	9.0	2.9E-05	3.0E-05	11.0	6.54	5.4E-10	2.6E+12
	42.5	72.0	4.4	3.2	4.9	10.2	2.9E-05	3.0E-05	11.0	6.53	5.5E-10	2.9E+12
	41.8	76.0	4.4	3.1	5.0	11.1	2.9E-05	3.0E-05	11.0	6.51	5.8E-10	2.9E+12
06-19-96	62.4	20.8	6.5	5.7	3.2	1.5	0	1.6E-07	5.6	6.85	9.9E-10	2.0E+11
25°C	62.6	22.8	6.6	5.8	3.1	1.8	0	1.6E-07	5.6	6.87	9.3E-10	2.1E+11
1 M	64.2	26.8	6.7	6.0	3.0	2.4	0	1.6E-07	5.5	6.85	9.8E-10	1.7E+11
	65.9	31.6	6.9	6.2	2.8	3.0	0	1.6E-07	5.5	6.82	1.1E-09	1.3E+11
	67.3	33.6	7.0	6.4	2.7	3.2	2.2E-06	2.4E-06	5.4	6.81	1.1E-09	1.1E+11
	68.1	35.2	7.1	6.5	2.6	3.4	2.2E-06	2.4E-06	5.4	6.81	1.1E-09	1.0E+11
	69.1	38.0	7.2	6.6	2.5	3.8	7.6E-06	7.8E-06	5.4	6.80	1.1E-09	9.0E+10
	69.4	40.0	7.3	6.6	2.5	4.0	7.6E-06	7.8E-06	5.4	6.80	1.1E-09	8.7E+10
	71.0	42.8	7.4	6.8	2.4	4.3	2.6E-05	2.6E-05	5.3	6.80	1.1E-09	7.4E+10
	70.9	44.4	7.4	6.8	2.4	4.5	2.6E-05	2.6E-05	5.3	6.80	1.1E-09	7.5E+10
06-20-96	85.8	14.0	9.0	8.7	1.1	0.3	0	5.1E-08	1.0	3.06	5.7E-07	1.7E+07
25°C	87.8	15.2	9.2	9.0	0.9	0.4	0	4.4E-08	1.0	3.06	5.7E-07	1.1E+07

179

	Hg ppb	time min	$P_{Hg b}$ ×10⁸ atm	$P_{Hg i}$ ×10⁸ atm					pH	a_{Cl_2} M	k_2 1/M-s
1 M	88.9	16.0	9.3	9.1	0.8	0.4	0	4.0E-08	1.0	3.06	5.7E-07 8.9E+06
	57.9	22.8	6.1	5.2	3.6	1.1	0	1.7E-07	2.4	3.07	1.4E-06 2.3E+08
	57.6	24.4	6.0	5.1	3.6	1.4	0	1.7E-07	2.4	3.07	1.4E-06 2.4E+08
	58.9	27.2	6.2	5.3	3.5	1.8	2.8E-06	3.0E-06	2.3	3.07	1.4E-06 2.1E+08
	59.3	30.0	6.2	5.3	3.4	2.3	2.8E-06	3.0E-06	2.3	3.07	1.4E-06 2.0E+08
	60.7	32.8	6.4	5.5	3.3	2.7	4.1E-05	4.1E-05	2.3	3.07	1.4E-06 1.8E+08
	62.5	37.2	6.5	5.7	3.2	3.3	4.1E-05	4.1E-05	2.3	3.07	1.4E-06 1.5E+08
	66.8	42.4	7.0	6.3	2.8	4.1	4.1E-05	4.1E-05	2.3	3.07	1.4E-06 9.4E+07
	59.4	44.0	6.2	5.4	3.4	4.3	2.7E-04	2.7E-04	2.3	3.08	1.4E-06 2.0E+08
	68.0	50.8	7.1	6.4	2.7	5.2	2.7E-04	2.7E-04	2.3	3.08	1.4E-06 8.3E+07
	75.8	56.0	7.9	7.4	2.0	5.8	2.7E-04	2.7E-04	2.3	3.07	1.4E-06 3.4E+07
	83.2	61.6	8.7	8.4	1.3	6.2	1.0E-03	1.0E-03	2.3	3.08	1.4E-06 1.2E+07
	84.6	65.2	8.9	8.6	1.2	6.4	1.0E-03	1.0E-03	2.3	3.08	1.4E-06 9.2E+06
	85.0	67.2	8.9	8.6	1.1	6.5	1.0E-03	1.0E-03	2.3	3.08	1.4E-06 8.7E+06

Table G-4 Detailed results of Hg° absorption in NaOCl-NaCl at low to intermediate pH at 55°C, with no external HgCl₂ injection. $[Hg^{++}]_i = [Hg^{++}]_{absorbed} + \dfrac{N_{Hg}}{k^\circ_{l.\,Hg^{++}}}$.

Run ID	Hg ppb	time min	$P_{Hg b}$ ×10⁸ atm	$P_{Hg i}$ ×10⁸ atm	N_{Hg} ×10⁹ mole s-m²	absorb [Hg⁺⁺] ×10⁸ M	[Hg⁺⁺]ᵢ ×10⁸ M	injected [NaOCl] ×10⁶ M	pH	a_{Cl_2} M	k_2 1/M-s
07-18-96	96.1	32.0	10.1	10.0	0.1	0.1	0.5	0.1	2.88	7.0E-08	1.6E+07
1M NaCl	93.7	46.8	9.8	9.7	0.3	0.3	1.1	0.4	2.91	1.9E-07	3.5E+07
55°C	60.5	74.0	6.3	5.6	3.0	2.6	10.1	1.0	2.95	5.3E-07	3.2E+09
	26.0	96.0	2.7	1.2	5.8	7.5	22.0	1.9	2.94	9.6E-07	1.3E+11
07-24-96	84.7	10.8	8.9	8.6	1.1	0.3	2.9	2.6	7.23	6.6E-11	1.3E+12
1M NaCl	35.9	28.8	3.8	2.5	5.0	3.0	15.6	8.6	7.46	9.3E-11	2.5E+14
55°C	25.9	42.0	2.7	1.2	5.8	6.6	21.2	13.7	8.03	1.4E-11	8.9E+15

Appendix H Using $a_{Cl_2,i}$ for Low pH Results of Hg Absorption in NaOCl-NaCl at 25°C

The bulk chlorine activity is corrected to give interfacial chlorine activity for chlorine desorption and reaction at the gas-liquid interface:

$$k^{\circ}_{l, Cl_2} (a_{Cl_2, b} - a_{Cl_2, i}) = k_{g, Cl_2} (H_{Cl_2} a_{Cl_2, i} - 0) + N_{Hg} \tag{H-1}$$

This resulted in:

$$a_{Cl_2, i} = \frac{k^{\circ}_{l.Cl_2} a_{Cl_2.b} - N_{Hg}}{k_{g.Cl_2} H_{Cl_2} + k^{\circ}_{l.Cl_2}} \tag{H-2}$$

The results are given in table H-1.

Table H-1 Hg absorption in NaOCl-NaCl at low pH (with HCl addition) at 25°C. $k_{g, Hg}$ = 0.39 mole/s-atm-m^2, k_{g, Cl_2} = 0.31 mole/s-atm-m^2, $k^{\circ}_{l, Hg^{++}}$ = 2.2x10^{-5} m/s, k°_{l, Cl_2} =2.9x10^{-5} m/s. No external HgCl$_2$ injection. The inlet Hg was 97.7 ppb.

Run ID	time	P_{Hgb} x10^8	P_{Hgi} x10^8	N_{Hg} mole	injected [NaOCl] x10^6	pH	$a_{Cl2,b}$ x10^7	$a_{Cl2,i}$
	min	atm	atm	s-m^2	M		M	M
05-10-96	21.6	7.6	7.0	2.2E-09	0.9	3.04	1.4	6.7E-11
0.1 M NaCl	66.4	2.3	0.6	6.7E-09	2.9	3.03	4.6	2.4E-10
05-16-96*	24.4	3.5	2.1	5.7E-09	1.7	2.98	10.6	9.4E-10
05-17-96	18.0	10.2	10.2	6.2E-12	0.1	0.96	1.2	1.3E-10
1 M NaCl	22.0	8.2	7.8	1.7E-09	0.7	0.96	7.2	7.1E-10
	80.8	4.0	2.6	5.3E-09	1.7	0.93	16.5	1.6E-09
05-23-96	20.8	10.1	10.1	9.4E-11	0.2	4.96	0.03	-2.6E-13
1 M NaCl	27.2	8.8	8.4	1.3E-09	1.0	4.98	0.2	-2.9E-11
	29.2	8.5	8.2	1.5E-09	1.0	4.99	0.2	-3.7E-11
	38.8	5.6	4.6	3.9E-09	2.7	5.08	0.4	-1.1E-10
	90.0	5.0	3.8	4.5E-09	4.1	5.15	0.5	-1.2E-10
	97.2	2.4	0.8	6.6E-09	7.7	5.32	0.6	-1.8E-10
05-28-96*	28.4	5.4	4.3	4.1E-09	1.2	1.04	12.4	1.2E-09
05-29-96	13.0	6.8	6.0	3.0E-09	1.7	4.85	0.4	-6.8E-11
1 M NaCl	63.7	2.3	0.6	6.7E-09	6.4	4.97	1.1	-1.3E-10

* with 1 M NaCl and 25°C

181

Although this correction reduced the chlorine activity by 2×10^3 M, the results are still underpredicted compared to the high pH results. For higher pH, such as pH = 5, the predicted $a_{Cl_2,i}$ is a negative value. This is due to the fact that there was little chlorine available in the bulk solution that it was depleted by reaction as soon as it was generated.

Glossary

A = gas - liquid contact area (m^2)

C = instantaneous bulk concentration in the liquid (M)

C_{Hg} = instantaneous bulk mercury concentration in the liquid (M)

$C_{Hg, initial}$ = initial injected $HgCl_2$ concentration in the liquid (M)

$[Cl_2]_b$ = Cl_2 concentration in the bulk liquid (M)

$[Cl_2]_i$ = Cl_2 concentration at the liquid side interface (M)

$[Cr_2O_7^=]_b$ = $Cr_2O_7^=$ concentration in the bulk liquid (M)

$[Cr_2O_7^=]_i$ = $Cr_2O_7^=$ concentration at the liquid side interface (M)

$D_{CO_2-H_2O}$ = diffusion coefficient of CO_2 in water ($m^2\ s^{-1}$)

D_{Hg-H_2O} = diffusion coefficient of Hg in water ($m^2\ s^{-1}$)

$D_{Hg^{++}-H_2O}$ = diffusion coefficient of Hg^{++} in water ($m^2\ s^{-1}$)

$D_{Hg(g)-Air}$ = interdiffusion coefficient of Hg and air ($m^2\ s^{-1}$)

$D_{Hg(g)-N_2}$ = interdiffusion coefficient of Hg and N_2 ($m^2\ s^{-1}$)

$D_{MnO_4^--H_2O}$ = liquid film diffusion coefficient of MnO_4^- ($m^2\ s^{-1}$)

$D_{SO_2-H_2O}$ = liquid film diffusion coefficient of SO_2 ($m^2\ s^{-1}$)

$D_{SO_2-N_2}$ = interdiffusion coefficient of SO_2 and N_2 ($m^2\ s^{-1}$)

G = gas flow rate (l min^{-1})

$[H_2O_2]_b$ = hydrogen peroxide concentration in the bulk liquid (M)

$[H_2O_2]_i$ = hydrogen peroxide concentration at the liquid side interface (M)

H_{Hg} = Henry's constant of Hg (atm M^{-1})

$[Hg(II)]_{absorbed}$ = bulk liquid Hg(II) conc. that absorbed from gas phase (M)

183

$[Hg(II)]_b$ = Hg(II) concentration in the bulk liquid (M)

$[Hg(II)]_i$ = Hg(II) concentration at the liquid side interface (M)

K_1 or K_2 = equilibrium constant

k_1 = first order rate constant (s^{-1})

k_2 = second order rate constant ($M^{-1} s^{-1}$)

k_3 = third order rate constant ($M^{-2} s^{-1}$)

k_3' = third order rate constant defined by equation (6-29) ($M^{-2} s^{-1}$)

k_g = gas film mass transfer coefficient (mole s^{-1} atm^{-1} m^{-2})

K_g' = normalized Hg flux, $\dfrac{N_{Hg}}{P_{Hgi}}$ (mole s^{-1} atm^{-1} m^{-2})

$k^\circ_{l, Hg}$ = physical liquid film mass transfer coefficient of Hg (m s^{-1})

$k^\circ_{l, Hg^{++}}$ = physical liquid film mass transfer coefficient of Hg^{++} (m s^{-1})

k°_{l, MnO_4^-} = physical liquid film mass transfer coefficient of MnO_4^- (m s^{-1})

k°_{l, SO_2} = physical liquid phase mass transfer coefficient of SO_2 (m s^{-1})

$[Mn(II)]_b$ = Mn(II) concentration in the bulk liquid (M)

$[Mn(II)]_i$ = Mn(II) concentration at the liquid side interface (M)

$[MnO_4^-]_b$ = permanganate concentration in the bulk liquid (M)

$[MnO_4^-]_i$ = permanganate concentration at the liquid side interface (M)

$[Na_2S]_b$ = Na_2S concentration in the bulk liquid (M)

n_g = gas phase agitation speed (rpm)

n_l = liquid phase agitation speed (rpm)

N_{Hg} = Hg flux (mole s^{-1} m^{-2})

$P_{CO_2, out}$ = outlet CO_2 partial pressure (atm)

P_{Hgb} = partial pressure of Hg in the bulk gas phase (atm)

P_{Hgi} = partial pressure of Hg at the gas side interface (atm)

184

$P_{Hg, in}$ = partial pressure of Hg in the inlet gas (atm)

$P_{Hg, out}$ = partial pressure of Hg in the outlet gas (atm)

R = gas constnat, $8.314 \dfrac{Pa\ m^3}{mole\ °K}$

t = time (s)

T = temperature (°K)

V = volume of the liquid solution (m^3)

x = distance measured from the gas-liquid interface (m)

a_{Cl^-} = activity of Cl$^-$ (M)

a_{Cl_2} = activity of aqueous Cl$_2$ (M)

a_{H^+} = activity of H$^+$ (M)

a_{HOCl} = activity of HOCl (M)

a_{OCl^-} = activity of OCl$^-$ (M)

γ_{Cl^-} = activity coefficient of Cl$^-$

γ_{Cl_2} = activity coefficient of aqueous Cl$_2$

γ_{HOCl} = activity coefficient of HOCl

γ_{Na^+} = activity coefficient of Na$^+$

γ_{NaCl} = activity coefficient of NaCl

γ_{OCl^-} = activity coefficient of OCl$^-$

185

References

Altshuller, E., Ortman, C., Analytical Chemistry, 32, 802-810 (1960).

Atkins, P. W., Physical Chemistry, 4th Ed., W. H. Freeman and Company, New York (1990).

Bakir, F., S. F. Damluji, L. Amin-Zaki, M. Murtadha, A. Khalidi, N. Y. Al-Rawi, S. Tikriti, H. I. Dhahir, T. W. Clarkson, J. C. Smith, and R. A. Doherty, "Methylmercury Poisoning in Iraq", Science, 181, 230 (1973).

Barbieri, R., Majorca, R., "Indagini con S^{35} sul meccanismo di formazione di tiosolfato e tritionato da H_2S + SO_2", La Ricerca Scientifica, 2337-2343, December (1960).

Baxendale, J., J. Keene and D. Stott, Pulse Radiolysis, p107, Academic Press, New York (1965).

Benschoten, J. and W. Lin, "Kinetic Modeling of Manganese(II) Oxidation by Chlorine Dioxide and Potassium Permanganate", Environ. Sci. Technol., 26, 1327-33 (1992).

Bergstrom, J., "Mercury Behavior in Flue Gases", Waste Management and Research, 4, 57 (1986).

Billing, C. E. and W. R. Matson, "Mercury Emissions from Coal Combustion", Science, 176, 1232-3 (1972).

Bloom, N.S., "Chemical Speciation of Mercury in Coal-Fired Power Plant Stack Gases: Overcoming Analytical Problems", in Proc. Conference on Managing Hazardous Air Pollutants: State of the Art, Washington, DC (1991).

Brosset, C., "The behavior of Mercury in the Physical Environment", Water, Air and Soil Pollution, 34, 145-166 (1987).

Brown, M. H., "The Toxic Cloud", Harper & Row, Publishers, New York (1987).

Chow, W., Miller M.J., Fortune J., Behrens, G., Rubin, E., "Managing Air Toxics Under the New Clean Air Act Amendments", Power Engineering, 95, 1, 30-34 (1991).

Clever, H. L., S. A. Johnson and M. E. Derrick, "The Solubility of Mercury and Some Sparingly Soluble Mercury Salts in Water and Aqueous Electrolyte Solutions", J. Phys. Chem. Ref. Data, 14(3), 631 (1985).

Collins, R., Cole, S., "Mercury Rising: Government Ignores the Threat of Mercury from Municipal Waste Incinerators", Clean Water Action, Washington D. C. (1990).

Connick, R. E. and Y. Chia, "The Hydrolysis of Chlorine and its Variation with Temperature", J. Am. Chem. Soc., 81, 1280 (1959).

Danckwerts, P. V., "Chap. 5, Absorption into Agitated Liquids", Gas-Liquid Reactions, McGraw Hill Book Company (1970).

DeVito, M.S., Conrad, V.B., Tumati, P.R., "Trace Element Sampling and Analysis from Coal-Fired Facilities", Consol, Inc., paper presented at Power-Gen 1992 conference, Orlando, FL, November 19 (1992).

DeVito, M.S., L. W. Rosendale and V. B. Conrad, "Comparison of Trace Element Contents of Raw and Clean Commercial Coals", presented at the DOE Workshop on Trace Element Transformations in Coal-Fired Power Systems, Scottsdale, AX, April 19-22 (1993).

Douglas, J., "Mercury in the Environment", EPRI Journal, p 4, December (1991).

Dyrssen, D., Wedborg, M., "The Sulphur-Mercury System in Natural Waters", Water Air and Soil Pollution, 56, 507-519 (1991).

Environmental Protection Agency, Code of Federal Regulations, title 40, part 266, App. IX, 525 (1992).

Federal Register, "Rules and Regulations", 60(243), 65387-436, December 19 (1995).

Felsvang, K., R. Gleiser, G. Juip, and K. Nielsen, "Air Toxics Control by Spray Dryer Absorption", presented at the 1993 SO_2 Control Symposium, August 24-27, Boston, MA (1993).

Gilmour, C. C. and E. A. Henry, "Mercury Methylation in Aquatic Systems Affected by Acid Deposition", Environmental Pollution, 71, 131-69 (1991).

Gleiser, R., and K. Felsvang, "Controlling Air Toxics from MSW and Utility Coal Fired Combustors", presented at the ICAC Forum 1993 -- Controlling Air Toxics and NOx Emission, Baltimore, MD, February 24-26 (1993).

Guest, T. L., and O. Knizek, "Mercury Control at Burnaby's Municipal Waste Incinerator", presented at the 84th Annual Meeting , Air & Waste Management Association, Vancouver, British Columbia, (1991).

187

Hall, B., P. Schager, and O. Lindqvist, "Chemical Reaction of Mercury in Combustion Flue Gases", Water, Air and Soil Pollution, 56, 3-14 (1991).

Hall, E. H., J. H. Oxley, and H. S. Rosenberg, "Mercury Emissions and Controls", status report, Battelle Memorial Institute, columbus, Ohio, June 1 (1993).

Hara N., "Capture of Mercury Vapor in Air with Potassium Permanganate Solution", Industrial Health, 13, 243 (1975).

Harris, D. C., "Quantitative Chemical Analysis", 2nd Ed., pp399, W. H. Freeman and Company (1987).

Hatch, R. and L. Ott, "Determination of Sub-Microgram Quantities of Mercury by Atomic Absorption Spectrophotometry", 40(14), Analytical Chemistry (1968).

Higbie, R., "The Rate of Absorption of a Pure Gas into a Still Liquid During Short Periods of Exposure", Trans. AIChE, 31, 365 (1935).

Hirschfelder, J. O., C. F. Curtis, and R. B. Bird, Molecular Theory of Gases and Liquids, Wiley, New York (1954).

Huang, H. S., C. D. Livengood, and S. Saromb, "Emissions of Airborn Toxics from Coal Fired Boilers: Mercury", DOE report ANL/ESD/TM-35, Argonne National Laboratory, September (1991).

Iverfeldt, A. and O. Lindqvist, "Atmospheric Oxidation of Elemental Mercury by Ozone in the Aqueous Phase", Atmos. Environ., 20(8), 1567-73 (1986).

Kobayashi, T., "Oxidation of Metallic Mercury in Aqueous Solution by Hydrogen Peroxide and Chlorine", J. Japan Soc. Air Pollut., 22(3), 230-6 (1987).

Lagowski, "Bleach Analysis by Redox Titration", Experiences in Chemistry, 124-6, McGraw-Hill, Inc. (1995).

Lide, D. R. (Ed.), CRC Handbook of Chemistry and Physics, 75th Ed., CRC Press, Inc., Boca Raton, FL (1994).

Lindberg, S. E., "Emission and Deposition of Atmospheric Mercury Vapor", Lead, Mercury, Cadmium and Arsenic in the Environment, T. C. Hutchinson and K. M. Meema, Eds., John Wiley and Sons Ltd., New York, pp. 89-106 (1987).

Lindqvist, O. and H. Rodhe, "Atmospheric Mercury ---- a review", Tellus, 37B, 136-159 (1985).

Lobo, V. M. M. and J. L. Quaresma, Handbook of Electrolyte Solutions, Elsevier Science Publishing Company, Inc., New York (1989).

Marrero, T. R. and E. A. Mason, "Gaseous Diffusion Coefficients", J. Phys. Chem. Ref. Data, 1(1), 3 (1972).

McCannon, C. S., Jr. and J. Woodfin, "An Evaluation of a Passive Monitor for Mercury Vapor", Am. Ind. Hyg. Assoc. J., 38, 378 (1977).

McGuire, L.M., "Sulfur Dioxide Absorption Experiments in Calcium Hydroxide Slurries", M.S. Thesis, UT-Austin, December (1990).

Medhekar, A. K, M. Rokni, D. W. Trainor, and J. H. Jacob, "Surface Catalyzed Reaction of Hg + Cl_2", Chem. Phys. Lett., 65(3), 600 (1979).

Meij, R., "The Fate of Mercury in Coal-Fired Power Plants and the Influence of Wet Flue-gas Desulfurization", Water, Air and Soil Pollution, 56, 21-33 (1991).

Menke, R. and G. Wallis, "Detection of Mercury in Air in the Presence of Chlorine and Water Vapor", Amer. Ind. Hyg. Assoc. J., 41, 120 (1980).

Metzger, M. and H. Braun, "In-situ Mercury Speciation in Flue Gas by Liquid and Solid Sorption Systems", Chemosphere, 16(4), 821-32 (1987).

Mikhailov, V. K. and M. I. Kochegarova, "Diffusion and Thermal Diffusion of Mercury Vapor in Air", Sb. Navch. Tr., Gos. Nauch.-Issled., Inst. Tsvet. Metal., 26, 138-44 (1967)

Monkman, J. L., P. A. Maffett and T. F. Doherty, "The Determination of Mercury in Air Samples and Biological Materials", Amer. Ind. Hyg. Assoc. J., 17, 418-20 (1956).

Mullaly, J. M. and H. Jacques, "The Diffusion of Mercury and of Iodine Vapors through Nitrogen", Philosophical Magazine, 48(288), 1105-22 (1924).

Munthe, J., Xiao, F., Lindqvist, O., "The Aqueous Reduction of Divalent Mercury by Sulfite", Water, Air and Soil Pollution, 56, 621-630 (1991).

Munthe, J., "The Aqueous Oxidation of Elemental Mercury by Ozone", Atmos. Environ., 26A, 1461-8 (1992).

Nakayama, K., "An Accurate Measurement of the Mercury Vapor Drag Effect in the Pressure Region of Transition Flow", Japanese Journal of Applied Physics, 7(9), 1114 (1968).

Nakazato, K., "Latest Technological Experience of the Removal of Mercury in Flue Gas and the management of Fly Ash from MSW Incinerator", Proc. Natl. Waste Process. Conf., 14, 163-169 (1990).

Nene, S. and V. C. Rane, "Kinetics of the Absorption of Mercury", Indian J. Technol., 19(1), 20-5 (1981).

Nguyen, X. T., assigned to Domtar Inc., Montreal, Canada, "Process for Mercury Removal", U. S. Patent 4,160,730, July 10 (1979).

Niro, European Patent Application 87306035.4, July 8 (1987).

Noblett, J. G. Jr., Owens, D. R., "Control of Air Toxics from Coal-Fired Power Plants Using FGD Technology", presented at the 1993 SO_2 Control Symposium, August 24-27, Boston, MA (1993).

Nriagu, J. O. and J. M. Pacyna, "Quantitative Assessment of Worldwide Contamination of Air, Water, and Soils by Trace Metals", Nature, 333, 134-139 (1988).

Owens, D. R., "Sulfite Oxidation Inhibited by Thiosulfate", Master's Thesis, The University of Texas at Austin (1984).

Parkinson, G. (Ed.), "A Simplified Scrubbing Process Cuts the Cost of Fluegas Cleanup", Chemical Engineering, 103(6), June (1996).

Parks, G. A. and R. E. Baker, assigned to Mountain Copper Company of California, Martinez, California, "Mercury Process", U. S. Patent 3,476,552, November 4 (1969).

Personal communication, Dr. Carl F. Richardson, Radian International, LLC, Austin, TX (1994).

Radian Corporation, "Estimating Air Toxics Emissions from Coal and Oil Combustion Sources", U.S. Environmental Protection Agency Report EPA-450/2-89-001, April (1989).

Raloff, J., "Mercurial Risks from Acid's Reign", Science News, 139, 152-6, March 9 (1991).

Ramel, C., "The Mercury Problem-A Trigger for Environmental Pollution Control", presented at the First International Conference on Environmental Mutagens, Asilomar, California, August 29-September 1 (1973)

Rawoof. M. and J. Sutter, "Kinetic studies of Permanganate Oxidation Reactions. II. Reaction with Ferrocyanide Ion", J. Phys. Chem., 71, 2767-71 (1967).

Reimann, D. O., "Mercury Output form Garbage Incinerators", Waste Management and Research, 4, 45 (1986).

Robinson, R. A. and H. S. Harned, "Some Aspects of the Thermodynamics of Strong Electrolytes from Electromotive Force and Vapor Pressure Measurements", Chem. Rev., 28, 419 (1941).

Schroeder, W. H., et al., "Toxic Trace Elements Associated with Airborne Particulates Matter: A Review", J. Air Pollu. Control Association, 37(11), 1267-85, November (1987).

Schroeder, W. H., G. Yarwood and H. Niki, "Transformation Processes Involving Mercury Species in the Atmosphere--Results form a Literature Survey", Water, Air, and Soil Pollut., 56, 653-66 (1991).

Shen, C. H. and G. T. Rochelle, "NO_2 absorption in limestone slurry for flue gas desulfurization", in proceedings of the 1995 SO_2 Control Symposium, Miami, FL, March 28-31 (1995).

Shendrikar, A. D., R. Filby, G. R. Markowski, and D. S. Ensor, "Trace Element Loss onto Polyethylene Container Walls from Impinger solutions from Flue Gas Sampling", Air Pollution Control Association, 34, 233-236 (1984).

Siegel, S. M and B. Z. Siegel, "Temperature Determinations of Plant-Soil-Air Mercury Relationships", Water, Air & Soil Pollu., 40, 443 (1988).

Sitaraman R., S. H. Ibrahim, and N. R. Kuloor, "A Generalized Equation for Diffusion in Liquids", J. Chem. Eng. Data, 8(2), 198 (1963).

Slemr, F., G. Schuster and W. Seiler, "Distribution, Speciation, and Budget of Atomospheric Mercury", J. Atmos. Chem., 3, 407-34 (1985).

Slemr, F. and E. Langer, "Increase in Global Atmospheric Concentrations of Mercury Inferred from Measurements over the Atlantic Ocean", Nature, 355, 434-7, January 30 (1992).

Smith, I. M., "Trace Elements from Coal Combustion Emissions", International Energy Agency Coal Research Report IEACR/01, London, England, June (1987).

Smith, R. D., "The Trace Element Chemistry of Coal during Combustion and the Emissions from Coal-Fired Power Plants", Progress in Energy Combustion Science, 6, 53-114 (1980).

Sorenson, J. A., G. E. Glass, K. W. Schmidt, J. K. Huber and G. R. Ross Jr., "Airborne Mercury Deposition and Watershed Characteristics in Relation

to Mercury Concentrations in Water, Sediments, Plankton, and Fish of Eighty Northern Minnesota Lakes", Assessment of Mercury Contamination in Selected Minnesota Lakes and Streams, E. B. Swain, (Ed.), Minnesota Pollution Control Agency, St. Paul, Minnesota, December (1989).

Spier, J. L., "The Determination of the Coefficient of Diffusion of Mercury Vapor and Cadmium Vapor in Nitrogen", Physica, 7(5), 381-4 (1940).

Stewart, C. T., Jr., "Air Pollution, Human Health and Public Policy", Lexington Books, D. C. Heath and Company, Lexington, Massachusetts (1979).

Swain, E. B. (Ed.), "Executive Summary: Assessment of Mercury Contamination in Selected Minnesota Lakes and Streams", Minnesota Pollution Control Agency, St. Paul, Minnesota, December (1989).

Takizawa, Y., "Epidemiology of Mercury Poisoning", The Biogeochemistry of Mercury in the Environment, Elsevier/North-Holland Biomedical Press, Amsterdam, Netherlands (1979).

Thomas, J., S. Gordon and J. Hart, "The Rates of Reaction of the Hydrated Electron in Aqueous Inorganic Solutions", J. Phys. Chem., 68, 1524-7 (1964).

Uchida, S., T. Kobayashi, and S. Kageyama, "Absorption of Nitrogen Monoxide into Aqueous $KMnO_4/NaOH$ and $Na_2SO_3/FeSO_4$ solutions", Ind. Eng. Chem. Process Des. Dev., 22, 323-29 (1983).

Vatavuk, W. M., "Estimating Costs of Air Pollution Control", Lewis Publishers, Chelsea, Michigan (1990).

Vaughan, B. E., K. H. Abel and D. A. Cataldo, "Review of Potential Impact on Health and Environmental Quality form Metals Entering the Environment as a Result of Coal Utilization", Pacific Northwest Laboratories, Battelle Memorial Institute, Richland, WA, August (1975).

Vogg, H., H. Braun, M. Metzger, and J. Schneider, "The Specific Role of Cadmium and Mercury in Municipal Solid Waste Incineration", Waste Management & Research, 4, 65-74 (1986).

Volland, C. S., "Mercury Emissions from Municipal Solid Waste Combustion", presented at the 84th Annual Meeting & Exhibition of Air & Waste Management Association, Vancouver, British Columbia, June 16-21 (1991).

Wesnor, J. D., "ABB's Investigations into the Utility Air Toxics Problem", presented at the 1993 SO_2 Control Symposium, August 24-27, Boston, MA (1993).

Wigfield, D. C. and S. L. Perkins, "Oxidation of Elemental Mercury by Hydroperoxides in Aqueous Solution" Can. J. Chem., 63, 275 (1985).

Whitman, W. G., "The Two-Film Theory of Gas Absorption", Chem. and Met. Eng., 29, 147 (1923).

Zohourslsen, O. and O. Christiansen, "Activated-carbon Addition Process for Control of Mercury and/or Dioxin Emissions", presented at the 1991 Dry FGD User Seminar, King of Prussia, PA, June 17-20 (1991).

Vita

Lingbing Zhao was born in Zhejiang, China on June 7, 1969, the youngest daughter of Qijin Zuo and Wanxian Zhao. After graduating from Taizhou High School in 1986, she entered Zhejiang University in September of that year and earned the degree of Bachelor of Science in Chemical Engineering in July, 1990. From 1990 to 1992, she attended the graduate school at East China University of Chemical Technology in Shanghai, China. She transferred to the University of Texas at Austin in September, 1992 and received Master of Science in Chemical Engineering in May, 1996. She worked part time for Radian International in Austin, Texas during the Summer and Fall of 1994. Employment has been accepted with Exxon Chemical Company in Baytown, TX.

Permanent address:　1632 W. 6th St. # M

　　　　　　　　　　Austin, TX　78703

This dissertation was typed by the author.